U. S. ARMY

TRANSPORTATION RESEARCH COMMAND
FORT EUSTIS, VIRGINIA

TRECOM TECHNICAL REPORT 64-1

GUST ALLEVIATION FEASIBILITY STUDY

Project 1D131201D159
(Formerly Task 9R38-10-005-04)
Contract DA 44-177-AMC-858(T)

April 1964

prepared by:

AUTONETICS
A Division of North American Aviation, Inc.
Anaheim, California

DISCLAIMER NOTICE

When Government drawings, specifications, or other data are used for any purpose other than in connection with a definitely related Government procurement operation, the United States Government thereby incurs no responsibility nor any obligation whatsoever; and the fact that the Government may have formulated, furnished, or in any way supplied the said drawings, specifications, or other data is not to be regarded by implication or otherwise as in any manner licensing the holder or any other person or corporation, or conveying any rights or permission, to manufacture, use, or sell any patented invention that may in any way be related thereto.

DDC AVAILABILITY NOTICE

Qualified requesters may obtain copies of this report from

<div align="center">

Defense Documentation Center
Cameron Station
Alexandria, Virginia 22314

</div>

This report has been released to the Office of Technical Services, U.S. Department of Commerce, Washington 25, D.C., for sale to the general public.

The findings and recommendations contained in this report are those of the contractor and do not necessarily reflect the views of the U.S. Army Mobility Command, the U.S. Army Material Command, or the Department of the Army.

This report has been reviewed by the U. S. Army Transportation
Research Command and is considered to be technically sound. The
report is published for the exchange of information and stimulation
of ideas.

JOHN E. YEATES
Project Engineer

JAMES G. MC HUGH
Group Leader
Aeromechanics Group

APPROVED.

FOR THE COMMANDER:

LARRY M. HEWIN
Technical Director

Project ID131201D 159
(Formerly Task 9R38-10-005-04)
Contract DA 44-177-AMC-858(T)
TRECOM Technical Report 64-1

April 1964

GUST ALLEVIATION FEASIBILITY STUDY

Prepared by
Autonetics
A Division of North American Aviation, Inc.
3370 East Anaheim Road, Anaheim, California

for
U.S. ARMY TRANSPORTATION RESEARCH COMMAND
FORT EUSTIS, VIRGINIA

PREFACE

This final report concludes a study effort conducted for the U.S. Army Transportation Research Command (USATRECOM) under Department of the Army Contract DA 44-177-AMC-858(T), dated 30 August 1962, by the Autonetics Division of North American Aviation, Inc. (NAA). The study was performed within Autonetics' Data Systems Division (DSD), formerly Computers and Data Systems Division, with the aid of the Columbus Division of NAA. Messrs. J. E. Yeates and R. L. Brugh of the contracting agency provided technical monitoring of the program.

The study was performed and this report was compiled by Messrs. J. D. Balducci, F. L. Adams, and C. H. McKinley of Autonetics, and M. A. Schwartzberg of Columbus. Messrs. H. L. Ehlers and E. C. Bridges of Autonetics and R. C. A'Harrah of Columbus provided program and technical direction. Acknowledgment is given to Messrs. K. J. Schussler, A. Katz, J. C. Karr, and A. Troy of Autonetics, and to Messrs. D. R. Cichy and J. A. Murphy of Columbus for their analytical assistance.

The gratitude of the authors is extended to Messrs. H. L. Ehlers and C. F. Rasmussen, Autonetics, and to Mr. R. Olshausen and Dr. G. M. Andrew, recently of Autonetics, for their time given in consultation and the benefit of their prior experience in the field of gust alleviation.

Credit is given to the Autonetics Technical Library for performance of the literature search and for the preparation of EM-1163-104, "Annotated Bibliography of Literature Concerning Gust Alleviation Techniques, Low-Altitude Atmospheric Turbulence, and Related Topics," dated 14 February 1963.

BLANK PAGE

CONTENTS

CONTENTS (Cont)

CONTENTS (Cont)

BLANK PAGE

ILLUSTRATIONS

TABLES

SYMBOLS

A	Alleviation
$\cancel{R}$	Aspect ratio
a	A coefficient; section lift-curve slope
a_{i_j}	Aerodynamic coefficient due to structural flexibility
B	A constant
b	Wing span, feet
C	A constant
C_D	Drag coefficient
C_L	Lift coefficient
C_M	Moment coefficient
C_H	Hinge moment coefficient
c	Chord, feet
$\bar{c}$	Mean aerodynamic chord, feet
c_L	Section lift coefficient
D	Drag, pounds
e	Efficiency factor; a coefficient
F	A function
f	Parasite drag factor, square feet; shaping network parameter, per second
f_n	Natural frequency, cps
g	Acceleration due to gravity, equal to 32.2 feet per second; shaping network paramete , per second
g_i	Damping coefficient of ith fuselage bending mode
h	Altitude or height, feet
I_{yy}	Pitch moment of inertia, slug feet squared
K	Gain factor
K_o	Dynamic contribution to gust sensitivity, a function of frequency
k	Shaping network parameter, per second
L	Lift; turbulence scale, feet
l	Distance, feet
$\mathcal{L}$	Induced drag factor
M	Mach number; mass-normalized pitching moment; mass, slugs
n_i	Generalized mass of ith fuselage mode, slugs
N	Number of exceedances per second

N_Z	Vertical acceleration, g's
q	Pitch rate, degrees per second or radians per second
$\bar{q}$	Dynamic pressure, pounds per square foot
R	Range, feet or miles
R_N	Reynolds number
S	Area, square feet
S_G	Ground run distance, feet
s	Laplacian operator, per second
J	Gust sensitivity, g's per feet per second
t	Time, seconds; thickness, feet
T	Thrust, pounds
U	Aircraft forward velocity, feet per second; unalleviated
u	Change in aircraft forward velocity, feet per second
V	Volts
W	Weight, pounds
w_g	Vertical gust velocity, feet per second
X	Mass-normalized drag coefficient
x	Distance, feet
y	Distance, feet
Z	Mass-normalized lift force coefficient
α	Angle of attack, degrees
α_g	Gust angle of attack, degrees
α_{g_s}	Simulated gust angle of attack, degrees
α_s	Sensed angle of attack, degrees
δ	Deflection angle, degrees
Δ	Increment
δ_E	Elevator deflection angle, degrees
δ_F	Flap deflection angle, degrees
δ_S	Control stick deflection
ϵ	Downwash angle, degrees
ζ	Damping ratio
γ	Flight path angle, degrees
λ	Taper ratio
Ω	Reduced gust frequency, radians per foot
κ	Span factor
Λ	Wing sweep angle, degrees
τ	Time increment, seconds
ω_i	Frequency of ith airplane bending mode, radians per second

ω_n	Natural frequency, radians per second
ϕ_i	Mode shape of ith airplane bending mode
Φ	Power spectrum
ρ	Atmospheric density, slugs per cubic foot
σ	Root mean square value
θ	Pitch angle, degrees
Γ	Tip dihedral angle, degrees
ξ_i	Generalized coordinate of ith airplane bending mode; thrust angle, radians
μ	Coefficient of friction
Ξ	Generalized bending force
$(\ )_o$	Denotes trim or steady-state value
$(\ )_W$	Denotes wing
$(\ )_T$	Denotes tail
$(\dot{\ })$	Denotes first derivative with respect to time
$(\ddot{\ })$	Denotes second derivative with respect to time
$(\ )_A$	Denotes alleviated value
$(\ )_U$	Denotes unalleviated value
$(\ )_e$	Denotes effective value

SUMMARY

This study report, based on a detailed analytical effort, provides a realist'c appraisal of the capabilities of known gust alleviation systems and determines the feasibility of utilizing these systems in future aircraft intended for sustained low level, high-subsonic-speed operations. Gust alleviation systems are defined as methods which intentionally or incidentally reduce vertical aircraft loading resulting from atmospheric turbulence.

The study considers a number of proposed systems and theoretical techniques. The systems fall into one of two broad categories: feedback control, termed active alleviation and aircraft geometry alteration, termed passive alleviation. Evaluation criteria include alleviation capability, pilot tolerance and endurance, stability, control, performance, structural effects, weight, cost, reliability, and fail-safety.

It is concluded that either a normal acceleration feedback system controlling flaps and elevators or a variable sweep wing design offers the most attractive method of obtaining desirable alleviation.

1

CONCLUSIONS

Based on the material presented in this report, it is concluded that two types of systems are most practical for inclusion in future aircraft designed for low-altitude, high-subsonic-speed operation. These are:

1. An active system employing a normal acceleration sensor and feedback of the sensed signal to trailing-edge wing flaps for lift control and to horizontal tail surfaces for balance of pitching moment. Alleviation obtained is approximately 40 percent of rms normal accelerations and 77 percent of the acceleration power spectral density (PSD) peak, i.e., at the aircraft short-period frequency. This system offers the most feasible approach to alleviation over a range of vehicle velocities.

2. A passive system consisting of a variable-sweep wing design which decreases loading in the swept position through reduction of the lift change due to angle of attack, i.e., lift-curve slope, C_{L_α} Potential alleviation is approximately 40 percent of rms normal accelerations and 50 percent of the acceleration power spectral density peak. This system is feasible if alleviation at high speed only is considered sufficient and if the associated range degradation is acceptable. This system exhibits advantages over the active system in the areas of cost and reliability.

The difference in PSD alleviation for the two systems, despite the similarity in rms values, results from the power peaking at active system servo frequencies. Thus, more high frequency loading is exhibited with the active system.

2

RECOMMENDATIONS

It is recommended that either the normal acceleration feedback system controlling flaps and elevators or the variable sweep wing concept be incorporated in vehicles intended for low-altitude, high-subsonic-speed operation.

In order to understand better the pilot fatigue problem, it is recommended that additional and detailed study be given to the problem of pilot tolerance and endurance with complex vibration spectra.

Because of the many possible variations in the highly ranked variable sweep system, it is recommended that a thorough study be conducted of this concept exclusively.

It is likely that gust alleviation capability will be required in conjunction with automatic terrain following (ATF) for low-altitude, high-speed (LAHS) penetration missions. Active alleviation system-ATF compatibility should be explored.

The simulated gust system as discussed in this report provides the highest degree of theoretical capability. It is recommended that adaptive control approaches be investigated to eliminate the critical dependence of this system on aircraft and system parameter variations. Such a solution may well provide alleviation to such a degree as to warrant the added system complexity.

It is recommended that investigators and contractors proposing stability augmentation systems or autopilots utilizing normal acceleration feedback examine their particular configurations for alleviation capability along the lines detailed in this report.

INTRODUCTION

Aircraft penetration of enemy defenses and territory can be considerably enhanced by flight at high speeds and minimum altitudes. High speed and the natural masking afforded by the terrain and earth curvature significantly decrease the probability of detection and the probability of kill. The LAHS flight, however, results in a greatly increased probability of clobber and possible degradation in pilot and equipment performance. The increased mental stress of precision flight, the greater acceleration levels resulting from terrain following maneuvers, and the higher turbulence levels encountered at lower altitudes, all contribute to performance degradation. Thus, the probability of success of an LAHS mission is influenced by the aircraft sensitivity to turbulence or gusts.

A vehicle designed primarily for low gust sensitivity normally results in sacrifices of performance and maneuverability at low dynamic pressures. The parameters of aircraft design which effect a low gust sensitivity will be discussed. LAHS missions cannot tolerate gust alleviation through aircraft velocity reduction or weather detection-course changing techniques, both of which prove effective in commercial aircraft or for less critical military missions. Consequently, some sort of gust alleviation system or device that can be incorporated into the basic design becomes desirable.

In this connection, the subject study contract was awarded by the U. S. Army Transportation Research Command to Autonetics. The purpose of the study was to provide the Army with a realistic appraisal of the capabilities of known gust alleviation systems and to determine the feasibility of utilizing these systems in future Army aircraft intended for sustained low level, high-subsonic-speed operation.

STUDY APPROACH

STUDY BASE

The problem of gust alleviation has been approached in many ways, varying even as to the means of measurement of the ability of an alleviation system to perform its design function. The necessity of an adequate study base is obvious, particularly when study approaches have varied as widely as have gust alleviation efforts. Establishment of a suitable study base included definition of the gust alleviation problem, formulation of an alleviation system list, description of atmospheric turbulence, establishment of evaluation criteria, definition of aircraft, and formulation of an analysis plan.

THE ALLEVIATION PROBLEM

Gust alleviation is defined as a reduction in turbulence-induced loading. The alleviation problem of concern to the subject study was that of the vehicle response in the longitudinal plane of motion to vertical gust disturbances. This restriction is based on the following assumptions:

1. Vehicle longitudinal and lateral dynamics may be considered separately.

2. Turbulence may be separated into vertical, lateral, and fore-aft components.

3. Fore-aft and lateral gust components are less significant since the largest vehicle surface area is exposed to the vertical gust component.

4. Lateral motion resulting from vertical gusts can be neglected if the wing span is small compared to the scale of turbulence.

The normal acceleration response to vertical gust disturbance is defined in terms of root mean square (rms) values as the gust sensitivity, $\mathcal{S}$, given by

$$\mathcal{S} = \frac{\sigma_{N_Z}}{\sigma_{w_g}} = \frac{\rho U\, C_{L\alpha}}{2\, W/S}\, K_o \tag{1}$$

5

where

$^{0}N_Z$ is the rms value of normal acceleration - g's

σ_{w_g} is the rms vertical gust velocity - feet per second

ρ is air density - slugs per cubic foot

U is aircraft forward velocity - feet per second

C_{L_α} is aircraft lift-curve slope - per radian

W/S is aircraft wing loading - pounds per square foot

K_o is a function of the turbulence spectrum and the aircraft dynamic response (primarily, short-period frequency and damping and, to a lesser degree, structural modes and phugoid motion). Changes in ρ, U, C_{L_α}, or W/S also affect K_o but result in a less significant alteration of $\mathcal{I}$ through this parameter.

The object of gust alleviation is to provide a reduction in $\mathcal{I}$ through alteration of one or more of these parameters. Reduction in aircraft velocity or increase in altitude (decrease in air density) is seen to provide a measure of alleviation. An aircraft with low C_{L_α} or high wing loading is necessarily less sensitive to gusts.

SYSTEMS

Through the Autonetics library, a survey of available literature was conducted on the subject of gust alleviation (reference 48). The systems found in the resulting reports were considered as being in one of two categories: active systems and passive systems.

Active systems are those systems using the elements of feedback control to alter the gust response of the vehicle. They are characterized by the employment of wind flow and/or inertial sensors and of electronic or mechanical feedback devices which activate aircraft control surfaces. The systems falling into this category can be classified as follows:

1. Autopilot, stability augmentation system (SAS), or pitch damper

2. Normal acceleration system

3. Angle-of-attack system

4. Combinations of the above

5. Simulated gust system

6. Miscellaneous techniques

Active systems are designed to alter the dynamic response or to provide an additive or multiplicative term to equation (1). These systems and the analysis of each are discussed in detail in Appendix IV.

Passive gust alleviation systems are those systems which provide reduction of the turbulence-induced loading through an airborne reconfiguration of vehicle geometry or by use of an auxiliary device. No sensing device is used to actuate the alleviator. Proposed techniques for providing passive alleviation include:

1. Folding wing

2. Telescoping wing

3. Variable sweep wing

4. Free-floating surfaces

5. Deflectors and spoilers

6. Miscellaneous techniques

Passive alleviation systems are designed to provide sensitivity reduction through decreases in lift-curve slope, C_{L_α}, or increases in wing loading, W/S. Description and analyses of these systems are provided in Appendix V.

TURBULENCE

The description of turbulence must realistically reflect the results of atmospheric research, must be compatible with the low-altitude mission, and must be capable of mathematical representation.

The random gust component can be characterized statistically by the power spectral or mean square density. Because extensive atmospheric research in recent years has contributed to a reliable representation of this quantity, a statistical approach to the definition of turbulence is desirable.

Among the most comprehensive analyses of low altitude atmospheric turbulence are those discussed in references 35 and 39. The power spectral density as provided in reference 35 and employed in this study is given by

$$\phi_{w_g}(\Omega) = \sigma_{w_g}^2 \frac{L(1 + 3\Omega^2 L^2)}{\pi(1 + \Omega^2 L^2)^2} \qquad (2)$$

where

L is the turbulence length - feet

Ω is a reduced frequency equal to $\frac{\omega}{U}$ - radians per foot

σ_{w_g} is the rms gust velocity - feet per second

Details of the turbulence description, including cumulative probability distributions of rms gust velocities, are given in Appendix I.

CRITERIA

The primary function of any gust alleviation system is to reduce the loads on the aircraft and to provide a less fatiguing ride. A system designed to perform this function necessarily introduces considerations other than the direct ability to alleviate, and feasibility criteria must encompass these factors.

Established criteria, as discussed in detail in Appendix II, consider both the sensitivity function, $\mathcal{J}$, and the frequency content of the acceleration power spectrum. The effects on pilot tolerance and endurance are determined and criteria are established in these areas. Systems are evaluated as to effects on aircraft performance, stability, and control. Structural effects are considered. Weight, cost, and reliability figures are calculated. Features or side effects peculiar to a particular system or group of systems are discussed.

No attempt is made to establish numerical evaluation functions or to place a relative importance factor on each criterion, since overall system and cost effectiveness are dependent largely on operational analyses and considerations of military requirements not within the scope of this effort. Any attempt by the contractor to provide numerical weighting to the evaluation process could prove to be misleading.

AIRCRAFT

A practical evaluation of gust alleviation concepts can best be accomplished on a comparative basis for a typical aircraft design. An aircraft designed to perform an LAHS surveillance mission was used to provide the basis for such a comparison.

The aircraft, termed the base-point airplane (BPA), is a two-man, two-engine, 18,000-pound vehicle. Its primary mission consists of cruise to and from the surveillance site at 0.4 Mach and 500-foot altitude for an approximately 300-nautical-mile radius, and dash at the site at 0.9 Mach and 500 feet for 20 minutes. The aircraft design is detailed in Appendix III.

ANALYSIS

Following the definition of the BPA, three degrees-of-freedom, rigid-body aerodynamic equations of motion were written as detailed in Appendix VI. Coefficients were calculated for the low-altitude condition over the velocity range from 0.4 Mach to 0.9 Mach. Flexibility equations also were determined, but investigation of structural modes was limited. Results of the literature search were tabulated, and a system study list was compiled.

Active systems were optimized for the BPA through the use of digital computer programming, analogue simulation, and determinant expansion and root locus (reference 44) analytical techniques. Passive systems were applied to the BPA, and corresponding aerodynamic parameters were calculated. An available IBM 7090 digital computer program was modified and allowed determination of the load spectra and sensitivity for the BPA over the velocity range. For the analogue simulation, magnetic tapes of the turbulence input were transcribed for various aircraft velocities. This was done by using a Gaussian noise generator and a filter corresponding to the characteristics of the turbulence spectrum. A diagram of the circuit mechanization used for analogue simulation is shown in Appendix VII.

As each system was investigated, calculations, computer programs, and simulation allowed evaluation in the areas of alleviation capability, pilot tolerance and endurance, performance, stability, and control. Mechanization studies of each system determined the relative weight, cost, and reliability of each system and allowed evaluation from maintainability and fail-safety standpoints.

9

STUDY RESULTS

SYSTEMS

The analyses and evaluation of the various alleviation schemes are detailed in Appendix IV, Active Systems, and Appendix V, Passive Systems. The results are summarized in the following text.

Table 1 lists the most promising systems, gives the system type, references reports of investigations concerning each, and briefly describes the system technique. The five systems noted in Table 1 showed enough promise to be worthy of complete investigation.

The systems which were eliminated from detailed investigation for one reason or another are listed in Table 2. The table again gives the system type, references, and characteristics. Reasons for elimination are noted.

PERFORMANCE

Some of the study results in the area of aircraft performance are described in Table 3. Only the systems studied to completion are listed. These are the normal acceleration system (N_Z), angle-of-attack system (α), telescoping wing (TW), folding wing (FW), and variable sweep wing (VS). The angle-of-attack system should not be confused with the simulated gust system, which was eliminated as shown in Table 2. The former uses an angle-of-attack sensor only, while the latter, when employing this sensor, uses it in combination with inertial sensors in an attempt to "measure" the gust.

Effects on aircraft range, takeoff distance, stability, controllability, and structural conditions are noted in Table 3. Note that the active systems (N_Z and α) are similar in that they exhibit a relatively minor effect on aircraft range but greatly affect stability and control of the vehicle.

The acceleration system can operate over a range of flight conditions with the use of stability augmentation and a control stick pickoff in conjunction with an artificial stick feel system. The feel system is a desirable feature in any event. The angle-of-attack system operates adequately only over a very limited range of conditions even with SAS and control considerations. A high degree of system sophistication may be capable of overcoming the stability and control drawbacks of this system, but with the

10

BLANK PAGE

Table 1. Systems Analyzed to Completion

System	Notation	Type	References	Characteristics
Normal acceleration	N_z	Active	25, 29, 34, 46	Utilizes signal from normal accelerometer to control flaps and elevators in attempt to directly counteract lift and balance moment
Angle-of-attack	α	Active	7, 25, 29, 34, 46	Utilizes signal from nose-mounted vane or probe to control flaps and elevators in attempt to directly counteract lift and balance moment
Telescoping wing	TW	Passive	21	*Utilizes retraction of outboard portion of wing into inboard section in attempt to increase wing loading and decrease lift-curve slope
Folding wing	FW	Passive	6, 38	*Utilizes folding of outboard portion of wing in attempt to increase wing loading and decrease lift-curve slope
Variable sweep wing	VS	Passive	1, 36	*Utilizes change in wing sweep in attempt to reduce lift-curve slope

*Lift-curve slope defined as change in lift coefficient due to change in angle of attack

11

Table 2. Systems Not Analyzed to Completion

System	Notation	Type	References	Characteristics	Reason for Elimination
Autopilots, stability augmentation systems and pitch dampers	SAS	Active	8	Utilizes signal from pitch rate gyro to control elevators and improve stability; also may use acceleration control; autopilots include relief and guidance modes	Little alleviation capability
Flap controllers	FC	Active	46, 49	Utilizes signal from normal accelerometer or angle-of-attack sensor to control flaps in attempt to counteract lift	Flap-induced moment destabilizing; little alleviation capability
Simulated gust	α_{g_s}	Active	5, 28	Utilizes vane or probe and/or inertial sensors in combination so as to "measure" or simulate gust signal and control flaps and elevators in attempt to reduce lift	System parameters are extremely critical functions of aircraft and environment - more complexity than required - requires relatively unreliable air data measurement

12

Table 2. (Cont)

System	Notation	Type	References	Characteristics	Reason for Elimination
Free-floating surfaces	FF	Passive	26	Allows portion of wing to move freely with air mass in attempt to increase wing loading - either chordwise or spanwise hinge	Chordwise - little alleviation capability; spanwise - potential less than that of folding wing; possible wing tip flutter
Spoilers and deflectors	S&D	Passive	9, 10, 11, 12	Projection into air mass in attempt to spoil flow and reduce lift-curve slope	Severe drag penalty
Alleviation airplane	AA	Active and Passive	23	Utilizes free floating surfaces in conjunction with angle-of-attack sensor to control flaps and elevators	Highly complex system with extreme weight penalty; difficult to interpret and evaluate with limited information available
Flexible wing spar	FS	Active	3, 15, 42	Utilizes flap or aileron geared to wing bending in attempt to reduce lift	Little alleviation capability, possible structural instability

13

Table 2. (Cont)

System	Notation	Type	References	Characteristics	Reason for Elimination
Wing slots	WS	Passive	19, 20, 42	Slot in wing is used for pressure equalization to reduce lift-curve slope	Little alleviation
Airjet spoilers	AS	Passive	19, 20	Utilizes ejection of air to spoil flow and reduce lift-curve slope	Severe drag penalty; complex nozzle and ducting requirements; appreciable power requirement
Optimization techniques	OT	Active	43	Derivation of sensors and signals to control lift and moment devices in optimum fashion	Results in simulated gust system at best; highly theoretical assumptions

Table 3. Performance Results

System	Aircraft Range*	Takeoff Distance	Stability	Control	Structural Effects
N_z	Decrease of less than 3 percent due to added weight and flap motion	No effect	Stability augmentation required, good stability achievable over range of flight conditions	Adequate controllability achievable if artificial stick feel system is available (g's proportional to stick force), stick force pickoff signal can be shaped and used as reference for alleviation signal	Possibility of structural mode excitation exists, requires judicious choice of sensor location and possible filtering, 60 pounds additional wing weight required to allow flap motion
q	Decrease of less than 3 percent due to added weight and flap motion	No effect	Inherent stabilization problem, adequate stability not readily achievable over range of flight conditions even with augmentation, good at any one chosen flight condition with SAS	Adequate controllability not achievable over range of flight conditions, without complex network variation with air data, can be good at any one chosen condition with rate gyro and/or stick pickoff	Possibility of structural mode excitation exists, requires judicious choice of sensor location and possible filtering, 60 pounds additional wing weight required to allow flap motion
TW	Decrease of 32 percent with wings extended during cruise and telescoped for dash - weight and drag considered	No effect	Little effect on longitudinal stability, lateral characteristics altered, use same SAS as BPA	Little effect	Little effect
FW	Decrease of 21 percent with wings extended during cruise and folded for dash - weight and drag considered	No effect	Little effect on longitudinal stability, lateral characteristics altered, use same SAS as BPA	Little effect	Little effect
VS	Decrease of 9 to 22 percent (depending on configuration) with wings unswept, during cruise and swept for dash - weight and drag considered	Possibility of 17 percent reduction - from 2000 feet to 1665 feet	Little effect, use SAS as BPA	Little effect	Reduction of accelerations due to flexibility; swept wing is stabilizing to structural modes

*Range calculations based on maintaining same vehicle gross weight as BPA; system incorporation results in decrease in available fuel.

following results: Improvement in stability would be accomplished with some sacrifice of alleviation capability, and improved controllability can be accomplished only with the type of sophistication that places this system in the simulated gust system category (see Table 2).

The passive systems (TW, FW, and VS) all result in a significant decrease in aircraft range, even with cruise in the unalleviated configuration. A variable-sweep configuration provides the capability for reduction of takeoff distance.

Active systems present the possibility of vehicle flexibility mode excitation. Choice of sensor location is dependent on the structural mode shapes, and proper location is required to avoid mode excitation. This consideration would likely result in slightly less alleviation of the rigid airframe response than that available with a sensor located at the center of gravity. Electronic body-bending filters also may be employed to ease the problem. Passive systems have little effect on the structural modes, with the exception of VS, which in the swept position tends to reduce structural vibrations.

ALLEVIATION

The alleviation capabilities of each system are illustrated in Table 4. Active systems exhibit a greater reduction in loading at the short-period frequency, (lowering at the power spectral density peak) but suffer from a notable increase at higher servo mode frequencies. The result is that active and passive systems provide comparable alleviation from a root mean square standpoint. The possibility of structural mode excitation arises from the higher frequency content exhibited by active system use.

Because the servos employed by active systems to actuate the flaps are nonlinear devices with limited rate of motion, the alleviation capabilities of these systems depend to some extent on the gust intensity. The quoted values are obtainable with realistic servos at gust velocities well into the thunderstorm category.

Active system employment affects the vehicle short-period response to such an extent that proper assessment of alleviation capability must include examination with stability augmentation incorporated. Hence, the alleviation values given in Table 4 for active systems are those with augmentation. The effects of passive system incorporation on stability are slight enough that evaluation with augmentation is not required. SAS is necessary to meet military stability specifications whether gust alleviation is incorporated or not.

16

BLANK PAGE

Table 4. Alleviation Capabilities

System	Sensitivity* Cruise CG	Sensitivity* Cruise Pilot	Sensitivity* Dash CG	Sensitivity* Dash Pilot	Percent Alleviation Based on rms Values Cruise CG	Cruise Pilot	Dash CG	Dash Pilot	Percent** Alleviation Based on PSD Peak	Probable Endurance *** (Minutes) Time to Reduced Efficiency Cruise	Dash	Time to Become Intolerable Cruise	Dash	Comments
BPA	0.022	0.020	0.054	0.051	0	0	0	0	0	32	1	140	8	
N_Z	0.018	0.015	0.037	0.030	18	25	31	41	77	96	3	220	56	Alleviation figures are those with SAS included and are accurate to thunderstorm-turbulence range. high frequency vibrations (servo frequencies) more prevalent
q	0.010	0.008	0.031	0.028	54	60	43	45	81	Pilot Outlasts Fuel	5	Pilot Outlasts Fuel	68	Alleviation figures are those with SAS included and are accurate to thunderstorm turbulence range. high-frequency vibrations prevalent but less than N_Z system
TW	0.014	0.013	0.032	0.030	36	35	41	41	49	150	3	260	56	Alleviation figures obtained without SAS, inclusion of SAS results in negligible effect on alleviation
FW	0.016	0.015	0.040	0.037	27	29	26	27	35	96	1	220	30	Alleviation figures obtained without SAS, inclusion of SAS results in negligible effect on alleviation
VS	≤0.016	≤0.014	0.041 to 0.033	0.037 to 0.030	≥27	≥30	24 to 38	27 to 42	40 to 50	120	< 1 to 3	240	30 to 56	Alleviation figures obtained without SAS, inclusion of SAS results in negligible effect on alleviation, quoted values dependent on final swept-wing configuration

*Calculations based on rigid heavy weight vehicle (full fuel load) at 5-percent static margin system optimised to dash condition

**Based on peak value of acceleration power spectra at pilot station, heavy weight vehicle, dash condition

***Based on criteria in Appendix II with mean weight vehicle (half-fuel load) and gust velocity of 7 feet per second (0.99 cumulative probability)

17

Alleviation capability is interpreted in Table 4 in terms of the endurance criterion given in Appendix II using gust intensity with 99-percent probability of occurrence. Note that the cruise portion of the mission requires little in the way of alleviation for operation at normal proficiency; all systems listed are capable of providing the required alleviation. On the other hand, none of the systems permits operation of the dash portion of the mission (20 minutes) at normal proficiency. All, however, allow dash at a tolerable level.

EQUIPMENT

From an equipment standpoint, as summarized in Table 5, it is seen that active systems generally are of lighter weight, while passive systems are more reliable. The weight of a thick wing VS compares favorably to that of an active system. The higher reliability of passive systems arises primarily because of their limited use. Operation of the system mechanism is required only for reconfiguration, which would most likely occur two times per flight. Active system operation is necessarily continuous.

System production costs are not separable by system category. System cost would be on the order of 0.5 to 2.5 percent of vehicle cost. Active system costs are capable of reduction through integration with the autopilot.

Maintenance of either type of system is determined primarily by the hydraulic and mechanical systems. Active systems appear to offer an advantage in this area, particularly when electronic packaging is integrated with the autopilot.

Fail-safety problems would require more design attention in an active system, where failure monitoring would be required.

CONCLUSIONS

Recommendation of a gust alleviation system for incorporation into future vehicles is approached best through a process of elimination. The systems of Table 2 are eliminated by virtue of the reasons cited. Of the remaining systems, both the telescoping (TW) and folding wing (FW) versions must be regarded as requiring too great a sacrifice in range capability because of the additional weight.

System choice thus is limited to consideration of three systems: N_z, α, and VS. Only the normal acceleration system is capable of providing significant alleviation over a range of flight conditions without severe

BLANK PAGE

Table 5. Equipment Summary

System	Weight Penalty (Pounds)	*Estimated Production Cost	Mean Time Before Failure (Flight Hours)	Comments
N_Z (non-redundant)	98	1.011	1,270	Reliability includes SAS since operation is dependent on SAS; cost can be reduced through integration with autopilot or SAS; maintenance except for servos is negligible with integrated packaging; monitoring of flap to elevator deflection ratio and limited authority flap servos required for fail safety
N_Z (Triple unit redundant)	105	1.020	870,000	
α (non-redundant)	106	1.011	1,270	Reliability includes SAS since operation is dependent on SAS; same as above except for angle-of-attack sensor which requires additional purchase, packaging, and maintenance even with autopilot integration; ability to provide pilot control not included in cost
α (Triple unit redundant)	112	1.021	870,000	
TW	1,200	1.023	3,200,000	Failure probability assumes operation twice per flight, no failure in tracks or bearings, and therefore may be slightly optimistic; tracks and bearings may require significant amount of maintenance attention
FW	630	1.005	3,200,000	Failure probability assumes operation twice per flight

Table 5. (Cont)

System	Weight Penalty (Pounds)	Production Cost	Mean Time Before Failure (Flight Hours)	Comments
VS	115 to 860	1.012 to 1.016	4,000,000	Light weight and low cost is for thick wing vehicle. Failure probability assumes no failure in the tracks or bearings, and therefore may be slightly optimistic. Tracks and bearings may require significant amount of maintenance attention.

*Costs for 200 production units normalized to BPA; BPA cost in neighborhood of $1,000,000; costs do not include SAS but assume SAS provided

BLANK PAGE

degradation in performance. While an angle-of-attack system offers better alleviation over the flight regime, the stability and control problems associated with its incorporation are such as to deter practical application. A variable sweep system also offers good alleviation over the flight range, but sweeping of the wings during cruise results in a severe range penalty due to a large increase in induced drag. Thus, if alleviation is desirable over a range of flight conditions, the normal acceleration system is the most feasible

On the other hand, alleviation only at high speeds may be considered acceptable. In this case all three systems are feasible, but further considerations may be taken into account as follows. First, the angle-of-attack system offers slightly better alleviation than any other system. The only disadvantage of the VS system is its effect on system range, which the study shows may be as little as 9 percent with a thick wing. The variable sweep system, in addition to meeting the requirements for alleviation at high speed, would still allow use of the system at low speed if necessary, a capability not provided by the angle-of-attack system. Though the range degradation would still be great, the cruise alleviation capability would always be present and particular mission requirements would dictate the extent of use. The acceleration system is still preferable to an angle-of-attack system for the same reason. The VS system is most feasible from cost and reliability standpoints.

In summary, the recommendation of this report is that either the normal acceleration system or the variable sweep system be considered for incorporation into future LAHS vehicles. The acceleration system should be utilized if alleviation is desirable over a range of flight conditions and/or if a 9 percent range degradation is acceptable. Cost and reliability figures would indicate a preference for the VS system. Detailed study of variable sweep designs may also show that reduction of the calculated range degradation is possible.

To consider whether it would be appropriate to alleviate only during the dash portion of the mission, it is important to note that the cruise portion of the mission can be accomplished at normal proficiency with no alleviation approximately 87 percent of the time (based on mean weight vehicle and RB-66 turbulence probability data). However, though the chosen mission consists of 2.5 hours of cruise and 20 minutes of dash, the total fuel allows more than 5 hours of cruise with no dash. For this reason, it may be preferable to provide cruise alleviation capability and consequent mission versatility.

BIBLIOGRAPHY

1. "Aerodynamic Design Manual," North American Aviation, Inc.,
    Columbus, Ohio.

2. A'Harrah, R. C., and Schulze, R. P., "An Investigation of Low-
    Altitude High Speed Flying and Riding Qualities of Aircraft,"
    Report No. NA 62H-397, NAA, Columbus, Ohio (not dated).

3. "An Analysis of the Effectiveness of a Gust Alleviating Device,"
    Aircraft Laboratory RDO No. 451-374 (ASTIA AD-50757), Wright
    Air Development Center, Dayton, Ohio, 1 July 1953.

4. "Annotated Bibliography of Literature Concerning Gust Alleviation
    Techniques, Low-Altitude Atmospheric Turbulence, and Related
    Topics," EM-1163-104, Autonetics, Anaheim, Calif., 14 February
    1963.

5. "Bending Suppression and Gust Alleviation Concept Study (Pro-
    posal)," EM-0363-258, Autonetics, DSD, Anaheim, Calif.,
    4 September 1962.

6. Blackaby, J. R., "Wind Tunnel Investigation at Low Speed of a
    Wing Having 63° Sweepback and a Dropped Tip," RM A55B14,
    NACA Washington, D. C., April 1955.

7. Cooney, T. V., and Schott, Russell L., "Initial Results of a Flight
    Investigation of the Wing and Tail Loads on an Airplane Equipped
    With a Vane-Controlled Gust-Alleviation System," TN 3746, NACA,
    Washington, D. C., 1956.

8. Crabill, N. A., An Analytical Investigation of the Gust-Alleviating
    Properties of a Simple Pitch Damper, TN 4173, NACA, Washing-
    ton, D. C., December 1957.

9. Croom, D. R., Shufflebarger, C. C., and Huffman, J. K., "Investi-
    gation of Forward-Located Fixed Spoilers and Deflectors as Gust
    Alleviators on an Unswept-Wing Model," TN 3705, NACA, Wash-
    ington, D. C., June 1956.

10. Croom, D. R., and Huffman, J. K., "Investigation at Transonic
    Speeds of Deflectors and Spoilers as Gust Alleviators on a 35° Swept
    Wing," TN 4006, NACA, Washington, D. C., June 1957.

11.   Croom, D. R., and Huffman, J. K., "Investigation at Low Speeds of Deflectors and Spoilers as Gust Alleviators on a Model of the Bell X-5 Airplane with 35° Swept Wings on a High-Aspect Ratio 35° Swept-Wing-Fuselage Model," TN 4057, NACA, Washington, D. C., June 1957.

12.   Croom, D. R., and Huffman, J. K., "Investigation of Deflectors as Gust Alleviators on a 0.09 Scale Model of the Bell X-5 Airplane With Various Wing Sweep Angles from 20° to 60° at Mach Numbers From 0.40 to 0.90," TN 4175, NACA, Washington, D. C., November 1957.

13.   DeYoung, J., "Theoretical Symmetric Span Loading Due to Flap Deflection for Wings of Arbitrary Plan Form at Subsonic Speeds," Report 1071, NACA, Washington, D. C., 1951.

14.   DeYoung, J., and Harper, C. W., "Theoretical Symmetric Span Loading at Subsonic Speeds for Wings Having Arbitrary Plan Form," Report 921, NACA, Washington, D. C., 1948.

15.   "Dynamic Analyses for the C-47 Airplane Gust Load Alleviation System," Report No. SM-14456, Douglas Aircraft Division, Santa Monica, Calif., 29 July 1952.

16.   Escobosa, A. S., "Unit Redundant Scheme for Higher Control System Reliability," IRE Proceedings of the 6th National Convention on Military Electronics, IRE, New York, N. Y., 1962.

17.   Fischel, J., and Vogler, R. D., "High Lift and Lateral Control Characteristics of an NACA 652-215 Semispan Wing Equipped With Plug and Retractable Ailerons and a Full-Span Slotted Flap," TN 1872, NACA, Washington, D. C., 1949.

18.   "Flying Qualities of Piloted Airplanes," Military Specification MIL-F-8785, NACA, Washington, D. C., 1 September 1954, Amended 17 April 1959.

19.   "Gust Alleviation Study, Part I, Estimation of the Control Derivatives for Flaps, Spoilers, and Other Control Devices Intended for Use as Gust Alleviators," WADC Tech. Report 57-750, Part 1 (ASTIA AD 2081-143), Fluidyne Engineering Corp., WADC, Dayton, Ohio, January 1958.

20. "Gust Alleviation Study, Part III, Prediction of the Alleviation of Gust Loads on a Rigid Restrained Wing, Utilizing Wing Installed Alleviator Devices," WADC Tech. Report 57-750 (ASTIA AD-2081-145), Part III, Fluidyne Engineering Corp., WADC, Dayton, Ohio, January 1958.

21. Hanna, R. H., "A Wind Tunnel Investigation of the Low-Speed Characteristics of a Telescoping Variable Area Wing," Report No. NA 62H-303, North American Aviation, Inc., Columbus, Ohio, 1 May 1962.

22. Harshe, M. L., "Summary Report on the VAX Parametric Design Study," Report NA 62H-15, North American Aviation, Inc., Columbus, Ohio, 15 January 1962.

23. Hirsch, Rene', "Etudes Et Essais D'un Avion Absorbeur De Rafales" (Studies and Tests on a Plane Which Absorbs Strong Wind Gusts), DOCAERO No. 42, France, January 1957.

24. Hoener, S. F., "Fluid Dynamic Drag," Published by the Author, Midland Park, New Jersey, 1958.

25. Hunter, Paul A., Kraft, Christopher C. Jr., and Alford, William L., "A Flight Investigation of an Automatic Gust-Alleviation System in a Transport Airplane," NASA TN D-532, NASA, Washington, D.C., 1961.

26. Jaquet, B. M., Queijo, M. J., and Lichtenstein, J. H., "Low-Speed Static Longitudinal Stability and Control Characteristics of a 60° Triangular-Wing Model Having Half-Delta Tip Controls, RM L51D20a, NACA, Washington, D.C., 27 June 1951.

27. Johnson, J. M., Jr., and Andrew, G. M., "A Preliminary Gust Alleviation Study for the Mohawk Aircraft (YAD-1)," NAA Report, No Number, (Not Dated).

28. Johnson, J. M., Jr., Andrew, G. M., and Olshausen, R., "Gust Alleviation Study for the B-70 Aircraft," NAA TM 3441-12-50, Autonetics, Anaheim, Calif.

29. Kraft, Christopher C. Jr., "Initial Results of a Flight Investigation of a Gust Alleviation System," NACA TN 3612, NACA, Washington, D.C., 1956.

30. "Low Speed Wind Tunnel Tests of a 0.20 Scale Model of the T2J-1 Airplane to Investigate Various Wing Fences and Fail Configurations, and to Determine the General Stability and Control Characteristics," Report NA57-612, North American Aviation, Inc., Columbus, Ohio, 4 December 1957.

31. McCullough, J. K., "Drag-Due-To-Lift of Thick, Cambered Wings," Aero-Thermo R&D Group Technical Note 62-1, North American Aviation, Inc., Columbus, Ohio, 23 February 1962.

32. Nelson, W. H., and Erickson, A. L., "The Effect of Aspect Ratio on the Subsonic Aerodynamic Characteristics of Wings with NACA 65-210 Sections," RM A9K18, NACA, Washington, D. C., February, 1960.

33. Perkins, C. D., and Hage, R. E., "Airplane Performance, Stability, and Control," Wiley & Sons, Inc., New York, N. Y., 1960.

34. Phillips, William H., and Kraft, Christopher C. Jr., "Theoretical Study of Some Methods for Increasing the Smoothness of Flight Through Rough Air," NACA TN 2416, NACA, Washington, D. C., 1951.

35. Press, H., Meadows, M. T., and Hadlock, I., "A Re-Evaluation of Data on Atmospheric Turbulense and Airplane Gust Loads for Application in Spectral Calculations," TR-1272, NACA, Washington, D. C., 1956.

36. Report No. RM-1188, Rand Corp., Santa Monica, Calif.

37. "Report of Test Project No. AVN 4860, 1/16 Phase III of Man Machine Environment Capability Studies and Test in Support of Surveillance Aircraft Development," U. S. Army Aviation Board, Ft. Rucker, Ala., 28 May 1962.

38. Riley, D. R., "Wind-Tunnel Investigation and Analysis of the Effects of End Plates on the Aerodynamic Characteristics of an Unswept Wing," TN-2440, NACA, Washington, D. C., August 1951.

39. Saunders, K. D., "B-66B Low Level Gust Study," WADD Technical Report 60,305, WADC, Dayton, Ohio, March 1961.

40. Schwartzberg, M. A., and Burch, J. L., "Lifting Capabilities of Wings With and Without High-Lift Devices," Report No. 8055, Martin Engineering, Martin Marietta Corp., Baltimore, Md., April 1956.

41. Sivells, J. C., and Spooner, S. H., "Investigation in the Langley 19-Foot Pressure Tunnel of Two Wings of NACA 65-210 and 64-210 Airfoil Sections With Various Type Flaps," TN 1579, NACA, Washington, D. C., May 1948.

42. "Some Aerodynamic Aspects of Gust Load Alleviation," Report No. SM-14819, (ASTIA AD-6509), Douglas Aircraft Co., Santa Monica, Calif., June 1953.

43. Toback, Murray, "On The Minimization of Airplane Responses to Random Gusts," TN 3290, NACA, Washington, D. C., 1957.

44. Truxal, John G., "Control Engineer's Handbook," McGraw-Hill Book Company, New York, N. Y., 1958.

45. USAF Stability and Control Handbook, October 1960.

46. Watt, W. G., and Nishimi, J. T., "CESSNA 310 Gust Alleviation Study," NAA IOL 60-3441-64-FCS-46, Autonetics, Anaheim, Calif., 8 December 1960.

47. Whelde, G., "Study of the Random Motion of the KC-135 Airplane in Atmospheric Turbulence," Document No. D6-3451, Boeing Airplane Company Transport Division, Seattle, Wash., 17 December 1962.

48. Young, A. D., and Hufton, P. A., "Note on the Lift and Profile Drag Effects of Split and Slotted Flaps," R&M 2545, British Aeronautical Research Council, England, September, 1941.

49. Zbrozek, J. K., "Theoretical Analysis of a Gust Alleviator Used on a Lancaster Aircraft and Comparison With Experiment," Royal Air craft, Establishment (Barnborough) Report No. Aero. 2654 (ASTIA AD-255240), Ministry of Aviation, London, England, January 1961.

APPENDIX I. TURBULENCE

DEFINITION

During recent years, several analyses have been conducted regarding turbulence spectra and the probability of encounter of various types of atmospheric disturbances. Among the most comprehensive are those discussed in references 35 and 39. The results indicate that random gusts can be characterized by relatively simple analytical functions.

The power spectral or mean square density, as provided by reference 35 and employed in this study, is

$$\phi_{w_g}(\Omega) = \sigma_{w_g}^2 \; \frac{L(1 + 3\Omega^2 L^2)}{\pi (1 + \Omega^2 L^2)^2} \tag{3}$$

where

Ω is a reduced frequency, $\dfrac{\omega}{U}$ - radians per foot

U is the aircraft forward velocity - feet per second

L is the turbulence length, proportional to the average eddy size - feet

σ_{w_g} is the root-mean-square gust velocity - feet per second

This expression was chosen because it had been used extensively in the past at Autonetics and since IBM 7090 digital computer programs had been developed for its use. A detailed mathematical description of this turbulence representation is presented in reference 35. The spectrum of reference 39 differs from the chosen one only in that slightly more power is evidenced at high frequencies. An analogue representation of this spectrum would correspond to that of reference 35 as shown in Figure 1.

A value of 1000 feet was chosen as a representative turbulence length for analysis, as suggested by reference 35. Smaller values of L, of course, result in higher gust corner frequencies and a slight increase in gust sensitivity. No loss of generality occurs with the choice of the turbulence length.

Atmospheric turbulence in-the-large (that is, throughout the world and for all time) can be considered to be a stationary Gaussian random process. The turbulence encountered for a given time or flight is, of course, limited by the duration, flight course, and weather conditions. The turbulence history here is reduced to a nonstationary Gaussian process that varies only in intensity. Thus, for localized investigations, a root-mean-square gust velocity can be assumed. This rms value can then be considered to vary according to some cumulative probability distribution. In the subject study, both the aircraft velocity and rms gust velocity were varied discretely.

The cumulative probability distributions of gust velocities from both references are shown in Figure 2. Interpretation of the study results may be made in light of either function. An interpretation of rms gust velocities in terms of weather conditions, as given in reference 47, is also shown.

ANALOGUE SIMULATION

An analogue circuit was mechanized which filtered the output of a Gaussian noise generator according to the desired spectra and recorded it on magnetic tapes for various aircraft velocities. Use of the tapes allowed repeatability of simulation runs and direct comparison of study results. The simulation circuits are discussed and illustrated in Appendix VII.

The analogue filter transfer function used to obtain the random gust function is given as

$$F(s) = \frac{\sigma_{w_g}}{\sigma_V} \left(\frac{L}{\pi U}\right)^{1/2} \frac{1 + \sqrt{3}\frac{L}{U}s}{\left(1 + \frac{L}{U}s\right)^2} \tag{4}$$

where

s is the Laplacian operator - per second

σ_V is the root-mean-square value of Gaussian noise generator output voltage - volts

28

DIGITAL SIMULATION

Digital computer programs that utilized the turbulence spectrum were available prior to this study. Changes in and additions to the programs aided the analytical effort necessary to apply the statistical approach. The relationship used to determine power spectral density of normal acceleration as a function of gust inputs is given as

$$\Phi_{N_Z}(\omega) = \Phi_{w_g}(\omega) \left| \frac{N_Z}{w_g}(\omega) \right|^2 \tag{5}$$

where

$$\left| \frac{N_Z}{w_g}(\omega) \right| \quad \text{is the absolute value of the aircraft transfer function for normal acceleration response to gust inputs - g's per feet per second}$$

$\Phi_{w_g}(\omega)$ is the power spectral density gust representation

Digital computer determinant expansion and power spectral techniques enabled solution for both the acceleration spectra and the aircraft sensitivity.

One criterion utilized in this study considered pilot tolerances as determined by the number of exceedances per unit time of various incremental g levels. For evaluation against this criterion, the following equation, as given in reference 39, was used:

$$N = \frac{1}{2\pi} \left[\frac{\int_0^\infty \omega^2 \phi_{N_Z}(\omega) \, d\omega}{\int_0^\infty \phi_{N_Z}(\omega) \, d\omega} \right]^{1/2} e^{-N_Z^2 / \sigma_{N_Z}^2} \tag{6}$$

where

N is the number of exceedances per second

N_Z is the g level to be exceeded

$$\sigma^2_{N_Z} = \int_0^\infty \Phi_{N_Z}(\omega) \, d\omega \qquad (7)$$

The available digital computer program was expanded to include solution of this expression for various g levels.

APPENDIX II. CRITERIA

The criteria utilized for system feasibility determination are detailed in this appendix.

ALLEVIATION

The problem of gust alleviation as defined in this study is restricted to reduction of vertical accelerations. Some investigations have used a criterion consisting of minimization of pitch rate as well as acceleration (see reference 43). Quantitative information on human reactions to angular rates is scant although studies presently in progress may lead to useful conclusions in this area. Angular rates encountered in aircraft are not detrimental to equipment or structure. For these reasons the use of angular rate criteria would be unjustified.

The primary measure for determining the ability of a gust alleviation system to perform its design function is its effect on the aircraft's sensitivity to gusts.

$$\text{Sensitivity } J = \frac{\sigma_{N_Z}}{\sigma_{w_g}} \text{ in g's per feet per second} \qquad (8)$$

where

σ_{N_Z} is the root mean square value of normal acceleration - g's

σ_{w_g} is the root mean square value of vertical gust velocity - feet per second

The sensitivity may be defined at the center of gravity (cg) or at any other fuselage location. The acceleration at a body station is given by

$$N_{Z_x} = N_{Z_{cg}} - \frac{l_x}{57.3 \, g} \ddot{\theta} \qquad (9)$$

where

l_x is the distance from cg to body station - feet - positive forward

$\ddot{\theta}$ is the pitch angular acceleration - degrees per second squared

31

The normalized vertical acceleration power spectral density peak also is used as a measure of alleviation. Alleviation based on this measure can differ markedly from that based on rms values. Therefore, care must be taken in evaluating quoted alleviation results. For example, examination of reference 27 indicates 91-percent alleviation using PSD peak values, and 75 percent based on rms values, as obtained for the Mohawk YAO-1.

Sensitivity values given in this report are based on a heavy weight rigid vehicle with 5 percent static margin unless otherwise noted. Percentage of alleviation used herein, unless otherwise noted, is defined as

$$\text{Percent A} = 100 \left(1 - \frac{\mathcal{S}_A}{\mathcal{S}_U}\right) \tag{10}$$

where

$\mathcal{S}_A$ is the sensitivity with alleviation

$\mathcal{S}_U$ is the sensitivity without alleviation

PILOT TOLERANCE AND ENDURANCE

Tolerance

Gust alleviation requirements can be interpreted in terms of human tolerance of accelerations. The best available information on human reaction to complex vibrations encountered in flight through rough air is contained in reference 37. For purposes of data analysis, this reference groups acceleration levels into several categories.

The following generalizations are made for each of the behavior categories depicted in Figure 3:

Category 1a: Smooth. No performance impairment. Lack of stimulation could produce lethargy.

Category 1b: Practically smooth. No appreciable performance impairment. Precise manipulations are performed easily and quickly.

Category 2a: Mild light. Most tasks are performed easily. Interference with precise manipulations such as writing is noticed, but is not appreciable.

32

Category 2b: Light. Effects may be bothersome at upper levels, but do not markedly interfere with the performance of most tasks. Marked interference occurs with precise tasks such as writing.

Category 3: Light to moderate. In-cockpit psychomotor coordinations suffer an increased decrement in this category, with a marked increase in time to read and adjust instruments. The task of controlling the airplane requires a considerable portion of the pilot's attention.

Category 4: Moderate. Instruments become difficult to read, and manipulations with the outstretched hand are quite difficult at the upper levels of this category. As the upper levels are approached, it becomes necessary to support the arms on the legs or brace them in some manner in order to avoid inadvertent stick movements.

Category 5: Moderate to severe. Manipulations other than those with the stick and throttle are practically impossible, and control of the aircraft requires the full attention of the pilot to the virtual exclusion of glances inside the cockpit. Pilot control of the aircraft becomes increasingly marginal.

Category 6: Severe. Pilot control is submarginal a considerable portion of the time. The pilot takes a severe physical pounding, and exposure of more than 5 to 10 minutes might result in physiological damage.

The preceding categories are determined by the number of exceedances of various acceleration levels in one second. This value for a Gaussian random process is approximated by the formula

$$N = \frac{1}{2\pi} \left[\frac{\int_0^\infty \omega^2 \phi_{N_Z}(\omega)\, d\omega}{\int_0^\infty \phi_{N_Z}(\omega)\, d\omega} \right]^{1/2} e^{-N_Z^2/\sigma_{N_Z}^2} \tag{11}$$

where

N is the number of exceedances per second

Some of the study data are interpreted in terms of this criterion to allow greater appreciation for alleviation, sensitivity, and frequency content of the resulting spectra.

The angular accelerations which contribute to the total acceleration at the pilot's fuselage station are utilized in this determination as given by equation 9. In general, the tendency is toward a reduction in the total accelerations because of the resultant pitching action of a statically stable vehicle.

Endurance

Pilot endurance of accelerations as a function of flight duration has been investigated by Cornell Aeronautical Laboratory (CAL) and the Columbus Division of North American Aviation, Inc. Figure 4 indicates the results of these studies in terms of pilot proficiency as a function of mission duration and rms g levels. The rms values indicated are based on spectra corresponding to the frequency response of a rigid airplane having a well damped short period natural frequency of about 0.8 cps.

Proper evaluation of endurance would consider the variations in vehicle velocity and the weight change due to fuel consumption. Since cumulative effects of varying g levels are not a basis for this criterion, and to avoid complication, the endurance herein is calculated on the following basis: (1) constant vehicle velocity and (2) sensitivity values based on a mean weight airplane (half fuel load). The actual sensitivity, varying inversely with weight, would be lower at the beginning of the mission and higher toward the end. The mean value gives a good indication of probable endurance.

AIRCRAFT RANGE

For a given flight speed, weight, and fuel load, the range of an aircraft is inversely proportional to the drag. The range ratio of the alleviated vehicle to the unalleviated one, assuming the same quantity of fuel, can be expressed as

$$\frac{R_A}{R_U} = \frac{(C_D S)_U}{(C_D S)_A} \tag{12}$$

For calculations of range variation resulting from any necessary structural weight changes and subsequent fuel-supply reduction, the following equation, based on the classical range determination by Breguet (reference 33), is used:

$$\frac{R_A}{R_U} = \frac{(C_D\,S)_U}{(C_D\,S)_A} \left[\frac{(W_F)_A}{(W_F)_U} \right]^{1.19} \tag{13}$$

where

W_F is the weight of the fuel.

The same initial gross weight and flight speeds are assumed.

Flight through turbulent air leads to a continual variation of aircraft flight attitude over a narrow range of angle of attack. The drag coefficients used in equations 12 and 13 should, therefore, be the rms values appropriate to the specific conditions being considered. The study results indicate that these rms values differ very little from the drag coefficient of the same configuration in flight through calm air at the same speeds. Consequently, for the purposes of range comparison, the calm air drag values have been used. For those systems which involve continual surface deflections, an rms drag increment due to the surface motion is taken into account.

STABILITY AND CONTROL

To ensure aircraft dynamic response consistent with existing requirements, it is necessary to consider vehicle stability and handling qualities. Military specifications (reference 18) require that short period damping shall be such that the normal acceleration response to a stick impulse shall damp to one-tenth amplitude in one cycle; i.e., have a damping ratio ζ greater than 0.34, for short period oscillations with periods less than 6 seconds. Normal stability augmentation and autopilot design requirements in industry are more stringent; a much-used criterion corresponding roughly to that resulting from CAL studies is shown in Figure 5. Also shown are the results of handling qualities investigations conducted at North American Aviation, Inc., Columbus Division, indicating that pilot preferences allow a much looser criterion in the higher frequency areas. Below 0.9 cps, the results agreed well with the CAL data. Above 0.9 cps, the pilot acceptance boundary was a line of constant time of one second to damp to one-tenth amplitude, independent of actual damping ratio.

The incorporation of an alleviation system should allow response within the stability requirements and not seriously degrade the rise time or steady state value of the response to stick commands.

STRUCTURAL EFFECTS

Use of a gust alleviation system may affect the vehicle aeroelastic modes and the effects on flexibility should be noted. Added airframe stress resulting from alleviation system incorporation and subsequent necessary structural weight changes are further considerations. The effects of structural vibrations on aircraft sensitivy and pilot fatigue are generally minor.

WEIGHT

The total weight penalty attributable to a gust allevation system is a consequence of (1) weight increase caused by incorporation of the system itself and (2) possible structural weight changes. It also is conceivable that a decrease in vehicle structural weight may be permissible with a reduction of the gust loads and consequent design to a lower load factor, through for this to be accomplished through use of an alleviation system would require a system that could not fail.

COST

The relative production costs for each alleviation system have been estimated. Design and development and maintainability are also discussed to allow appreciation for costs in these areas.

RELIABILITY AND FAIL-SAFETY

System reliability figures are calculated in terms of failure probability wherever possible. Equipment mechanizations are considered to take maximum advantage of state-of-the-art techniques for enhancing reliability and fail-safety. The redundancy technique used for active systems is presented in reference 16.

It should be noted that failure of the gust alleviation system need not necessarily result in mission abortion. Mission accomplishment in the absence of an alleviator would be largely a function of the immediate turbulence conditions and the ability of the particular crew to operate under these conditions.

APPENDIX III. BASE-POINT AIRPLANE

A practical evaluation of various gust alleviation concepts can be accomplished best by using a single basic vehicle designed to perform the intended mission. An aircraft called the base-point airplane (BPA), designed to perform an LAHS surveillance mission, is used to provide the basis for system comparison.

SPECIFICATIONS

The aircraft specifications for this study are defined as follows:

1   Maximum velocity at sea level - 0.9 Mach

2   Cruise velocity at 500-feet altitude - 0.4 Mach

3   Gross weight - 18,000 pounds

4   Takeoff distance over 50-foot obstacle - 2,000 feet

5   Maximum load factor - 7.33

6   Surveillance equipment weight - 1500 pounds

7   Two engines

8   Two-man crew

The primary aircraft mission requirements consist of the following:

1   Cruise to and from the surveillance site at 0.4 Mach and altitude of 500 feet for approximately 300-nautical mile radius

2   Dash at the surveillance site at 0.9 Mach and altitude of 500 feet for 20 minutes

GEOMETRY

The geometry of the BPA is illustrated in Figure 6 and listed in Table 6. The design has not been optimized since such a procedure would require an extensive study in itself. The selection of the BPA provides a reasonable, conventional design capable of a creditable job on the

37

Table 6. BPA Planform Geometry

Wing area	277.0
Aspect ratio, wing	4.0
Taper ratio	0.5
Sweep of $c/2$	0
Airfoil section	64A206
Wing span	33.3
Chord, root	11.1
Chord, tip	5.55
Chord, mean aerodynamic	8.625
Area, vertical tail	$0.15\,S_w$
Area, horizontal tail	$0.275\,S_w$
Aspect ratio, vertical tail	1.4
Aspect ratio, horizontal tail	3.0
Taper ratio, vertical tail	0.6
Taper ratio, horizontal	0.4
Length, vertical and horizontal tails	$1.5\,c_w$
Single-slotted flap	
Chord	$0.25\,c_w$
Span	$0.2\,b_w \longrightarrow 0.65\,b_w$
Plain aileron	
Chord	$0.25\,c_w$
Span	$0.65\,b_w \longrightarrow 1.0\,b_w$
Drop-nose flap	
Chord	$0.5\,c_w$
Span	$0.2\,b_w \longrightarrow 1.0\,b_w$

required mission. The 6-percent thick straight wing with an $R = 4$ is estimated to result in an aircraft drag divergence Mach number of 0.882. as obtained from references 1 and 36. Some airfoil camber has been included to improve the aircraft's high lift characteristics and cruise performance.

A single-slotted trailing edge flap and a droop nose flap have been selected to meet the 2,000-foot takeoff requirement. These devices are not necessarily optimum but are adequate to provide the required performance.

Aircraft propulsion is provided by two turbofan engines determined by appropriately scaling those of a Pratt and Whitney TF-30 engine to match the high speed drag estimated for the BPA. The static thrust-to-weight ratio, $(T/W)_{STATIC}$, is 0.496 for a gross weight of 18,000 pounds.

The fuselage length and shape, nacelle locations, and general aircraft configuration are modeled after designs suggested by the study of reference 22. Bulges under each wing house the double-bogie landing gear recommended for STOL operation. Representative tail sizes were selected as listed in Table 6.

PERFORMANCE AND GUST RESPONSE

The BPA design resulted in compliance with specifications; the aircraft has a maximum sea level velocity of 0.9 Mach, a total takeoff distance of 2,000 feet over a 50-foot obstacle at a gross weight of 18,000 pounds, and a cruise radius of 330 nautical miles at 500-foot altitude with a 20-minute sea level dash period at 0.9 Mach.

Handling qualities at all flight speeds for a wide range of center of gravity travel are indicated in Figure 7. These handling qualities are acceptable within the criteria of reference 2. Stability augmentation is necessary at higher static margins for compliance with military specifications. Low dynamic pressure flight conditions would no doubt illustrate a requirement for augmentation at any static margin. Stability augmentation is accepted as a basic flight aid in all modern higher performance aircraft.

The gust sensitivity of the BPA as a function of Mach number is shown in Figure 8. The reduction in pilot station sensitivity noted with higher static margin arises from the faster short-period response. Short-period frequency is roughly proportional to the square root of M_α, the equivalent of static margin. The higher static margin vehicle pitches into the relative wind more rapidly, thus acting in direct opposition to the acceleration resulting from the change in lift. The pilot senses the sum of the two effects, which is now reduced. The quicker alinement with the relative wind also offsets some of the direct loading, as is evidenced by the slight reduction in sensitivity at the cg.

39

It should be noted that while an increase in static margin can provide a measure of alleviation, some of the advantage is lost again when the stability augmentation system is added to the basic vehicle. Normal stability augmentation system design would result in a decrease of the higher frequencies resulting from high static margin. Military acceptance of the NAA Columbus study results and consequent change in requirements to allow the higher frequency response could thus result in the provision of a significant measure of alleviation through increase in static margin.

The gust sensitivity of a vehicle is a function of the short-period frequency. Figure 9 shows the possible range of sensitivity for the BPA at 0.9 Mach with a fixed lift-curve slope, wing loading, and M_q.

Changes in aircraft dynamic stability, i.e., variations in ζ and ω_n, result in alteration of the gust response. Decreased sensitivity is achieved through an increase in the short period natural frequency and/or an increase in damping.

Short-period frequency at a particular flight condition is determined primarily by M_α or static margin. The faster responding vehicle provides a more noticeable reduction in total accelerations at positions forward of the center of gravity. As a result, pilot proficiency improves with increase in static margin.

Changes in aircraft design to effect alleviation through improved damping do not readily result in the expected sensitivity reduction. This is true since the damping ratio is determined primarily by M_q. Therefore, a change also occurs in the transfer function numerator which tends to offset the improvement gained by increased damping. However, damping ratio changes can also be effected through a change in $M_{\dot{\alpha}}$. Increases in the magnitude of this parameter are obtained through design involving lengthening of the tail moment arm and a corresponding reduction in horizontal tail surface area.

It also should be pointed out that decrease in the lift-curve slope will decrease the damping ratio, although the change in the latter has a much less significant effect on sensitivity than has the static change.

All further references to the BPA in this report are for a 5-percent static margin vehicle unless otherwise noted.

The correspondence between the two mission phases of the BPA and the pilot proficiency boundaries is shown in Figures 10 and 11. Figure 10 shows that during cruise, 13-percent of the flights would result in reduced pilot proficiency due to turbulent conditions. Figure 11 shows that 64 percent of the flights will be performed at reduced pilot proficiency during dash. Approximately 3-percent of the total number of flights will encounter intolerable atmospheric conditions during the attempted dash portion of the mission at 0.9 Mach. Calculations are based on a mean weight sensitivity (half fuel load).

Figure 12 is an analogue simulated time history showing the response of the BPA at 0.9 Mach to a random gust having an rms value of 4 feet per second. Peak accelerations, which are a function of the gust amplitude, are shown to exceed 0.5 g several times during the 100-second run. Tolerance and error buildups in the simulation mechanization lead to slightly different numerical results than those generally quoted throughout the report. The latter are digital computer results and can be considered the more accurate.

MISSION PERFORMANCE

A weight analysis for the base-point airplane with an assumed take-off gross weight of 18,000 pounds resulted in the following estimated distribution of weight:

$$\frac{W_{structure}}{W} = 0.32$$

$$\frac{W_{propulsion\ system}}{W} = 0.16$$

$$\frac{W_{crew\ +\ fixed\ useful\ load}}{W} = 0.03$$

$$\frac{W_{equipment\ +\ payload}}{W} = 0.14$$

$$\frac{W_{fuel}}{W} = 0.35$$

Mission performance capability was calculated for an estimated 6300-pound fuel capacity. A cruise radius of 330-nautical miles at 0.4 Mach and 500-foot altitude with a 20-minute sea-level dash at 0.9 Mach at the surveillance site is estimated to be a feasible mission for the BPA. Details of the calculations are as follows:

1. Takeoff gross weight = 18,000 pounds

2. Fuel weight = 6,300 pounds

3. Warmup and takeoff: 5 minutes at NRP at sea level:

   Fuel = 1.05 x 2 x 2190 x 5/60 = 384 pounds

4. Cruise to and from surveillance site at 0.4 Mach at 500-feet altitude with an average cruise weight of 15,000 pounds

   Required thrust is given by $\bar{q} S \left[C_{D_o} + C_L^2 / \pi \, A\!R \, e \right]$ (14)

   Thrust/engine = $\dfrac{(234)\,(277)}{2} \left[0.0180 + 0.0995\,(0.231)^2 \right]$ = 755 pounds

   Fuel flow = 545 pounds/hour/engine

   Time = 2.5 hours

   Cruise fuel = 1.05 x 2 x 545 x 2.5 = 2860 pounds

5. Dash at surveillance site at 0.9 Mach and sea level for 20 minutes:

   Fuel = 1.05 x 2 x 3390 x 20/60 = 2370 pounds

6. Reserve fuel:

   a. 5-percent of initial fuel

      Fuel = 0.05 x 6300 = 315 pounds

   b. Fuel for 20 minutes at maximum endurance at sea level (calculated at aircraft gross weight):

      Thrust/engine = $\dfrac{(135.5)\,(277)}{2} \left[0.0180 + 0.0995\,(0.48)^2 \right]$ = 765 pounds

Fuel flow = 522 pounds/hour/engine

Fuel = 1.05 x 2 x 522 x 20/60 = 366 pounds

Cruise range = 2.5 hours x 264 knots = 660-nautical miles

AERODYNAMIC CHARACTERISTICS

The aircraft profile drag at cruise velocity and altitude is estimated at C_{D_o} = 0.0180. The relative aerodynamic cleanness of the configuration is shown in Figure 13. A 17-percent increase to C_{D_o} = 0.0211 at 0.9 Mach is estimated.

An airplane efficiency factor, e = 0.8, has been calculated for the BPA by the method of reference 31. This efficiency factor is assumed to be constant throughout the operational Mach-number range. The total drag coefficient for the BPA is

$$C_D = C_{D_o} + \frac{C_L^2}{\pi \, \mathcal{R} \, e} = C_{D_o} + 0.0995 \, C_L^2 \qquad (15)$$

The wing lift-curve slope for the BPA was determined to be C_{L_α} = 0.066 at 0.4 Mach and 0.093 at 0.9 Mach. The fuselage and nacelle contributions to lift, particularly at low angles of attack, are negligible. The curve of wing lift-curve slope versus Mach of Figure 14, therefore, represents the aircraft tail-off values of lift-curve slope. The curve of horizontal tail lift-curve slope versus Mach was computed as for the wing.

The maximum lift coefficient of the BPA was estimated by the methods of reference 40. The tail-off clean wing $C_{L_{max}}$ is 0.99 and the increment due to the high lift devices is 0.86. The effect on $C_{L_{max}}$ of possible changes in wing thickness and aspect ratio is shown in Figure 15. The takeoff ground run was calculated using a $C_{L_{max}}$ of 1.80 with

the thrust and tail contributions to lift at takeoff assumed nearly compensating. The ground run distance was calculated from the expression

$$S_G = \frac{1}{\rho g} \frac{W/S}{(C_L)_{T.O.} \left[(T/W)_{0.707V_{T.O.}} - \mu \right]} \tag{16}$$

with $\mu = 0.025$ and $C_{L_{T.O.}} = 0.9 \, C_{L_{max}}$ and a mean thrust-to-weight ratio during the takeoff run of $(T/W)_{0.707V_{T.O.}} = 0.46$. The wing loading at takeoff is $W/S = 65$. The nomograph in Figure 16 permits rapid estimation of the effects on takeoff distance of variations in aircraft gross weight, wing loading, thrust/weight ratio, and the related thrust requirements for high-speed flight. The relation between total takeoff distance over a 50-foot obstacle and the ground run, which is included as a portion of the nomograph, was established by a correlation of flight-test data for numerous aircraft. For the BPA, under the conditions outlined above, the total takeoff distance over a 50-foot obstacle is 2,000 feet.

The downwash variation at the tail is estimated as $\partial \epsilon / \partial \alpha = 0.55$ at 0.2 Mach by the method of reference 45. The variation with Mach number shown in Figure 14 was determined by adjusting the low speed value by the ratio of

$$C_{L_{\alpha_1}} M_1 / C_{L_{\alpha_2}} M_2 = 0.2$$

The wing aerodynamic center is estimated to be at $0.25 \, \bar{c}_W$ at Mach numbers below 0.8. An aft movement of the wing ac with Mach number above 0.8 places it at $0.35 \, \bar{c}_W$ at 0.9 Mach.

The incremental change in ac location due to the fuselage and nacelles is $-0.10 \, \bar{c}_W$ for Mach ≤ 0.9.

The tail-off and tail-on lift and pitching moment curves for the BPA are shown in Figures 17 and 18 for a center of gravity position at $0.25 \, \bar{c}_W$.

Due to the wing camber, $\alpha_o = -1$ degree and $C_{m_o} = -0.02$ at Mach numbers below 0.8. Both of these values are reduced to zero at 0.9 Mach.

Longitudinal control has been assumed to be provided by the horizontal tail deflected in its entirety rather than utilizing an elevator.

The effects of flap and aileron deflection on the lift and drag of the BPA are shown in Figures 19 and 20 and reference 30. The centers of pressure of the lift due to deflection of these devices are shown in Figure 21. These estimates are based on the information to be found in references 17, 40, 41, 45, and 48. A generalized method for determining the lift contribution of a trailing-edge device at small deflections is presented later. The downwash variation with trailing-edge-device deflection shown in Figure 21 was determined as

$$\frac{\partial \epsilon}{\partial \delta} = \left(\frac{\partial \epsilon}{\partial \delta}\right) \frac{C_{L_\delta}}{C_{L_\alpha}} = \left(\frac{\partial \epsilon}{\partial \alpha}\right) \alpha_\delta \kappa \qquad (17)$$

The stability derivatives of the BPA through the range of flight-Mach numbers are listed in Table 7. These derivatives are expressed in dimensional form for direct insertion into the equations of motion given in Appendix VI. The following constants were used in obtaining these derivatives:

$S = 277$ square feet $I_{yy} = 300,000$ slugs per square foot

$\bar{c}_W = 8.625$ feet $l_T/\bar{c}_W = 1.5$

$m_i = 559$ slugs $\rho = 0.002377$ slugs per cubic foot

The thrust derivative, T_u, can be obtained from Figure 22. Stability derivatives for the flap and aileron of the BPA used as gust alleviation devices also are included in Table 7.

Table 7. BPA Stability Derivatives

Parameter	Static Margin	Dimensions	Mach Number			
			0.40	0.55	0.725	0.90
X_u		1/sec	-0.014	-0.0195	-0.024	-0.026
X_α		fps	5.8	4.5	1.5	-3.5
M_u		1/ft-sec	0	-0.00017	-0.00035	-0.00045
M_α	0.05	$1/sec^2$	-4.0	-8.0	-0.15	-26
M_α	0.20	$1/sec^2$	-15.5	-33	-59	-105.5
M_q		1/sec	-0.7	-1.0	-1.45	-2.0
$M_{\dot\alpha}$		1/sec	-0.4	-0.6	-0.97	-1.65
Z_α		fps^2	-500	-1000	-1860	-3300
$Z_{\dot\alpha}$		fps	-1.6	-2.4	-4.0	-6.9
Z_u		1/sec	-0.15	-0.13	-0.106	-0.09
Z_q		fps	-2.9	-4.2	-6.0	-8.4
X_{δ_F}		fps^2	-9	-17.3	-30	-46
Z_{δ_F}		fps^2	-95	-198	-360	-623
M_{δ_F}	0.05	$1/sec^2$	-0.4	-1.0	-3.8	-20
M_{δ_F}	0.20	$1/sec^2$	-3.3	-6.2	-14.1	-42
$Z_{\dot\delta_F}$		1/sec	-0.4	-0.64	-1.04	-1.67
$M_{\dot\delta_F}$		1/sec	-0.1	-0.16	-0.245	-0.38
X_{δ_A}		fps^2	-5.1	-10	-16.2	-25.5
Z_{δ_A}		fps^2	-58	-102	-190	-325
M_{δ_A}	0.05	$1/sec^2$	-1.0	-1.5	-4.5	-12
M_{δ_A}	0.20	$1/sec^2$	-2.2	-4.4	-9.3	-21
$Z_{\dot\delta_A}$		fps	-0.15	-0.21	-0.35	-0.55
$M_{\dot\delta_A}$		1/sec	-0.038	-0.042	-0.08	-0.13

Table 7. (Cont)

Parameter	Static Margin	Dimensions	Mach Number			
			0.40	0.55	0.725	0.90
$Z_{\dot{\alpha}_g}$		fps	1.30	1.52	1.98	1.50
$M_{\dot{\alpha}_g}$		1/sec	0.30	0.35	0.48	0.38
Z_{δ_E}		fps^2	-100	-200	-380	-680
M_{δ_E}		1/sec^2	-24	-51	-89	-145

Profile drag estimations were determined as follows:

Mach = 0.4 at 500-Foot Altitude

	$S_{WET(ft^2)}$	$f \; (ft^2)$
Wing (exposed)	432	1.43
Tails	235.4	0.875
Fuselage	422	1.45
Nacelles	187	0.705
Landing Gear Pods	34.8	0.43
Totals	1,311.2	4.890

With 2-percent increases in wetted area and parasite drag factor to allow for miscellaneous aircraft protuberances, the low-speed profile drag is determined as follows:

S_{WET} = 1340 square feet   f = 5.0

C_{D_o} = f/S = 5.0/277 = 0.0180

The profile drag has been assumed to be constant with increasing Mach number to 0.8 Mach. Beyond this speed, C_{D_0} increases to a value of 0.0211 at 0.9 Mach.

The relation used to estimate wing lift-curve slopes for all configurations included in this study is

$$C_{L_\alpha} = \frac{AR\,(c_{L_\alpha})}{\frac{AR}{\cos \Lambda_{.5c}}\,\beta + C} \tag{19}$$

where

$c_{L_\alpha} = 0.108$ for a NACA 64A206 section

$C = 3.34 - 0.11\,AR$ as determined from test data on a straight wing in reference 32

$$\beta = \sqrt{1 - M^2}$$

A generalized plot based on the above equation is presented in Figure 23 from

$$\frac{C_{L_\alpha}}{\kappa} = \frac{1}{9.12\left(\dfrac{\beta}{\cos \Lambda_{.5c}}\right) + \dfrac{30.45}{AR} - 1} \tag{20}$$

where

$$\kappa = c_{L_\alpha} / 0.1097$$

and

C_{L_α} is lift-curve slope per degree of α.

The lift increment due to small deflections of a trailing-edge flap or aileron C_{L_δ}, can be expressed as a function of the percent of wing chord and wing span covered by the device.

$$C_{L_\delta} = f(C_{L_\alpha}, \ \alpha_\delta, \ \kappa) \tag{21}$$

where

C_{L_α} is the wing lift-curve slope

$\alpha_\delta = C_{L_\delta}/C_{L_\alpha}$ is a function of the flap chord (22)

κ is a function of the flap span

Values of α_δ and κ applicable to a straight wing with either single-slotted or plain trailing-edge devices are presented in Figure 24.

VIBRATION DATA

The following data apply for the base-point configuration airplane:

$m_1 = 34.300$ slugs $\omega_1 = 96.712$ radians per second

$m_2 = 8.267$ slugs $\omega_2 = 115.742$ radians per second

$g_i = 0.02$ for $i = 1, 2$

Figure 25 gives the fuselage mode shapes for the first two airplane modes. Note that the shapes are plotted versus fuselage station, in inches, and the shapes $\frac{d\phi_i}{dx}$ required in the rate gyro sensing equation are per foot. Flexibility parameters applicable to the structural equations in Appendix VI are listed in Table 8.

49

Table 8. BPA Flexibility Parameters.

Parameter	Value	Units	Parameter	Value	Units
$a^R_{1,3/m}$	0.12999	ft/slug	$a^I_{1,3/m}$	-0.02747	ft^2/slug
$a^R_{1,4/m}$	0.04180	ft/slug	$a^I_{1,4/m}$	0.82429	ft^2/slug
$a^R_{2,3/I_{yy}}$	0.02058	ft^2/slug-ft^2	$a^I_{2,3/I_{yy}}$	0.14555	ft^3/slug-ft^2
$a^R_{2,4/I_{yy}}$	0.00496	ft^2/slug-ft^2	$a^I_{2,4/I_{yy}}$	0.04146	ft^3/slug-ft^2
$a^R_{3,1/m_1}$	0.573	ft^2/slug	$a^I_{3,1/I_{yy}}$		
$a^R_{3,2/m_1}$			$a^I_{3,2/m_1}$	53.618	ft^3/slug
$a^R_{3,3/m_1}$	0.72105	ft/slug	$a^I_{3,3/m_1}$	12.357	ft^2/slug
$a^R_{3,4/m_1}$	0.08433	ft/slug	$a^I_{3,4/m_1}$	-4.3394	ft^2/slug
$a^R_{3,7/m_1}$	6.1721	ft^2/slug	$a^I_{3,7/m_1}$		
$a^R_{3,8/m_1}$	-1.3316	ft^2/slug	$a^I_{3,8/m_1}$	0.12999	ft/slug
$a^R_{4,1/m_2}$	36.301	ft^2/slug	$a^I_{4,1/m_2}$		
$a^R_{4,2/m_2}$			$a^I_{4,2/m_2}$	227.33	ft^3/slug
$a^R_{4,3/m_2}$	0.99025	ft/slug	$a^I_{4,3/m_2}$	15.623	ft^2/slug

Table 8. (Cont)

Parameter	Value	Units	Parameter	Value	Units
$a^R_{4,4/m_2}$	0.56344	ft/slug	$a^I_{4,4/m_2}$	24.946	ft^2/slug
$a^R_{4,7/m_2}$	3.9365	ft^2/slug	$a^I_{4,7/m_2}$		

51

APPENDIX IV.   ACTIVE SYSTEMS

Analysis and results of active system investigation are detailed in this appendix, followed by summary and further considerations of the more promising systems.

PITCH DAMPERS AND AUTOPILOTS

Autopilots and pitch dampers or stability augmentation systems (SAS) are considered as active system techniques which artificially alter the aircraft dynamic response. Pitch dampers or SAS utilize inertial sensors, electronic computation, and hydraulic or mechanical servo actuators to augment the aircraft short period stability. Autopilots, in addition to providing short period stabilization, employ outer-loop control or pilot relief modes such as attitude hold, altitude hold, mach hold, and automatic terrain following. The alteration in short-period response as provided by these systems may alleviate or aggravate the response due to gusts.

For aircraft operating over an extreme range of flight conditions, an SAS must be designed specifically for the vehicle or must contain adaptive ability, i. e. , the ability to alter the control system parameters as a function of the environment or measured response. Most SAS's utilize a pitch rate signal as obtained from a rate gyro to control the elevator and to provide improved damping. Normal design employs short period criteria such as the one indicated in Figure 5 (CAL studies).

A pitch SAS that would result in acceptable qualities is shown in functional form in Figure 26. This system employs an electronically compensated pitch rate feedback signal. The compensation or signal shaping employed is not necessarily optimum, but indicates the normally desired trend of SAS design and allows evaluation as a gust alleviator. The choice of compensation allowed evaluation over a large range of vehicle static margin.

The canceler or washout circuit employed on the rate gyro output serves to wash out or eliminate the steady-state pitch rate value from the feedback signal, thus allowing maneuverability. The washout time constant must be short enough to allow the commanded rate to be reached within a reasonable time, yet long enough so as not to interfere with the short period stability. This can be accomplished for the BPA low altitude

conditions with a 2-second time constant. The effect of the washout on response to a step stick command is shown in Figure 27. Vehicles having a short period response that would be adversely affected by a short time constant are forced to employ control stick pickoffs in addition to a longer term washout.

The root loci plots of Figure 28 illustrate, in the complex frequency plane, the change in damping and frequency obtainable with the SAS for 5-percent and 20-percent static margin vehicles as a function of the gain $K_{\dot\theta}$. The nominal value of $K_{\dot\theta}$ shown is equal to 0.06 degree per degree per second. The increase in damping afforded by the SAS is accompanied by a decrease in the natural frequency. Hence, little or no alleviation occurs (see Figure 9).

An alternate approach to stability augmentation and alleviation would appear to be the feedback of a pure pitch rate signal, since, as the locus plot of Figure 29 illustrates, an increase in natural frequency would result (with servo modes included) without significant change in damping ratio. This would appear to effect a sensitivity reduction. Unfortunately, from an alleviation viewpoint, pitch rate feedback acts in the same way as a change in M_q, and the numerator of the transfer function,

$$\frac{N_{Z_w}}{g}(s) = \frac{Z_\alpha}{gU} \frac{(s^2 - 2M_q s)}{(s^2 + 2\zeta\omega_n s + \omega_n^2)} \tag{23}$$

where s is the Laplacian operator, is also altered. The overall result is little or no change in sensitivity. This is further illustrated by the plot of Figure 30, which illustrates the acceleration amplitude in response to gust inputs as a function of frequency, with and without the rate feedback. Systems employing mechanical damping, such as the mass-overbalanced elevator of reference 8, provide essentially the same results.

Autopilots include stability augmentation, which acts to provide the same sort of change in short-period dynamics Most outer-loop commands operate under slowly changing conditions, and therefore affect the gust response negligibly. An exception to this may be the case of an automatic terrain-following mode. Terrain following and gust alleviation compatibility

appears to be an area worthy of further investigation. Autopilots or dampers operating with normal acceleration in conjunction with pitch rate are a design possibility. Acceleration feedback acts to alter the static sensitivity, frequency, and damping with no change in the numerator of equation 23.

With acceleration feedback to the surface, the static sensitivity is altered as follows:

$$\frac{Z_\alpha}{gU} \rightarrow \frac{Z_\alpha}{gU} \frac{L}{1 + \dfrac{F_{N_Z} Z_{\delta_E}}{57.3g}} \tag{24}$$

where F_{N_Z} is the feedback operator. If $F_{N_Z} Z_{\delta_E}$ can be made large enough, the static sensitivity will be significantly reduced. Acceleration feedback to the elevator alone is destabilizing, and pitch rate feedback is needed for good stability. Even with pitch rate feedback, only small acceleration gains are possible in a straightforward feedback loop where F_{N_Z} is a constant. Z_{δ_E}, the measure of elevator control force, may be increased, but larger values more readily result in instability. Thus, the product $F_{N_Z} Z_{\delta_E}$ is the important factor for stability as well as for alleviation.

Complex autopilots employing shaping or integration of the acceleration signal or containing some measure of self-adaptation could conceivably result in a measure of alleviation. Full investigation of such systems and application to the BPA would effectively involve a sophisticated autopilot design and examination of many individual complex systems not within the scope of this program.

It can be concluded that augmentation systems employing pitch rate only cannot provide significant alleviation, but that complex systems employing some form of acceleration feedback may result in a measure of alleviation. It is recommended that any proposed autopilots or augmentation systems utilizing acceleration feedback be investigated for alleviation capability along the lines of this report.

NORMAL ACCELERATION CONTROL

A frequently proposed active gust alleviation system employs normal acceleration feedback to bi-directional flaps for directly off-setting the lift and to tail surfaces for counteraction of flap-produced moment. This system is discussed in references 25, 34, and 46. Preliminary discussions assume the accelerometer to be mounted at the center of gravity. The normal acceleration system, designated N_Z, provides an alteration of the static portion of the gust sensitivity, and also affects the vehicle dynamic response.

System Concept

The N_Z system investigated is shown in block diagram form in Figure 31. The system, providing the signal gains are maintained in a ratio inversely proportional to the surface-produced moments, i.e., $K_{N_{Z_E}} = K_{N_{Z_F}} (M_{\delta_F}/M_{\delta_E})$, alters the static gust response as follows:

$$\frac{Z_\alpha}{gU} \rightarrow \frac{Z_\alpha}{gU} \left[\frac{1}{1 - K_{N_{Z_F}} (Z_{\delta_F} - M_{\delta_F}/M_{\delta_E} \times Z_{\delta_E})} \right]$$

Thus, as $K_{N_{Z_F}}$ is increased, the sytem ideally results in a corresponding decrease in sensitivity. Z_{δ_F} is negative and large in comparison to the second term.

Since the moment ratio is a function of velocity, best results at constant gain may be realized at only one condition of flight. The gain adjustment can be made for the high-speed case where sensitivity is highest, if the system remains effective at lower speeds. The damping ratio ζ decreases as a function of $K_{N_{Z_F}}$ but the frequency ω_n remains essentially as for the basic aircraft, providing the gain ratio is maintained.

Dynamic Response

The root locus plots of Figure 32 show that the short-period frequency for 0.9 Mach remains nearly constant. At other flight speeds, where the flap to elevator gain ratio is not equal to $M_{\delta_F} / M_{\delta_E}$, the natural frequency changes rapidly. The decrease in damping is noted at all flight speeds. The static decrease in sensitivity is shown in Figure 33 as a function of $K_{N_{Z_F}}$. A comparative plot illustrating the effect of the

dynamics change and inclusion of servo and sensor dynamics is also shown. The previously discussed SAS was utilized to regain damping. The locus plots of Figure 34 illustrate the increase in damping ratio at 0.9 Mach and 0.4 Mach. Rate gyro and accelerometers were assumed to have a second-order linear dynamic response of 16 cps. Linear servo dynamics included a 4-cps elevator power servo and a 3-cps flap power servo. Series servos having a 7-cps response were used. Variation in linear flap power servo dynamics over a range from 2 to 7 cps showed little effect on the sensitivity. Studies based on response to sharp-edged or step gusts, with the associated high frequency content, could result in erroneous conclusions as to the importance of linear servo dynamics. The true turbulence spectrum content is primarily low frequency. Realistic servos would be unable to respond to high-frequency disturbances.

The rate limits of the actuation device warrant further consideration. Higher amplitudes of commanded motion at a particular frequency necessarily result in higher actuator rate of travel. With higher input signal amplitudes, the rate limit is eventually reached and the response is no longer linear, a fact not considered with simple linear dynamics. Thus the ability to alleviate becomes a function of the gust velocity. The effect of flap power servo rate limiting becomes pronounced with high gust velocities and high system gains. The sensitivity as a function of rms gust velocity is illustrated in Figure 35 for flap loop gains of 5.5 and 7.5 degrees per g. A flap servo rate limit equivalent to 30 degrees per second is used. The phase shift resulting from non-linearity is enough to result in vehicle limit cycling with a gain $K_{N_{Z_F}}$ of 11.0 and an rms gust velocity of 8 feet per second. It is seen that a gain of 5.5 with the 30-degree-per-second limit provides good alleviation well beyond the thunderstorm range.

All dynamics and rate limits of the discussion appear to be easily realizable. The servo response is limited primarily by compliance, and it is estimated that flap power servos can be designed with a 5 cps response with 10,000-pound force output and a stroke of ±2 inches. Elevator deflections and rates are small, and no problems result with these actuation devices.

A high-gain system provides better alleviation at low gust velocities but, because of rate limiting, results in both stability and sensitivity problems at higher gust velocities. A low gain system, on the other hand, while less effective as an alleviator, assures significant sensitivity reduction to extremely high gust velocities. The sensitivity as a function of aircraft velocity is shown in Figure 36 for the low gain system. A time history of the gust response as obtained on the simulator is shown in Figure 37.

Acceleration feedback gust alleviation presents the problem of the alleviation system's tendency to counteract the g's developed from a stick command. Satisfactory response is dependent upon application of a signal proportional to the commanded g's for use in canceling the signal from the alleviator. Such a signal can be provided if a conventional artificial stick feel system (commanded g-load proportional to applied stick force) is employed in the vehicle. Such systems are a desirable feature even in the absence of a gust alleviator. A stick force transducer can be utilized, the measured force being proportional to the commanded acceleration. The transducer signal can be shaped by a lag network and combined with the accelerometer output as shown in Figure 38. The lag serves to avoid initial overcontrol while the commanded load is building up. Combining this signal with the accelerometer output enables the sensed maneuver g's to be canceled from the alleviation command, i.e., not interpreted as gust loads. The end result is that alleviation is provided about stick-commanded g's rather than about zero g's.

The described method was simulated on the analogue computer. Figure 39 illustrates the normal acceleration at the cg for simultaneous alleviation and pilot-commanded g's. Pilot commands of 1-g steps and sinusoids are presented; the low-amplitude random accelerations (compare with Figure 37) about these commands indicate effective gust alleviation. The same method may accommodate outer loop autopilot g commands in such modes as automatic terrain following. Compatibility with this mode, however, is an important enough problem to warrant further investigations.

Systems using a form of split or auxiliary elevator, such as that discussed in references 25 and 29, appear to offer no additional advantages. Controllability is available only over a limited range of flight conditions.

Figure 40 illustrates the location of the system equipment necessary to the acceleration system with SAS. The accelerometer is shown at a point other than the cg, since it should be located so as to minimize the airframe structural vibration pickup.

If wing flaps are to be used as dual purpose landing and gust allevi-
ation control surfaces, the alleviating function will be fully available in
the longitudinal plane during aileron-induced maneuvers. However, if
the ailerons double as alleviating surfaces, a condition of signal-sharing
will exist such that all electrical commands (gust alleviation and pilot
relief modes) will be summed together as inputs to the series servos with
opposite phasing to left and right surfaces; while the alleviation signals
will enter with the same phasing, producing symmetrical deflections.
Because alleviation generally requires only a small amount of the avail-
able surface displacement (see time history of gust response in Figure 37),
proper alleviation surface deflections will be obtained under all but extreme
maneuvers. It is conceivable that for large maneuver deflections, addi-
tional deflection commands for alleviation would result in position limiting.

A point in favor of using flaps rather than ailerons is that the former
are nearer the wing root, with larger design stresses available. For
landing the vehicle, it becomes necessary to use a standard controller,
e.g., a relatively slow screw-jack actuator, in parallel with the alleviation
servo. This will provide the large downward surface displacement not
available from the limited authority alleviation servo. If ailerons are
used as the alleviation system lift devices, an advantage is that the nor-
mally required aileron power servos may be designed to perform a dual
role for maneuvering and alleviating. It is assumed that series servos
will be added to the power servos. A series servo also is required for
the elevator to obtain stability augmentation and gust alleviation.

The product $K_{N_{Z_F}} Z_{\delta_F}$ is the important factor in determining allevi-

ation capability. Since the value of $K_{N_{Z_F}}$ can be limited by nonlinear

servo effects, as discussed, it would appear that the largest control
force possible would be the most desirable. However, larger surfaces
would necessarily result in lower available servo rates, and a tradeoff
obviously is indicated.

Flap motions with the alleviation system described are a function
of the gust velocity and would vary approximately according to Figure 41,
which is based on analogue-simulation results. The change in range due to
the increased drag resulting from flap motion can be seen from Figure 41
to be minor, on the order of 1 percent. An additional 1.5-percent range
degradation can be attributed to the additional weight of the system and
structural weight increases necessitated by high speed flap motion. The
latter is estimated to be 30 pounds per wing, or 2 pounds per square foot
of flap area. Thus, the overall range degradation attributable to system
incorporation is less than 3 percent.

ANGLE-OF-ATTACK CONTROL

A system employing a type of wind-flow sensor to generate an error signal for flap and elevator commands has been presented in several references. Among these are references 7, 25, 29, 34, and 49. The sensors studied have been either a vane or a pressure-probe type mounted on a nose boom. Both serve to generate a signal

$$\alpha_s = \alpha_o + \alpha + \alpha_g e^{s\tau} - \frac{l_{cg}}{U} \dot{\theta}$$

where

α_o is trim angle of attack

s is the Laplacian operator

$\tau = \dfrac{l_{cp}}{U}$ is the time for gust to reach cp after being sensed

l_{cp} is the distance from sensor to center of pressure

l_{cg} is the distance from sensor to center of gravity

Thus $e^{s\tau}$ represents the time lead obtained by sensing the gust angle of attack ahead of where it affects the vehicle aerodynamically. It can be seen that, while the intent of the use of such a sensor is to obtain a measurement of the gust angle of attack α_g, the motion of the vehicle also is a significant contributor to the sensed signal. Several investigators have proposed elimination of these other components by various means. Such systems are herein termed simulated gust systems and are not the subject of the present discussion. Rather, this section deals only with a system using the single sensed signal α_s.

The manner in which this system affects the gust sensitivity is not as apparent as for an acceleration feedback system. In general, the α and $\dot{\theta}$ terms alter the short period dynamic response, and the α_g term tends to minimize the effect of numerator dynamics of the transfer function. If α_g were the only component sensed, the gust sensitivity could theoretically be made equal to zero through complete cancellation of numerator dynamics.

System Concept

The angle-of-attack sensing system, designated α, is shown in block diagram form in Figure 42. As with the acceleration system, the sensed signal is amplified and used to actuate the flaps. A portion of the signal, gained as a function of the surface moment ratio $M_{\delta_F}/M_{\delta_E}$, is fed as before to the elevators to counteract the flap-produced moment. This adjustment would optimally correspond to that necessary for operation at the dash speed.

The steady component of angle of attack, α_o, must be canceled out so that changes in the trim angle of attack with velocity or weight will have no effect on the sensed signal.

Dynamic Response

Figures 43 and 44 show that as long as the gain ratio $K_{\alpha_F}/K_{\alpha_E}$ is varied and maintained equal to the surface moment ratio, a single value of flap gain, $K_{\alpha_F} = 4.5$ degrees per degree, will serve to provide good alleviation. The results hold through the aircraft velocity range. However, if the gain ratio is held constant, no ratio will servo over the studied flight regime, as illustrated by Figure 45. In fact, no constant ratio will result in a stable system over the velocity range. This indicates a need for stability augmentation and/or adaptive gain changing.

The gain ratio was adjusted for optimum operation at 0.9 Mach. The previously discussed stability augmentation system was then added, resulting in the stability indicated in Figure 46. Damping at lower aircraft velocities remains far from optimum. Higher gaining on the pitch rate signal in an attempt to provide increased low speed damping would result in very poorly damped or unstable servo modes. In addition, the short-period response at 0.9 Mach is seriously degraded, becoming highly overdamped. It is conceivable that a different SAS could be designed to provide satisfactory short period characteristics for all flight conditions. The stabilization difficulties, nevertheless, appear to be an inherent deficiency of the angle-of-attack system if a significant range of vehicle velocity is to be satisfied.

A washout on the probe or vane signal could not be employed successfully to provide desired handling qualities. The short time constant that would be necessary adversely affects what is already a stability

problem. Longer time constants begin to interfere with the ability to sense low-frequency gusts. The α component of the sensed signal remains to interfere with controllability. An integrating actuator or other type of canceler is needed for trim.

Controllability may be obtained through additional inertial sensing and cancellation of the α component of the sensed signal, or with a stick pickoff. The former is discussed later as a simulated gust approach. The latter is useful over only a limited flight regime, since neither stick displacement nor stick force can be considered proportional to α over a range of conditions. Optimization for a particular flight condition would result in compromised control at other conditions. Gain changing techniques have not been proposed previously, but conceivably could result in adequate controllability.

The gust sensitivity obtained with the angle-of-attack system and SAS is shown in Figure 47 as a function of airplane velocity. A time history of the response to 4 fps rms gusts for 0.9 Mach is shown in Figure 48. No further advantages appear to be offered by use of a split elevator.

Equipment Considerations

The angle-of-attack sensing system is relatively independent of servo rate limiting. Figure 49 illustrates the sensitivity as a function of gust velocity with a 3 cps flap power actuator, rate-limited at 30 degrees per second. In general, relative control surface motion is less with the angle-of-attack system than for the acceleration system. This can be attributed to the inherent lead provided by nose-boom mounting of the sensor. Significant increases in alleviation capability also are noted as a result of the sensor location. The lead time gained by locating the sensor on the boom rather than at the wing amounts to 29 milliseconds at 0.9 Mach and 61 milliseconds at 0.4 Mach. The sensitivity reduction is thus improved by 15 percent at 0.9 Mach and by 25 percent at 0.4 Mach.

The equipment necessary for installation of an angle-of-attack system is illustrated in Figure 50. The considerations of flap-actuator mechanization are the same as those discussed for the acceleration system. The two basic types of applicable angle-of-attack sensors follow:

1. Vane Type. With the vane-type transducer, the sensing vane normally is alined fore and aft. Both positive and negative angles are detected via the sensing vane (airfoil) deflector.

The units contain self-regulating heaters and require roughly 200 watts of heater power to avoid icing. The pickoff device may be synchro, potentiometer, or linear voltage differential transformer (LVDT). For redundant system mechanization, the vane-type transducer can be furnished with two or three pickoff elements.

2. Probe Type. The probe-type transducer utilizes a cylindrical sensor probe, with two slots located toward its far end and running parallel to its axis, which normally protrudes and faces forward into the airstream. Airflow around the probe produces across each slot pressure that is transmitted to two separate chambers in the transducer by individual channels in the probe. Deviations of the probe axis from the flight velocity vector result in a pressure differential between the two chambers. A butterfly vane responds to pressure variation and transmits movement through a feedback mechanism rotating the probe until the chamber pressures are equalized. Output elements are either synchros or potentiometers.

Characteristics of an angle-of-attack sensor which were not considered in this study include any possible nonlinear effects, boom flexibility, and definition of the pressure field about the sensor. The effect of the angle-of-attack system operation on range capabilities is essentially the same as with the normal acceleration system. Flap deflections are about the same magnitude, but the rates of deflection are less than those obtained with acceleration feedback. System and structural weight increases are estimated to contribute to an overall range degradation of less than 3 percent. As for the acceleration system, ailerons deflecting in a nondifferential manner may be used in place of bi-directional flaps.

SIMULATED GUST SYSTEM

Different active gust alleviation schemes that have been approached can be grouped into a single category and considered as attempts to measure the gust and utilize it as a control signal to actuate the flaps and elevators. The systems of references 5 and 28 and a system studied at CAL

fall into this category, herein termed the simulated gust system. The term "simulated" is used since no device exists which measures the actual gust or gust angle of attack. Rather, a combination of sensors is used, the outputs of which are combined in such a fashion that the total signal is proportional to the gust velocity or gust angle of attack.

No alteration of the stability or control characteristics of the vehicle should occur.

Derivation of Gust Signal

The approach taken in references 5 and 28 for gust measurement is based on mathematical summation of the aerodynamic lift and pitching moment perturbation equations and solution of the resulting equation for α_g. Neglecting smaller terms and assuming both flap and elevator controllers, the resulting equation is

$$\alpha_g = aN_Z + B\delta_E + C\delta_F + \alpha \tag{27}$$

where a is a function of the aircraft and flight condition parameters. At a particular flight condition, it is a constant. B and C are always constants. A low frequency approximation is used, wherein

$$\alpha \cong \frac{D\,\dot\theta}{s+e} \tag{28}$$

where

s is the Laplacian operator

D is a constant

e is a function of flight condition

Thus, the resulting equation for the gust signal is

$$\alpha_{g_s} = aN_Z + B\delta_E + C\delta_F + \frac{D}{s+e}\,\dot\theta \tag{29}$$

N_Z may be sensed with a vertical accelerometer, $\dot\theta$ may be sensed with a pitch rate gyro, and δ_E and δ_F may be determined by servo position pickoffs. The gains and lag are formed electronically. The formulation of this gust signal is illustrated in block diagram form in Figure 51.

63

Possible errors in this approach may result from the omission of the smaller terms, approximation of α, location of the accelerometer, servo nonlinearities, and estimation of the various lift and moment equation coefficients.

The second approach to obtaining the gust signal utilizes an angle-of-attack sensor which yields

$$\alpha_s = \alpha_0 + \alpha + \alpha_g e^{sT} - 1_{cg/U} \dot{\theta} \tag{30}$$

where

α_0 is the trim angle of attack

The trim angle-of-attack α_0 must be canceled or washed out. Two approaches may be taken to eliminate the α term. The first is to use the lagged pitch rate approximation as shown previously. The second uses the fact that

$$N_z = \frac{U \dot{\gamma}}{57.3 \, g} = \frac{U(\dot{\theta} - \dot{\alpha})}{57.3 \, g} \tag{31}$$

This equation can be solved for α, yielding

$$\alpha = \int \left(\dot{\theta} - \frac{57.3 \, g N_z}{U} \right) dt \tag{32}$$

A combination of pitch rate and vertical acceleration, where the latter is programmed as a function of airspeed, can be electronically integrated to obtain α as follows:

$$\alpha = \frac{1}{s + k_1} \left(\dot{\theta} - \frac{57.3 \, g N_z}{U} \right) \tag{33}$$

where k_1 is the reciprocal of the integration time constant.

The lag from sensor to cp can be approximated with a truncated series expansion of the exponential series, i.e., $e^{-\tau s} \cong 1 - \tau s$, or an electronic delay can be fabricated. Either way, the delay must be made a function of aircraft velocity. The portion of the sensed signal due to pitch rate is small and can be neglected. Indicated airspeed must be utilized for gain programming. The resultant equation to be mechanized is

$$\alpha_{g_s} = \left[\alpha_s \frac{s}{s + k_2} + \frac{1}{s + R_1} \left(\frac{57.3 \, g \, N_z}{U_{IAS}} - \dot{\theta} \right) \right]$$

$$\left[1 - \frac{l_{cp}}{U_{IAS}} \left(\frac{s}{s + k_3} \right) \right] \quad (34)$$

The formulation of this signal is illustrated in block diagram form in Figure 52.

Errors in this expression may result from the approximate integration, the time delay approximation, neglect of the $\dot{\theta}$ contribution to the sensed angle of attack, the use of indicated airspeed rather than inertial velocity, and the attempted cancellation of the trim angle of attack. The latter may interfere somewhat with the ability to sense low frequency gusts. Center-of-gravity and center-of-pressure shifts also contribute a small error.

Application of Gust Signal

The gust signal as measured, or simulated, is used to control flaps and elevators. The signal must be operated on in order to perform this control function.

The object of the system is, of course, to minimize the loading resulting from gusts. A determinant consisting of the aerodynamic equations of motion and elevator and flap control equations,

$$\delta_F = F_1 \, \alpha_{g_s} \quad (35)$$

$$\delta_E = F_2 \, \alpha_{g_s} \quad (36)$$

can be formed, where F_1 and F_2 are arbitrary functions to be deter-
mined. α_{gs} is temporarily assumed to be equal to α_g, and perfect
servos and sensors are assumed. The determinant can be used to solve
for the transfer function N_Z/w_g and the latter set equal to zero, i.e.,
perfect alleviation. The unknown functions may be solved for in any of
three ways. Since there are two unknown functions and only one equa-
tion, some relationship between the two must be assumed, or another
equation must be determined.

A method using the latter approach is to determine also the trans-
fer function $\dot\theta/w_g$, and set it equal to zero as well. With this approach,
it is found that the resulting functions, F_1 and F_2, are unrealizable.
They cannot be formed by electronic or mechanical means.

A second method is to assume that the functions are of the form

$$F_i = a_i s + b_i \tag{37}$$

The resulting transfer function numerator is of the fourth order, and
like coefficients can be equated for determination of the unknowns.

The third approach is to assume a relationship between F_1 and F_2
whereby the functions are inversely proportional to the moments
resulting from surface deflection.

The latter two methods result in essentially the same determi-
nation. That is, the surface signals should be gained in the inverse
ratio of resulting moment and shaped by a network of the form
$(s+f)/(s+g)$. The block diagram of Figure 53 illustrates this controller.

Gust Response and Performance

Assuming that the gust is perfectly sensed or simulated, the loads
resulting from gusts with this type of system are theoretically zero. This
must be true, since the basis for derivation of the system is that the
loads are zero. The vehicle characteristic equation which determines
the stability is unaltered by incorporation of the system. It also can be
seen, through the appropriate determinant expansion, that the response
to stick commands N_Z/δ_s or $\dot\theta/\delta_s$ is unaltered by incorporation of the
system. Thus, the system theoretically provides perfect alleviation,
with no alteration of vehicle stability or control.

As a test of the ability of the system to meet its theoretical capa-
bility, the system was incorporated into the analogue computer simulation.
The shaping parameters as determined for the 0.9 Mach flight condition
were used. Assumptions that provided the basis for analytical determi-
nation also were assumed for the simulation. That is, unity servo and

66

and sensor dynamics, and ideal sensing of the gust angle of attack were used. The control signal was the output of the magnetic tapes which provided the actual gust disturbance, which is clearly the best signal that a simulated gust system could produce.

Figure 54 illustrates the sensitivity obtained with incorporation of the idealized system as a function of the nominal elevator gain. As might be expected, the alleviation obtainable is not ideal and,furthermore,is a critical function of gain. Less than 8-percent variation in gain results in a vehicle more sensitive to gusts than was the vehicle with no system. The inability to achieve the predicted alleviation can be attributed to parameter tolerance buildup. Thus,the degree to which vehicle characteristics are known and the tolerance to which system parameters can be held determine the ability of the system to provide alleviation.

The optimum control gains and shaping determined for the 0. 9 Mach flight conditon were used with 0. 4 Mach aircraft dynamics. Aggravation rather than alleviation resulted. In both cases studied, the control signal was the actual gust, and errors caused by gust signal formation would further decrease the system effectiveness.

The degre. to which an angle-of-attack sensing system resembles this type of system shows why the former also tends to be critically dependent upon flight parameters. The anomaly results from the so-called open-loop nature of the system, as opposed to the closed-loop nature of a true control system. A closed-loop system utilizes a feedback signal to alter that output which is sensed and maintains a continuous monitor over it. The subject system obviously has no effect on the gust itself, which is the sensed signal. Therefore, it is an open-loop system with no direct measure of how well it is performing its function. The manner in which the flaps and elevators move to counteract the effect of the gust is based solely on the predicted response to all three inputs.

Since wind tunnel investigations produce measurements of vehicle characteristics that are accurate only to within perhaps 20 percent, an accuracy exceeded on the simulator, the ability to predict the response is necessarily limited. For this reason, and since the system is predicated on a high degree of complexity with no more alleviation evidenced than with less complex systems, it must be concluded that present application under practical conditions is questionable. The system appears to lend itself to an adaptive approach. Perhaps parameter adjustment as a function of sampled acceleration power could be employed. In view of the high degree of theoretical promise afforded by such a system, it is recommended that investigations along these lines continue. Resultant alleviation capability may well justify a high degree of system sophistication.

FLEXIBLE WING SPAR

A gust alleviation system which has been tested in flight is discussed in references 3, 15, and 42. The system operates to counteract the effect of a gust on the aircraft by aileron deflection determined by and geared to the bending of the wing under the gust load. The aileron deflection angle is dependent on wing flexibility and the gearing ratio between the aileron and wing bending. For the system as flight tested, alleviation of aircraft accelerations was about 9 percent at flight Mach numbers of the order of 0.2. Higher aileron deflection to wing-bending gearing ratios resulted in an unstable system. Surface inertia and response time requirements for satisfactory in-phase operation at high flight speeds are extremely difficult to achieve. Instability can result easily.

ALLEVIATION AIRPLANE

The gust alleviation airplane described in reference 23 is an interesting development of an airplane designed specifically to alleviate the effect of gusts through both active and passive means. This approach appears to utilize the floating characteristics of the flaps and an auxiliary empennage mechanically linked to flaps and elevators. Maneuverability is obtained because of the linkage, but it appears to be limited in application to a small flight regime. Detailed alleviation analysis is difficult with the limited information available on the system. The detailed design problems, system weight, and lack of promise of considerable alleviation appear to prohibit utilization of such a system for the purposes considered here.

OPTIMIZATION TECHNIQUES

The problem of obtaining the optimum active gust alleviator was approached in two ways. The first was through utilization of a unique digital computer program called direct search optimization. The second involved determinant expansion with feedback terms written in generalized form. Both were subjected to the constraints of stability, controllability, and alleviation. These approaches result in a simulated gust system.

A theoretical study employing the Wiener optimum filter theory was conducted and reported in reference 43. The theoretical requirements included a minimization of a combination of acceleration and pitch rate. The derived filter in this case corresponds to the characteristics of the system to be obtained. The author assumes that a gust sensing device is available and that independently operating force and moment can be applied. A system based on this analysis would effectively be a simulated gust system with optimum shaping for minimization of a combination of acceleration and pitching rate.

FLAP CONTROLLER

References 46 and 49 are instances of study where control of the flaps only has been proposed as a gust alleviation system. Normal acceleration or angle-of-attack sensing can be used as a controlling signal. As a result of lift-surface deflection, pitching moments are produced for which no counteraction is developed with such a system. The generated moment is a function of the center-of-pressure and center-of-gravity locations, and of the flap deflection and rate. Only very small gains and, hence, minute flap deflections are possible with such a system. Phugoid motion rapidly tends toward instability with increasing gain, with the frequency becoming intolerably high.

It can be concluded that the flap-produced pitching moment is significant and that moment countering is necessary.

ACTIVE SYSTEM EVALUATION

Alleviation

Of the active systems investigated in this study, only those systems which employ both lift and moment controllers provide sufficient alleviation to merit use as a gust alleviator. Simple systems designed specifically for pitch stabilization do not provide significant alleviation, but the possible change in gust response characteristics warrants inclusion of gust considerations into stabilization system design criteria. Normal acceleration or angle-of-attack sensing is fundamental to active system alleviation. Some of the characteristics of the more promising systems, i. e. , the flap-elevator acceleration system with SAS and the angle-of-attack system with SAS, are summarized here.

The rigid-body sensitivities for the active systems are shown in Figure 55 as a function of Mach number, for comparison purposes. The alleviation afforded at the pilot station by these systems is indicated in Figure 56 in terms of the normalized vertical acceleration power spectral density. It can be seen from this figure why care must be taken in interpretation of percent alleviation figures. For example, in the case of the acceleration system, the percent alleviation figure based on peak PSD values is 77 percent at the pilot station. This compares to 41 percent based on rms values.

The angle-of-attack system shows an 81-percent reduction of the PSD peak and 45 percent based on rms values. The simulated gust system is not illustrated on the alleviation charts, since mathematical derivation would result in perfect alleviation, and any value obtained on a computer would be a function of computer tolerances. There exists no way of determining the alleviation that would be evidenced, other than a probability analysis using estimated aerodynamic accuracies and system parameter tolerances.

The angle-of-attack system clearly exhibits the best alleviation. It should be realized that proper stabilization of the vehicle with an angle-of-attack system would degrade the alleviation obtained at lower aircraft velocities. The alleviation capability tends to be a somewhat critical function of system gains. The normal acceleration system exhibits less alleviation capability than the angle-of-attack system over the studied flight regime. Alleviation obtained at high speed, the condition to which both systems were optimized, is comparable. The alleviation obtainable with an active system is a function of the flap servo rate limits, but it has been shown that proper gaining can result in the quoted alleviation to rms gust intensities beyond 15 feet per second.

Pilot Tolerance and Endurance

The pilot endurance probability at the dash condition and for a mean weight vehicle is shown for the acceleration and angle-of-attack systems in Figure 57. The pilot can operate at normal proficiency 95 percent of the time with the acceleration system and 97 percent of the time with the angle-of-attack system, based on RB-66 turbulence probability data and the chosen endurance criterion.

The active system capabilities in terms of endurance may be somewhat misleading, since, as previously stated, the endurance criterion is based on a vehicle short-period response spectrum, while the active system spectra exhibit peaking at the higher servo frequencies. This fact is illustrated in Figures 58 and 59, which show the N_z system acceleration power spectrum in comparison with that of the folded-wing vehicle. While the two systems exhibit comparable alleviation based on rms values, it can be seen from Figure 58 that the reduction in PSD peak is noticeably greater with the active system. Therefore, there must be more power exhibited at higher frequencies with the active system. This fact is borne out by Figure 59, which illustrates the high frequency content resulting from peaking at the closed-loop servo frequencies.

The high-frequency content may be bothersome, as pointed out by Figure 60, which illustrates the active system frequency content in terms of pilot behavior categories. Analysis and evaluation become rather difficult when the system exceedance plots pass through a number of behavior categories. Obviously, the margin for evaluation becomes more nebulous at the lower g increments, where the categories are not widely separated. Thus, though it is clear that alleviation results cannot be interpreted on rms values alone, no decisive tolerance determination can be made. It is noteworthy, however, that the high-frequency vibrations are of small amplitude and perhaps can be eliminated from having an effect on pilot behavior with the use of a spring-mounted seat. The high-frequency acceleration content would be evidenced with any active system. The present evaluation is based on rigid vehicle response. Structural vibrations would, of course, have an additional minor effect on pilot tolerance and endurance.

Performance, Stability, and Control

The effect of active system incorporation on aircraft range is estimated to be less than 3 percent. A decrease on the order of 1 percent is noted due to the increase in drag resulting from flap deflection. The remainder arises from the decrease in allowable fuel resulting from the overall weight penalty, including system weight and necessary structural weight increases.

Pitch stability augmentation is required with both active and passive systems, but is necessary to active system alleviation evaluation. The stability obtainable with the angle-of-attack system is a critical function of system gain. The stability augmentation system studied was not capable of providing adequate stabilization with an angle-of-attack system over a range of flight conditions. Though proper stabilization may be possible with a more sophisticated SAS, the stability problem is an inherent one. Proper stabilization would tend to decrease the amount of alleviation. Stabilization to military specifications at any one flight condition is obtainable.

The acceleration system can be stabilized to specifications over the studied flight regime. Pilot control in the presence of the alleviator can be achieved with an acceleration system if the vehicle is equipped with an artificial stick feel system. A signal proportional to commanded g's can be obtained with a stick force transducer and, when shaped with a simple lag network, can be used to cancel out the alleviation feedback signal.

No such simple method of obtaining a signal proportional to α exists for cancellation of the feedback signal in an angle-of-attack system. Complex systems attempting to do so are classified as simulated gust systems, shown to be of limited practical value. Control can be obtained at a particular condition of flight with an angle-of-attack system by means of a stick transducer or possibly with pitch rate feedback.

The stability and control problems associated with an angle-of-attack system restrict its use to a very limited flight regime. Incorporation of this system would provide no alleviation capability at other flight conditions.

Structural Effects

Active systems employing both lift and moment controlling surfaces require additional wing structural weight. An increase in structural weight of 2 pounds per square foot of flap area is estimated for the type of flap deflections encountered. Thus, a structural weight penalty of approximately 60 pounds is associated with active system incorporation.

Active system incorporation poses the possibility of excitation of vehicle structural modes. Though the two-surface control tends to make the problem a more difficult one, the excitation of flexibility modes is a possibility encountered in design of nearly every autopilot. The approaches

taken to avoid structural mode excitation include proper sensor location and design of body-bending filters. Sensor location at a point other than the cg may result in a slight decrease in alleviation capability.

Equipment Considerations

The weight penalties, production costs, and mean time between failure (MTBF) of the active systems are summarized in Table 9. Both single systems and triple-unit redundant systems are considered. Triple-unit redundancy, as discussed in reference 16, is a philosophy used in providing high reliability in electronic and electromechanical systems. Reliability figures include SAS reliability, since alleviation system functioning is dependent on SAS operation. System cost, weight, and reliability for acceleration and angle-of-attack systems are comparable.

Table 9. Active System Weight, Cost, and Reliability

System	Total Weight Penalty (Pounds)	*Estimated Production Cost	**Mean Time Before Failure (Flight Hours)
Normal acceleration (non-redundant)	98	1.011	1270
Normal acceleration (triple-unit redundant)	105	1.020	870,000
Angle-of-attack (non-redundant)	106	1.011	1270
Angle-of-attack (triple-unit-redundant)	112	1.021	870,000

* Normalized to BPA cost of 1.000, for 200 production units

** Reliability includes SAS since functioning is dependent on SAS operation

A typical active system mechanization is shown in Figure 61. Active system designs lend themselves readily to integration with the autopilot; design, development, production, and maintenance costs can all be reduced through such integration.

Maintenance of active systems is comparable to that normally encountered with a stability augmentation system and would be reduced by integration. Periodic replacement of sensors and servos is required. The latter, with modern-day electronic packaging techniques, represent the single largest system maintenance effort. The additional servos required, and increased servo activity would necessitate a corresponding increase in maintenance.

Active system failure and the associated probability of large flap deflections could result in severe consequences. In order to assure fail-operational capability, the ratio of flap and elevator signals must be continuously monitored and the system automatically disengaged when the ratio deviates from specified bounds. The disengage signal can be utilized to recenter and lock the flap series servo. In addition, the flap servo should be of limited authorit' to ensure complete ability of the pilot to control the vehicle in case of failure.

The majority of the most likely failure modes are precluded by the triple-unit redundancy technique, which includes redundant sensors, electronics, servo valve pilot stages, feedback transducers, and actuator shaft seals. A bistable switching valve could automatically revert to a standby hydraulic supply in the event of pressure loss in the primary supply.

Conclusions

Of the active systems investigated, it is concluded that only a normal acceleration system controlling flaps and elevators is capable of providing significant alleviation over a range of flight conditions. Though the angle-of-attack system meets the requirements at the dash condition, it affords no capability for gust alleviation over a range of speeds, and incorporation of this system would result in some sacrifice of mission versatility.

The high theoretical alleviation capability without sacrifice of stability and control, as afforded by a simulated gust system, is such that continued effort in this area should be pursued. If a self-adaptive technique can be developed whereby a high degree of alleviation is assured over a wide range of flight conditions, a high degree of system complexity may well be justifiable.

APPENDIX V. PASSIVE SYSTEMS

The analysis and results of passive system investigation are detailed individually in this appendix, followed by summary and further considerations of the more promising systems.

FOLDING WING

The passive system alleviation concept of folding each wing tip of an aircraft under turbulent conditions has as its objective a reduction of the aircraft's gust sensitivity through a decrease in the projected wing area (increased W/S) and a simultaneous reduction of wing aspect ratio (decreased C_{L_α}). The effective aspect ratio of a folded wing, which determines its aerodynamic characteristics, is not the same as its geometric aspect ratio in the wing chord plane because of the end-plating effect of the folded tips on the load-carrying portion of the wing.

Figures 62 and 63 indicate little, if any, change in the effective aspect ratio of a wing due to tip folding except for extreme taper ratios. This relative independence of C_{L_α} on wing folding, when based on projected wing area, is apparently also the case for partial wing folding or tip dihedral. Since there is no reduction of C_{L_α} with wing folding, the gust alleviating capabilities of this system result primarily from increased wing loading.

Aerodynamic Characteristics

Evaluation of the gust alleviation capability with folded wing tips was conducted for an assumed folding of the outer 40 percent of the wing span. The 40-percent folding corresponds to the maximum allowable for telescoping, and thus permits the folded wing system to be evaluated against a telescoping wing system having the same properties. The alleviation provided by a folded wing configuration, however, is shown to correspond almost directly to the amount of wing folded.

The airplane configuration with 40-percent folding, designated FW, is shown in Figure 64. The projected wing area is 188.5 square feet, a 32-percent reduction from that of the BPA with wing unfolded. FW planform geometry is listed in Table 10.

The lift-curve slope and downwash variations with Mach number are given in Figure 65. Effect of the folded wing tips on geometry and drag of the BPA is shown in Figure 66. The relation between folded and unfolded wing geometric aspect ratios (see Figure 67) is

$$\frac{\mathscr{R}_o}{\mathscr{R}} = 1 + \frac{4 \ (h/b)}{1 + \lambda_o} \tag{38}$$

where subscript o denotes unfolded wing. A more general form of this relation, which allows for partial folding (tip dihedral), is:

$$\frac{\mathscr{R}_o}{\mathscr{R}} = \frac{1 + 4 \ (h/b) \left[\frac{1}{(1 + \lambda_o)} (1 + \lambda_o \cos \Gamma) + (h/b) \cos \Gamma \right]}{\left[1 + 2 \ (h/b) \cos \Gamma \right]^2} \tag{39}$$

where $\mathscr{R}$ is the aspect ratio of the folded wing as projected in the chord plane of the fixed portion of the wing.

Various sizes and shapes of end plates were tested on a straight wing as reported in reference 38. The results indicate relatively little effect on variations in end-plate shape and upper or lower wing surface location. The significant parameter is the ratio of end-plate height to wing span as shown in Figure 62. The effective aspect ratio, $\mathscr{R}_e$, is compared to the geometric aspect ratio, $\mathscr{R}$, of the wing in the chord plane. These results, for aspect ratio effect on wing lift-curve slope, can be used to compare the effective aspect ratio of a folded wing to the geometric aspect ratio of the wing without folding, $\mathscr{R}_o$, as in Figure 63. It is seen that the effective aspect ratio for wings of moderate taper ratio with folded tips is essentially the same as that of the unfolded wing. The wing lift-curve slope then is independent of wing folding when it is based on the projected wing area. This is further coorborated for wing tip dihedral by data in reference 6. As reported therein, a wing with Λ_{LE} = 63 degrees, $\mathscr{R}$ = 3.5, λ = 0.25 and 15 degree dihedral was tested with the outer 40 percent of its semispan drooped at 0 degree, 40 degrees, and 60 degrees relative to the wing chord plane. In each case, the lift-curve slope, based on the projected wing area, was almost precisely the same ($C_{L_\alpha} \cong 0.042$).

Calculated stability derivatives with wings folded are listed in Table 11.

Table 10. FW Planform Geometry With Wings Folded

Wing area	188.5
Aspect ratio	2.12
Taper ratio	0.7
Sweep of c/2	0.0
Airfoil section	64A206
Wing span	19.98
Chord, root	11.1
Chord, tip	7.7
Chord, mean aerodynamic	9.52

Gust Response and Performance

Gust sensitivity of FW is shown in Figure 68 as a function of Mach number for static margins of 5 and 20 percent. Static reduction is 32 percent based on the increase in wing loading. Overall sensitivity reduction for FW is seen to vary from 26 to 33 percent over the speed and static stability range, a variation arising from the change in short-period dynamics. The dynamics are illustrated in Figure 69. Inclusion of SAS would alter these values somewhat, but the change would be slight. Alleviation as provided by a folding-wing configuration can be considered to correspond directly to the amount of folding. A time history of the FW gust response, as obtained during simulation and shown in Figure 70, can be compared to that of the BPA to illustrate the reduction in sensitivity.

The effect of folded wing tips on aircraft range is shown in Figure 71. First, neglecting the weight penalty of a folded-wing configuration, the effect of the change in drag due to wing folding is shown for cruise and dash. This effect is in accordance with equation 12. Secondly, the structural weight penalty, estimated to be 630 pounds for FW, is considered and compensated for by a corresponding decrease in the available fuel. If the 20-minute dash at 0.9 Mach is performed with the wings folded, and the cruise portion of the mission is flown at 0.4 Mach with the wings in their extended position, a 21-percent decrease in aircraft range results.

It should be noted that although folding the wing tips decreases the sensitivity to vertical gusts, the lateral-gust sensitivity is increased because of the larger vertical surface area. Consequently, the net improvement in the aircraft's gust response from the pilot's point of view may not be as great as indicated by consideration of the vertical motions alone.

Table 11. FW Stability Derivatives With Wings Folded

Parameter	Static Margin	Dimensions	Mach Number 0.40	0.55	0.725	0.90
X_u		1/sec	-0.0167	-0.0169	-0.019	-0.026
X_α		fps^2	0.6	-0.5	-3.5	-9.1
M_u	0.05	1/ft-sec	-0.00005	-0.0001	-0.00015	-0.0003
M_u	0.20	1/ft-sec	-0.00022	-0.00037	-0.00062	-0.001
M_α	0.05	1/sec^2	-3.0	-6.0	-11.0	-19.5
M_α	0.20	1/sec^2	-12	-24	-44	-78.5
M_q		1/sec	-0.8	-1.15	-1.65	-2.43
$M_{\dot\alpha}$		1/sec	-0.52	-0.76	-1.27	-2.20
Z_α		fps^2	-340	-675	-1250	-2250
$Z_{\dot\alpha}$		fps	-2.02	-3.0	-4.9	-8.6
Z_u		1/sec	-0.152	-0.12	-0.096	-0.093
Z_q		fps	-3.15	-4.5	-6.5	-9.5
$Z_{\dot\alpha_g}$		fps	1.1	1.5	1.52	0.9
$M_{\dot\alpha_g}$		1/sec	0.28	0.38	0.40	0.24
Z_{δ_E}		fps^2	-100	-200	-380	-690
M_{δ_E}		1/sec^2	-26	-52	-97	-178

TELESCOPING WING

The passive system concept of a telescoping wing is similar to that of the folding wing, but carried a step farther. The telescoping wing retracts a portion of the normal wing tip into the inboard wing contour and thus eliminates its influence on the aircraft's aerodynamic characteristics. The gust alleviating objectives are a decrease of the exposed wing area (increased W/S) and a reduction of wing aspect ratio (decreased C_{L_α}). Application of wing telescoping alters the geometric aspect ratio and wing area in the same manner as wing folding. The geometric aspect ratio in this case is also the effective aspect ratio.

Aerodynamic Characteristics

The BPA with telescoping wing was evaluated for gust alleviation with an assumed telescoping of the outboard 40 percent of the wing span. This allows 20 percent of the wing to house the telescoping mechanism. The altered configuration, designated TW, is shown in Figure 72. The projected wing area is reduced 32 percent to 188.5 square feet as for FW. Planform geometry of TW is listed in Table 12.

The lift-curve slope and downwash variations with Mach number are given in Figure 73. Effect of telescoped wing tips on lift and drag of the BPA is shown in Figure 74.

Estimated performance information for TW is based on the idealized assumption that no discontinuities in the wing contour are required to permit retraction of the wing tip. Test data obtained for a more practical configuration, reference 21, as shown in Figure 75, suggest a decrease in $C_{L_{max}}$ and an increase in drag due to the required wing discontinuities. The effect of the drag increment with tips extended, as suggested by this figure, results in a 1-percent range decrement at 0.4 Mach. It is possible, however, that proper contouring of the wing at the tip juncture or an arrangement of wing fences may largely eliminate the deleterious effects of the discontinuity.

Table 12. TW Planform Geometry With Wings Telescoped

Wing area	188.5
Aspect ratio	2.12
Taper ratio	0.7
Sweep of c/2	0.0
Airfoil section	64A206
Wing span	19.98
Chord, root	11.1
Chord, tip	7.77
Chord, mean aerodynamic	9.52

Calculated stability derivatives and vibration data with wings telescoped are listed in Tables 13 and 14, respectively. The following data apply to this configuration:

$m_1 = 27.698$ slugs $\omega_1 = 98.878$ radians per second

$m_2 = 7.022$ slugs $\omega_2 = 174.026$ radians per second

$g_i = 0.02$ for $i = 1, 2$

Figure 76 gives the fuselage mode shapes in each of the first two airplane modes.

Table 13. TW Stability Derivatives With Wings Telescoped

Parameter	Static Margin	Dimensions	Mach Number 0.40	0.55	0.725	0.90
X_u		$1/\text{sec}$	-0.0197	-0.17	-0.0175	-0.023
X_α		fps^2	-5.1	-6.25	-8.5	-12.0
M_u	0.05	$1/\text{ft-sec}$	-0.00005	-0.00006	-0.0001	-0.00016
M_u	0.20	$1/\text{ft-sec}$	-0.00016	-0.0003	-0.0004	-0.00065
M_α	0.05	$1/\text{sec}^2$	-2.3	-4.2	-8.0	-13.1
M_α	0.20	$1/\text{sec}^2$	-8.9	-17.9	-31.7	-53.0
M_q		$1/\text{sec}$	-0.8	-1.13	-1.66	-2.43
$M_{\dot{\alpha}}$		$1/\text{sec}$	-0.47	-0.65	-1.05	-1.80
Z_α		fps^2	-250	-500	-900	-1500
$Z_{\dot{\alpha}}$		fps	-1.8	-2.5	-4.1	-7.0
Z_u		$1/\text{sec}$	-0.148	-0.112	-0.09	-0.082
Z_q		fps	-3.15	-4.5	-6.45	-9.5
$Z_{\dot{\alpha}_g}$		fps	1.35	1.92	2.40	2.47
$M_{\dot{\alpha}_g}$		$1/\text{sec}$	0.34	0.50	0.63	0.65
Z_{δ_E}		fps^2	-100	-200	-380	-690
M_{δ_E}		$1/\text{sec}^2$	-26	-52.5	-98	-176

Table 14. TW Flexibility Parameters With Wings Telescoped

Parameter	Value	Units	Parameter	Value	Units
$a^R_{1,\,3/m}$	0.10952	ft/slug	$a^I_{1,\,3/m}$	0.59740	ft²/slug
$a^R_{1,\,4/m}$	0.06104	ft/slug	$a^I_{1,\,4/m}$	0.31629	ft²/slug
$a^R_{2,\,3/I_{yy}}$	0.02019	ft²/slug ft²	$a^I_{2,\,3/I_{yy}}$	0.14815	ft³/slug-ft²
$a^R_{2,\,4/I_{yy}}$	0.01706	ft²/slug-ft²	$a^I_{2,\,4/I_{yy}}$	0.08593	ft³/slug-ft²
$a^R_{3,\,1/m}$	-0.686	ft²/slug	$a^I_{3,\,1/m_1}$		
$a^R_{3,\,2/m}$			$a^I_{3,\,2/m_1}$	109.36	ft³/slug
$a^R_{3,\,3/m_1}$	0.98742	ft/slug	$a^I_{3,\,3/m_1}$	8.3665	ft²/slug
$a^R_{3,\,4/m_1}$	0.94930	ft/slug	$a^I_{3,\,4/m_1}$	5.7816	ft²/slug
$a^R_{3,\,7/m_1}$	7.2508	ft²/slug	$a^I_{3,\,7/m}$		
$a^R_{4,\,1/m_2}$	4.667	ft²/slug	$a^I_{4,\,1/m}$		
$a^R_{4,\,2/m_2}$			$a^I_{4,\,2/m_2}$	215.01	ft³/slug
$a^R_{4,\,3/m_2}$	2.0399	ft/slug	$a^I_{4,\,3/m_2}$	17.385	ft²/slug
$a^R_{4,\,4/m_2}$	1.9984	ft/slug	$a^I_{4,\,4/m_2}$	15.328	ft²/slug
$a^R_{4,\,7/m_2}$	13.232	ft²/slug	$a^I_{4,\,7/n_2}$		

Gust Response and Performance

Gust sensitivity of TW is shown in Figure 77 as a function of Mach number for static margins of 5 and 20 percent. Sensitivity reduction on the order of 37 to 47 percent is indicated for the speed and static stability range considered. Inclusion of an SAS would alter these figures only slightly. The short-period dynamics for telescoped wings are illustrated in Figure 78. A time history of the TW gust response as obtained during simulation is shown in Figure 79.

The effect of telescoping the wing tips on aircraft range is shown in Figure 80. The percent changes in range considering drag effects only were determined by means of equation 12.

The higher induced drag with telescoped wing at 0.4 Mach is detrimental to aircraft range, whereas the reduced profile drag at 0.9 Mach results in increased range capability at that speed. A structural weight penalty of 1,200 pounds is associated with the ability to telescope the wings. By reducing the fuel load and maintaining the same 18,000-pound gross takeoff weight, there is a net loss in cruise range of 32 percent even with the wings extended during the cruise portion of the mission. The calculation is based upon the assumption of no discontinuities in wing contour.

VARIABLE SWEEP WING

A variable-sweep wing offers several possibilities for passively reducing gust sensitivity. The wing lift-curve slope can be decreased due to the increase sweep angle of the wing and its reduced aspect ratio. The possibility also exists that the wing area can be reduced by using sweepback. The extent of these changes in any given case depends on the specific technique employed to effect the change in sweep, as well as the geometry of the unswept configuration.

The BPA has been assumed to incorporate variable sweep as shown in Figure 81. This configuration is designated VS_1. A low-aspect-ratio (wide-chord) wing is not a desirable planform for variable sweep purposes and is used here only to facilitate a comparison. In order to illustrate the broader possibilities of variable sweep if applied to a different basic configuration, an alternate approach, designated VS_2, also is considered.

VS_1 requires the addition of a wing glove at the leading edge and a rounded section at the trailing edge of the inboard portion of the wing. Sweep has been limited to 60 degrees of the leading edge for the outboard wing panel and 45 degrees for the glove. The wing geometry of VS_1 is defined in terms of an equivalent conventional wing as shown in Table 15, and the aerodynamic characteristics were determined for this equivalent wing. Variable sweep in this application resulted in an increased wing area in the swept position.

The drag divergence Mach number of VS_1 is estimated to be 0.96 on the basis of the methods of references 1 and 36.

On the basis of the swept-wing area of 324 square feet, it is estimated that $C_{D_o} = 0.0155$ at 0.4 Mach and 0.0160 at 0.9 Mach. The airplane efficiency factor with wing swept back is e = 0.63 throughout the Mach number range of interest. The lift-curve slope and downwash variations with Mach number are shown in Figure 82. Calculated stabil. derivatives and vibration data for VS_1 with wings swept are listed tables 16 and 17, respectively. The following data apply to this configuration.

$m_1 = 34.123$ slugs $\qquad \omega_1 = 98.640$ radians per second

$m_2 = 9.256$ slugs $\qquad \omega_2 = 110.344$ radians per second

$g_i = 0.02$ for $i = 1, 2$

Figure 83 gives the fuselage mode shapes in each of the first two airplane modes.

Table 15. VS_1 Planform Geometry With Wings Swept*

Wing area	324.0
Aspect ratio	2.16
Taper ratio	0.66
Sweep of c/2	47.5
Airfoil section	
Wing span	26.5
Chord, root	14.74
Chord, tip	9.74
Chord, mean aerodynamic	12.38
*VS_1 unswept geometry is as for BPA except for addition of glove and rounded inboard trailing edge	

Table 16. VS_1 Stability Derivatives With Wings Swept

Parameter	Static Margin	Dimensions	0.40	0.55	0.725	0.90
X_u		1/sec	-0.0175	-0.0175	-0.0186	-0.032
X_α		fps^2	-6.5	-7.5	-10.5	-16.6
M_u	0.05	1/ft-sec	-0.00005	-0.00009	-0.00016	-0.0003
M_u	0.20	1/ft-sec	-0.0002	-0.00037	-0.00068	-0.00115
M_α	0.05	$1/sec^2$	-4.0	-7.0	-13.7	-24.0
M_α	0.20	$1/sec^2$	-15.1	-28.7	-55.2	-96
M_q		1/sec	-0.96	-1.36	-1.95	-2.76
$M_{\dot\alpha}$		1/sec	-0.3_	-0.51	-0.85	-1.45
Z_α		fps^2	-350	-700	-1290	-2250
$Z_{\dot\alpha}$		fps	-1.6	-2.4	-3.8	-6.2.
Z_u		1/sec	-0.148	-0.115	-0.095	-0.09
Z_q		fps	-2.91	-3.85	-5.6	-8.54
Z_{α_g}		fps	1.33	1.60	1.80	2.30
$M_{\dot\alpha_g}$		1/sec	0.30	0.45	0.55	0.55
Z_{δ_E}		fps^2	-100	-200	-380	-690
M_{δ_E}		$1/sec^2$	-22.5	-45	-84.5	-154

Table 17. VS_1 Flexibility Parameters With Wings Swept

Parameter	Value	Units	Parameter	Value	Units
$a^R_{1,\,3/m}$	0.08342	ft/slug	$a^I_{1,\,3/m}$	0.27817	ft^2/slug
$a^R_{1,\,4/m}$	0.10066	ft/slug	$a^I_{1,\,3/m}$	0.89412	ft^2/slug
$a^R_{2,\,3/I_{yy}}$	0.02043	ft^2/slug-ft^2	$a^I_{2,\,3/I_{yy}}$	0.13336	ft^3/slug-ft^2

Table 17. (Cont)

Parameter	Value	Units	Parameter	Value	Units
$a^R_{2,\,4}/I_{yy}$	0.00572	$ft^2/slug\text{-}ft^2$	$a^I_{2,\,4}/I_{yy}$	0.08221	$ft^3/slug\text{-}ft^2$
$a^R_{3,\,1}/m_1$	-3.274	$ft^2/slug$	$a^I_{3,\,1}/m_1$		
$a^R_{3,\,2}/m_1$			$a^I_{3,\,2}/m_1$	62.192	$ft^3/slug$
$a^R_{3,\,3}/m_1$	1.1156	$ft/slug$	$a^I_{3,\,3}/m_1$	10.198	$ft^2/slug$
$a^R_{3,\,4}/m_1$	-0.33090	$ft/slug$	$a^I_{3,\,4}/m_1$	-4.1455	$ft^2/slug$
$a^R_{3,\,7}/m_1$	6.5571	$ft^2/slug$	$a^I_{3,\,7}/m_1$		
$a^R_{4,\,1}/m_2$	17.554	$ft^2/slug$	$a^I_{4,\,1}/m_2$		
$a^R_{4,\,2}/m_2$			$a^I_{4,\,2}/m_2$	267.65	$ft^3/slug$
$a^R_{4,\,3}/m_2$	-0.54856	$ft/slug$	$a^I_{4,\,3}/m_2$	-11.036	$ft^2/slug$
$a^R_{4,\,4}/m_2$	1.8394	$ft/slug$	$a^I_{4,\,4}/m_2$	27.265	$ft^2/slug$
$a^R_{4,\,7}/m_2$	0.12725	$ft^2/slug$	$a^I_{4,\,7}/m_2$		

Gust sensitivity of VS_1 is shown as a function of Mach number in Figure 84 for static margins of 5 and 20 percent. With a 5-percent static margin, gust alleviation is on the order of 24 to 29 percent The alleviation is illustrated further by the time history of Figure 85. The short period dynamic characteristics of VS_1 are illustrated in Figure 86.

The effect on the aircraft range is shown in Figure 87. The higher induced drag of the swept version is detrimental at cruise Mach numbers but is outweighed by the profile drag reduction at the dash speed. More economical high speed flight thus is possible with the wings swept back. The 860-pound structural weight penalty of variable sweep, when compensated for by a reduced fuel weight, decreases aircraft range at cruise speed by 21.5 percent in comparison to that of the BPA.

Thick-Wing Performance

A further consideration for a variable-sweep configuration is the elimination of the necessity for a thin wing in high-speed flight. If the wing of VS_1 in the unswept position is increased in thickness from 6 to 12 percent, the structural weight decrease reduces the overall weight penalty to 115 pounds and enables the aircraft to carry a greater fuel load. The range decrease is 9 percent for the thick wing version as opposed to 21.5 percent for the thin-wing VS_1. The range decrement now is due largely to the increased profile drag of the thicker wing. In addition, use of a 12-percent thick wing in the unswept position with the same high-lift devices can increase $C_{L_{max}}$ to 2.10. Takeoff distance over a 50-foot obstacle at a wing loading of 65 is thus reduced from 2000 to 1740 feet. Estimated performance for VS_1 with a 12-percent thick wing was based on the following drag characteristics:

Wings swept back at 0.9 Mach: $C_{D_o} = 0.0186$

$e = 0.755$

Wings unswept at 0.4 Mach: $C_{D_o} = 0.0184$

$e = 0.805$

Alternate Variable Sweep Wing, VS_2

The preceding analysis of variable sweep for gust alleviation purposes can prove to be somewhat misleading because of the limited applicability of this concept to the BPA configuration. In order to indicate the more desirable characteristics achievable by means of variable sweep, an additional, although less extensive, analysis has been made of an alternate configuration. For this purpose, an entirely new wing is incorporated on the basic airplane, as shown in Figure 88, and the configuration is designated VS_2. Table 18 indicates the geometry of VS_2. In order to retain some basis for comparison of this configuration with the BPA, the wing area in the unswept position, excluding the glove, has been maintained at 277 square feet.

The high unswept aspect ratio of VS_2 permits considerable sweepback of the wing while retaining a smooth wing contour for high-speed flight. By comparison with VS_1, the increased sweepback of VS_2 (64 degrees as compared to 47.5 degrees), reduced swept-wing aspect ratio (1.85 to 2 16), and smaller wing area (290 square feet to 324 square feet) are conducive to decreased gust sensitivity. The lift-curve slope of VS_2 in the swept-back condition is estimated as 0.04 at 0.9 Mach. In comparison with the BPA for the same wing loading, $(Z_\alpha)_{VS_2} = 0.45 (Z_\alpha)_{BPA}$. This indicates a gust alleviation potential of 55 percent in contrast to 35 percent for VS_1 calculated on the same basis. Considerations of aircraft dynamics and the turbulence spectrum will reduce these percentages, but the relative comparison should remain substantially the same. Thus a 42-percent sensitivity reduction to 0.030 g's per feet per second is indicated for the pilot station at 0.9 Mach.

Table 18. VS_2 Planform Geometry

	VS_2 (Unswept)	VS_2 (Swept)
Wing area	277.0	290.0
Aspect ratio	7.66	1.85
Taper ratio	0.5	0.66
Sweep of c/2	0.0	64.0
Airfoil section	64A212	
Wing span	46.0	
Chord, root	8.03	
Chord, tip	4.01	
Chord, mean aerodynamic	6.25	

It is estimated that the aircraft structural weight will be 17 percent greater than that of the BPA. A total fuel load of 5450 pounds is permissible within the study takeoff gross weight limit of 18,000 pounds. With a 20-minute dash at 0.9 Mach, the cruise range with wings unswept is estimated to be 13 percent less than that of the BPA.

The wing planform of VS_2 provides improved low-speed performance over the BPA. The thicker wing, in an unswept position, combined with the higher aspect ratio provides a $C_{L_{max}}$ of 2.2 for the same type and relative size of high-lift devices as used on the BPA. Takeoff distance thus can be reduced from 2,000 feet to 1,665 feet for the same gross weight.

Other Design Approaches

Another possible design approach would be to maintain the 2000-foot takeoff distance by decreasing the wing area with the planform of VS_2 unchanged. The resulting configuration will exhibit reduced gust sensitivity and have a reduced structural weight so that its fuel load and range will be greater than that of VS_2. The possible variable sweep designs are sufficiently numerous to require an independent study and are of such a nature that considerable attention to detail is required.

FREE-FLOATING SURFACES

Many gust-alleviating concepts can be classified under the general heading of free-floating, or rotatable, surfaces. This classification covers those systems which can release a portion of the load-carrying wing surface from its rigid continuity with the remainder of the wing and permit it to float freely with the relative wind. The surfaces released can be the trailing-edge flaps, the ailerons, or a portion of the main wing, generally the outer span, specifically constructed to permit freedom of rotation.

A sizeable portion of the wing tips conceivably can be permitted freedom to rotate about a chordwise hinge line at the inboard end of the releasable tip. In calm air, the tips will then tend to float at some known dihedral angle, determined by the balance between the moment due to the weight of the tip and the lift on the tip. The wing tip also may be designed to float freely about a spanwise hinge line ahead of the tip aerodynamic center. In any of these approaches, the basis of the concept is to reduce the load-bearing surface area in the presence of gusts (increased W/S), thus reducing the gust sensitivity. For purposes of analysis, it is more convenient to consider these systems in terms of an effectively decreased lift-curve slope rather than a reduced wing area.

Aerodynamic Characteristics

The lift coefficient of a wing with some portion of its surface deflected can be expressed as

$$C_L = C_{L_\alpha} \alpha + C_{L_\delta} \delta. \tag{40}$$

Then the lift-curve slope with partial surface deflection is

$$(C_{L_\alpha})_\delta = C_{L_\alpha} + C_{L_\delta} (\partial \delta / \partial \alpha). \tag{41}$$

The surface floating angle with angle of attack is determined by the hinge moments acting on the deflected surface,

$$\frac{\partial \delta}{\partial \alpha} = -\frac{C_{H_\alpha}}{C_{H_\delta}} \tag{42}$$

$$(C_{L_\alpha})_\delta = C_{L_\alpha} - C_{L_\delta} (\frac{C_{H_\alpha}}{C_{H_\delta}}). \tag{43}$$

For a full-chord deflectable portion of the wing surface, $C_{H_\alpha}/C_{H_\delta} \cong 1.0$. Except for possible induced flow effects of the fixed portion of the wing, the above ratio is identically 1.0. Then

$$(C_{L_\alpha})_\delta = C_{L_\alpha} - C_{L_\delta}. \tag{44}$$

Examination of test data in reference 26 for a 60-degree delta wing with full-chord deflected tips indicated negligible induced upwash effect of the fixed wing on the flow at the tops (Figure 89 and reference 13). If this is the case for such an extreme configuration, the assumption that $\frac{\partial \delta}{\partial \alpha} = -1$ is acceptable for straight and mildly swept wings.

Under the above conditions, equation 44 is applicable to a free-floating wing tip configuration; and since

$$C_{L_\delta} = C_{L_\alpha} (1 - \alpha_\delta \kappa) \tag{45}$$

and $J_\delta = 1.0$ for a full-chord flap, then

$$C_{L_\delta} = C_{L_\alpha} (1 - \kappa) \tag{46}$$

where κ is almost exclusively a function of the flap span. Agreement of this relation with the data of reference 26 is shown in Figure 89.

The rotating-wing-tip and folded-wing-tip concepts would have identical effects on the wing lift-curve slope, for equal effected wing tip areas, if $C_{L_\delta}/C_{L_\alpha}$ were equal to S_{tip}/S. However, for a wing of 0.5λ the spanwise loading is such that $C_{L_\delta}/C_{L_\alpha} < S_{tip}/S$ so that $S(C_{L_\alpha})_R > S(C_{L_\alpha})_F$.

When partial chord flaps or ailerons are permitted to float freely, their floating angle is determined by the relation expressed in equation 42. Ordinarily $C_{H_\alpha}/C_{H_\delta} < 1.0$ except possibly for a well set-back hinge. With the expression for C_{L_δ} from BPA data,

$$(C_{L_\alpha})_{\delta_F} = C_{L_\alpha} (1 - \alpha_\delta \kappa \frac{C_{H_\alpha}}{C_{H_\delta}}). \tag{47}$$

For gust alleviation purposes, it would be ideally desirable to have $C_{L_\alpha} = 0$ for

$$C_{H_\alpha}/C_{H_\delta} = 1/\alpha_\delta \kappa , \tag{48}$$

a value ordinarily much larger than 1.0. Normally, $C_{H_\alpha}/C_{H_\delta}$ is of the order of 0.5 for trailing-edge devices.

The amount of flap deflection required to counteract the effect of a gust is:

for $\qquad C_{H_\alpha}/C_{H_\delta} = 1.0, \quad \delta_F = \dfrac{w_g/U}{\alpha_\delta \kappa} ;$

for $\quad C_{H_\alpha}/C_{H_\delta} = 0.5, \quad \delta_F = 2\dfrac{w_g/U}{\alpha_\delta\,\kappa}$

In calm air, the drag of a straight wing with a freely-floating tip is similar to that of the same wing with a folded tip of the same size except for additional drag due to the gap at the floating tip-fixed wing juncture. In turbulent air, the oscillations of the floating tip introduce additional drag related to the root-mean-square value of its deflection angle, a function of the distribution and intensity of the turbulence as well as the response characteristics of the tip.

Gust Response and Performance

The maximum achievable reduction in gust sensitivity with tips rotatable about a chordwise hinge line is the same as that of a folded wing. However, since turbulent air encompasses both up and down gusts, the resultant tip action will consist of a limited, and essentially equal, range of deflection angles about its normal position. Small net changes in tip dihedral, about 10 degrees, have relatively little effect upon the overall wing lift. Consequently, this particular concept offers little potential for gust sensitivity reduction.

If the wing tip is designed to float freely about a spanwise hinge, the maximum potential is also the same as for a folded wing. For a given size of wing tip effected in either concept, the same area of wing will be unloaded. However, the presence of the tip, whether in the vertical plane as for the folded wing or the horizontal plane as for the rotating tip, serves to end-plate the remainder of the wing and thus maintains a high effective aspect ratio. The rotating tip can be treated as a full-chord flap, and

$$(C_{L_\alpha})_R = C_{L_\alpha}\,(1 - \kappa) \tag{49}$$

In accordance with the preceding equation, the effective lift-curve slope with different extents of free-floating tips can be calculated. The effective gust alleviation factor, $C_{L_\alpha}S$, is shown in Figure 90 for TW and FW, as well as for floating tips. The telescoping wing which avoids end-plating of the fixed portion of the wing is obviously the most effective. The alleviation factor of the rotating wing tip is very similar to, but slightly less effective than, that of the folded wing as expected. It is also noted that the folded wing will have less drag than a rotating tip

91

of equivalent size. A weight analysis of a 40-percent semispan rotating tip on the BPA indicates a 17-percent increase in the aircraft structural weight in contrast to an 11-percent increase for the folded wing, FW.

The preceding analysis indicates that the rotating-wing-tip concept will provide gust alleviation and aircraft performance somewhat similar, but inferior, to that achievable with a folding wing. The possibility of wing tip flutter also exists.

SPOILERS AND DEFLECTORS

The passive alleviation method of projecting a spoiler or deflector (lower surface spoiler, similar to split flap) from a wing surface will reduce the lift-curve slope of the wing if the projection is at a forward chordwise station of the wing. Spoilers and split flaps in their more commonly used locations, 70 to 80 percent of the wing chord, do not appreciably affect the wing lift-curve slope. The forward located spoiler or deflector induces flow separation from the wing surface behind it, thereby altering the airfoil characteristics and effectively reducing the section lift-curve slope, c_{L_α}.

Aerodynamic Characteristics

Devices which reduce wing lift-curve slope by causing flow separation from the wing also introduce additional drag. Information is presented which permits a reasonable estimate of the minimum drag increment, $(\Delta C_{D_0})_D$, associated with a forward-located spoiler or deflector projection. For the present purpose, it is assumed that the only significant change in the aircraft drag polar due to these devices is an increase in C_{D_0}. It is noteworthy that a spoiler will produce some negative shift of the lift coefficient at which minimum drag occurs, ΔC_{L_0}, whereas a deflector will produce a positive shift.

In order to maintain the lowest possible drag level while achieving maximum gust alleviation, it appears desirable to use a maximum of deflector projection with a minimum of deflector span. The permissible spanwise extent of the deflector as used on the BPA is limited to an inboard location, $0.45\,b_w$, that will not result in excessive buffeting of the tail, and to an outboard location, $0.65\,b_w$, that will not interfere with the effectiveness of the aileron, reference 11. The test data also suggest that the deflector be located well forward on the wing, $x_D/c \cong 0.10$, where its drag contribution is less, but no degradation in gust alleviating capability, ΔC_{L_α}, is apparent. Figure 91 shows the effect of deflectors on lift-curve slope and minimum drag coefficient.

Three-dimensional test data obtained for wings with deflectors at forward wing locations are presented in references 9 through 12. Effective section lift-curve slopes, c_{L_α}, have been determined from these data by accounting for planform and Mach number effects through the use of the convenient charts for the determination of lift-curve slope which are included in reference 14. The results of this analysis are shown in Figures 92 and 93 as the ratio of the two-dimensional lift-curve slopes with and without deflectors present. This ratio is a function of three geometric parameters: the amount of deflector projection, the chordwise location of the deflector, and the spanwise extent of the deflector. Partial spanwise projection is represented by an effective or average section c_{L_α}.

The effect of a deflector on the lift-curve slope of a wing of arbitrary planform can be estimated by using the information in Figures 92 and 93 in the relationship

$$\frac{(C_{L_\alpha})_D}{C_{L_\alpha}} = \frac{a_D}{a}\left[\frac{\frac{\pi\,AR}{a\cos\Lambda} + 1}{\frac{\pi\,AR}{a\cos\Lambda} + \frac{a_D}{a}}\right] \tag{50}$$

where

$$a = \text{section lift-curve slope}$$

$$a_D = \text{section lift-curve slope with deflector projected}$$

$$\Lambda = \text{sweep of wing quarter-chord line}$$

$$C_{L_\alpha} = \text{clean wing lift-curve slope}$$

$$(C_{L_\alpha})_D = \text{wing lift-curve slope with deflector projected}$$

A spoiler or deflector projected normal to a wing surface is, to some extent, comparable to a flat plate fully exposed to an airstream. Drag data for the latter case are presented in reference 24 and shown here in Figure 94. A comparison of deflector drag data from reference 11 indicates similar trends with deflector geometry as with the fully exposed flat plates. The close agreement between the absolute values of drag coefficient for the fully exposed flat plate and the particular comparative case shown in Figure 94 ($x_D/c = 0.35$) must be regarded

as fortuitous in view of the strong influence of deflector chordwise location on the drag increment as indicated in the upper half of the figure. The effect of Mach number on the drag increment due to a deflector is very marked as shown in Figure 95.

The drag increment considered in the preceding paragraph is the increase in minimum drag, $(\Delta C_{D_o})_D$, due to a deflector. Just as for deflection of a trailing-edge flap or spoiler, there is a change in the lift coefficient at which the minimum drag occurs, C_{L_o}, due to deflectors, but the results are somewhat inconsistent. The much higher Reynolds numbers of flight will considerably reduce this C_{L_o} shift due to deflectors. This effect is neglected in the present analysis, but it should be noted that the positive shift due to a deflector will prove more favorable for the maintenance of the lowest possible in-flight drag than the negative shift due to a spoiler.

Larger changes in wing lift-curve slope can be obtained with combinations of spoilers, slots, and deflectors than with deflectors alone. However, increased drag penalties also accrue, and these effects apparently are consistent with the effects of the deflector alone and can be determined by extrapolation of the deflector data already presented as shown in Figure 96.

Gust Response and Performance

Gust sensitivity comparison of the BPA with and without deflectors projected is limited to consideration of the parameter Z_α/gU, which is a direct function of the changes in lift-curve slope. The comparison is shown in Figure 97. Changes in aircraft dynamics and flexibility characteristics will have only a small effect on the relative sensitivity levels indicated by this simplified comparison. The reduction in gust sensitivity of the BPA due to deflector projection is obviously small.

The large increments in drag associated with deflector projection limit the maximum sea-level flight Mach number as shown in Figure 98.

Large decrements in aircraft range capability are seen as a consequence of the drag introduced by the deflectors. The indications are that reduced maximum flight speeds and large decreases of aircraft range will result, with relatively little reduction in sensitivity.

The use of deflectors and associated devices is detrimental to aircraft stability. Typical increments in the longitudinal stability parameter, C_{M_α}, due to the use of these devices in wind tunnel tests, are shown in Figure 99.

The preceding discussion has been based upon information available for forward-located deflectors. The same conclusions are generally applicable to similarly located spoilers or combinations of these devices, with or without associated slots in the wing. It is evident from symmetry that either a spoiler or a deflector, of similar size and location on a wing will provide identical reductions in C_{L_α} and increments in C_{D_o}.

CHORDWISE WING SLOTS

The concept of chordwise slots opened at one or more spanwise stations along the wing is discussed in references 19, 20, and 42. Simplifying assumptions made in developing the theory, and the lack of knowledge concerning viscous effects and slot structural carry-through interference effects, suggest that theoretical results be viewed with caution.

The opening of chordwise slots at one or more stations along the wing span permits air flow from the lower to the upper wing surface at the slot when the aircraft is in level flight. The result is a local equalization of pressure similar to that normally occurring at the wing tip. In that respect, it also is similar to an aspect ratio reduction. The wing is effectively divided into wing segments, each of reduced aspect ratio, leading to a net decrease in wing lift-curve slope. The theory indicates the possibility of about 20-percent gust alleviation for an aircraft such as the BPA on the basis of lift-curve slope reduction alone.

Associated with the effect of chordwise wing slots on lift will be some drag increase and stability changes. These effects depend considerably upon the contouring of the slots and the exposed carry-through wing structure. In addition, operating mechanisms are required to effect slot opening and closure, and some wing weight increase is required to compensate for structural deficiencies at the slots.

There is no information available either to corroborate or to negate the theoretical conclusions concerning chordwise slots.

AIRJET SPOILERS

Consideration is given to spoilers, consisting of airjets from the wing surface, to serve as gust alleviators in references 19 and 20. The presentation in these references is based on admittedly limited information. Indications are given of reasonable promise for this system when it is considered in place of mechanical spoilers. The air requirements for a jet system acting in the same manner as mechanical spoilers or deflectors are not known but are expected to be inordinately high, especially for high flight dynamic pressures. The effect of an airjet deflector on the wing aerodynamic characteristics is the same as that of a mechanical spoiler; that is, any decrease in lift-curve slope due to wing flow spoilage will be accompanied by the same large drag increases which prove so detrimental to aircraft performance in the case of the mechanical deflectors. In view of the high drag penalty and the appreciable engine power bleed required, as well as the relatively more complex ducting and nozzle requirements of a blowing system, it appears likely that an airjet spoiler or deflector system would be less attractive than the relatively unattractive mechanical deflector system.

PASSIVE SYSTEM EVALUATION

Alleviation

Of the passive systems investigated in this study, only those involving major in-flight alterations of wing geometry provide significant alleviation without prohibitive penalities in performance. Some of the characteristics of telescoping wing, folding wing, and variable-sweep wing, the three most promising systems, are summarized here.

The rigid-body sensitivities for the passive systems are shown in Figure 100 as a function of Mach number. The alleviation afforded at the pilot station by these systems is indicated in Figure 101 in terms of the normalized vertical-acceleration power spectral density. Only VS_1 is indicated as a variable-sweep configuration in these figures. Alleviation obtainable with the alternate configuration, VS_2, has only been estimated and is expected to provide greater than 40-percent alleviation based on rms values and approximately a 50-percent reduction in PSD peak.

Notice that alleviation as provided by passive systems does not result in the high-frequency power exhibited by active systems. The result of passive systems incorporation is simply to provide a less sensitive airframe, with little or no side effects other than those caused by increased weight. Primary load reduction occurs at the short-period frequency, and increased loading at other frequencies is not in evidence.

The variable-sweep and telescoping-wing systems provide better alleviation than a folding wing, a fact attributed to the wing end-plating effect with the latter. Each of the passive systems should be employed optimally only at high speed to avoid large induced drag penalties, but these systems do provide capability for alleviation at low speed.

Pilot Tolerance and Endurance

The pilot endurance probability at the dash condition with a mean weight vehicle is shown in Figure 102 for the three configurations. It is seen that the dash portion of the mission can be accomplished at normal pilot proficiency more than 80 percent of the time.

The system alleviation capabilities are illustrated further in terms of pilot behavior in Figure 103.

Performance, Stability, and Control

Significant degradation in aircraft range is a by-product of passive system incorporation, resulting primarily from the large weight penalty. As has been shown, a thick-wing version of the BPA can result in a relatively small weight penalty, one comparable to active systems. A 9-percent range degradation at dash speed has been estimated for this configuration, due primarily to the increased profile drag. The significant point to be made is that range penalties of this order of magnitude or less are achievable with detailed design effort.

Longitudinal stability and control characteristics are not significantly altered by passive system incorporation. Stability augmentation should be provided regardless of gust alleviation for meeting of military requirements. Lateral stability is altered with a passive system but poses no problems not capable of being handled by a lateral SAS. It has been shown that a variable-sweep configuration allows for the possible reduction of takeoff distance.

Structural Effects

The weight penalties caused by passive system incorporation are tabulated in the next section. Passive systems exhibit little effect on structural mode vibrations, with the exception of a swept-wing configuration. The latter has a stabilizing effect on vehicle flexibility and reduces the resulting vibrations.

Equipment Considerations

The weight penalties, production costs, and MTBF's of the passive systems are summarized in Table 19. System weight penalties exceed those of active systems with the exception of a thick-wing variable-sweep configuration. Though the wing thickness of the other configurations could be altered to provide a decrease in weight, the critical Mach number would be lowered so that no range advantage would accrue over

the thinner wing. System costs are comparable to those of active systems. Reliability exceeds that of active systems since operation occurs as little as two times per flight, whereas active system operation is necessarily continuous.

The hydromechanical subsystems of the general configuration shown in Figure 104 provide the necessary passive system reconfiguration. Maintenance of the folding-wing system will be limited primarily to periodic seal replacement. The telescoping and variable-sweep wing systems might additionally require a significant amount of attention to the bearing and track assembly. Bearing replacement would be periodic, and adjustments of the track to maintain tolerance of fit could be performed as required. Fail-safety requirements are less stringent than those of an active system. Fail-safety during reconfiguration could be provided with a series of mechanical pins which allow the wings to be reconfigured only on a synchronized basis. Failure in the normal configuration, though resulting in possible mission abortion, should cause no loss of the aircraft. Failure in the alleviating configuration could be significant, necessitating excessive fuel consumption and high-speed landing.

Table 19. Passive System Weight, Cost, and Reliability

System	Total Weight Penalty (Pounds)	*Estimated Production Cost	**Mean Time Before Failure (Flight Hours)
Telescoping wing	1200	1.023	3,200,000
Folding wing	630	1.005	3,200,000
Variable sweep wing (Thin wing VS$_1$)	860	1.016	4,000,000
Variable sweep wing (Thick wing VS$_1$)	115	1.012	4,000,000
Variable sweep wing (VS$_2$)	860	-	4,000,000

*Normalized to BPA cost of 1.000 for 200 production units

**Reliability based on operation twice per flight and no failure in tracks or bearings

Conclusions

Of the passive systems investigated, it is concluded that only the variable sweep configuration is feasible as a gust alleviator. The folding- and telescoping-wing configurations result in too great a range penalty.

Although all the promising characteristics of a swept-wing design have not been demonstrated with the same configuration (i.e., best alleviation was illustrated with VS_2, while low cost and light weight were exhibited by a thick wing VS_1), the study results do allow the conclusion that a swept-wing version is feasible. The possible design approaches to a variable-sweep-wing aircraft are myriad, and it is believed that with sufficient study, a design capable of combining the better features can be achieved. Since considerable attention to detail is required, it is recommended that an independent study of variable-sweep-wing designs be conducted.

The swept wing, in order to provide sufficient range capability, is utilized optimally only at high speed, a fact that makes it somewhat less attractive than an active system. However, the probability of encountering intolerable atmospheric conditions at low speed is small, and alleviation at high speed only may be considered satisfactory. The swept wing does provide a degree of mission versatility, since if the range penalty is acceptable during a particular mission, then wings can be swept during cruise. The unattractive feature, when comparison is made to the active acceleration system, remains in the presence of a range penalty even with wings swept at high speed only. The variable sweep is more attractive than any active system from cost and reliability standpoints.

APPENDIX VI. EQUATIONS OF MOTION

RIGID AIRFRAME EQUATIONS

The aircraft three-degree-of-freedom equations of motion are rigid-body perturbation equations; i.e., steady-state terms have been subtracted and the variables are perturbation values from a steady-state reference. The force and moment derivatives have been developed separately for wing-body and tail contributions for most of the derivatives. Stability axis derivatives have been assumed and the force equations (drag and lift) are written in the stability axis system. although for small angles of attack, very little difference exists between the equations for stability and body axes. Axis system and sign conventions are illustrated in Figure 105.

The effects of the gust are treated separately for the wing and the tail. In addition, the effect of the gust alleviation device (flap) on the tail is included. Lift, drag, and moment terms are included that can be applied to any gust alleviation device employed. Many of the unimportant or negligible forces and moment terms have been dropped out to simplify the equations.

The airframe perturbation equations of motion as employed in this study are:

Drag (stability axis)

$$\dot{u} + g\theta \cos \gamma_o = \sum_{i=0}^{m} X_i + \cos \xi \, T_u u$$

Lift (stability axis)

$$\dot{\alpha} U_o - q U_o + g\theta \sin \gamma_o = \sum_{i=0}^{m} Z_i - \sin \xi \, T_u u$$

Moment (body axis)

$$\dot{q} = \sum_{i=0}^{m} M_i + \frac{Z_T m}{I_{yy}} T_u u$$

where

u, θ, and α are perturbation values.

If ξ and Z_T are assumed to be 0 in these equations,

$$\cos \xi\, T_u u = T_u u$$

$$\sin \xi\, T_u u = 0$$

$$\frac{Z_T m}{I_{yy}} T_u u = 0 \; .$$

The terms $g\,\theta \cos \gamma_0$ and $g\,\theta \sin \gamma_0$ account for the perturbation of the gravity component from an initial position, γ_0.

The development of the force and moment terms X_i, Z_i, and M_i follows.

Aerodynamic Force Terms in the X Direction

The aerodynamic force terms in the X direction are

$$X_i = X_u u + X_{\dot{u}} \dot{u} + X_\alpha \alpha + X_\alpha \frac{w}{U} + X_{\dot{\alpha}} \dot{\alpha} + X_{\dot{\alpha}} \frac{\dot{w}}{U} + X_q q +$$

$$X_{\dot{q}} \dot{q} + X_{\delta_E} \delta_E + X_{\dot{\delta}_E} \delta_E + X_{\delta_F} \delta_F + X_{\dot{\delta}_F} \delta_F$$

Derivatives that are neglected because they are small are

$$X_{\dot{u}}, \; X_{\dot{\alpha}}, \; X_q, \; X_{\dot{q}}, \; X_{\delta_E}, \; X_{\dot{\delta}_E}, \; \text{and } X_{\dot{\delta}_F}$$

The remaining terms are

$$X_i = X_u u + X_\alpha \left(\alpha + \frac{w}{U}\right) + X_{\delta_F} \delta_F$$

In the above equation, no separation of wing-body and tail derivatives is required, since tail-drag terms are small compared to wing-body terms. X_u and X_α may be considered to be complete (tail-on) airplane derivatives.

X_{δ_F} is retained, since flaps are used as the gust alleviation device and the drag is appreciable.

Aerodynamic Force Terms in the Z Direction

Force terms in the Z direction are

$$Z_1 = Z_u u + Z_{\dot{u}}\dot{u} + Z_\alpha \alpha + Z_{\alpha_g}\frac{w_g}{U} + Z_{\dot{\alpha}}\dot{\alpha} + Z_{\dot{\alpha}_g}\frac{\dot{w}_g}{U} +$$

$$Z_q q + Z_{\dot{q}}\dot{q} + Z_{\delta_E}\delta_E + Z_{\dot{\delta}_E}\dot{\delta}_E + Z_{\delta_F}\delta_F + Z_{\dot{\delta}_F}\dot{\delta}_F$$

The following derivatives are neglected since they are small:

$$Z_{\dot{u}}, \quad Z_{\dot{q}}, \quad Z_{\dot{\alpha}_g}, \quad \text{and } Z_{\dot{\delta}_F} \quad .$$

The wing-body and tail contributions to the derivatives,

$$Z_\alpha, \quad Z_{\dot{\alpha}}, \quad Z_q, \quad \text{and } Z_{\delta_F} \quad ,$$

are separated to account for the time lag for the gust disturbance and the downwash variations to reach the tail.

The development of the tail contributions to the appropriate derivatives follows.

The angle of attack at the tail is:

$$\alpha_T = \alpha - \epsilon = \alpha - \partial\epsilon/\partial\alpha \; \alpha \quad \text{(straight flight)}$$

(fixed incidence of tail with respect to α is 0).

The angle of attack at the tail at any given time, t, during unsteady conditions can be given by

$$\alpha_T(t) = (\alpha)_t - (\partial\epsilon/\partial\alpha \, \alpha)_{t+\Delta t} + (\alpha_g)_{t+\Delta t} - (\partial\epsilon/\partial\alpha \, \alpha_g)_{t+\Delta t} -$$

$$(\partial\epsilon/\partial\delta_F \, \delta_F)_{t+\Delta t} + (q^1{}_T/U)_t$$

where subscript t refers to the value of the term at time t and subscript t + Δt refers to the value of the term at time t + Δt, where Δt is positive.

The term $(ql_T/U)_t$ accounts for the induced angle of attack due to airplane pitch rate.

The above expression can be rewritten with the exponential operator $e^{-\Delta ts}$ (pure time lag) used to account for the time lagged terms.

$$\alpha_T(t) = (\alpha)_t - (\partial\epsilon/\partial\alpha\,\alpha)\,e^{-\Delta ts} + \alpha_g\,e^{-\Delta ts} - (\partial\epsilon/\partial\alpha\,\alpha_g)\,e^{-\Delta ts} -$$

$$(\partial\epsilon/\partial\delta_F\,\delta_F)\,e^{-\Delta ts} + (ql_T/U)_t$$

where

$$s = \frac{d}{dt}$$

Further, $e^{-\Delta ts}$ can be expanded in a power series to

$$e^{-\Delta ts} = 1 - \Delta ts + \frac{\Delta t^2 s^2}{2!} + \frac{\Delta t^3 s^3}{3!} + \ldots$$

The first two terms can represent the operator sufficiently, and can even give more accurate vehicle response results than the use of $e^{-\Delta ts}$ in some cases.

The time lag, Δt, is the time for an airflow disturbance to travel from the wing to the tail.

$\Delta t = l_T/U$, where l_T is the tail arm.

Rewriting the expression for tail angle of attack and using $e^{-\Delta ts} = 1 - \Delta ts$

$$\alpha_T(t) = \alpha - \partial\epsilon/\partial\alpha\,\alpha\,(1 - l_T/Us) + \alpha_g\,(1 - l_T/Us) - \partial\epsilon/\partial\alpha\,\alpha_g\,(1 - l_T/Us) -$$

$$\partial\epsilon/\partial\delta_F\,\delta_F\,(1 - l_T/Us) + ql_T/U \; ;$$

or

$$\alpha_T(t) = \alpha - \partial\epsilon/\partial\alpha \ \alpha + \partial\epsilon/\partial\alpha \ \dot\alpha \ l_T/U + \alpha_g - \dot\alpha_g \ l_T/U - \partial\epsilon/\partial\alpha \ \alpha_g +$$

$$\partial\epsilon/\partial\alpha \ \alpha_g \ l_T/U - \partial\epsilon/\partial\delta_F \ \delta_F + \partial\epsilon/\partial\delta_F \ \delta_F \ l_T/U + q \ l_T/U .$$

Rearranging and multiplying and dividing all rate terms by $\bar{c}/2U$

$$\alpha_T(t) = \alpha(1 - \partial\epsilon/\partial\alpha) + \partial\epsilon/\partial\alpha \ (\frac{\dot\alpha \bar{c}}{2U}) \frac{2 l_T}{\bar{c}} + \alpha_g \ (1 - \partial\epsilon/\partial\alpha) - (\frac{\dot\alpha_g}{2U}) \frac{\bar{c} \ 2 l_T}{\bar{c}}(1 - \partial\epsilon/\partial\alpha)$$

$$= \partial\epsilon/\partial\delta_F \ \delta_F + \partial\epsilon/\partial\delta_F \ (\frac{\delta_F \bar{c}}{2U}) \frac{2 l_T}{\bar{c}} + (\frac{q \bar{c}}{2U}) \frac{2 l_T}{\bar{c}}$$

The lift on the tail for unsteady conditions can be given by

$$(C_L)_T = C_{L_{\alpha_T}} \ \alpha_T(t), \ \delta_E, \ (C_{L_o})_T \text{ and } \epsilon_o = 0$$

$$(C_L)_T = C_{L_{\alpha_T}} \left[\alpha \ (1 - \partial\epsilon/\partial\alpha) + \partial\epsilon/\partial\alpha \ (\frac{\dot\alpha \bar{c}}{2U}) \frac{2 l_T}{\bar{c}} + \right.$$

$$\alpha_g \ (1 - \partial\epsilon/\partial\alpha) - (\frac{\dot\alpha_g}{2U}) \frac{\bar{c} \ 2 l_T}{\bar{c}} \ (1 - \partial\epsilon/\partial\alpha) -$$

$$\left. \partial\epsilon/\partial\delta_F \ \delta_F + \partial\epsilon/\partial\delta_F \ (\frac{\delta_F \bar{c}}{2U}) \frac{2 l_T}{C} + (\frac{q \bar{c}}{2U}) \frac{2 l_T}{\bar{c}} \right] .$$

It is assumed that $d\,t/dt$ will never be high enough to require the use of the unsteady aerodynamic lift-curve slope.

The tail derivatives are obtained from the above expression as follows:

$$(\partial C_L/\partial\alpha)_T = C_{L_{\alpha_T}} \ (1 - \partial\epsilon/\partial\alpha) = (C_{L_\alpha})_T$$

$$\left[\frac{\partial C_L}{\partial\left(\frac{\dot{\alpha}\bar{c}}{2U}\right)}\right]_{-T} = C_{L_{\alpha_T}} \partial\epsilon/\partial\alpha \frac{2l_T}{\bar{c}} = (C_{L_{\dot{\alpha}}})_T$$

$$(\partial C_L/\partial\alpha_g)_T = C_{L_{\alpha_T}}(1 - \partial\epsilon/\partial\alpha) = (C_{L_\alpha})_T$$

$$(\partial C_L/\partial\delta_F)_T = C_{L_{\alpha_T}} \partial\epsilon/\partial\delta_F = (C_{L_{\delta_F}})_T$$

$$\left[\frac{\partial C_L}{\partial\left(\frac{q\bar{c}}{2U}\right)}\right]_T = C_{L_{\alpha_T}} \frac{2l_T}{\bar{c}} = (C_{L_q})_T$$

In dimensional derivative form,

$$(Z_\alpha)_T = -\frac{\rho SU^2}{2m}(C_{L_\alpha})_T$$

$$(Z_{\dot{\alpha}})_T = -\frac{\rho SU\bar{c}}{4m}(C_{L_{\dot{\alpha}}})_T$$

$$(Z_{\alpha_g})_T = -\frac{\rho SU^2}{2m}(C_{L_\alpha})_T = (Z_\alpha)_T$$

$$(Z_q)_T = -\frac{\rho SU\bar{c}}{4m}(C_{L_q})_T$$

$$(Z_{\delta_F})_T = -\frac{\rho SU^2}{2m}(C_{L_{\delta_F}})_T \quad .$$

The wing-body derivatives can then be included to give complete airplane derivatives:

$$Z_{\delta_F} = (Z_{\delta_F})_W + (Z_{\delta_F})_T$$

105

$$Z_q = (Z_q)_W + (Z_q)_T$$

$$Z_\alpha = (Z_\alpha)_W + (Z_\alpha)_T$$

$$Z_{\dot\alpha} = (Z_{\dot\alpha})_W + (Z_{\dot\alpha})_T$$

$$Z_{\alpha_g} = (Z_{\alpha_g})_W + (Z_{\alpha_g})_T = (Z_\alpha)_W + (Z_\alpha)_T$$

The total aerodynamic force along the Z axis is then

$$Z_i = Z_u u + \left[(Z_\alpha)_W + (Z_\alpha)_T\right]\left[\sigma + \frac{w_g}{U}\right] + \left[(Z_{\dot\alpha})_W + (Z_{\dot\alpha})_T\right]\dot\alpha +$$

$$\left[(Z_q)_W + (Z_q)_T\right]q + Z_{\delta_E}\delta_E + \left[(Z_{\delta_F})_W + (Z_{\delta_F})_T\right]\delta_F$$

Aerodynamic Moment Terms About Y Axis

Aerodynamic moment terms about Y axis are:

$$M_i = M_u u + M_{\dot u}\dot u + M_q q + M_{\dot q}\dot q + M_\alpha \alpha + M_\alpha \frac{w_g}{U} + M_{\dot\alpha}\dot\alpha +$$

$$M_{\dot\alpha_g}\frac{w_g}{U} + M_{\delta_E}\delta_E + M_{\dot\delta_E}\dot\delta_E + M_{\delta_F}\delta_F + M_{\dot\delta_F}\dot\delta_F$$

The following derivatives are neglected since they are small;

$$M_{\dot u}, \ M_{\dot q}, \ \text{and } M_{\dot\delta_E}$$

The wing-body and tail contributions to the derivatives

$$M_\alpha, \ M_{\dot\alpha}, \ M_{\alpha_g}, \ M_{\dot\alpha_g}, \ M_{\delta_F}, \ M_{\dot\delta_F}, \ \text{and } M_q$$

are separated for the same reason and in the same manner as the corresponding Z_i derivatives.

The moment resulting from the tail for unsteady conditions can be given by

$$(C_M)_T = C_{M_{\alpha_T}} \alpha_T(t), \quad \delta_E, \quad C_{M_o} \text{ and } \epsilon_o = 0 \quad .$$

Substituting the expression for $\alpha_T(t)$ developed for the Z_i derivatives,

$$(C_M)_T \quad C_{M_{\alpha_T}} = \left[\alpha(1 - \partial\epsilon/\partial\alpha) + \partial\epsilon/\partial\alpha \left(\frac{\dot{\alpha}\bar{c}}{2U}\right) \frac{2l_T}{\bar{c}} + \alpha_g(1 - \partial\epsilon/\partial\alpha) - \right.$$

$$\left(\frac{\dot{\alpha}_g \bar{c}}{2U}\right) \frac{2l_T}{\bar{c}}(1 - \partial\epsilon/\partial\alpha) - \partial\epsilon/\partial\delta_F \, \delta_F +$$

$$\left. \partial\epsilon/\partial\delta_F \left(\frac{\dot{\delta}_F \bar{c}}{2U}\right) \frac{2l_T}{\bar{c}} + \left(\frac{q\bar{c}}{2U}\right) \frac{2l_T}{\bar{c}} \right]$$

The tail moment derivatives are then obtained from the above expression:

$$(\partial C_M/\partial\alpha)_T = C_{M_{\alpha_T}} (1 - \partial\epsilon/\partial\alpha) = (C_{M_\alpha})_T$$

$$\left[\frac{\partial C_M}{\partial \left(\frac{\dot{\alpha}\bar{c}}{2U}\right)} \right]_T = C_{M_{\alpha_T}} \partial\epsilon/\partial\alpha \, \frac{2l_T}{\bar{c}} = (C_{M_{\dot{\alpha}}})_T$$

$$(\partial C_M/\partial\alpha_g)_T = C_{M_{\alpha_T}} (1 - \partial\epsilon/\partial\alpha) = (C_{M_\alpha})_T$$

$$\left[\frac{\partial C_M}{\partial\left(\frac{\dot{\alpha}_g \bar{c}}{2U}\right)} \right]_T = -C_{M_{\alpha_T}} (1 - \partial\epsilon/\partial\alpha) \frac{2l_T}{\bar{c}} = -(C_{M_q})_T + (C_{M_{\dot{\alpha}}})_T$$

$$(\partial C_M/\partial\delta_F)_T = -C_{M_{\alpha_T}} \partial\epsilon/\partial\delta_F = (C_{M_{\delta_F}})_T$$

$$\left[\frac{\partial C_M}{\partial \left(\frac{\delta_F \bar{c}}{2U}\right)}\right]_T = C_{M_{\alpha_T}} \partial \epsilon / \partial \delta_F \frac{2l_T}{\bar{c}} = (C_{M_q})_T \partial \epsilon / \partial \delta_F$$

$$\left[\frac{\partial C_M}{\partial \left(\frac{q\bar{c}}{2U}\right)}\right]_T = C_{M_{\alpha_T}} \frac{2l_T}{\bar{c}} = (C_{M_q})_T$$

The wing-body derivatives can then be included to give complete air-plane moment derivatives:

$$M_\alpha = (M_\alpha)_W + (M_\alpha)_T$$

$$M_{\dot\alpha} = (M_{\dot\alpha})_W + (M_{\dot\alpha})_T$$

$$M_{\alpha_\delta} = (M_{\alpha_\delta})_W + (M_{\alpha_\delta})_T = (M_\alpha)_W + (M_\alpha)_T$$

$$M_{\dot\alpha_\delta} = (M_{\dot\alpha_\delta})_W + (M_{\dot\alpha_\delta})_T = (M_{\dot\alpha})_W + \left[(M_{\dot\alpha})_T - (M_q)_T\right]$$

$$M_{\delta_F} = (M_{\delta_F})_W + (M_{\delta_F})_T$$

$$M_{\dot\delta_F} = (M_{\dot\delta_F})_W + (M_{\dot\delta_F})_T = (M_{\dot\delta_F})_W + (M_q)_T \,^\epsilon\delta_F$$

$$M_q = (M_q)_W + (M_q)_T$$

The total aerodynamic moment input to pitching acceleration is

$$M_i = M_u u + \left[(M_\alpha)_W + (M_\alpha)_T\right]\left[\alpha + \frac{w_g}{U}\right] + \left[(M_{\dot\alpha})_W + (M_{\dot\alpha})_T\right]\dot\alpha +$$

$$\left[(M_{\dot\alpha})_W + (M_{\dot\alpha})_T - (M_q)_T\right]\frac{\dot{w}_g}{U} + \left[(M_q)_W + (M_q)_T\right]q + M_{\delta_E}\delta_E +$$

$$\left[(M_{\delta_F})_W - (M_{\delta_F})_T\right]\delta_F + \left[(M_{\dot\delta_F})_W + (M_{\dot\delta_F})_T\right]\dot\delta_F$$

The three equations are now rewritten within the previous assumptions and with angles and angular rates in degree units but derivatives in radian units.

$$\dot{u} + g \frac{\theta}{57.3} \cos \gamma_0 - X_u u + X_\alpha \left(\frac{\alpha}{57.3} + \frac{w_g}{U} \right) + X_{\delta_F} \frac{\delta_F}{57.3} + T_u u$$

$$\frac{\dot{\alpha} U}{57.3} - \frac{Uq}{57.3} + g \frac{\theta}{57.3} \sin \gamma_0 - Z_u u + \left[(Z_\alpha)_W + (Z_\alpha)_T \right] \left[\frac{\alpha}{57.3} + \frac{w_g}{U} \right] +$$

$$\left[(Z_{\dot{\alpha}})_W + (Z_{\dot{\alpha}})_T \right] \frac{\dot{\alpha}}{57.3} + \left[(Z_{\delta_F})_W + (Z_{\delta_F})_T \right] \frac{\delta_F}{57.3} +$$

$$\left[(Z_q)_W + (Z_q)_T \frac{q}{57.3} \right] + Z_{\delta_E} \frac{\delta_E}{57.3}$$

$$\dot{q} = M_u u + \left[(M_\alpha)_W + (M_\alpha)_T \right] \left[\frac{\alpha}{57.3} + \frac{w_g}{U} \right] + \left[(M_{\dot{\alpha}})_W + (M_{\dot{\alpha}})_T \right] \frac{\alpha}{57.3} +$$

$$\left[(M_{\dot{\alpha}})_W + (M_{\dot{\alpha}})_T - (M_q)_T \right] \frac{\dot{w}_g}{U} + \left[(M_q)_W + (M_q)_T \right] \frac{q}{57.3} +$$

$$M_{\delta_E} \frac{\delta_E}{57.3} + \left[(M_{\delta_F})_W + (M_{\delta_F})_T \right] \delta_F + \left[(M_{\dot{\delta}_F})_W + (M_q)_T \delta_F \right] \dot{\delta}_F$$

FLEXIBILITY EQUATIONS

The equations of motion of a flexible airplane can be written in generalized form as

$$m_r \ddot{\xi}_r = \Xi_r$$

$$m_i \ddot{\xi}_i = g_i \omega_i m_i \dot{\xi}_i + \omega_i^2 m_i \xi_i = \Xi_i$$

where r = 1...6 designate the six rigid-body degrees of freedom and i = 1...refer to the elastic degrees of freedom. Assuming that the airplane flexibility can be represented adequately by two vibration modes, the longitudinal equations of motion can be written

$$m\ddot{X} = \Sigma F_X$$

$$m\ddot{Z} = \Sigma F_Z$$

$$I_{yy}\ddot{\theta} = \Sigma M_\theta$$

$$m_i\ddot{\zeta}_i = g_i\omega_i \quad m_i\dot{\zeta}_i = \omega_i^2 \quad m_i\zeta_i = \Xi_i \quad i = 1,2$$

Since the rigid-body equations have been presented already, only the flexibility-correction terms to the rigid-body equations and the two model equations will be given here. The detail form of the equation is

$$\dot{U} + g\frac{\theta}{57.3}\cos\gamma_o = \text{(rigid terms)}$$

$$\frac{\dot{\alpha}}{57.3}U - \frac{\dot{\theta}}{57.3}U + g\frac{\theta}{57.3}\sin\gamma_o = \text{(rigid terms)} - q\frac{a^R_{1,3}}{m}\xi_1$$

$$-q\frac{a^R_{1,4}}{m}\xi_2 = q/U\frac{a^I_{1,3}}{m}\dot{\xi}_1 - q/U\frac{a^I_{1,4}}{m}\dot{\xi}_2$$

$$\frac{\ddot{\theta}}{57.3} = \text{(rigid terms)} - q\frac{a^R_{2,3}}{Iyy}\xi_1 - q\frac{a^R_{2,4}}{Iyy}\xi_2 - q/U\frac{a^I_{2,3}}{Iyy}\xi_1 - q/U\frac{a^R_{z,y}}{Iyy}\dot{\xi}_2$$

$$\ddot{\xi}_1 = -g_1\omega_1\dot{\xi}_1 - \omega_1^2\xi_1 - q\frac{a^R_{3,1}}{m_1}\frac{\alpha}{57.3} - q\frac{a^R_{3,3}}{m_1}\xi_1 -$$

$$q\frac{a^R_{3,4}}{m_1}\xi_2 - q/U\frac{a^I_{3,2}}{m_1}\frac{\dot{\theta}}{57.3} - q/U\frac{a^I_{3,3}}{m_1}\dot{\xi}_1 -$$

$$q\frac{a^R_{3,7}}{m_1}\frac{\delta_E}{57.3} - q\frac{a^R_{3,8}}{m_1}\frac{\delta_F}{57.3} - q/U\frac{a^I_{3,4}}{m_1}\dot{\xi}_2$$

$$\ddot{\xi}_2 = -g_2 \omega_2 \dot{\xi}_2 - \omega_2^2 \xi_2 - q \frac{a^R_{4,1}}{m_2} \frac{a}{57.3} - q \frac{a^R_{4,3}}{m_2} \xi_1 -$$

$$q \frac{a^R_{4,4}}{m_2} \xi_2 - q/U \frac{a^I_{4,2}}{m_2} \frac{\dot{\theta}}{57.3} - q/U \frac{a^I_{4,3}}{m_2} \dot{\xi}_1 -$$

$$q/U \frac{a^I_{4,4}}{m_2} \dot{\xi}_2 - q \frac{a^R_{4,7}}{m_2} \frac{\delta_E}{57.3} - q \frac{a^R_{4,8}}{m_2} \frac{\delta_F}{57.3}$$

These equations apply to the BPA and to all passive systems.

SENSOR EQUATIONS

The linear acceleration at any fuselage station is determined from

$$\ddot{Z}_{FS} = \dot{Z}_{cg} - (X_{cg} - X_{FS}) \ddot{\theta}_{cg} + \sum_{i=1}^{2} \phi_{i_{FS}} \ddot{\xi}_i \quad .$$

The pitch velocity sensed by a rate gyro at any fuselage location is given by

$$\dot{\theta}_{FS} = \dot{\theta}_{cg} + \sum_{i=1}^{2} (\frac{d\phi_i}{dx})_{FS} \dot{\xi}_i \quad .$$

AERODYNAMIC COEFFICIENTS

Strip theory aerodynamic influence coefficients were determined using a modified quasi-steady theory. Although lift-lag effects were neglected, the method used is not pure quasi-steady since rate terms are included. Generalized aerodynamic coefficients were then calculated by multiplying the aerodynamic influence coefficients by modal down-wash and by modal deflections, viz.

$$\left[a \right] = \left[\phi \right]^r \left[AIC \right] \left[\frac{w}{U} \right] \quad .$$

These coefficients were determined for 0.9 Mach and are presented in the appropriate airplane sections.

APPENDIX VII. ANALOGUE MECHANIZATION

The analogue computer circuit mechanizations utilized in the simulation study are shown with standard symbology in Figure 106. Airframe, control, and turbulence circuit mechanizations are included. Turbulence for various flight conditions (gust filter corner frequency is proportional to aircraft velocity) was recorded on the multichannel FM tape recorder in 100-second sections. One channel is used to turn on and reset the computer automatically. The level of turbulence (rms value) is set by adjusting the tape output amplitude. A turn-on time delay keeps rms circuits from dividing by zero time at the outset of each run.

The mechanization employs a function-selector section to permit, without rewiring, study of active systems with various feedback signals. A pure time delay was mechanized to simulate the delay of gust encounter from angle-of-attack sensor to center of pressure.
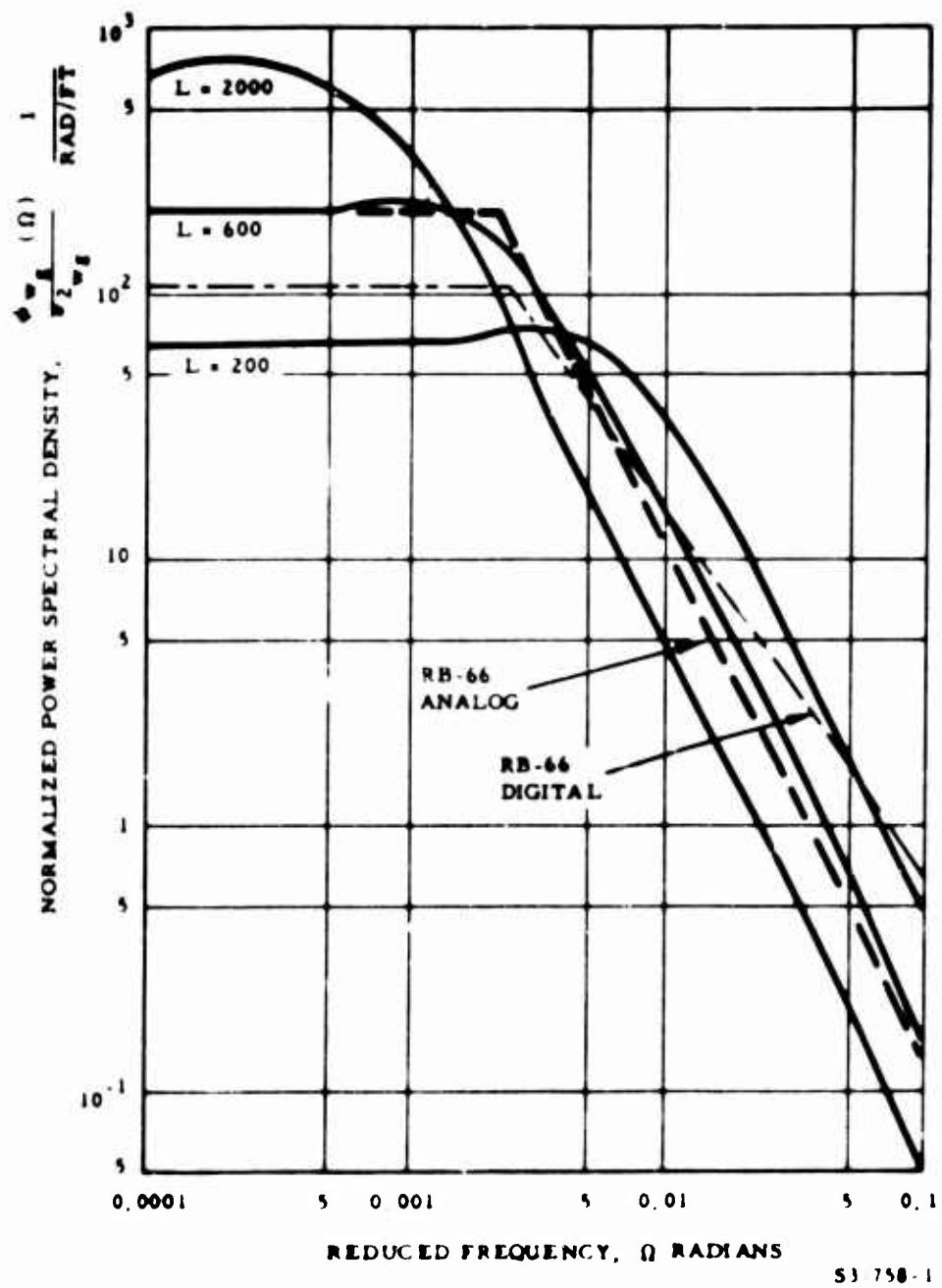
Figure 1. Analytic Turbulence Representation
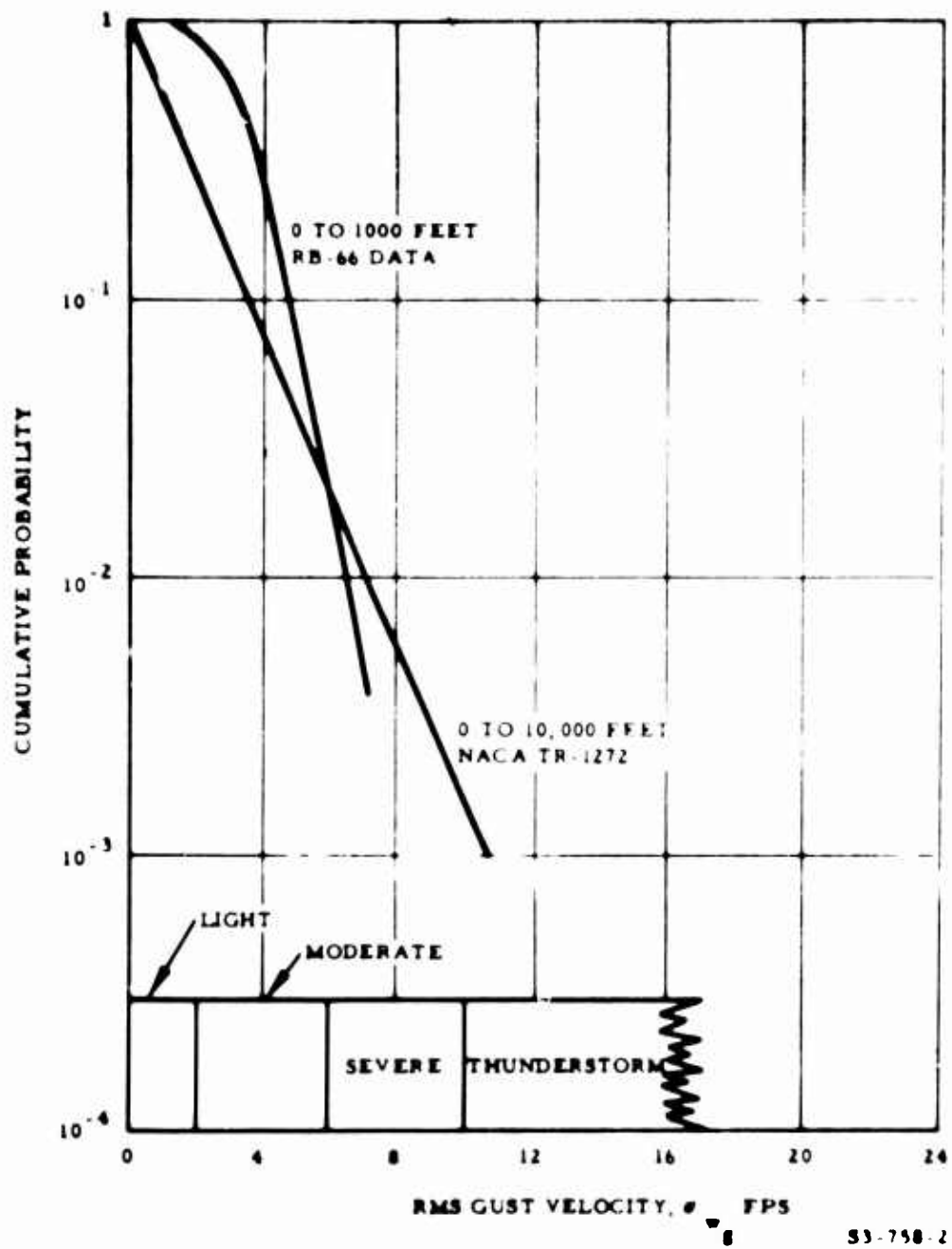
Figure 2. Cumulative Distribution of RMS Gust Velocity
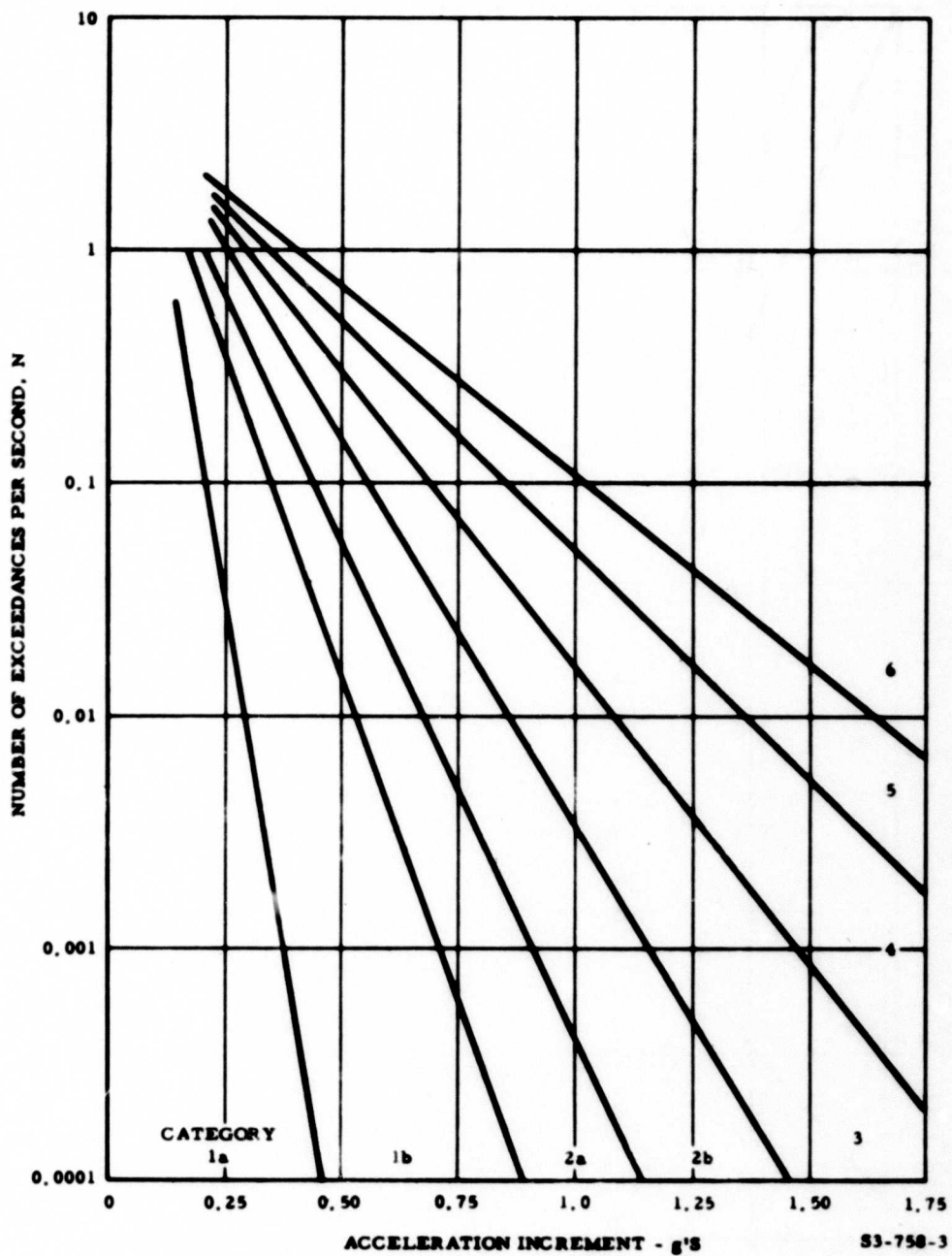
Figure 3. Behavior Categories
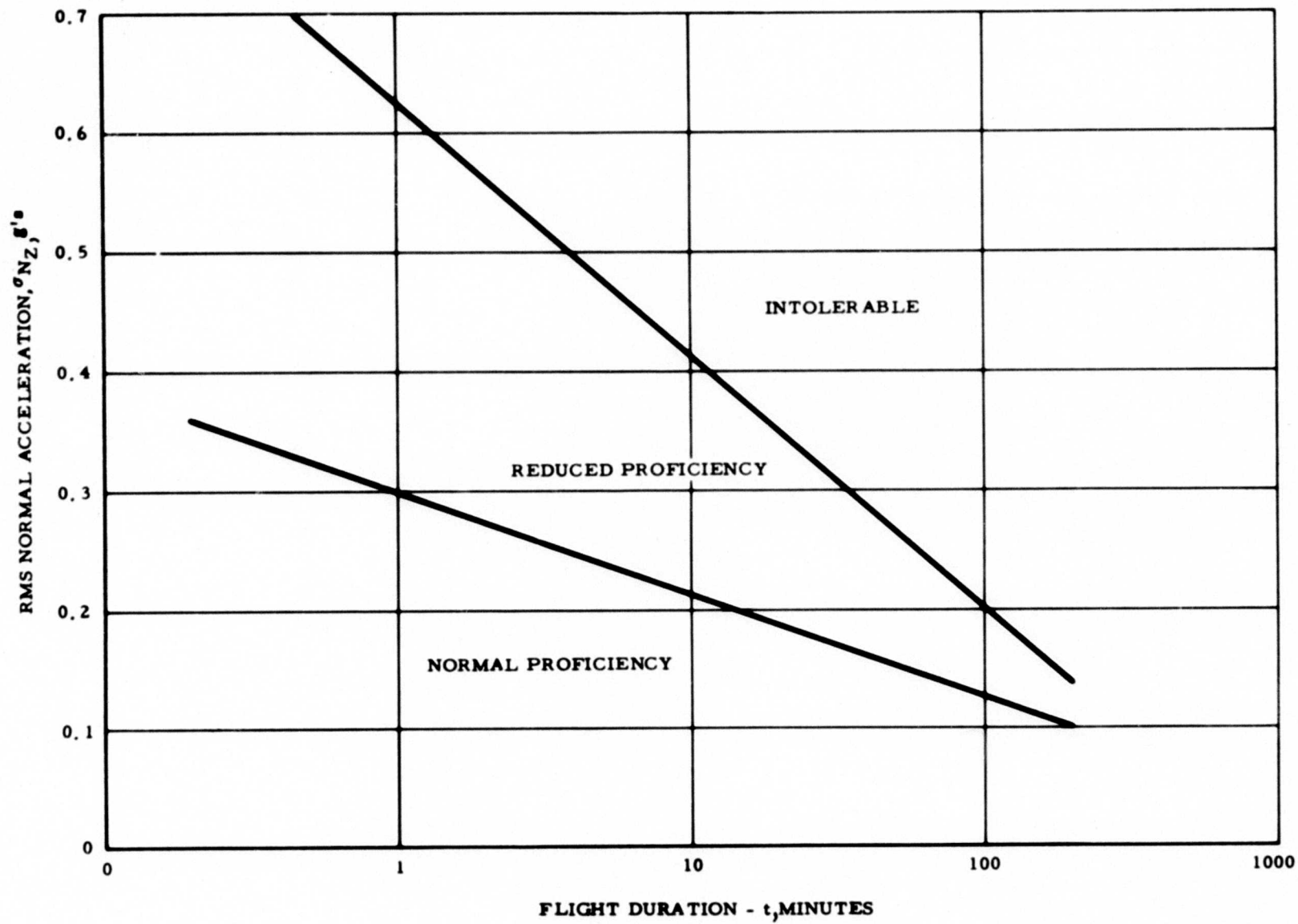
Figure 4.   Endurance Boundaries

116

BLANK PAGE
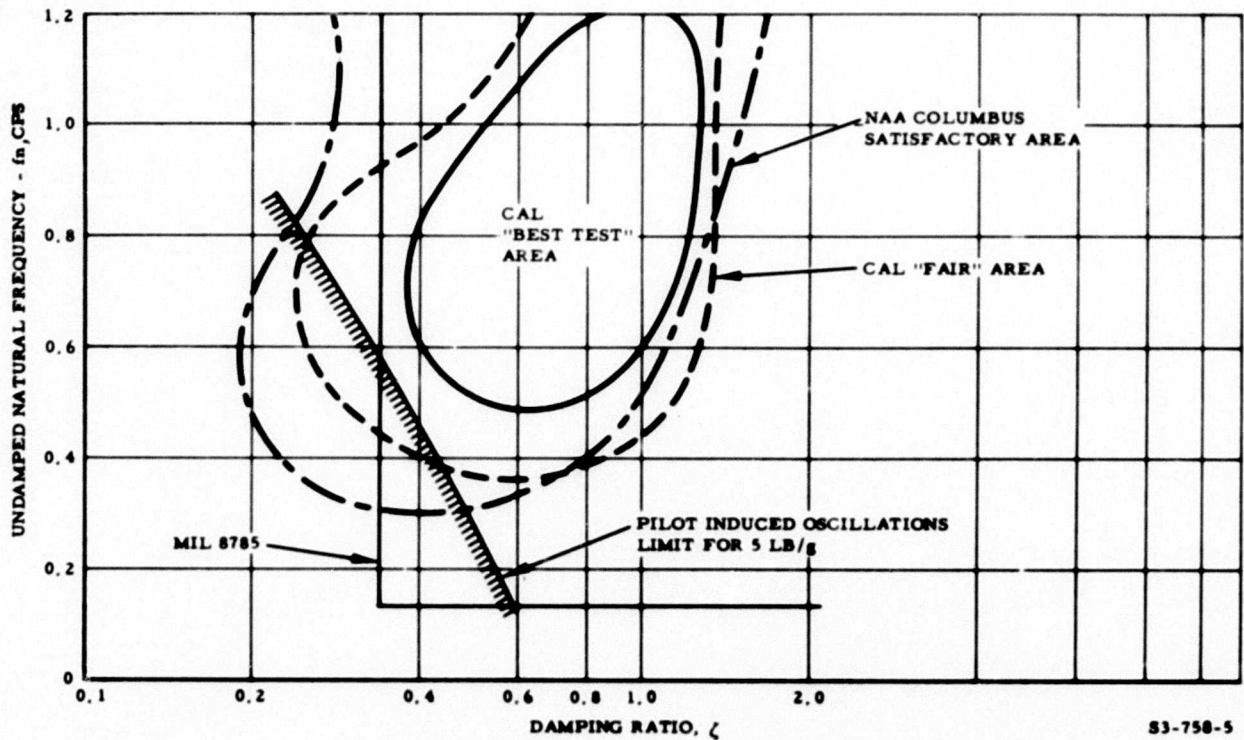
Figure 5. Short Period Damping and Frequency Criterion

V_{MAX} @ SEA LEVEL = 0.9 M   W = 18,000 LBS
V_{CRUISE} @ SEA LEVEL = 0.4 M   S = 277 SQ FT
CRUISE RADIUS = 300 NM   Æ = 4.0
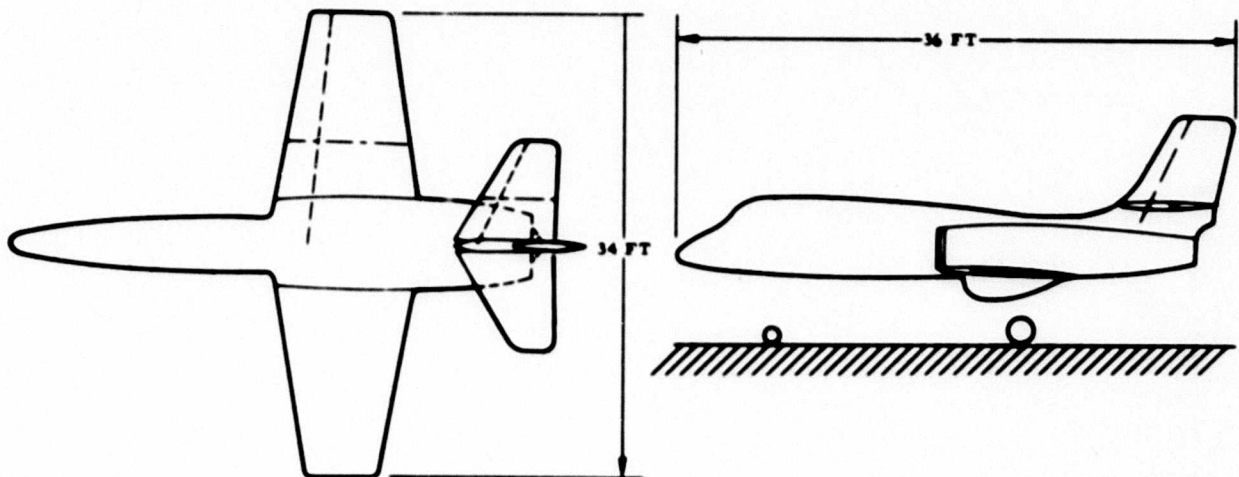
Figure 6. Base Point Airplane (BPA)
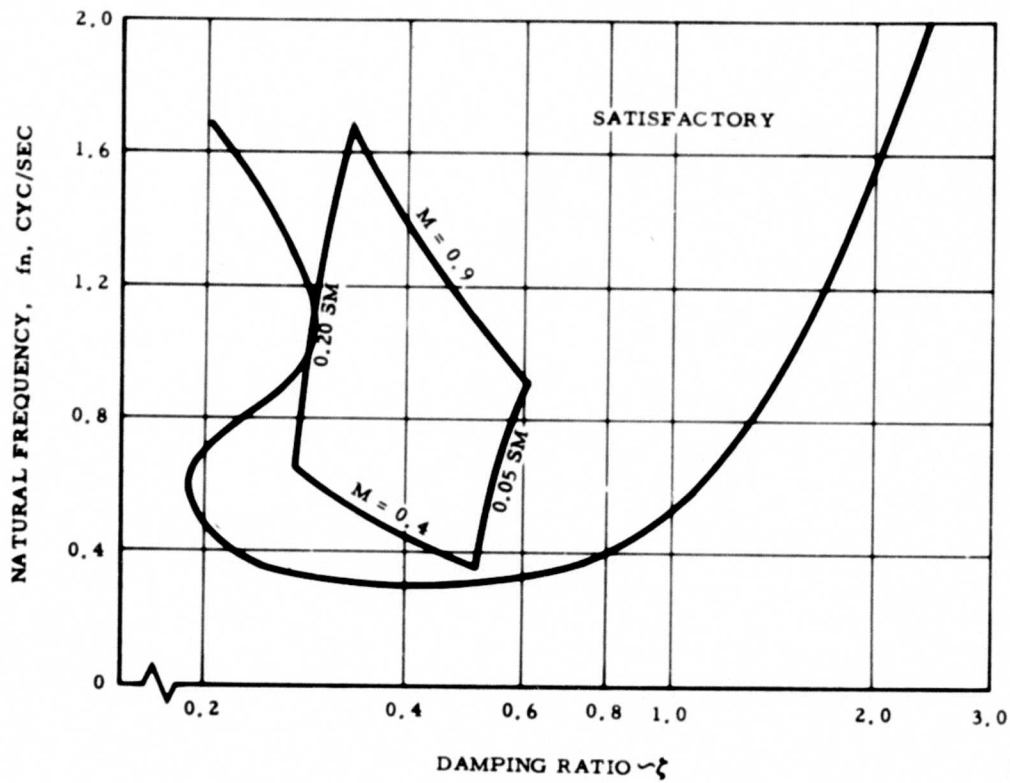
117

Figure 7.   Short Period Characteristics of BPA
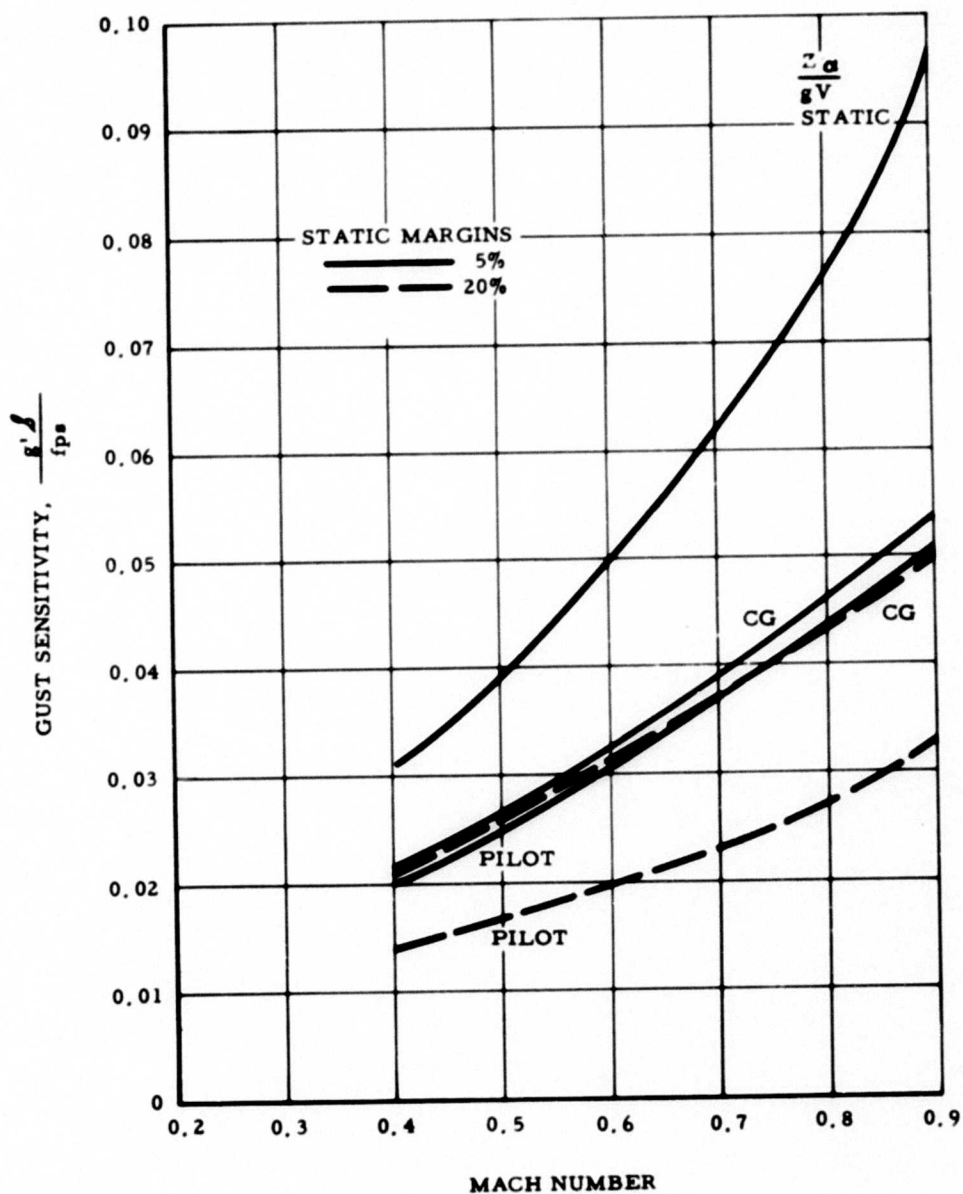
Figure 8. Gust Sensitivity of BPA

S3-758-8
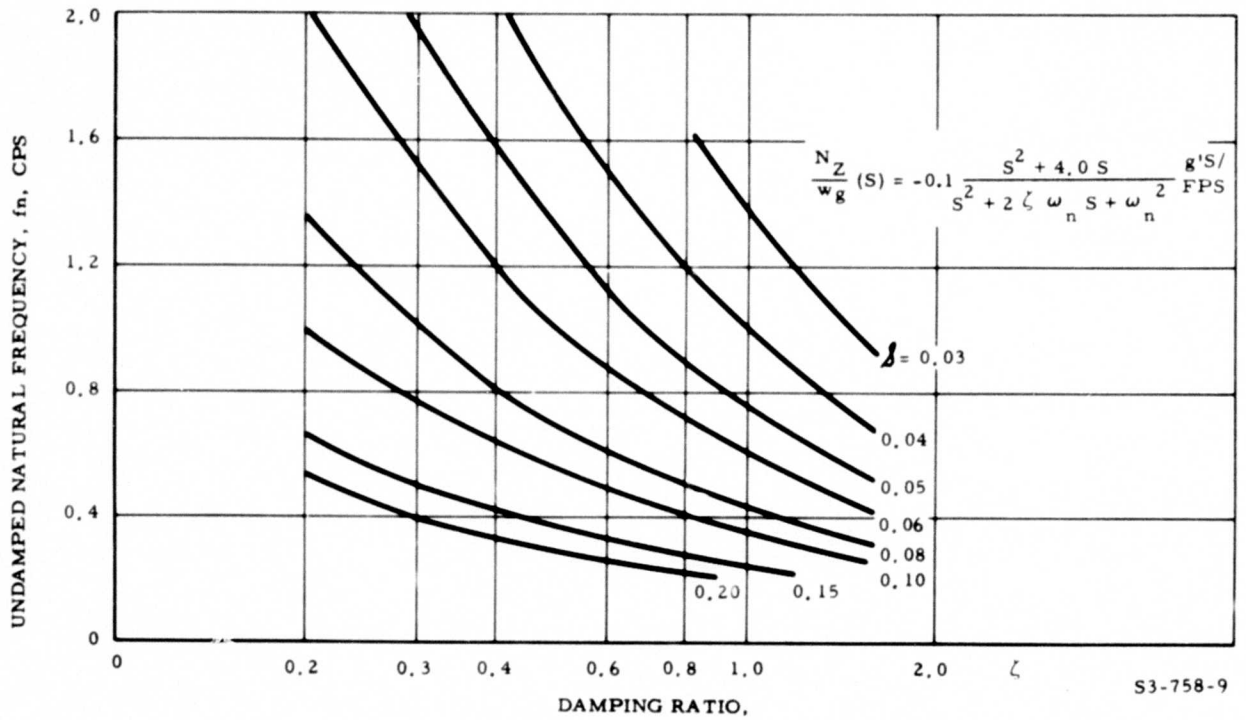
Figure 9. Gust Sensitivity of BPA Having Variable
Short Period Characteristics

120
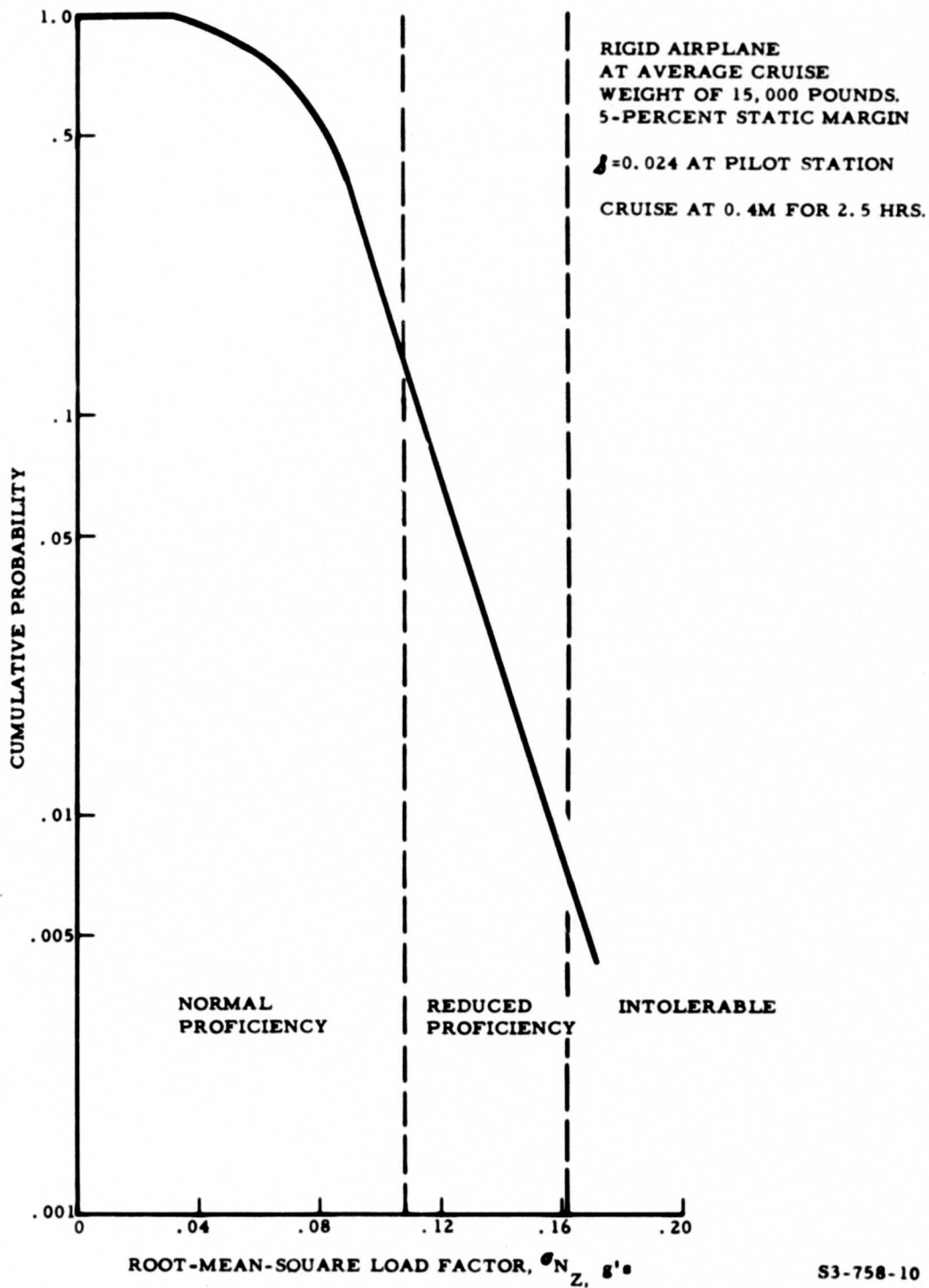
Figure 10. BPA Cruise Endurance Probability

121
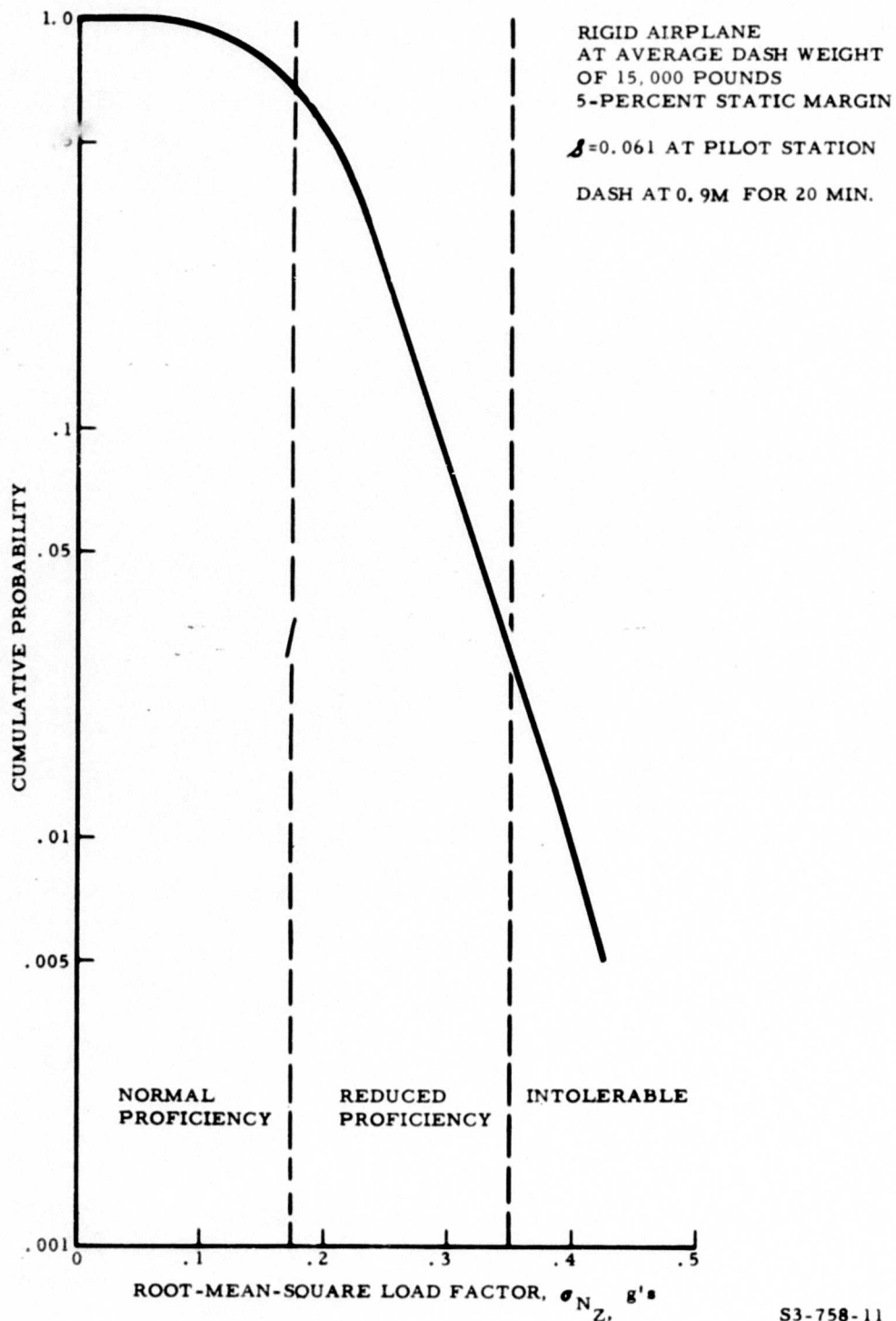
Figure 11. BPA Dash Endurance Probability

S3-758-11

122
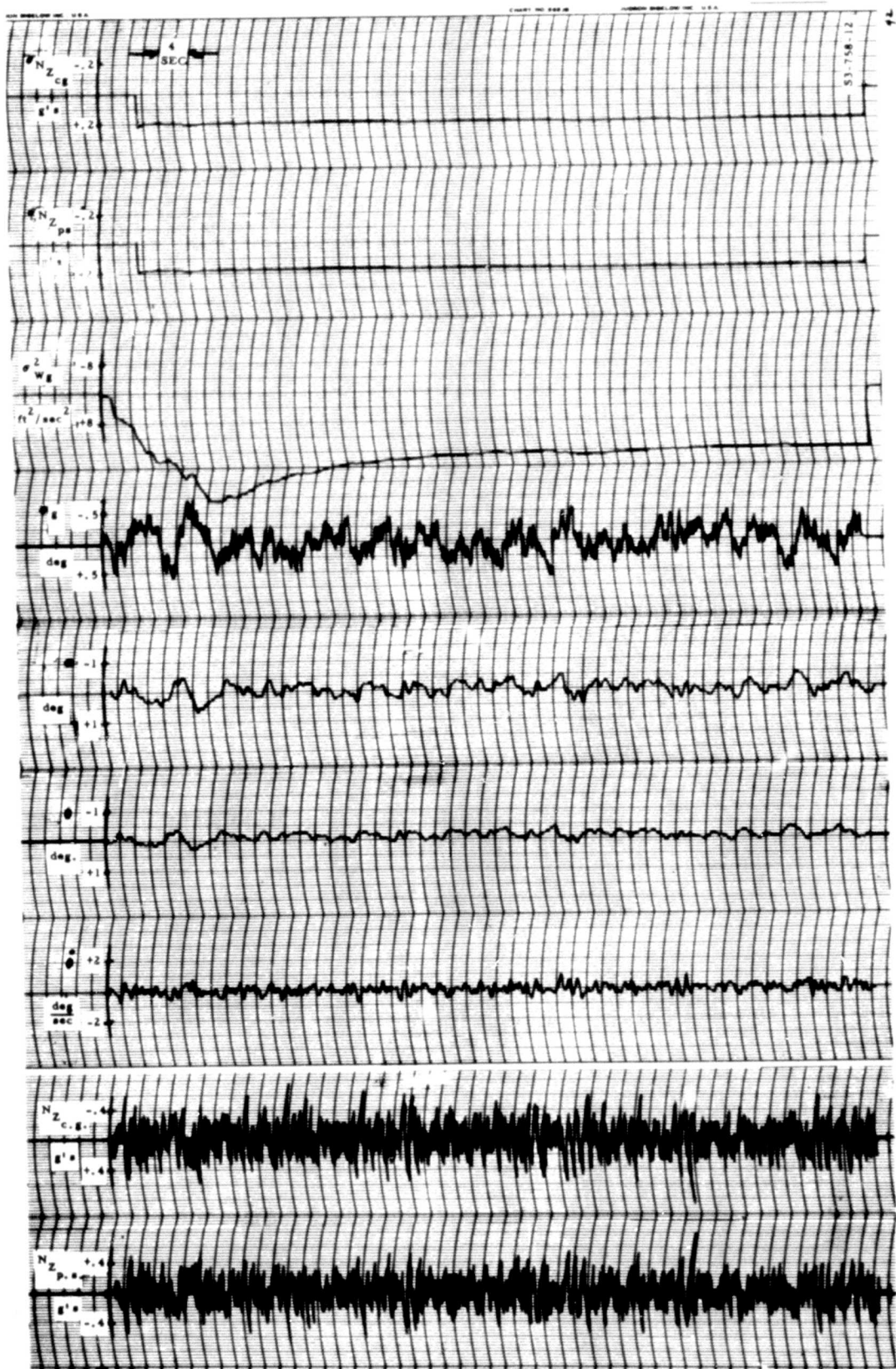
Figure 12. Time History of BPA Gust Response at 0.9 Mach

123
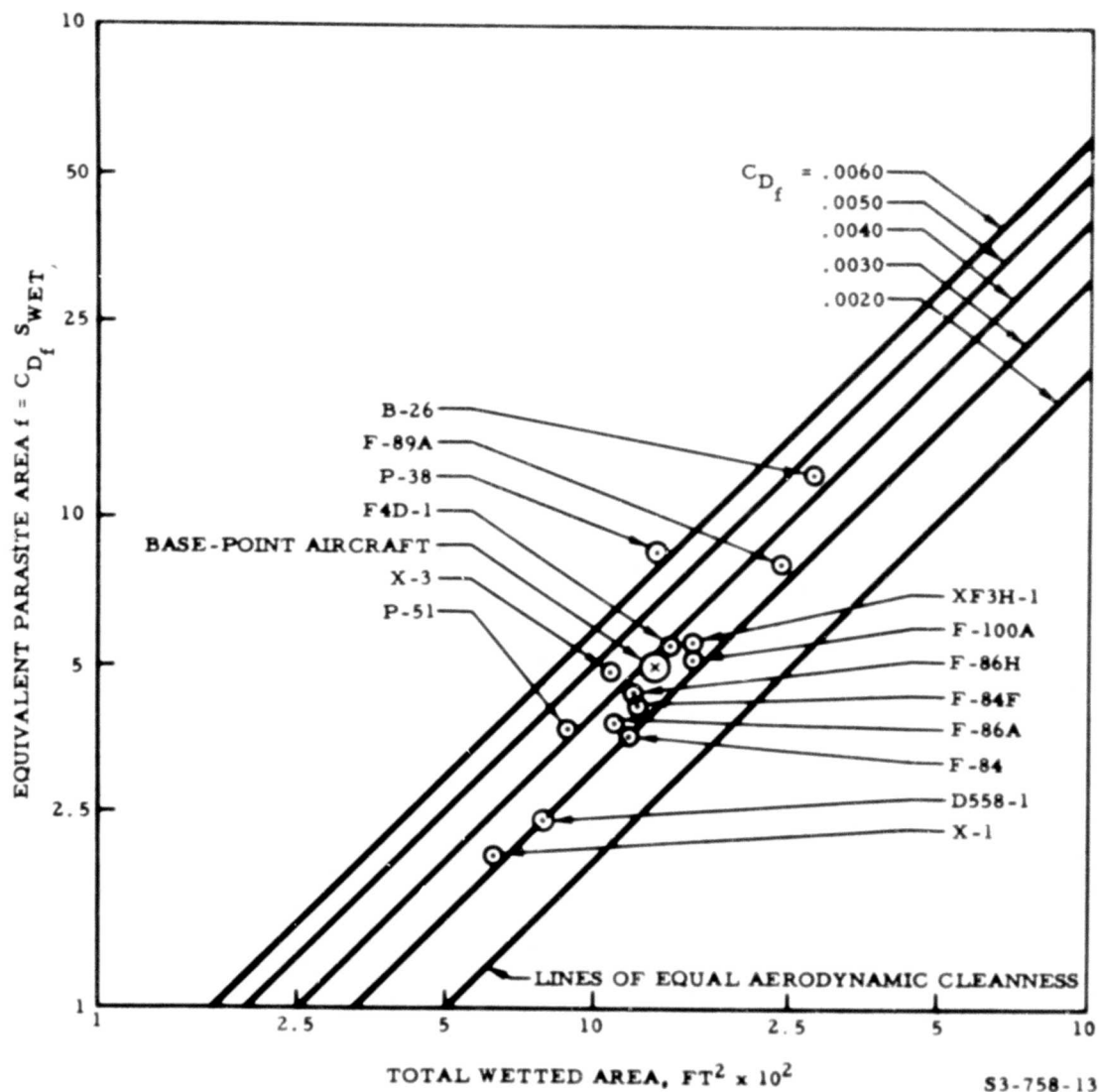
Figure 13. Equivalent Parasite Drag Area of Complete Airplanes
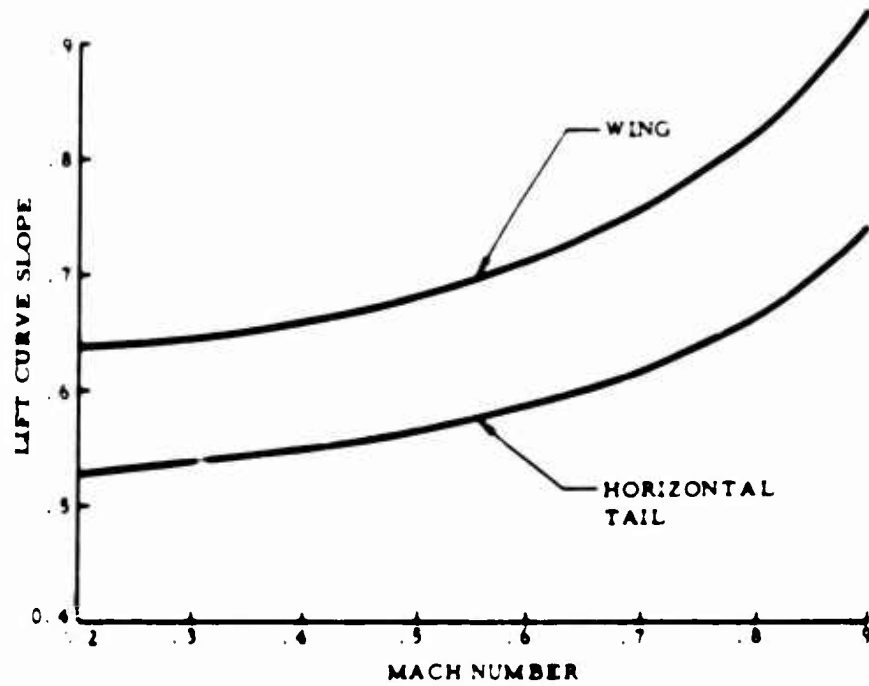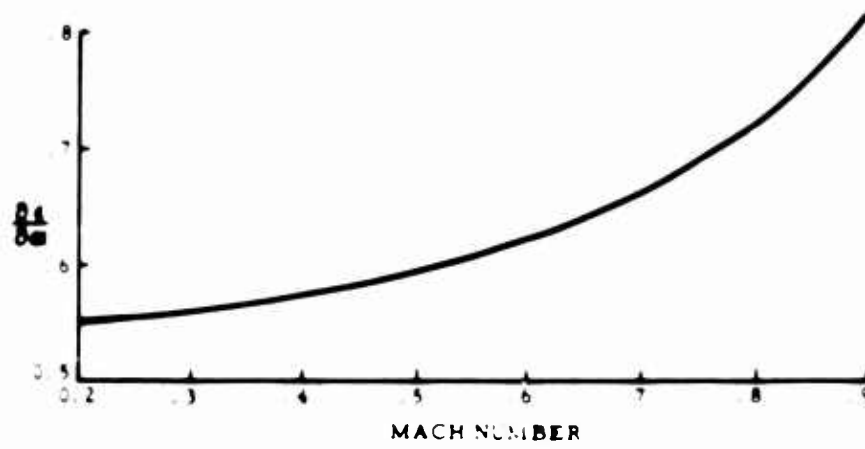
Figure 14. Effect of Mach Number on Lift Curve
Slope and Downwash of BPA
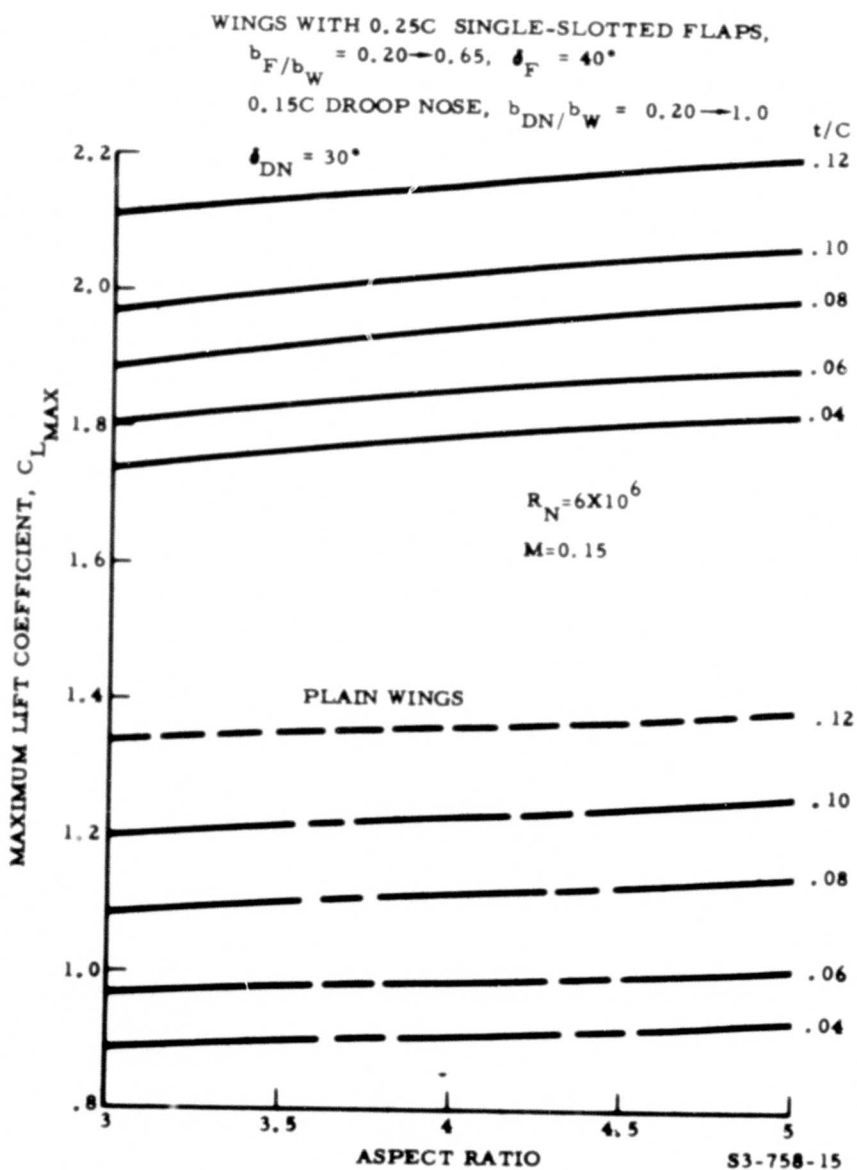
Figure 15. Maximum Lift Coefficients of Unswept Wings With 64A2xx Sections
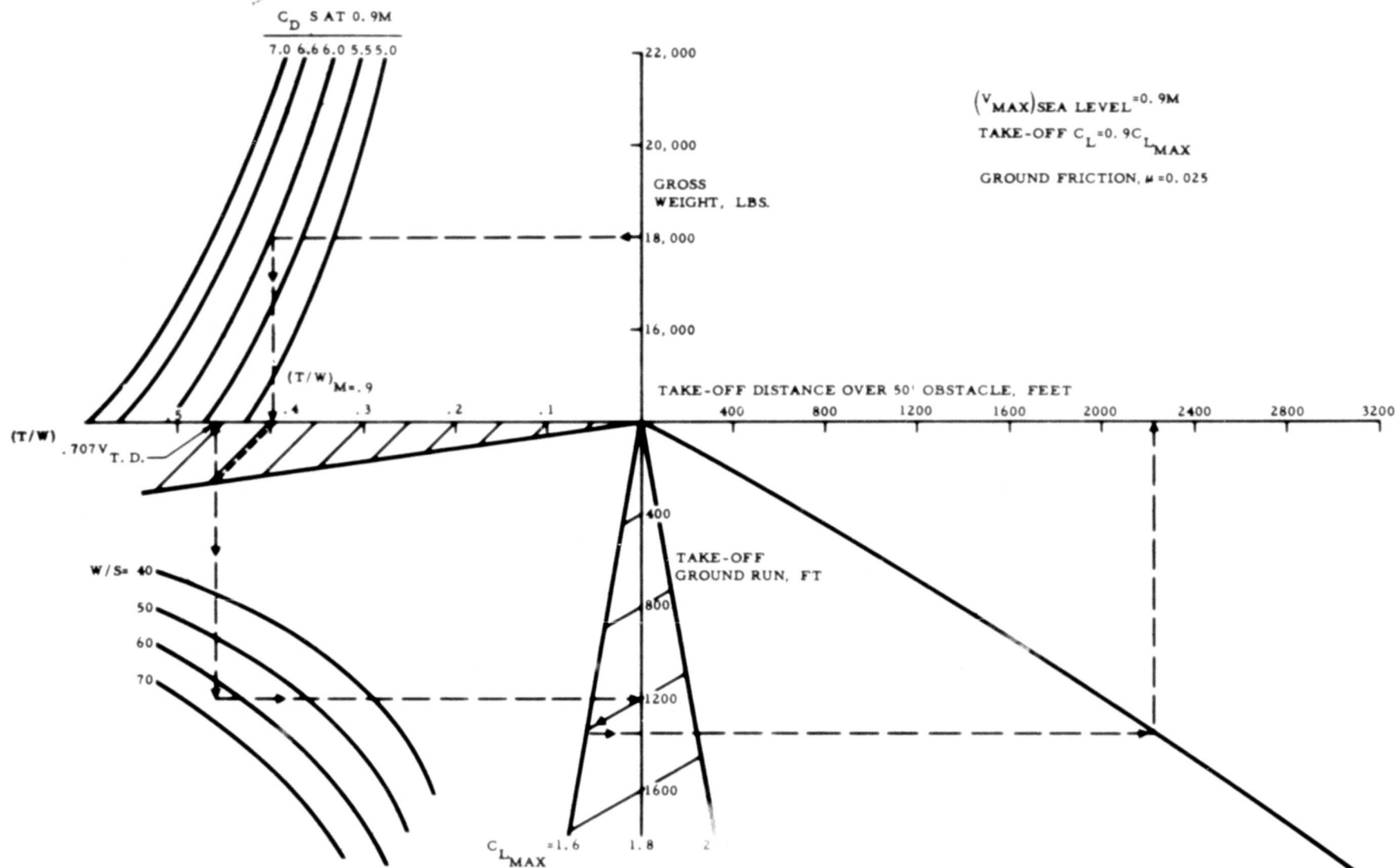
Figure 16. Takeoff Distance Nomograph
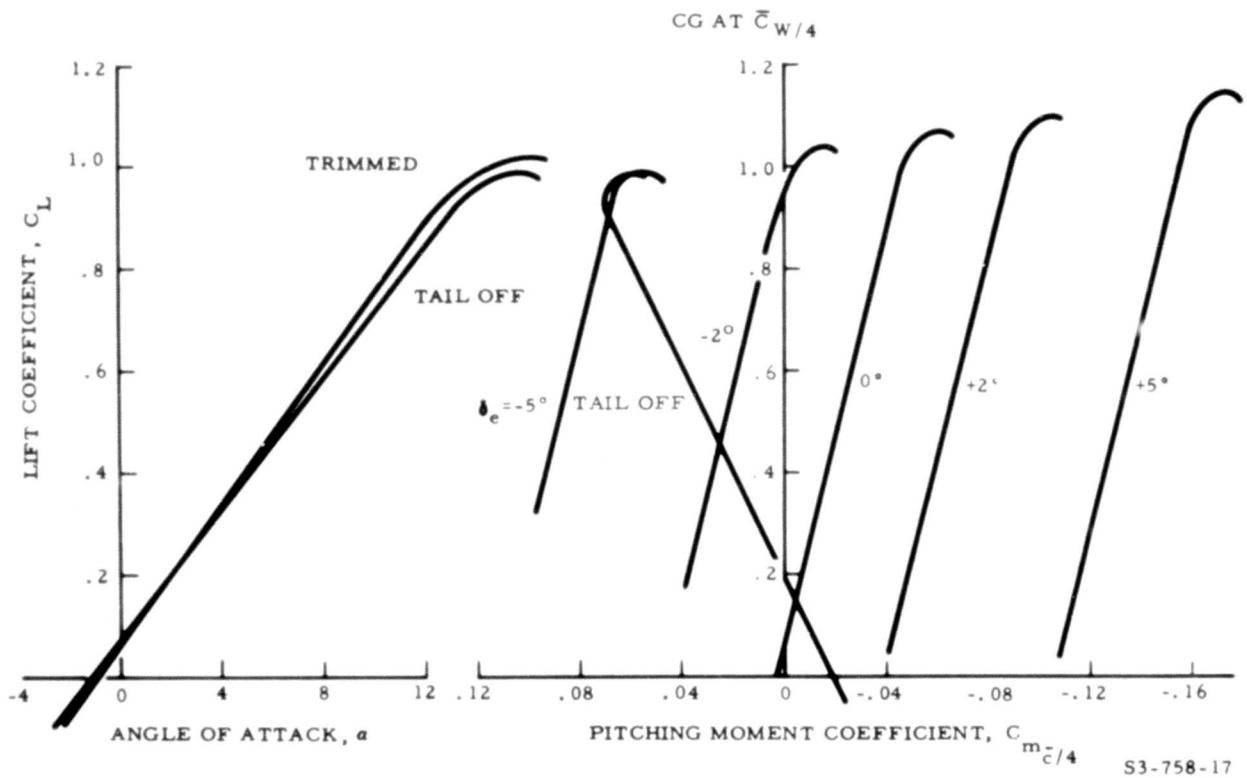
Figure 17. Lift and Pitching Moment at 0.4 Mach
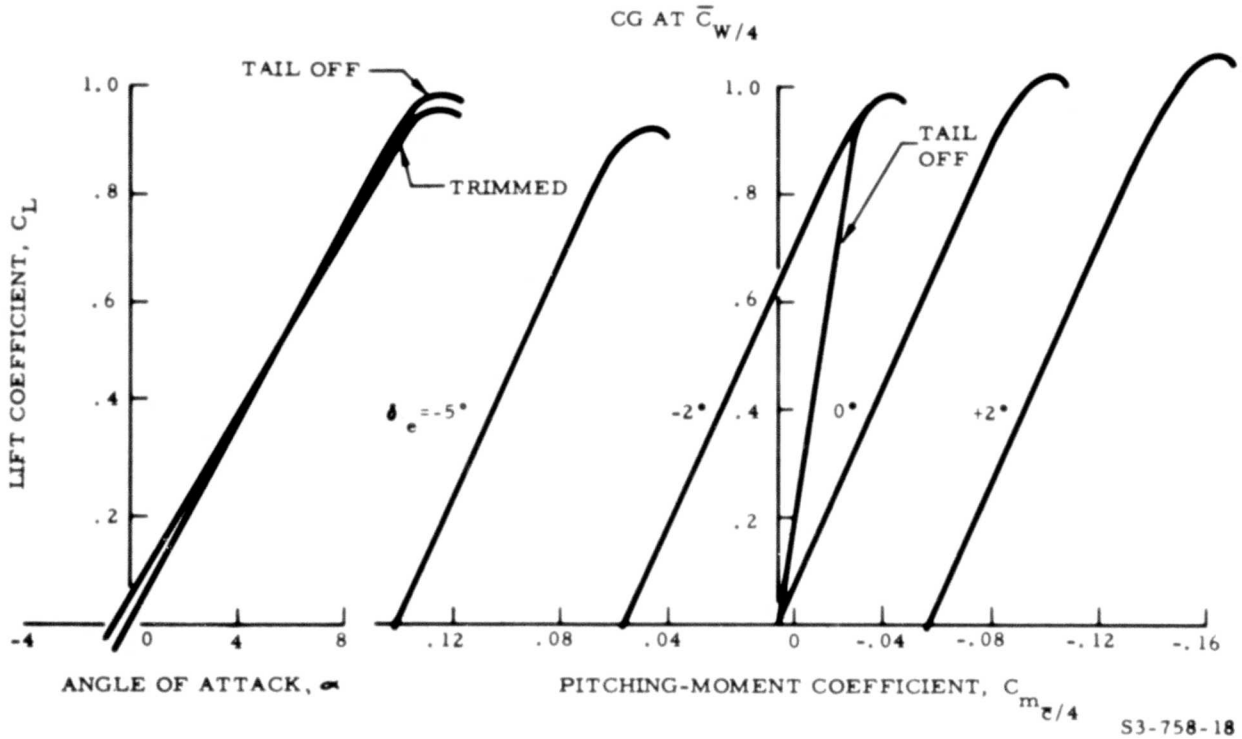
Figure 18. Lift and Pitching Moment at 0.9 Mach

128
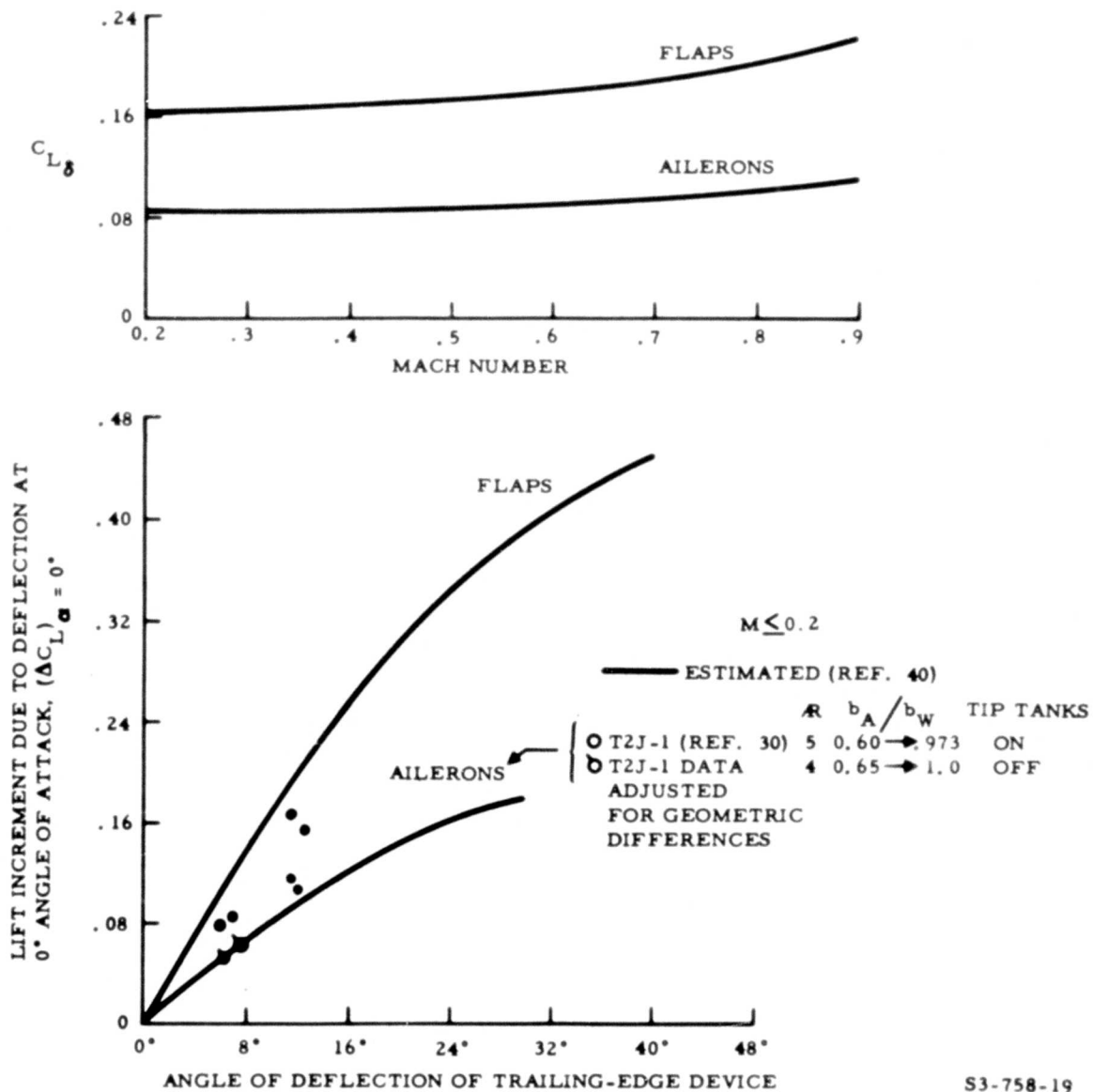
Figure 19. Lift Due to Flap or Aileron Deflection
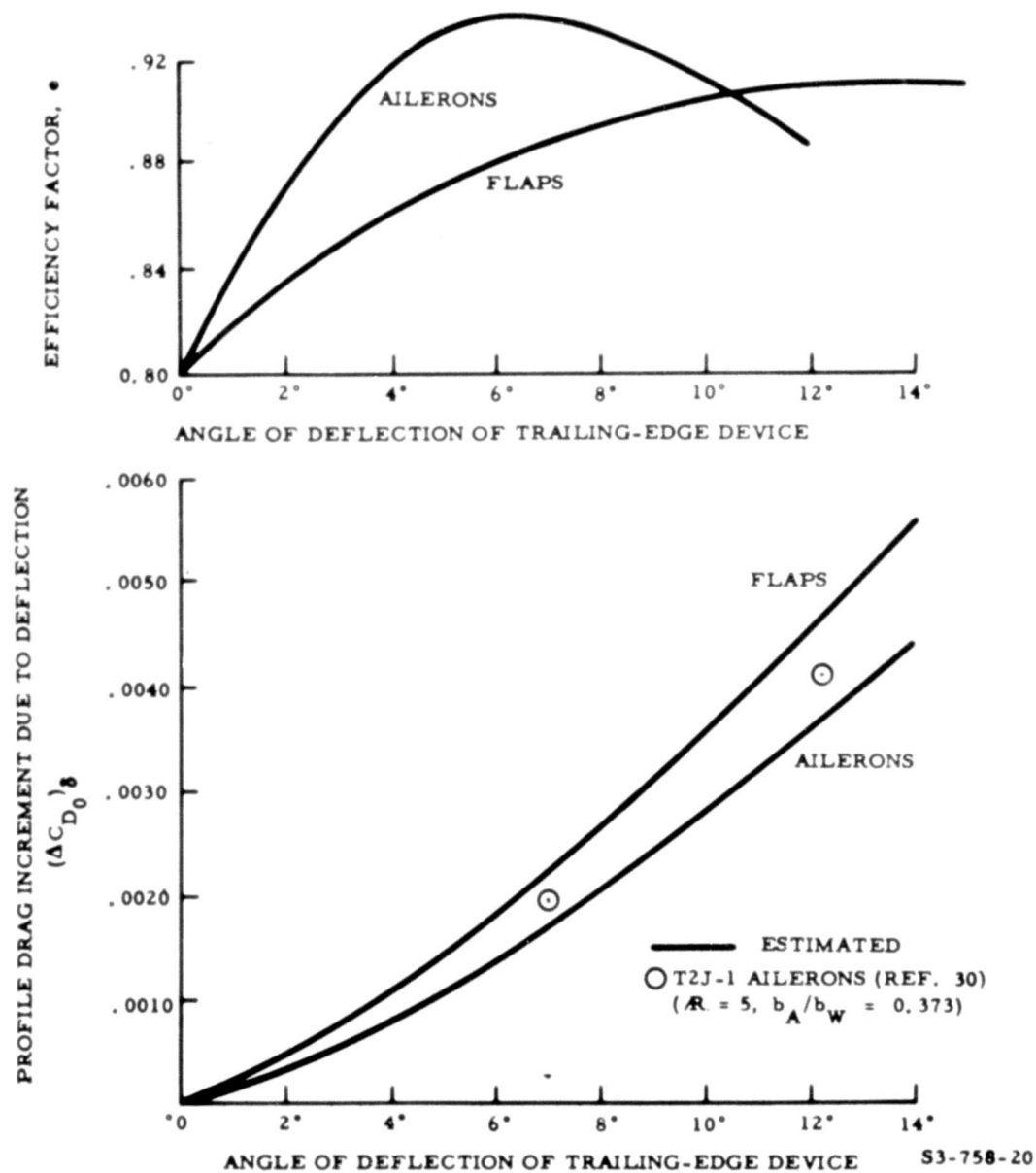
Figure 20. Drag Due to Flap or Aileron Deflection

130
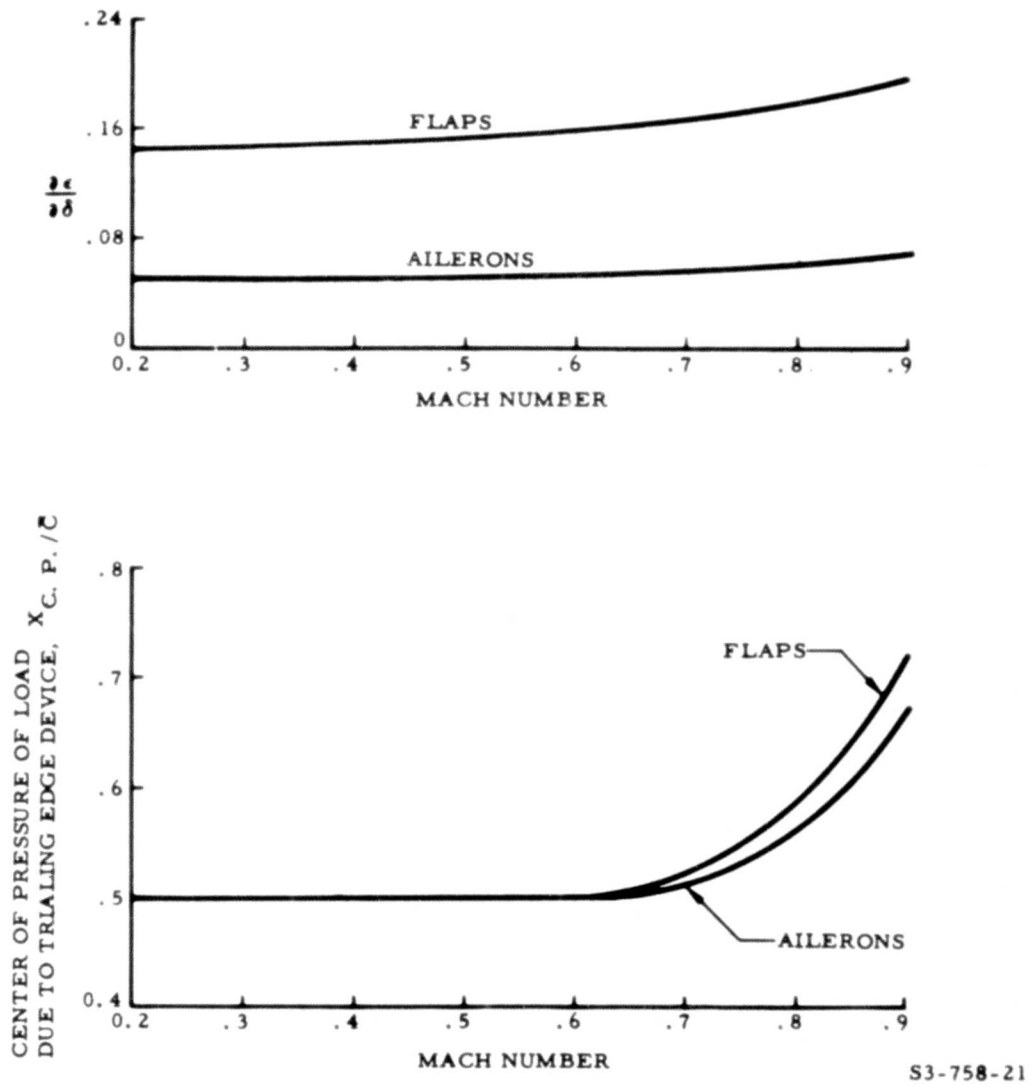
Figure 21. Downwash and Load Center of Pressure Due
to Flap or Aileron Deflection

S3-758-21

131
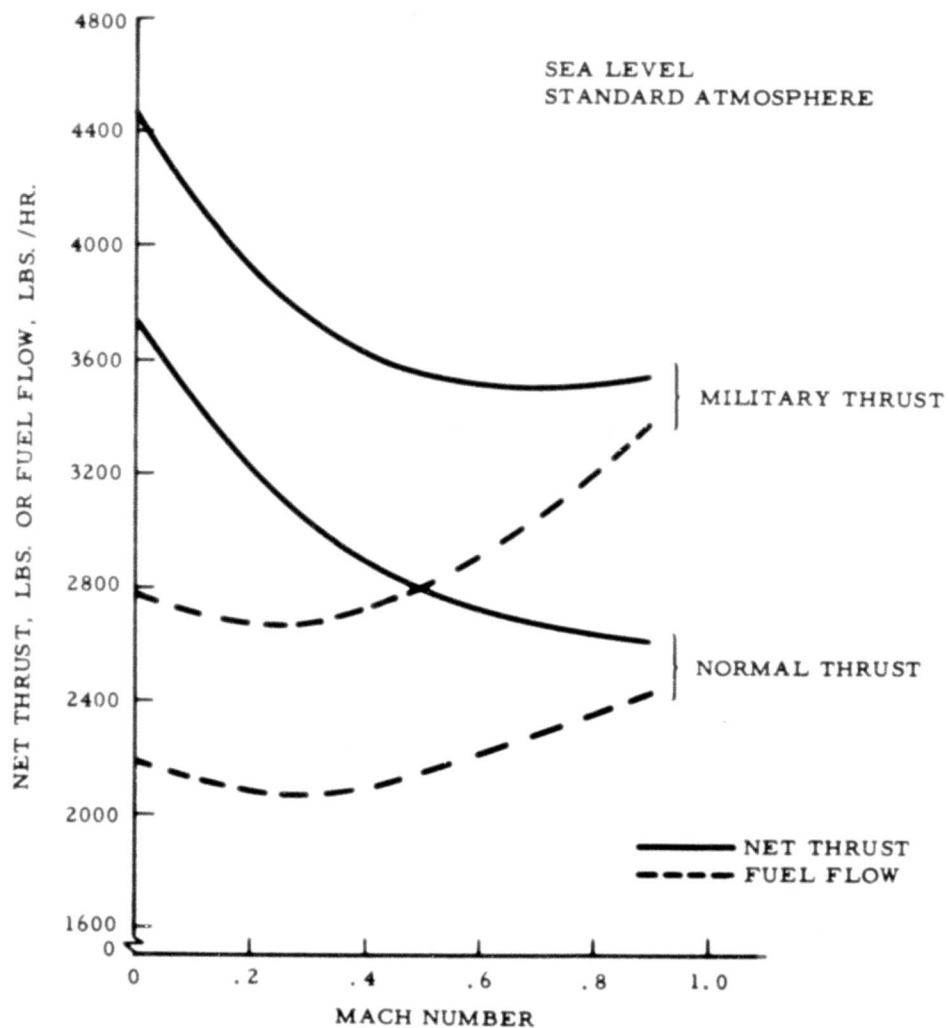
Figure 22. Engine Thrust and Fuel Flow Characteristics

S3-758-22

132

$$\frac{C_{L\alpha}}{K_1} = \frac{1}{9.12\left(\frac{\beta}{\cos \Lambda_{.5C}}\right) + \frac{30.45}{AR} - 1}$$

$$\beta = \sqrt{1 - M^2}$$

$$K_1 = C_{L\alpha}/.1097$$

$$C_{L\alpha} \text{ PER DEGREE}$$
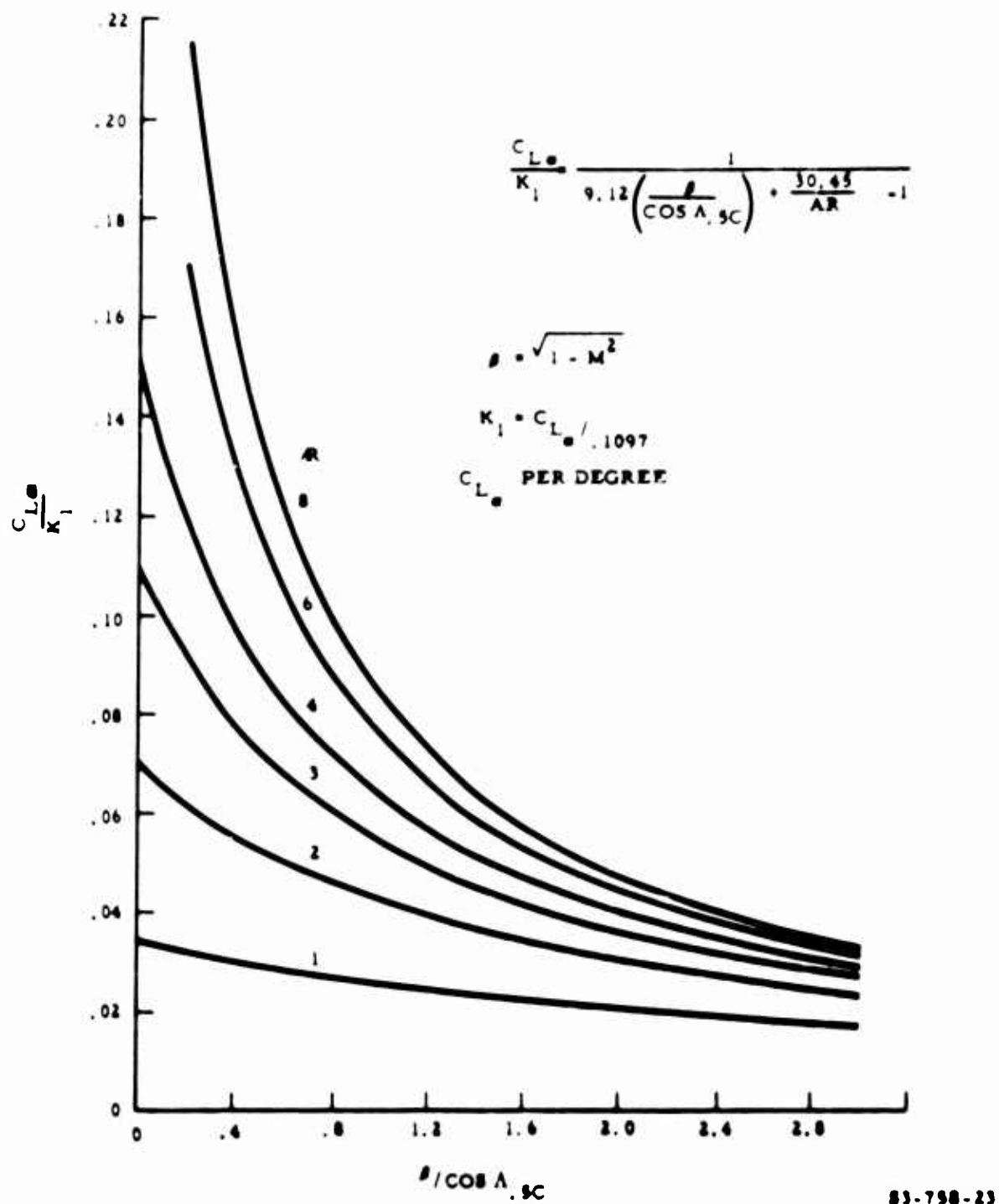
Figure 23.   Curves for Estimation of Wing Lift Curve Slope

133
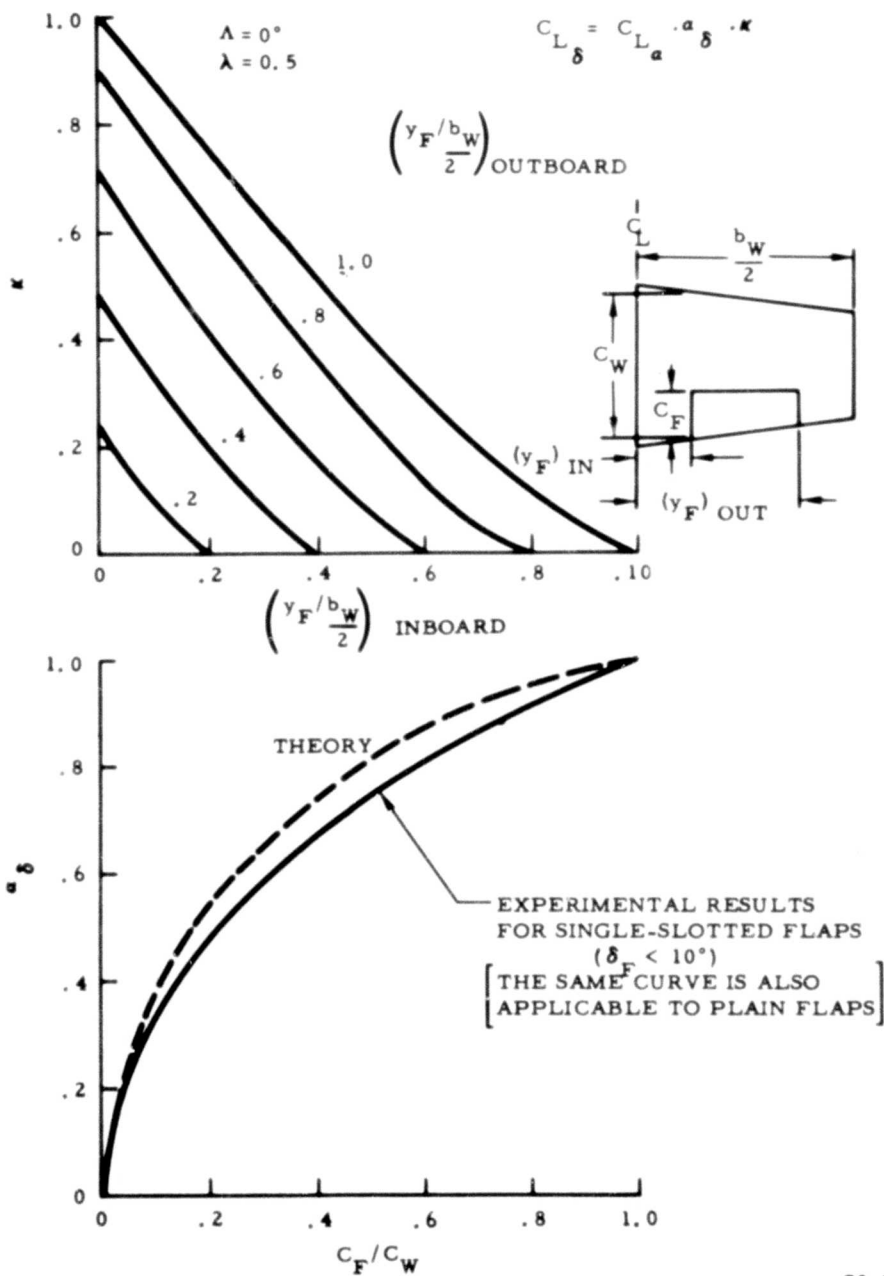
Figure 24.   Curves for Estimation of Lift Due to Trailing
Edge Device

134
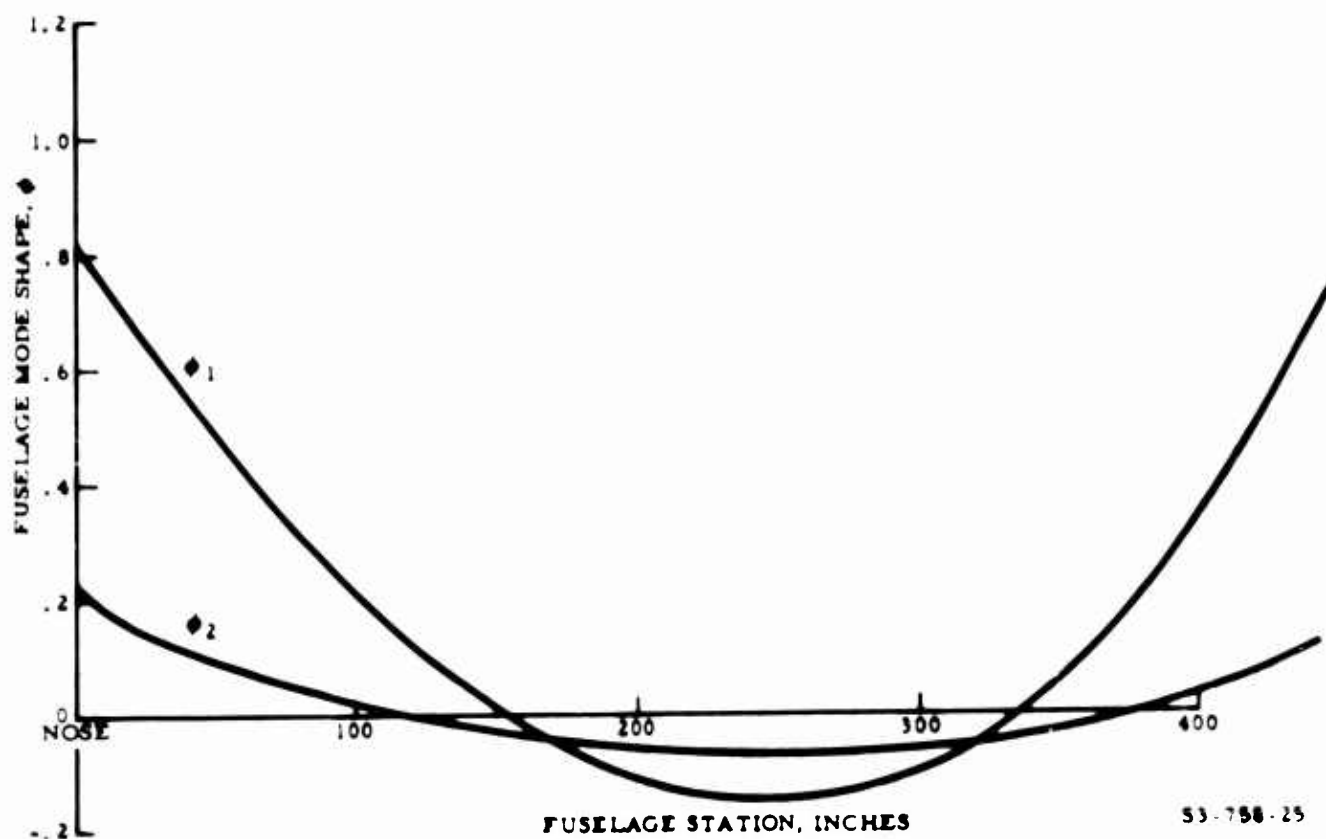
Figure 25. BPA Fuselage Mode Shapes
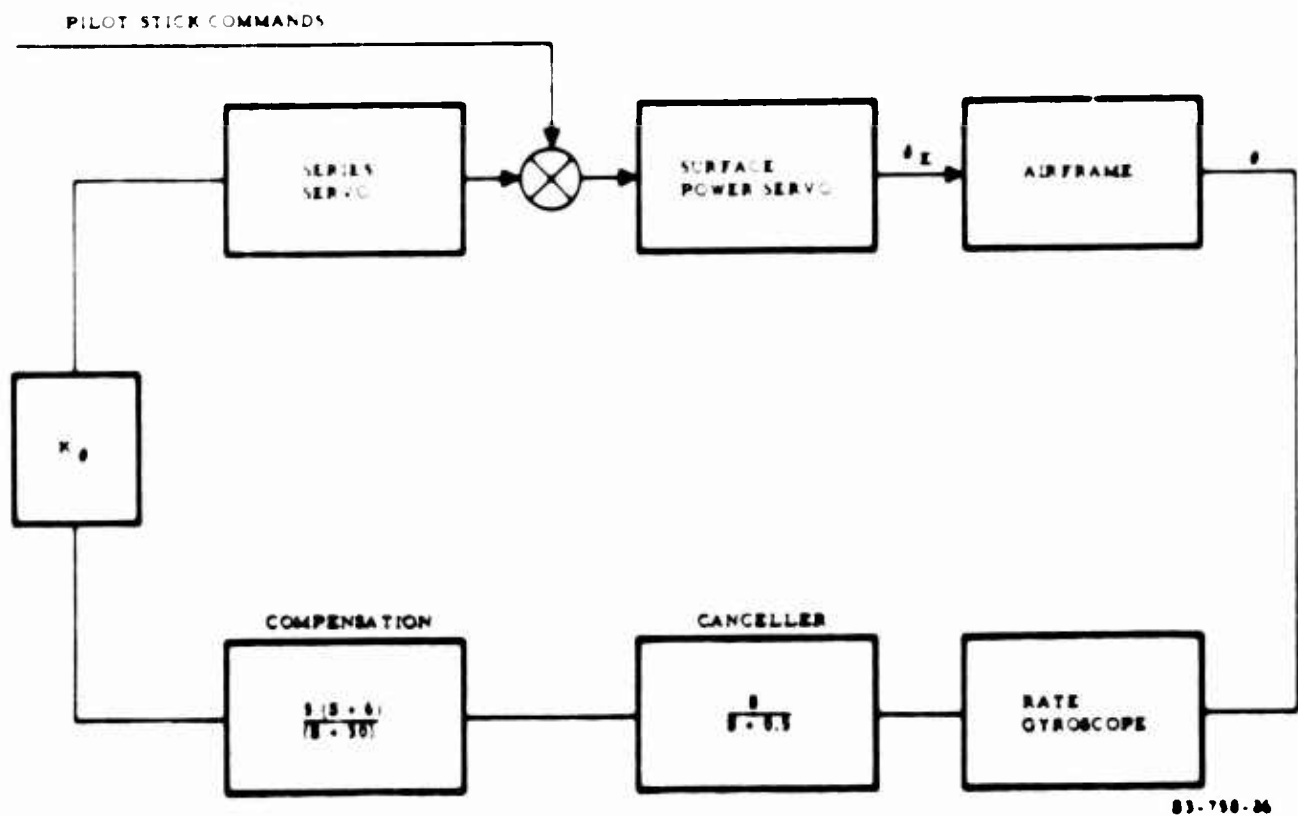
Figure 26. Pitch Stability Augmentation System Block Diagram

135
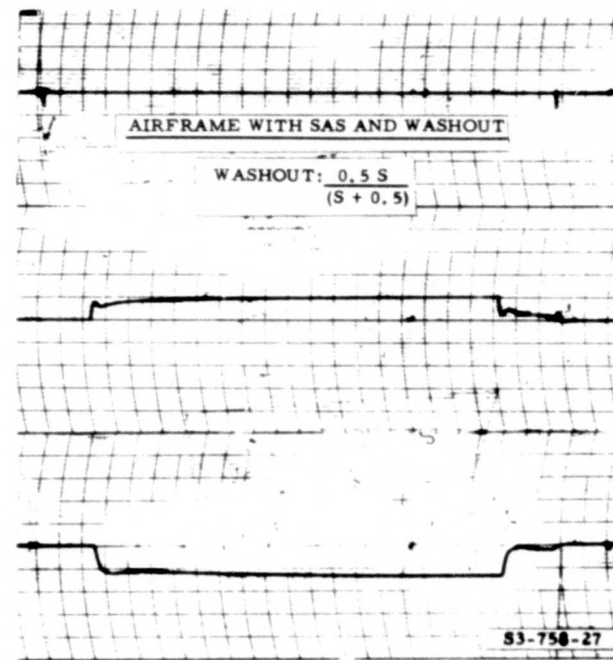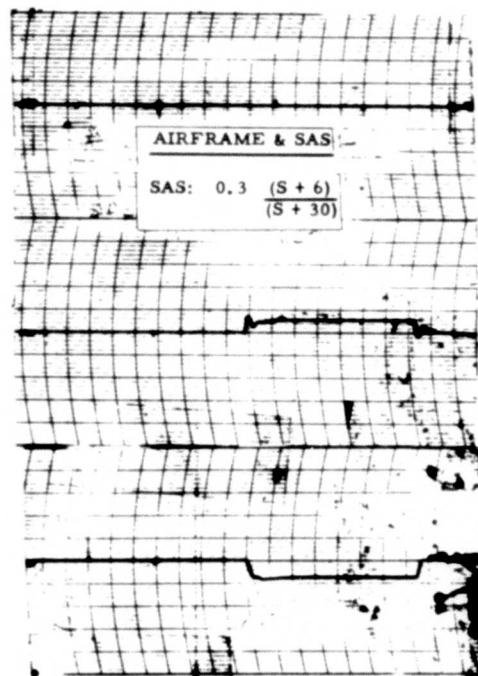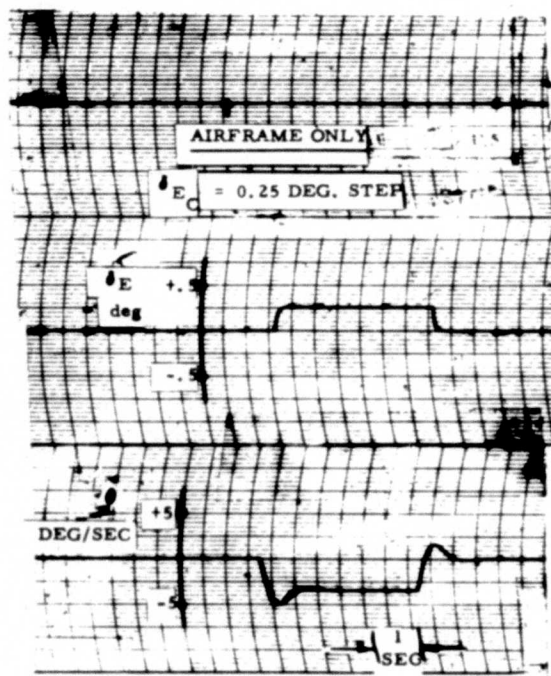
Figure 27. Effect of SAS on Response to Stick Command

BLANK PAGE
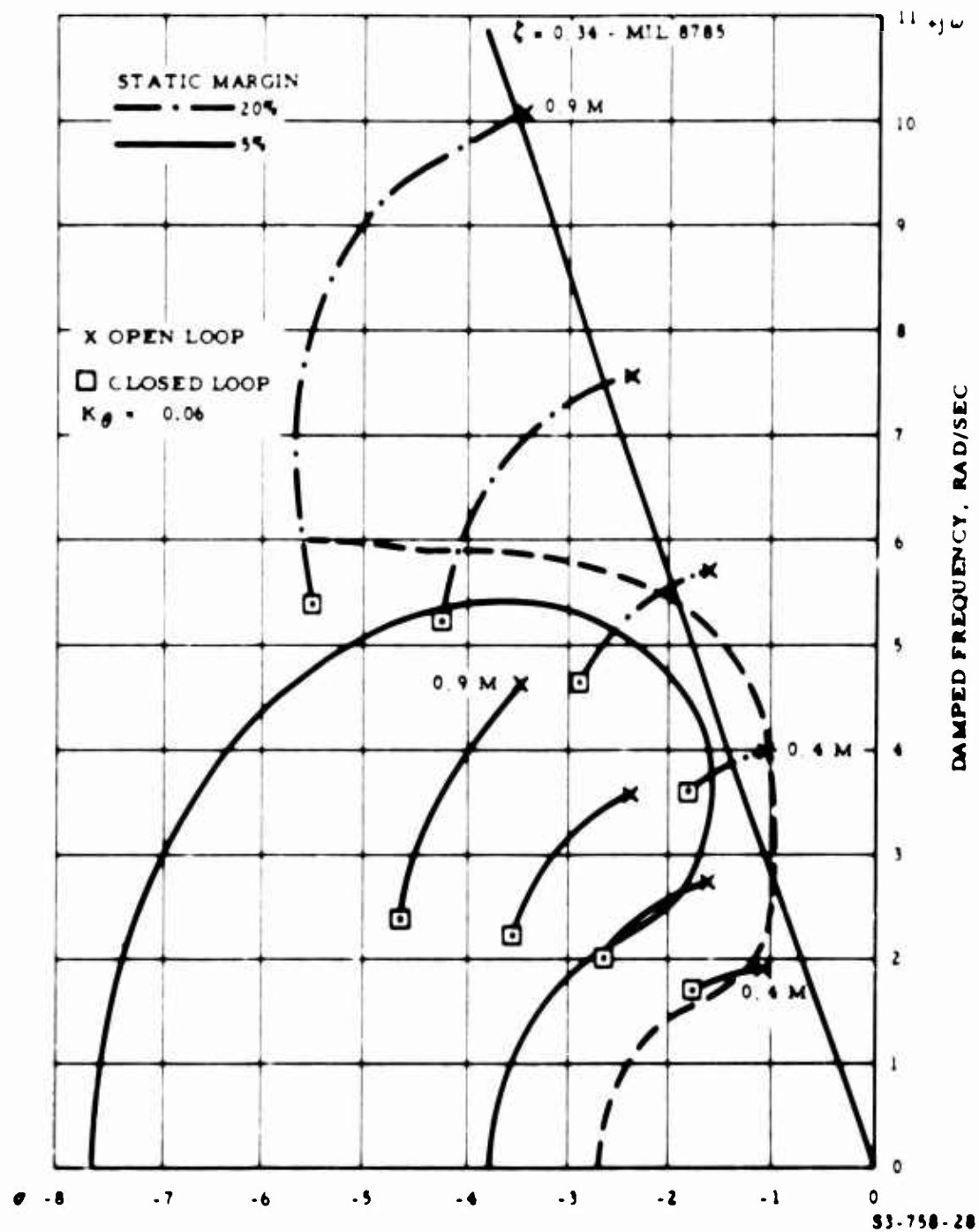
Figure 28. Short Period Loci With Stability Augmentation
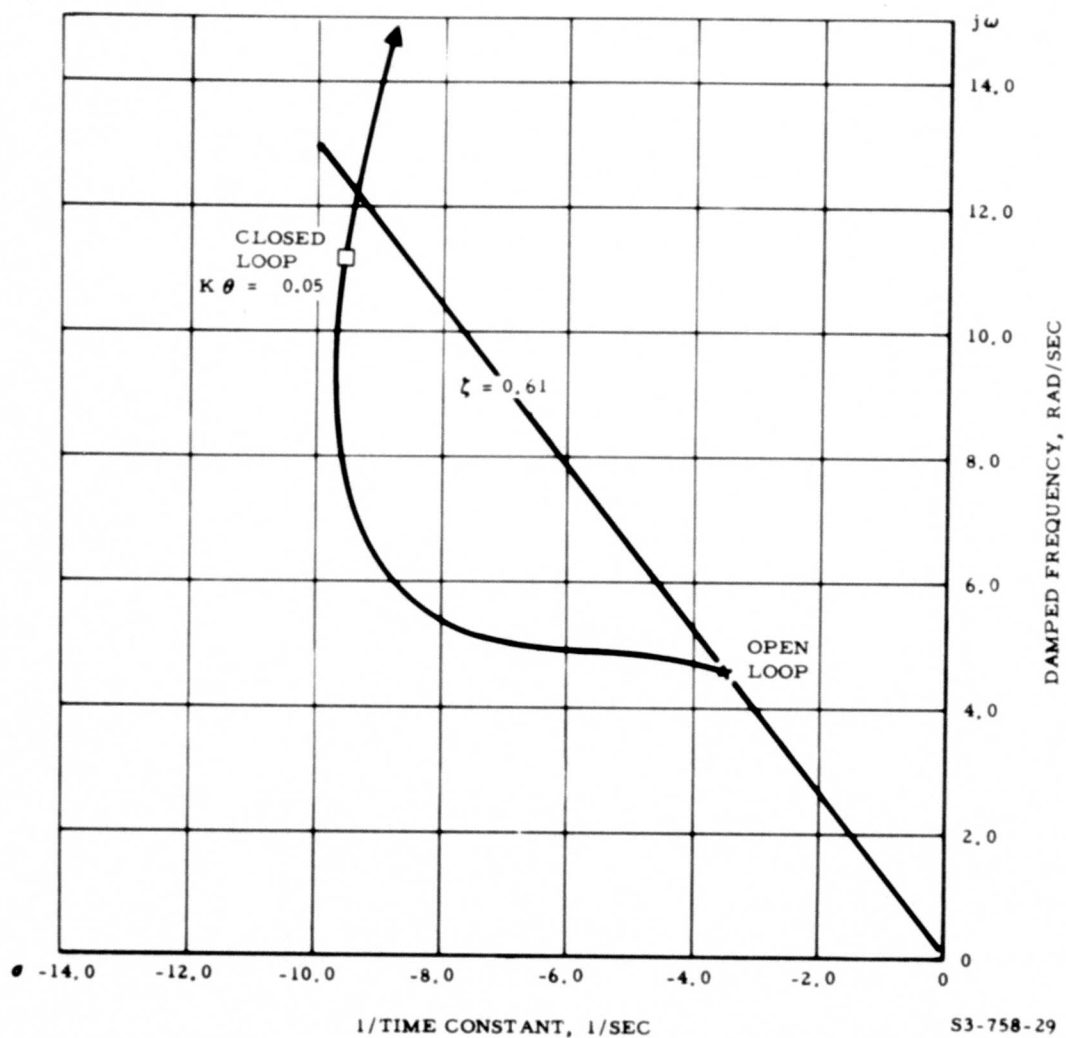
Figure 29. Short Period Locus With Simple Pitch Rate Feedback

S3-758-29

138

BLANK PAGE
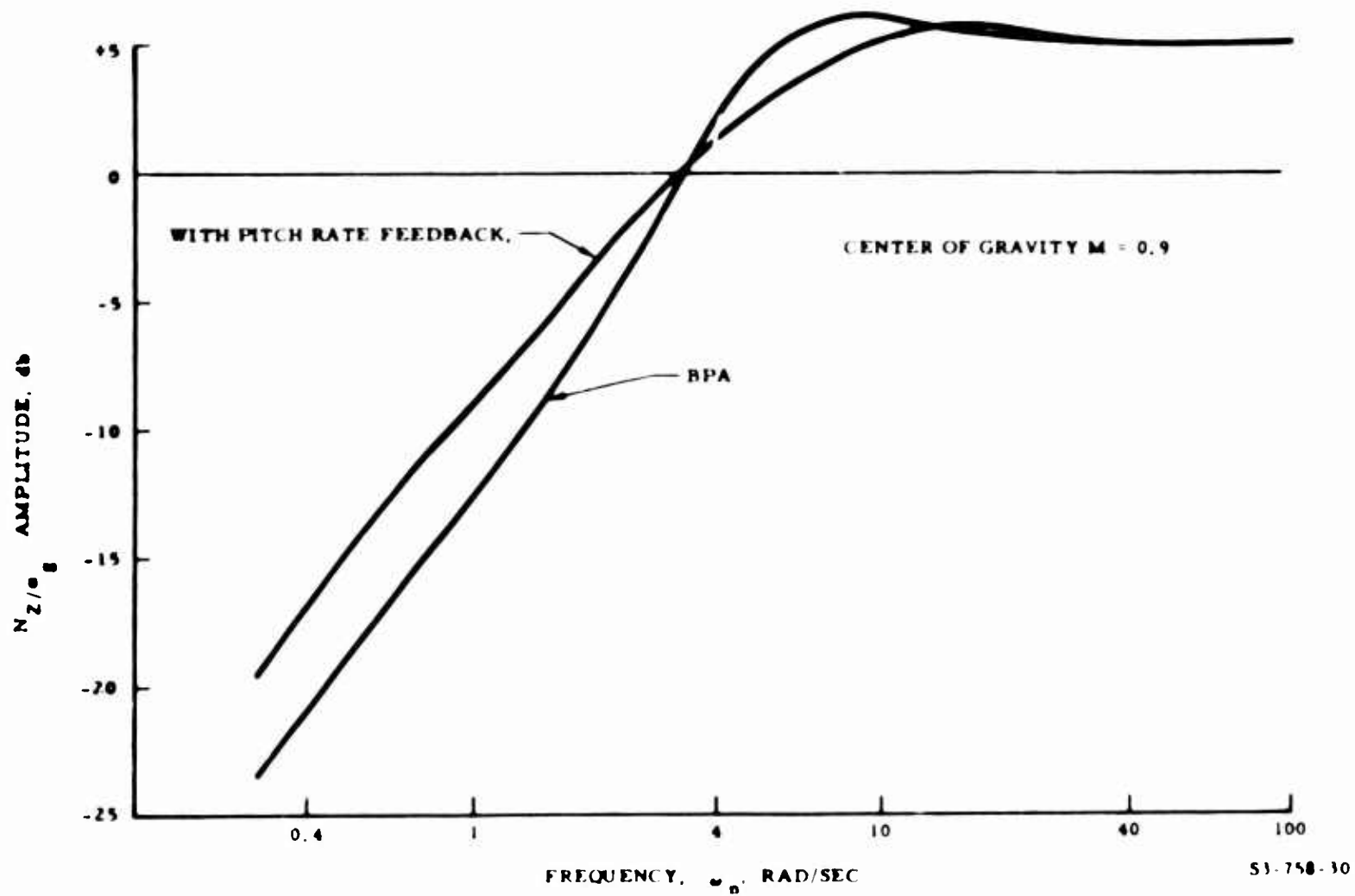
Figure 30. Effect of Pitch Rate Feedback on Acceleration
Response to Gust Disturbances

S3-758-30
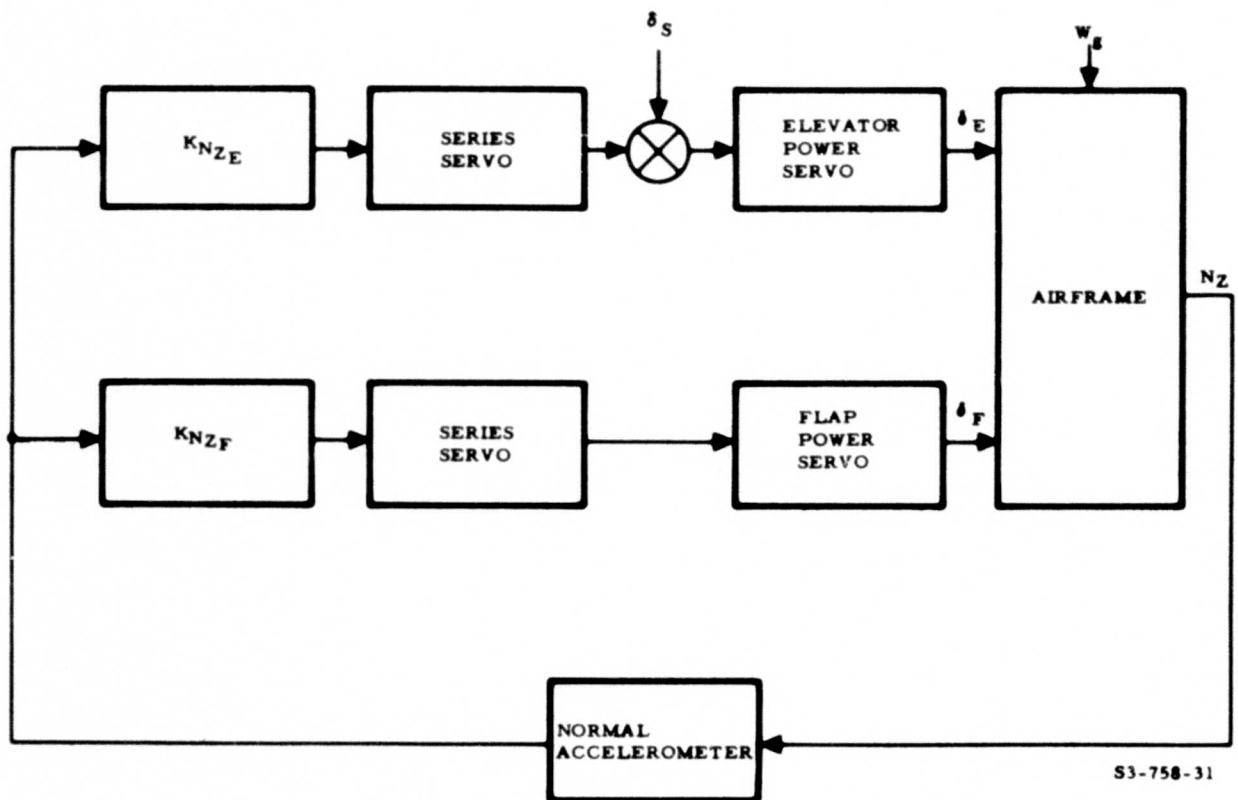
Figure 31. Block Diagram of Normal Acceleration System
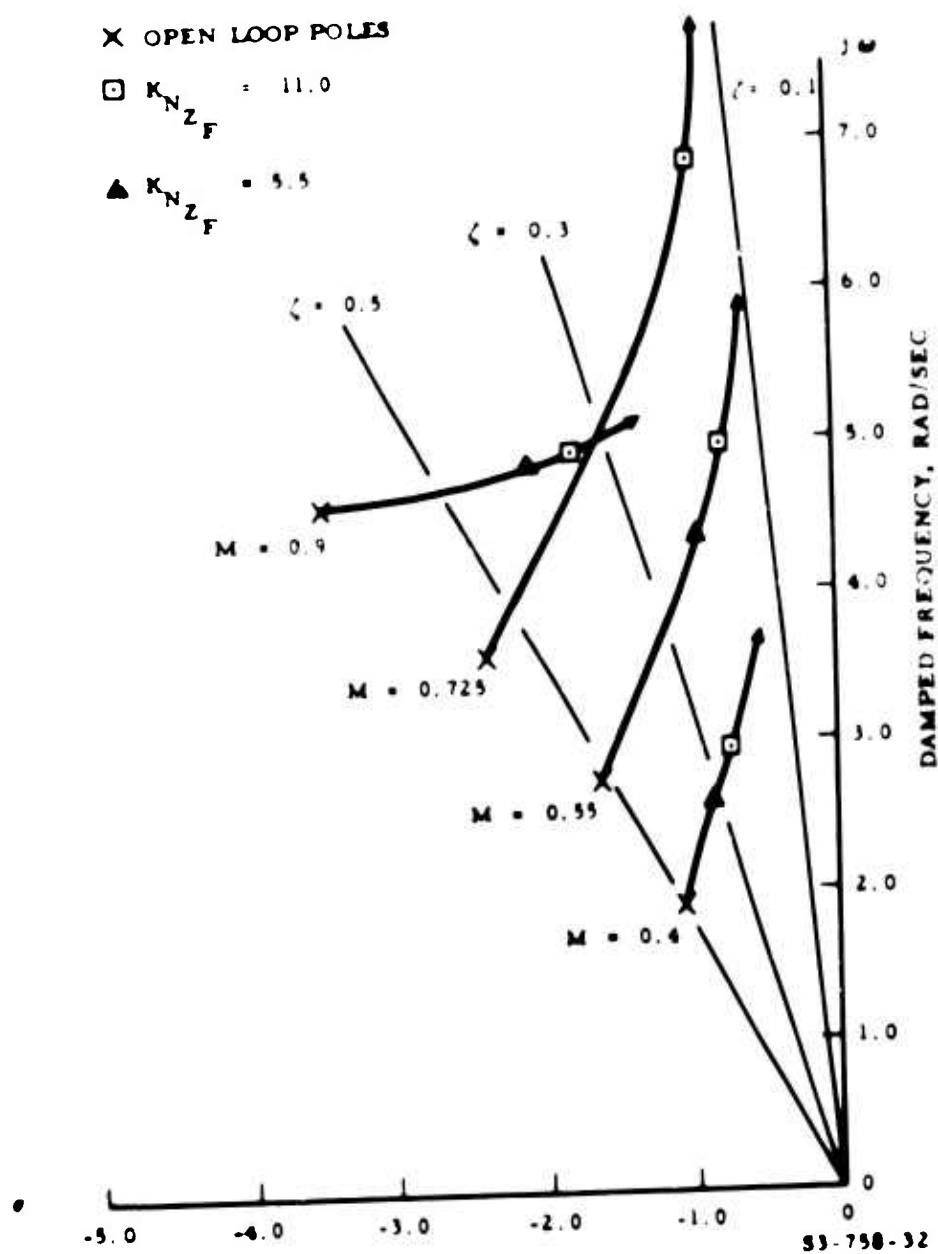
Figure 32. Short Period Loci With N_Z System
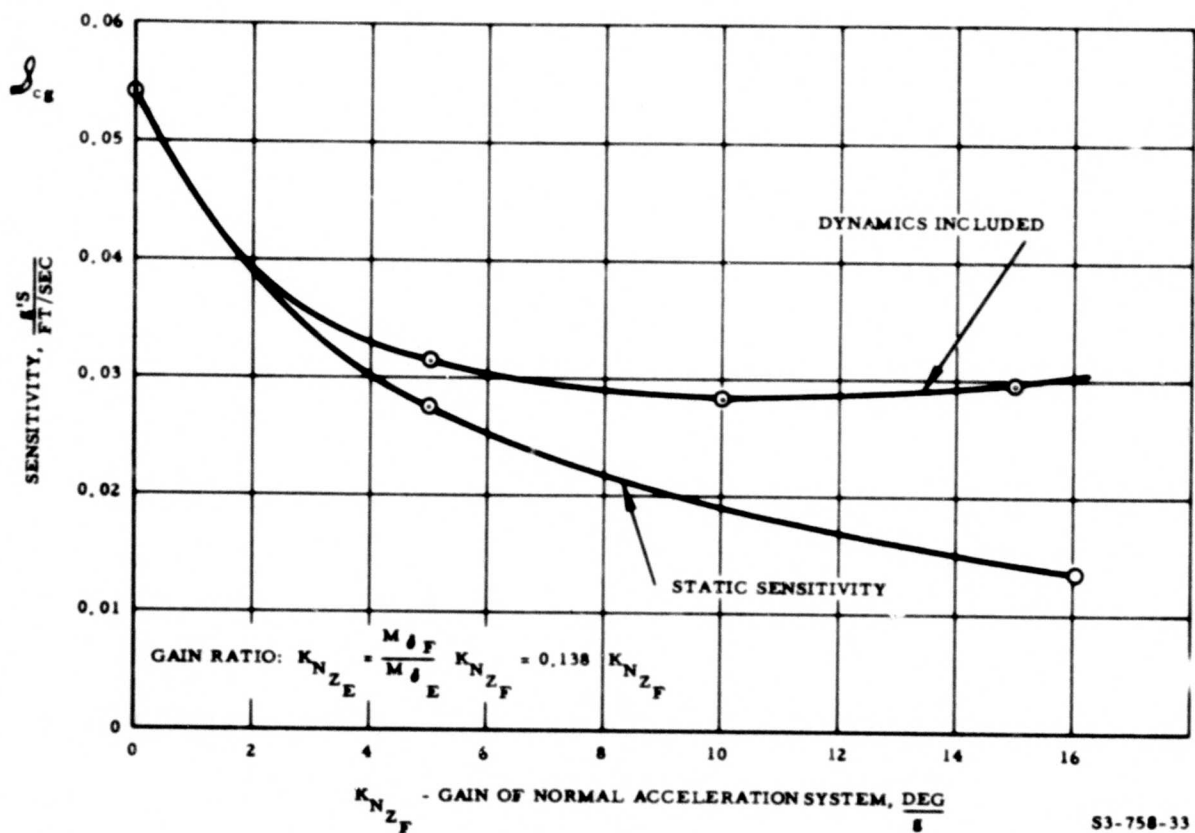
Figure 33. Effect of N_Z Gain on Gust Sensitivity

S3-758-33

142
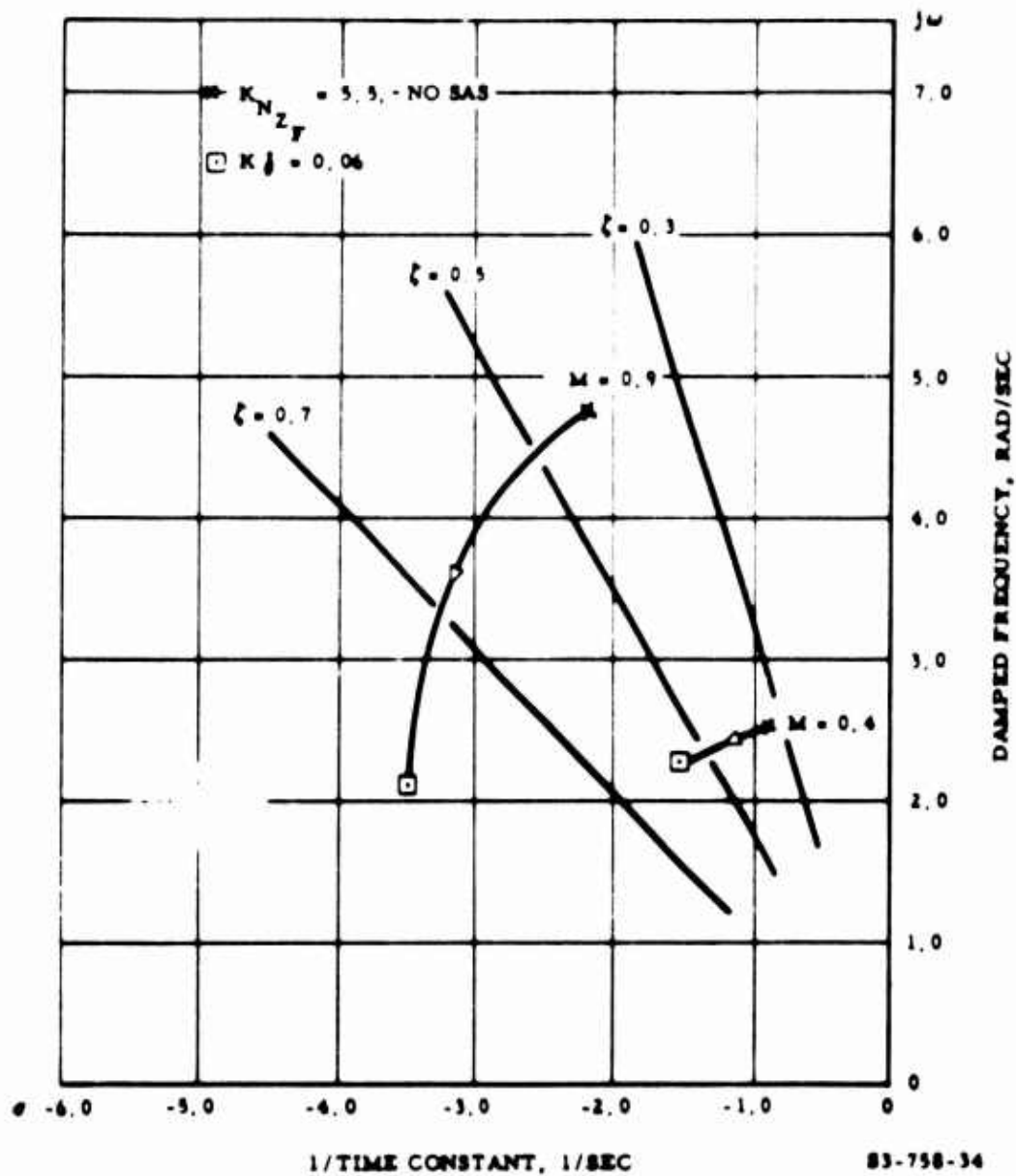
Figure 34. Short Period Loci With SAS Added to N_Z System

143
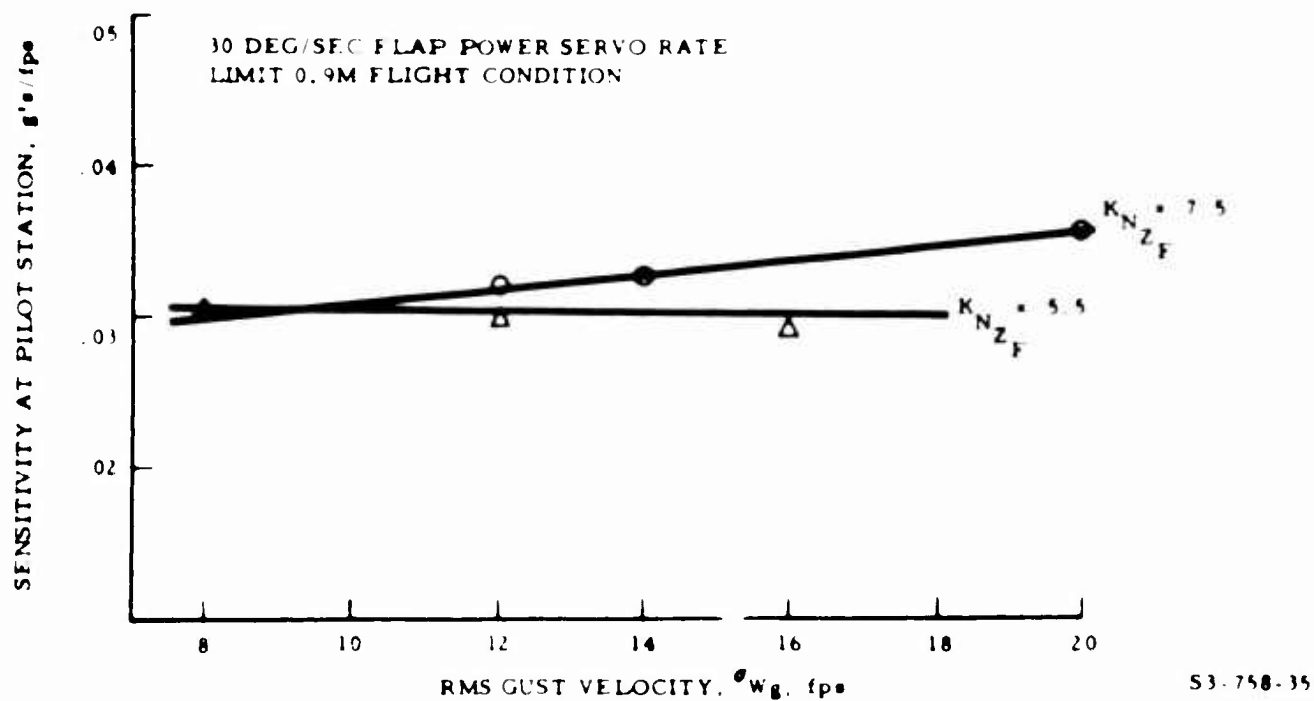
Figure 35. Effect of Flap Power Servo Rate Limit on
Gust Sensitivity, N_Z System
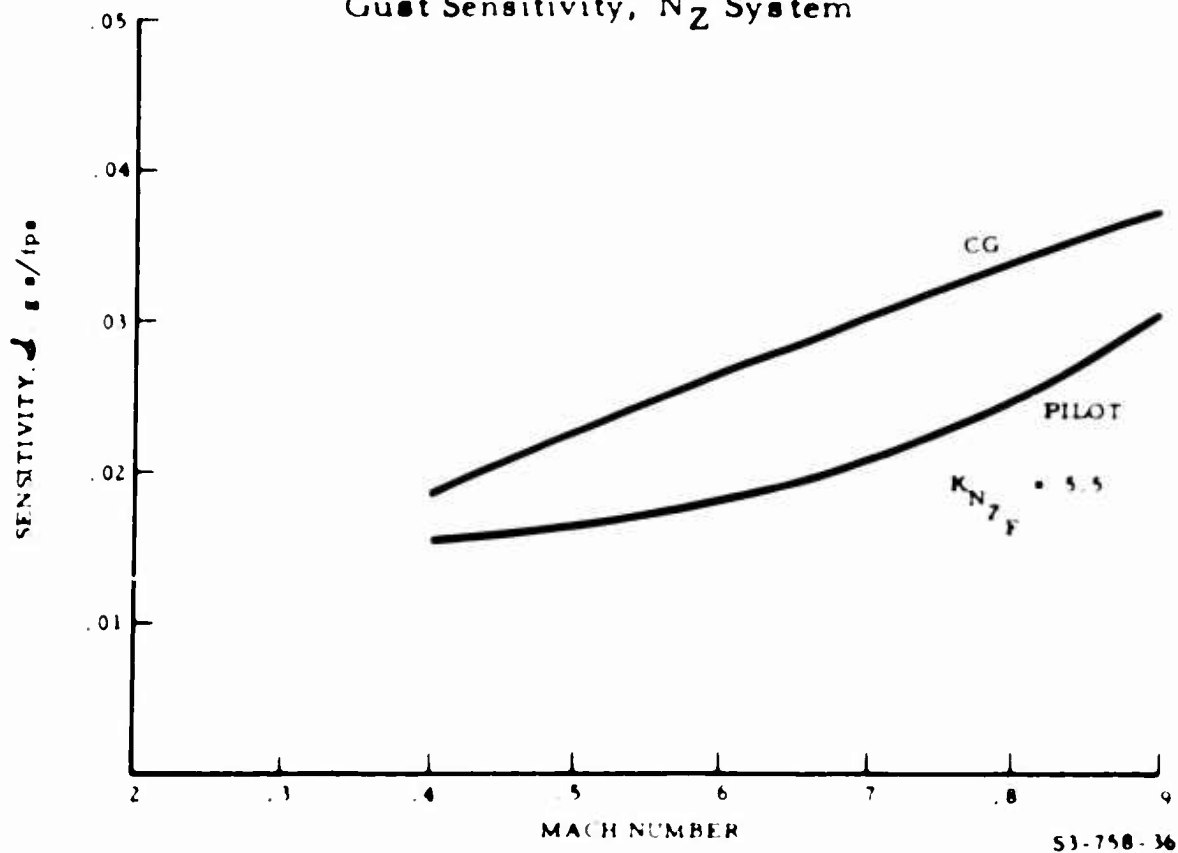
Figure 36. Gust Sensitivity With Normal
Acceleration System and SAS

144
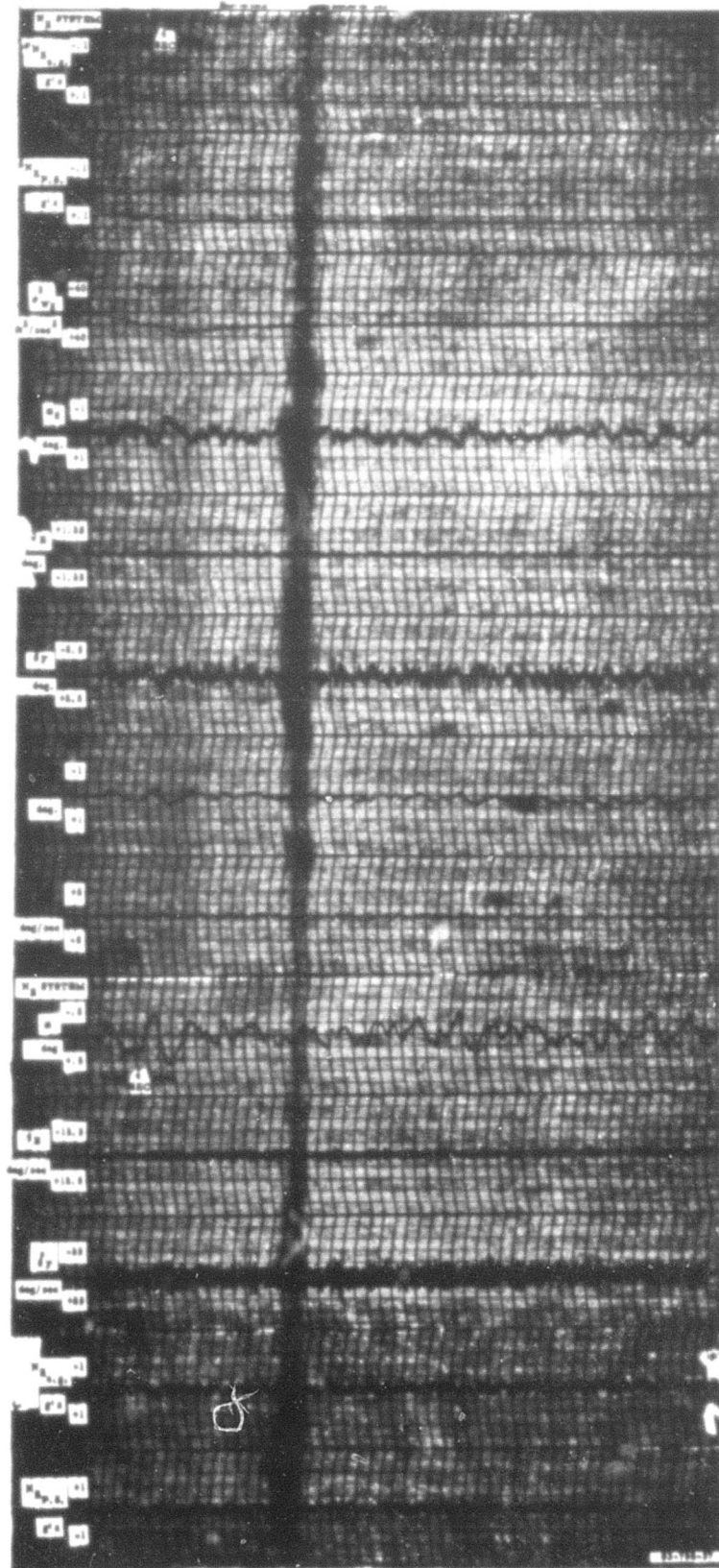
Figure 37.   Time History of Gust Response at 0. 9 Mach
With N_z System and SAS
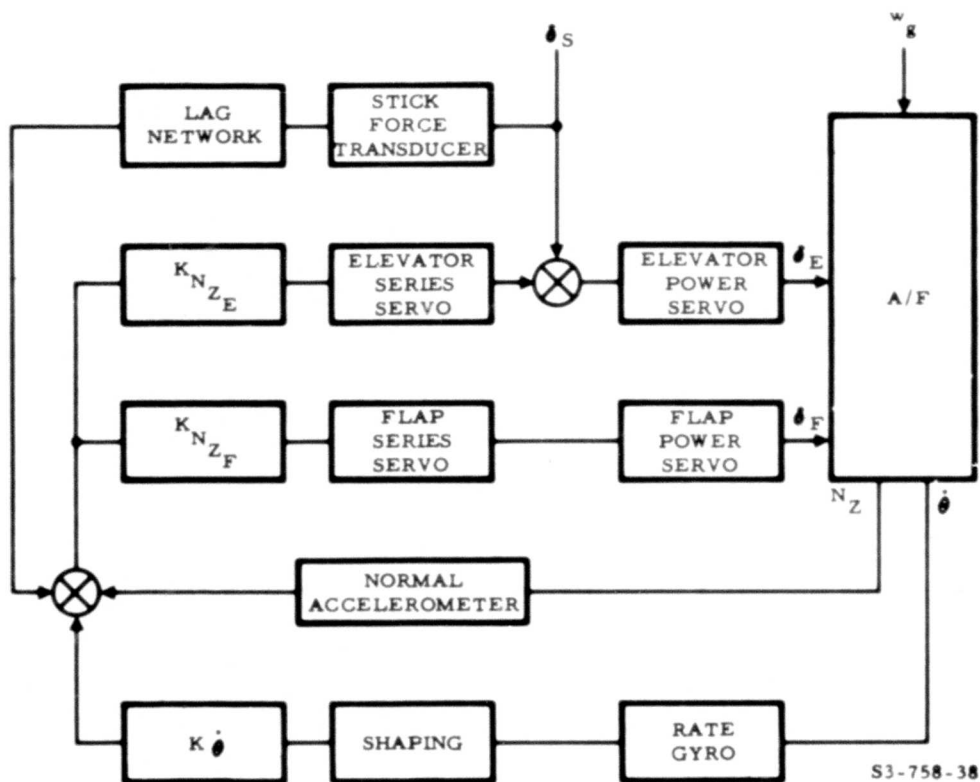
Figure 38. Block Diagram of N_Z System With SAS and Provision for Pilot Control

146
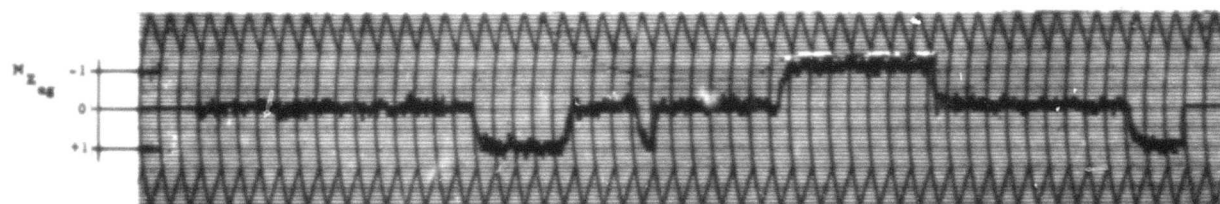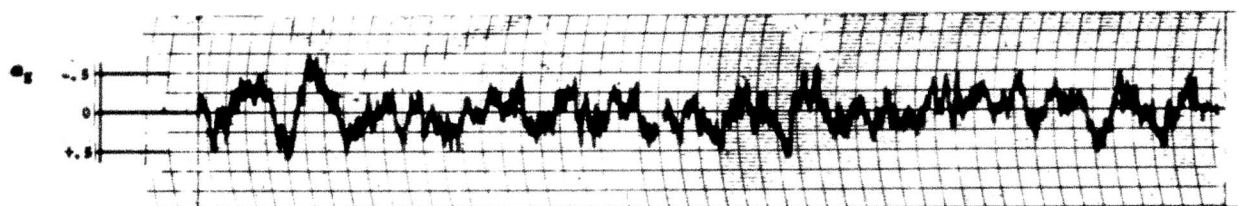
a. Step Commands
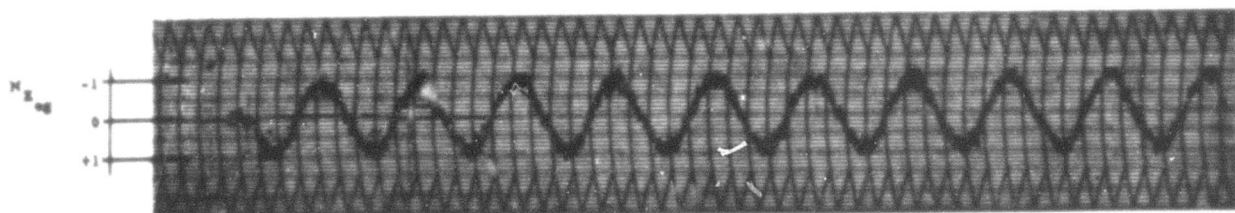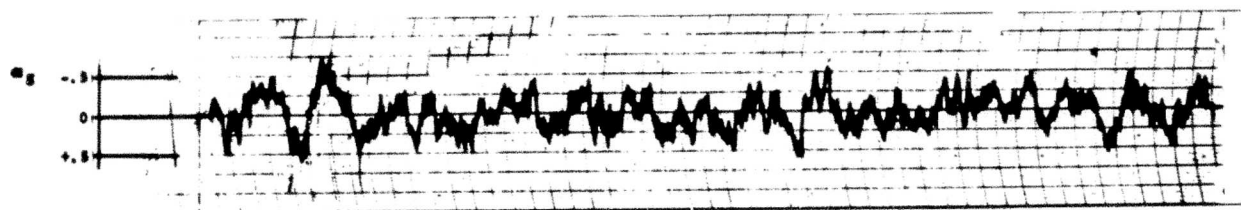
b. Sinusoidal Command

83-758-39

**Figure 39.   Time History of Simultaneous Alleviation
and Pilot g- Commands**

147

FLAP POWER ACTUATOR

RATE GYROSCOPE AND
ELECTRONICS PACKAGE

ELEVATOR

FLAP SERIES SERVO

ELEVATOR SERIES
SERVO

STICK FORCE
TRANSDUCER

FLAP

NORMAL ACCELEROMETER
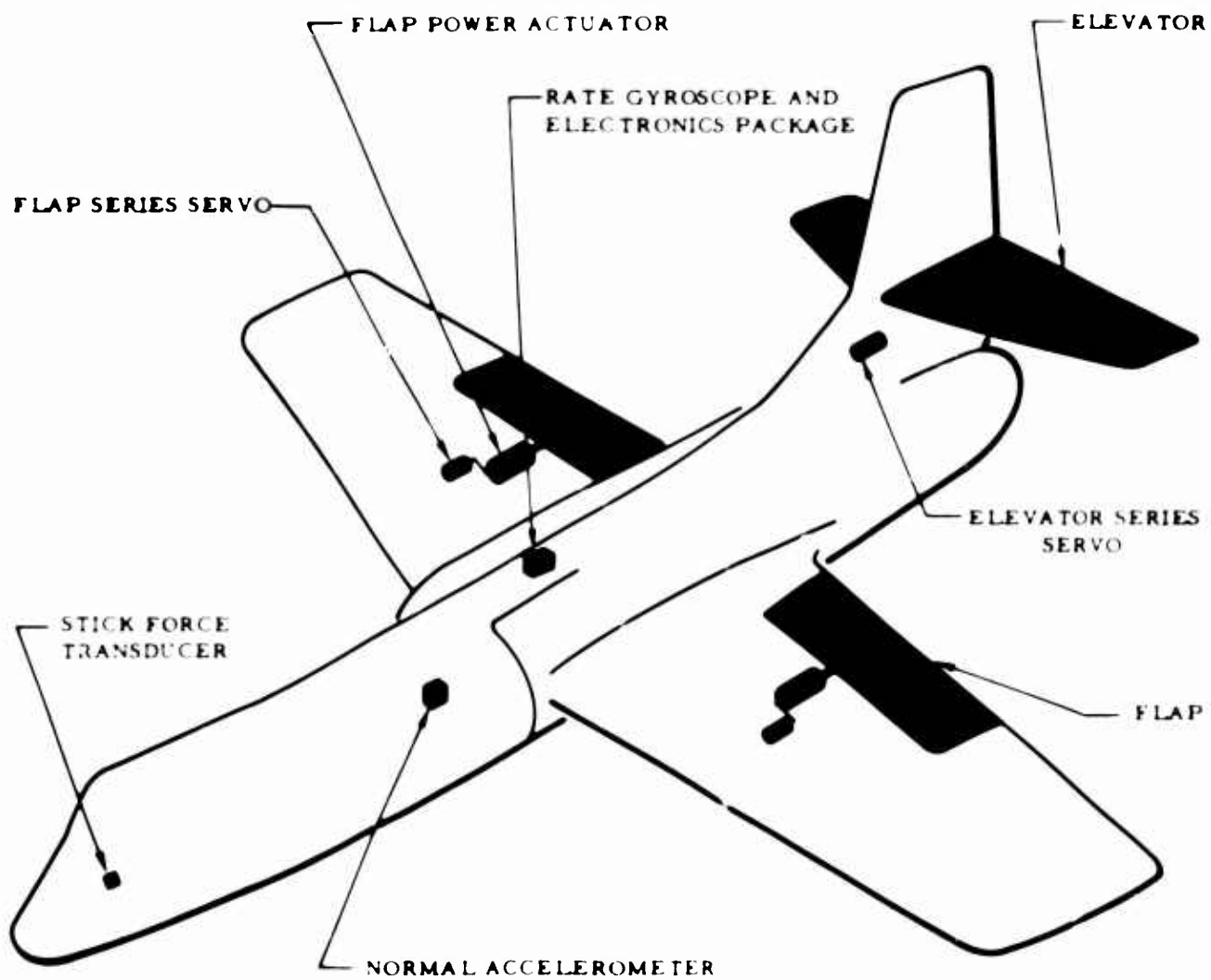
S3-758-40

Figure 40.   Equipment Location - Normal Acceleration
System With SAS

148
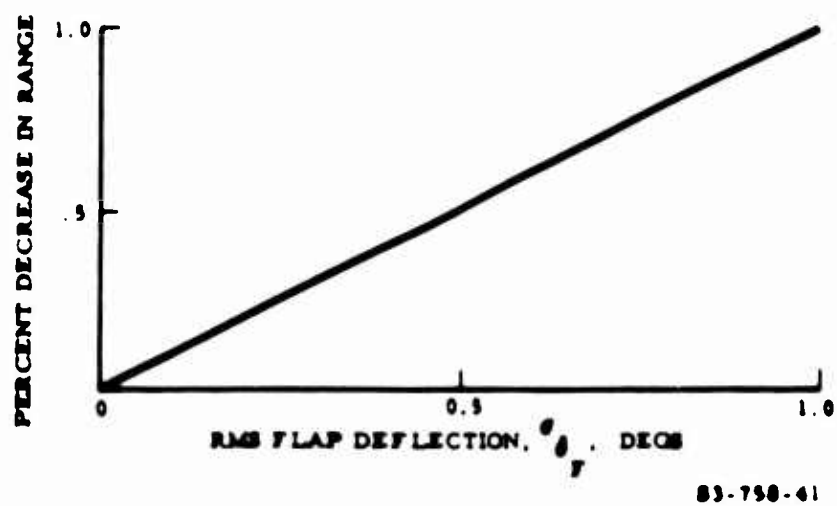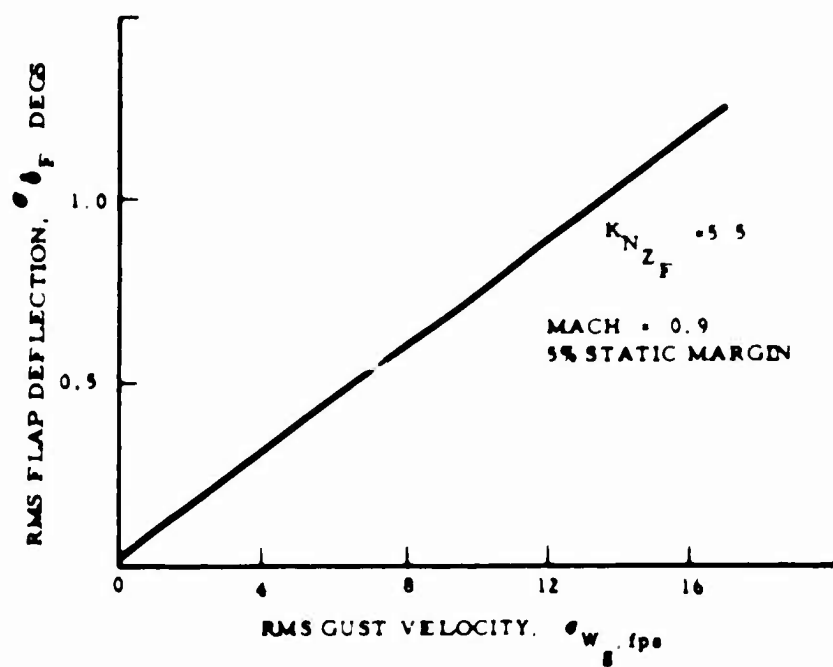
Figure 41.   Range Degradation Due to Flap Motion
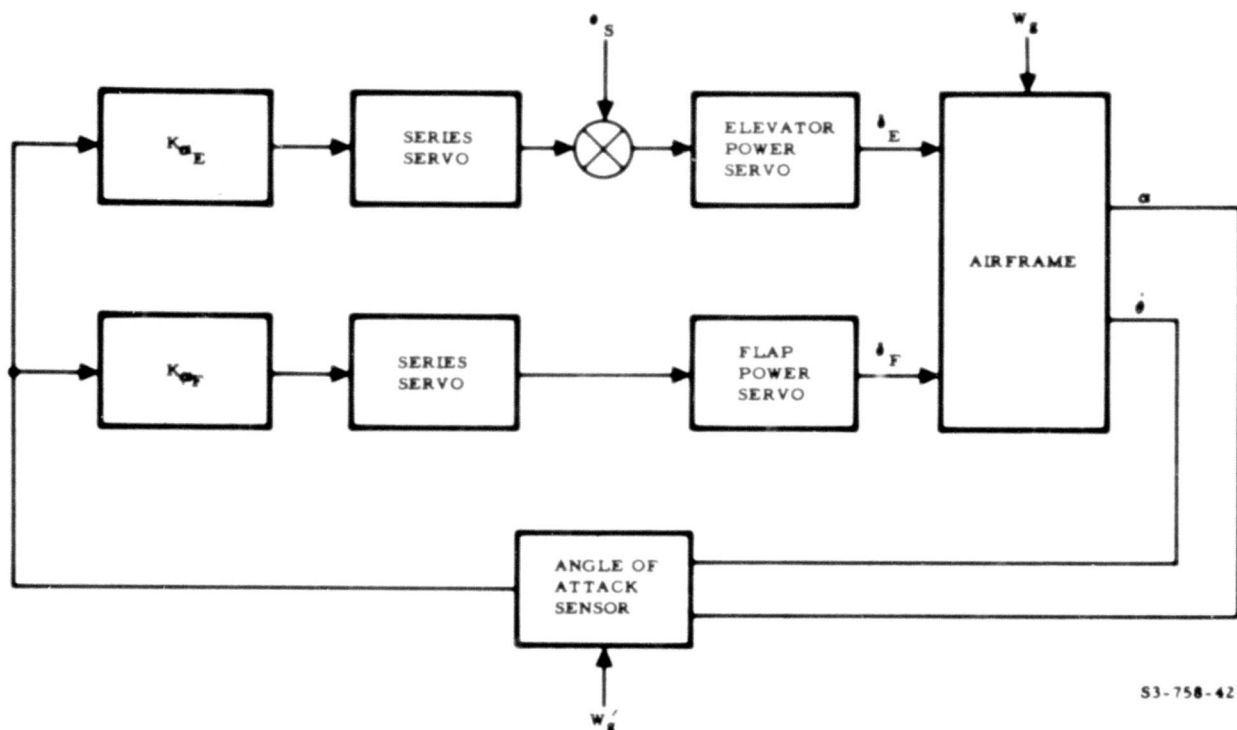
Figure 42. Block Diagram of Angle-of-Attack System, α
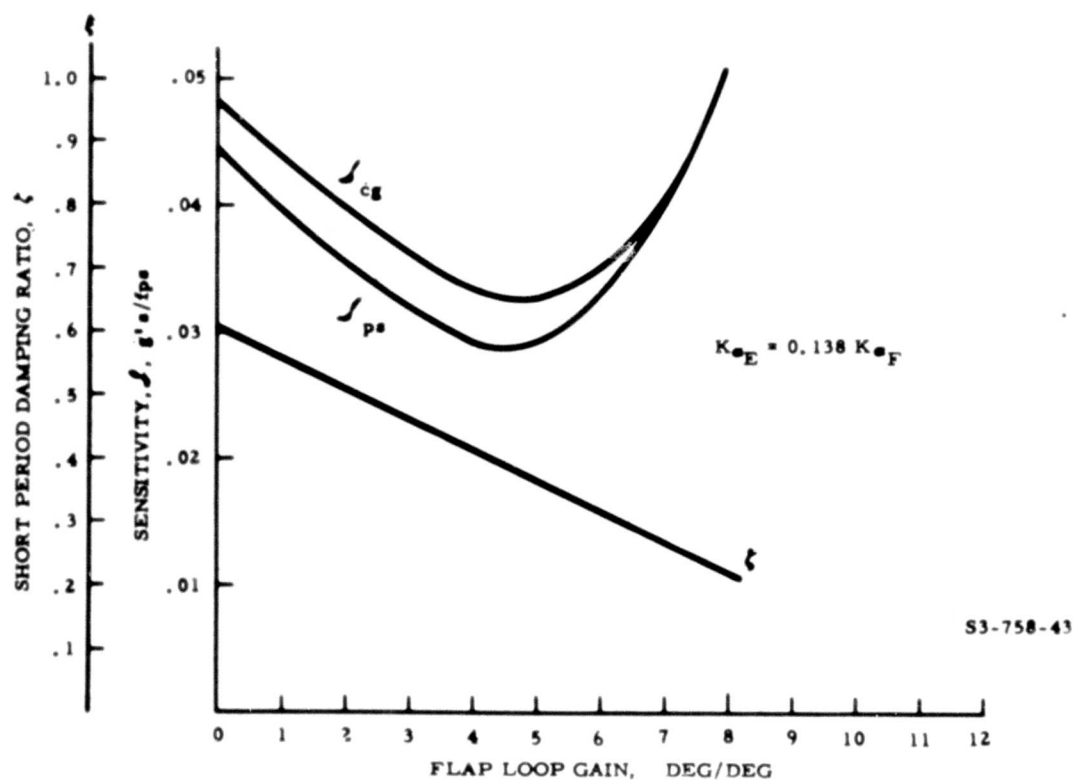
Figure 43. Effect of Flap Gain on Sensitivity and Damping
at 0.9 Mach, α System

150
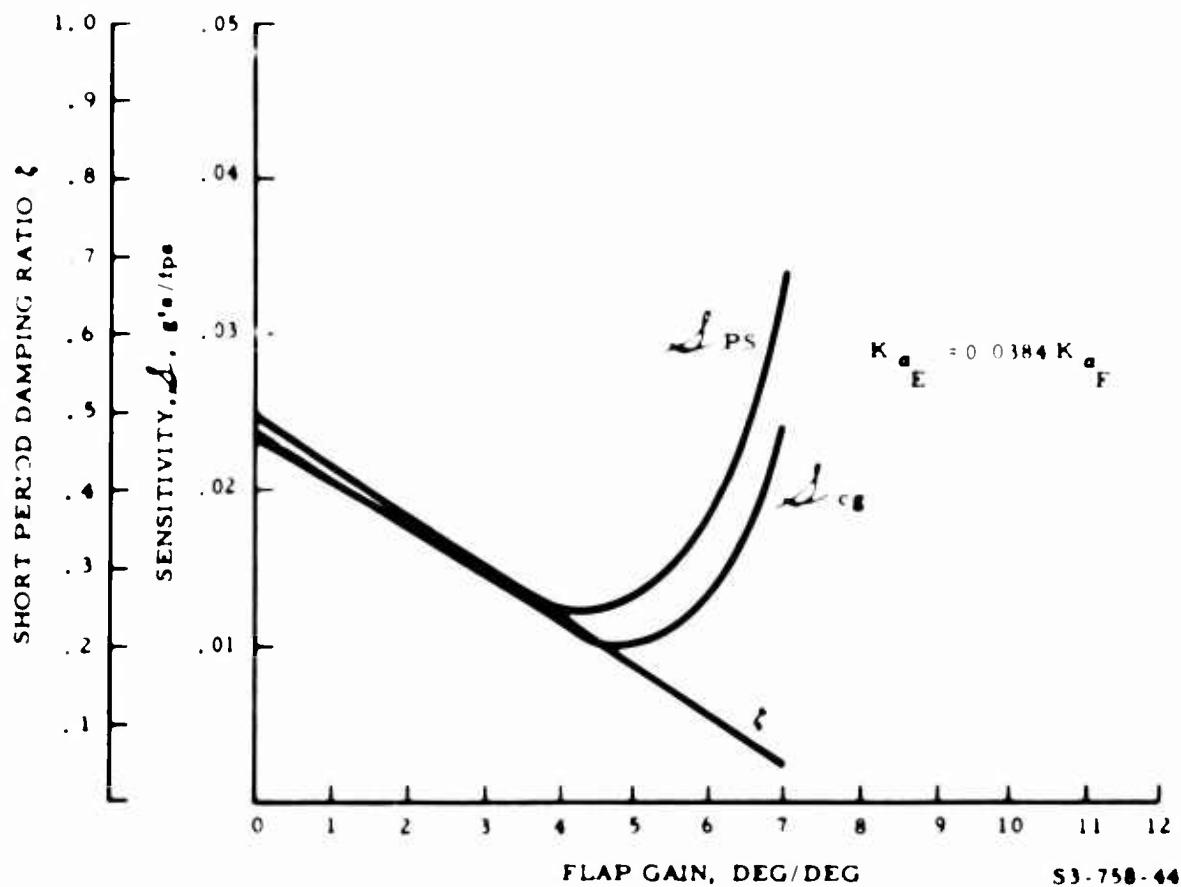
Figure 44. Effect of Flap Gain on Sensitivity and Damping at 0.4 Mach, α System

151
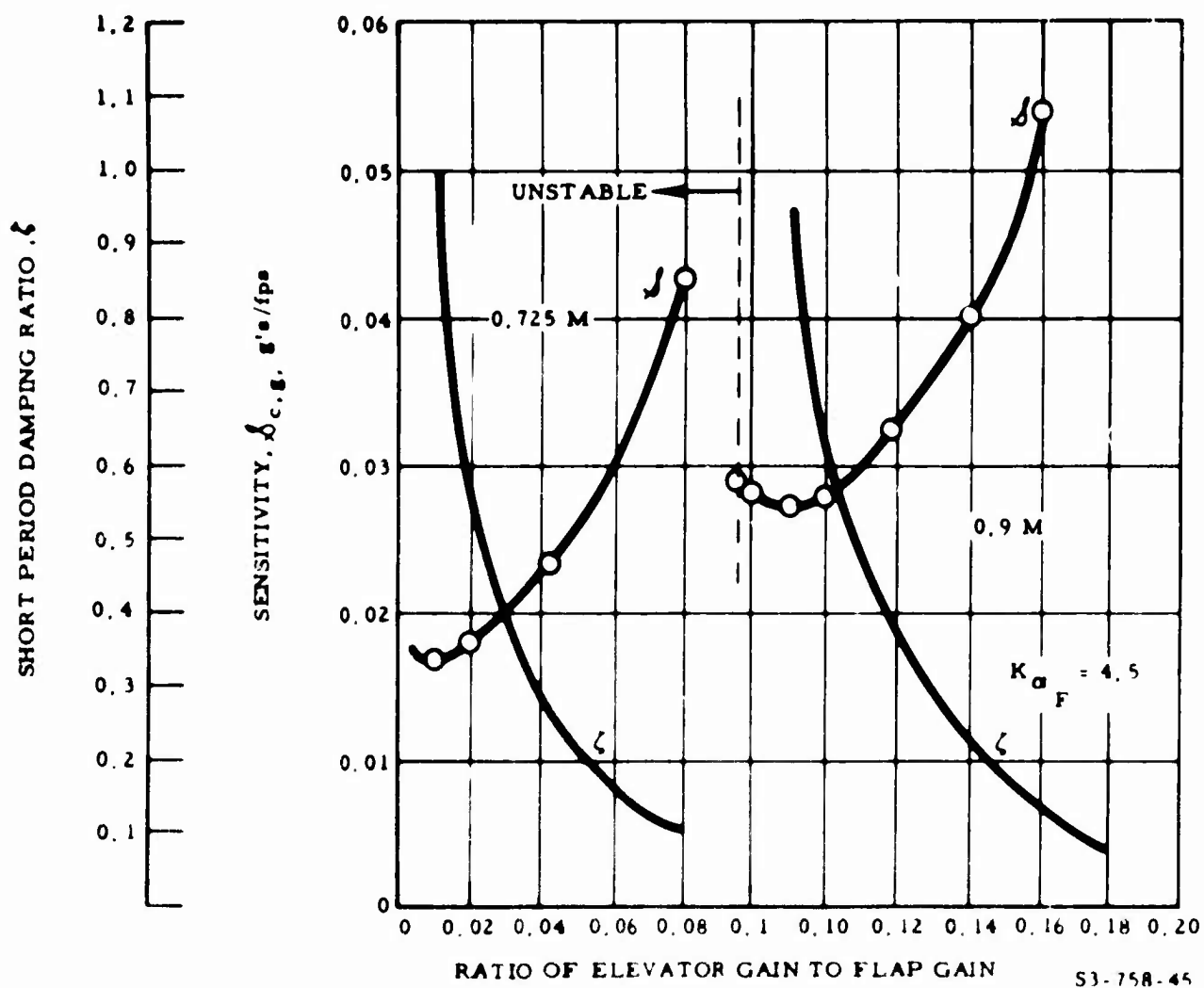
Figure 45.   Effect of Gain Ratio on Sensitivity and
Damping, α System

$K_{\theta_F} = 4.5, \quad K_E = 0.138 \, K_F$

$\boxdot \quad K_G = 0.06$
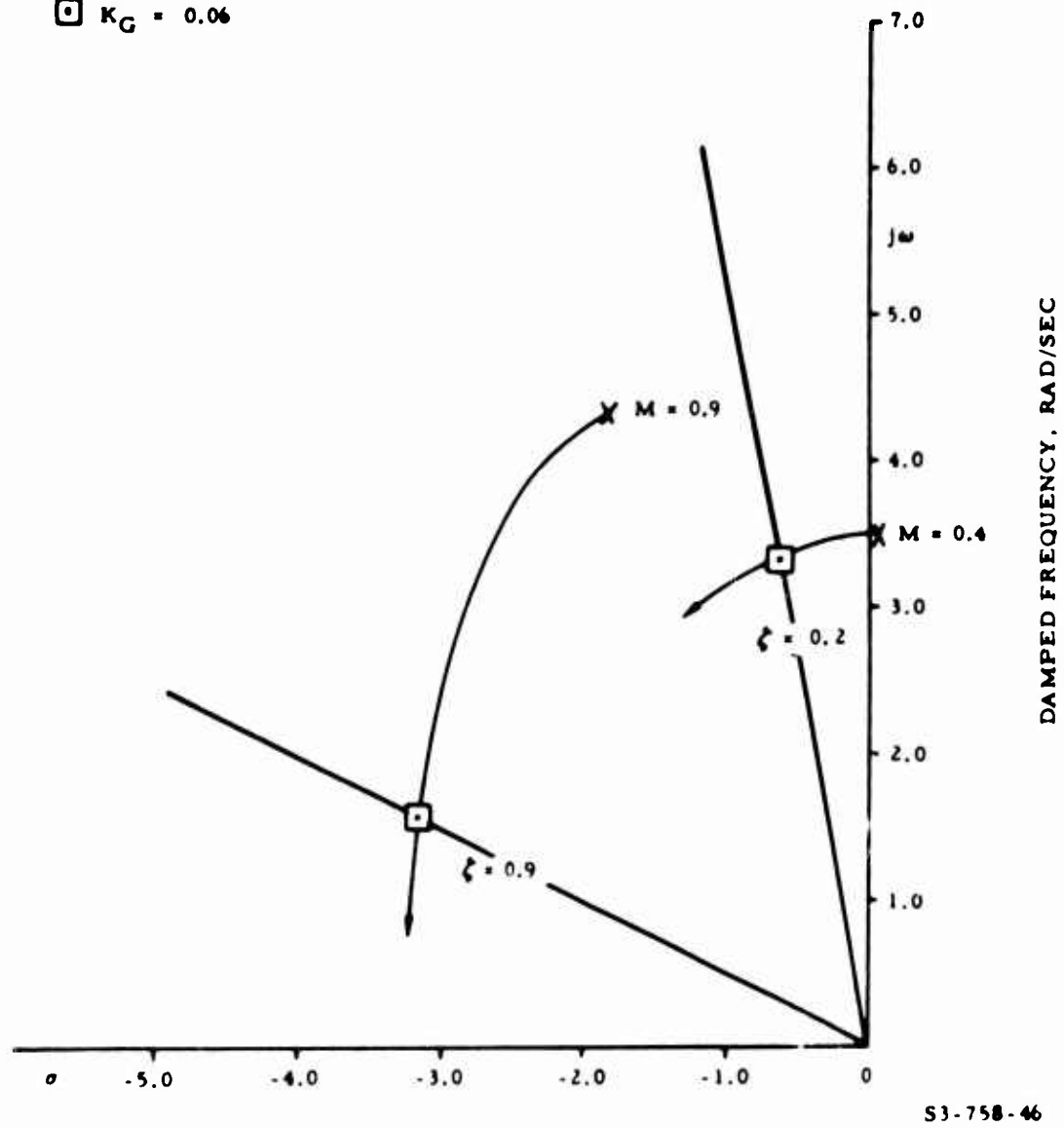
Figure 46. Short Period Loci With SAS Added to α System

S3-758-46

153
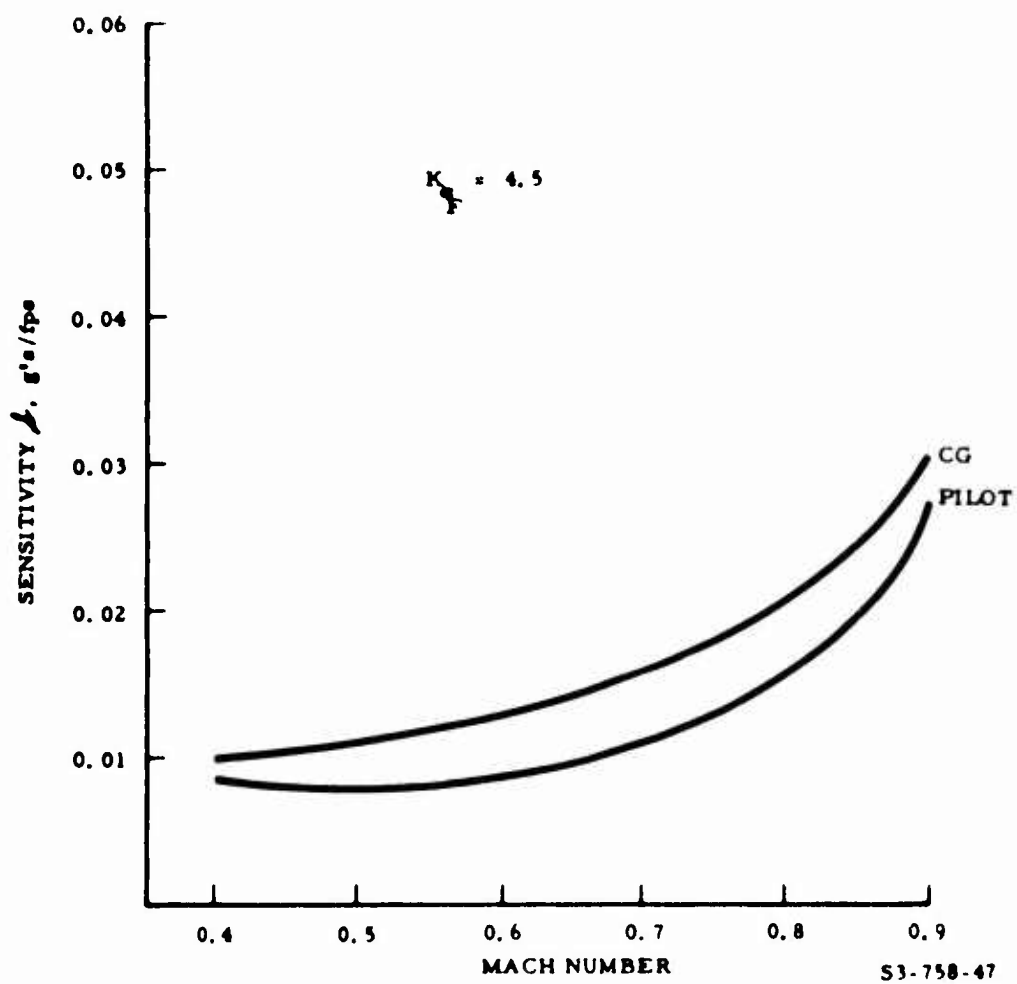
Figure 47. Gust Sensitivity With Angle-of-Attack System and SAS
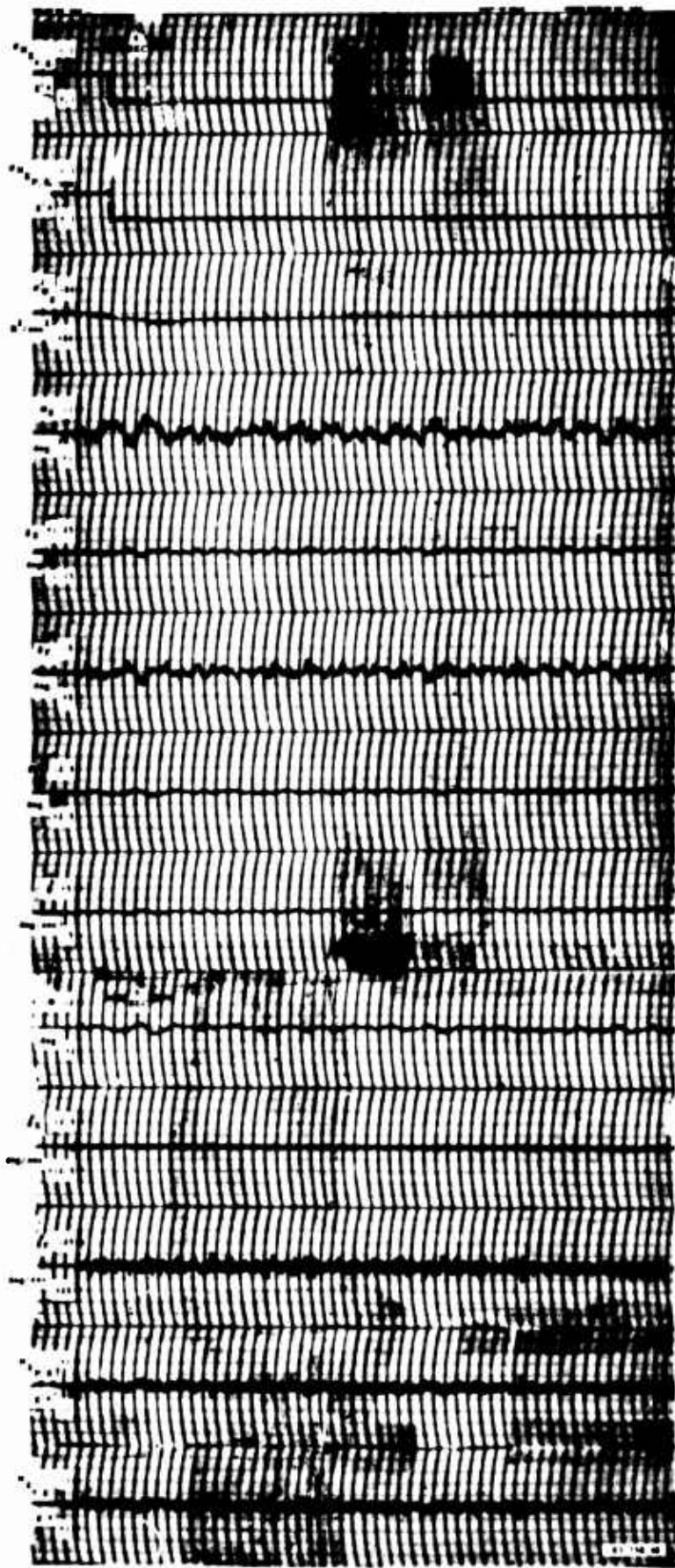
Figure 48. Time History of Gust Response at
0.9 Mach With α System and SAS

155
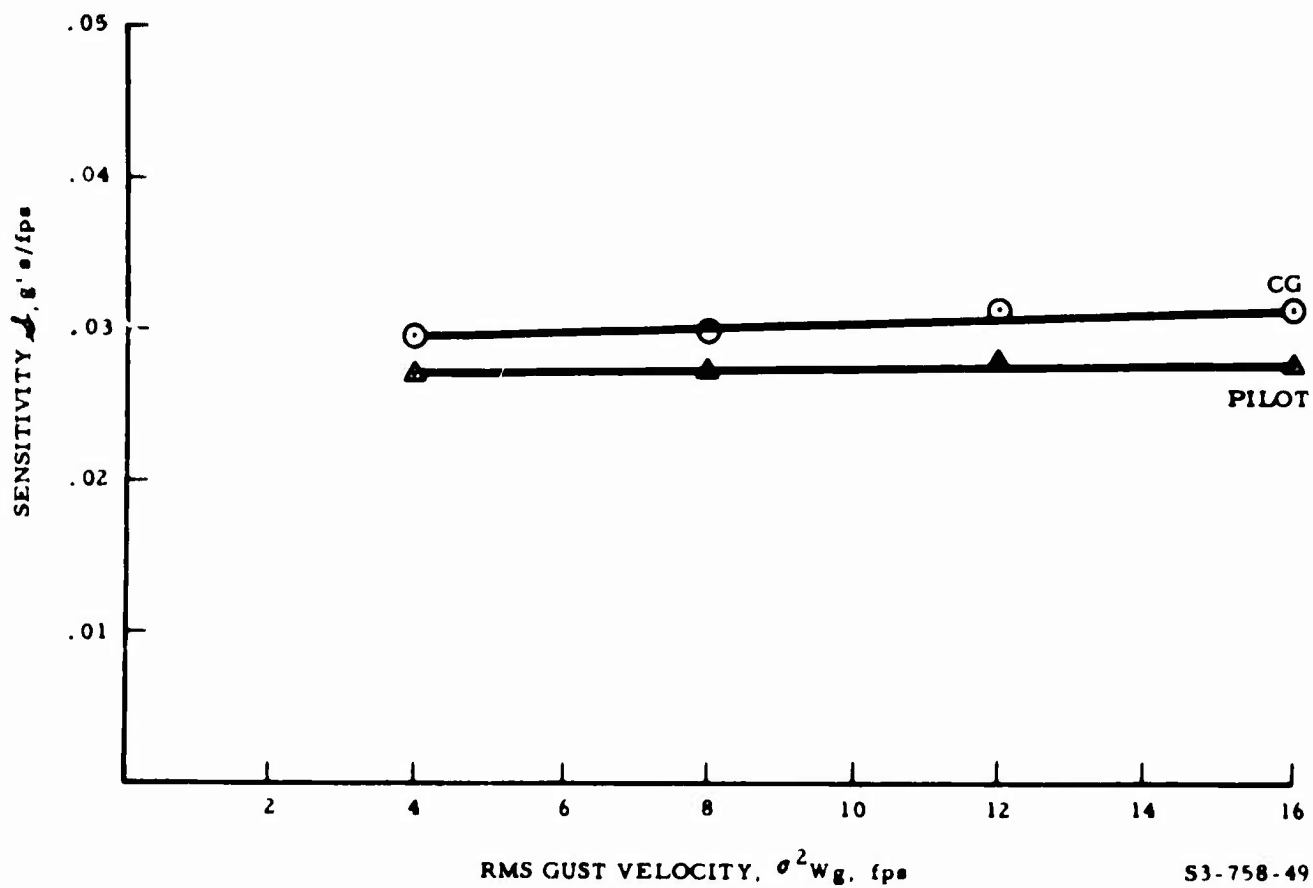
Figure 49. Effect of Flap Power Servo Rate Limit on Gust Sensitivity, α System

FLAP POWER ACTUATOR — — RATE GYROSCOPE AND
ELECTRONICS PACKAGE — ELEVATOR

FLAP SERIES SERVO —

ELEVATOR SERIES
SERVO

STICK
FORCE TRANSDUCER

FLAP

ANGLE OF ATTACK SENSOR
(VANE OR PRESSURE PROBE)

S3-758-50
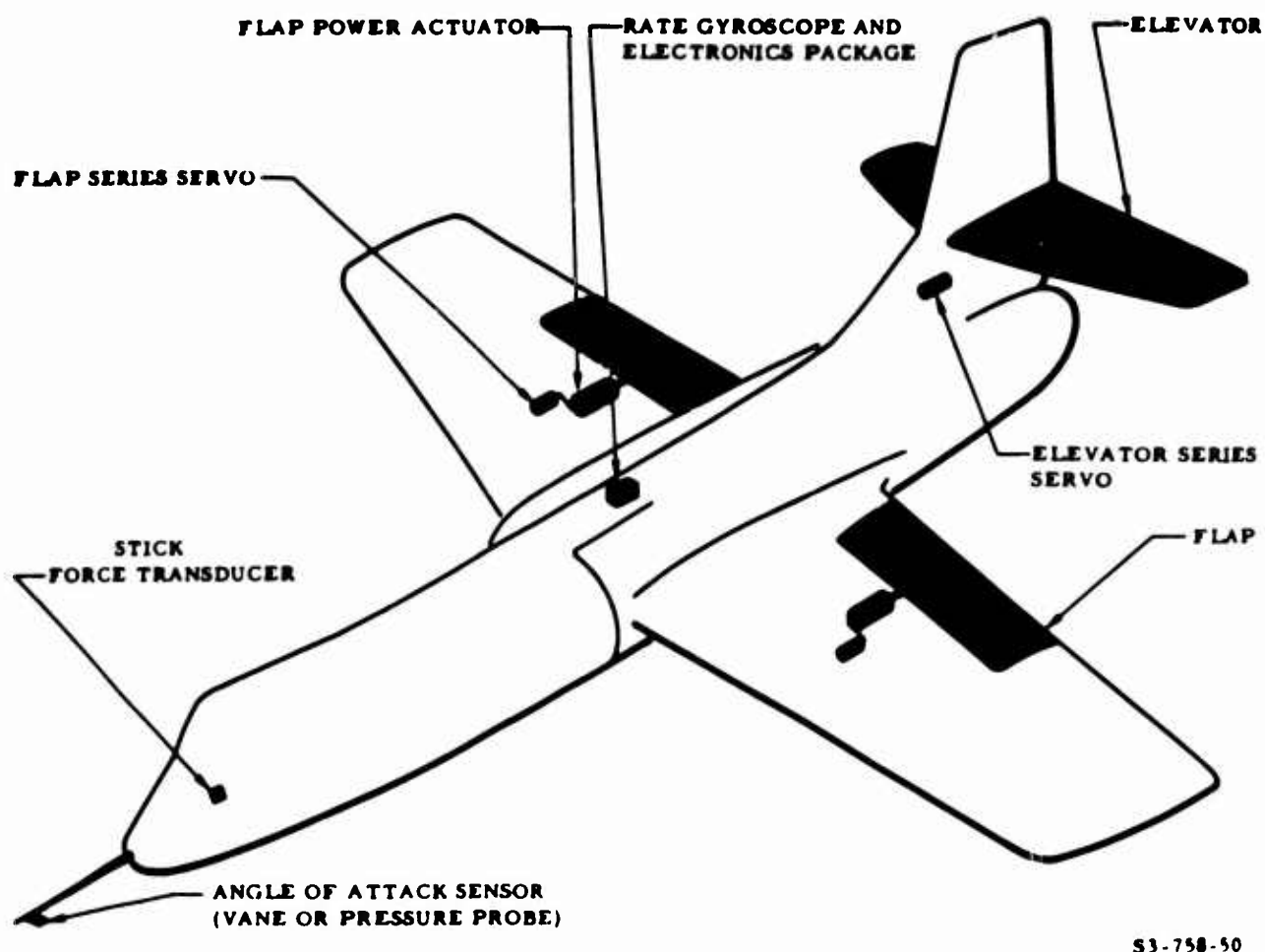
Figure 50. Equipment Location, Angle-of-Attack System With SAS

157
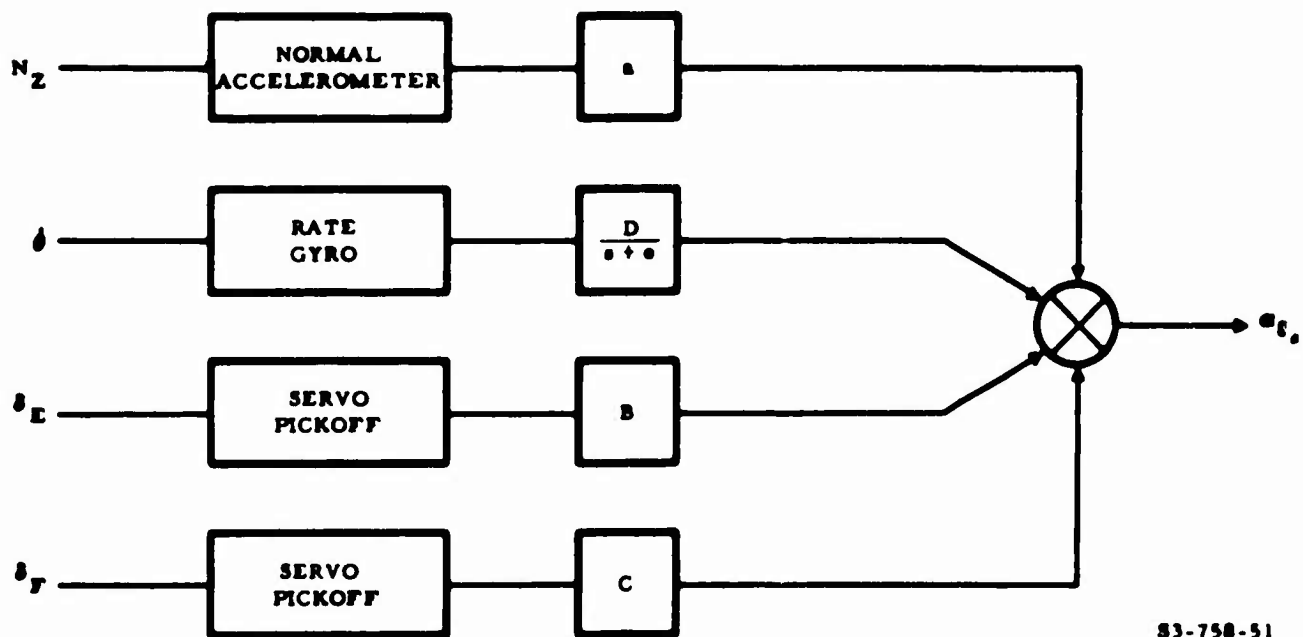
83-758-51

Figure 51.   Gust Signal Formulation With Inertial Sensors
and Servo Pickoffs

158

BLANK PAGE
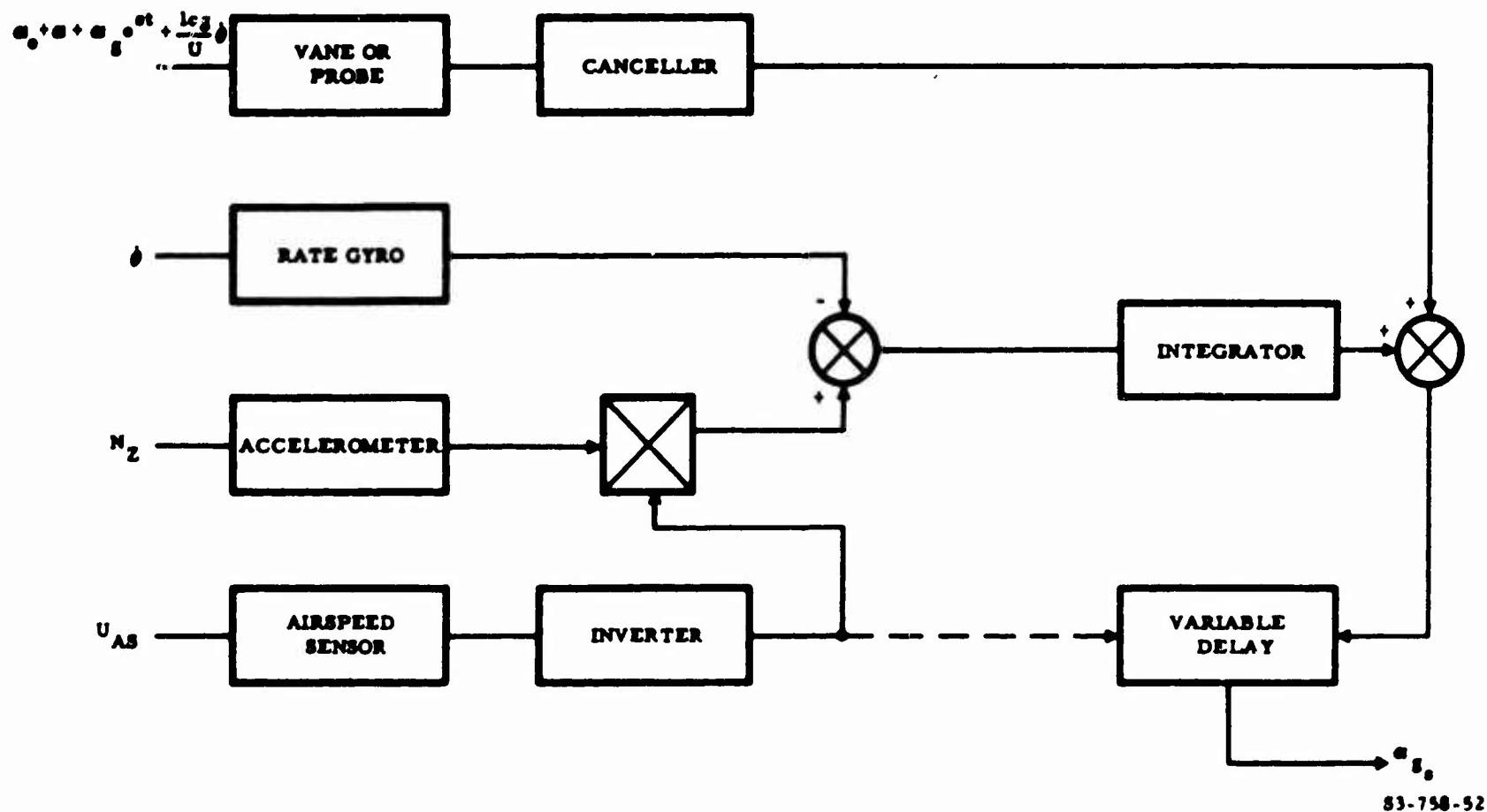
83-758-52

Figure 52. Gust Signal Formulation With Angle-of-Attack and Inertial Sensors
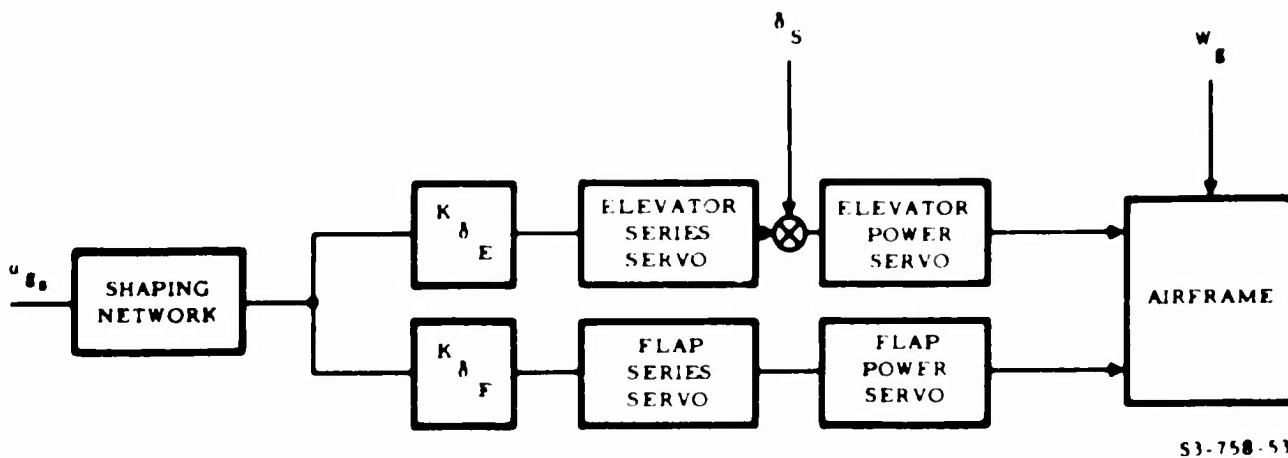
Figure 53. Utilization of Simulated Gust Signal

FRACTION OF NOMINAL ELEVATOR LOOP GAIN
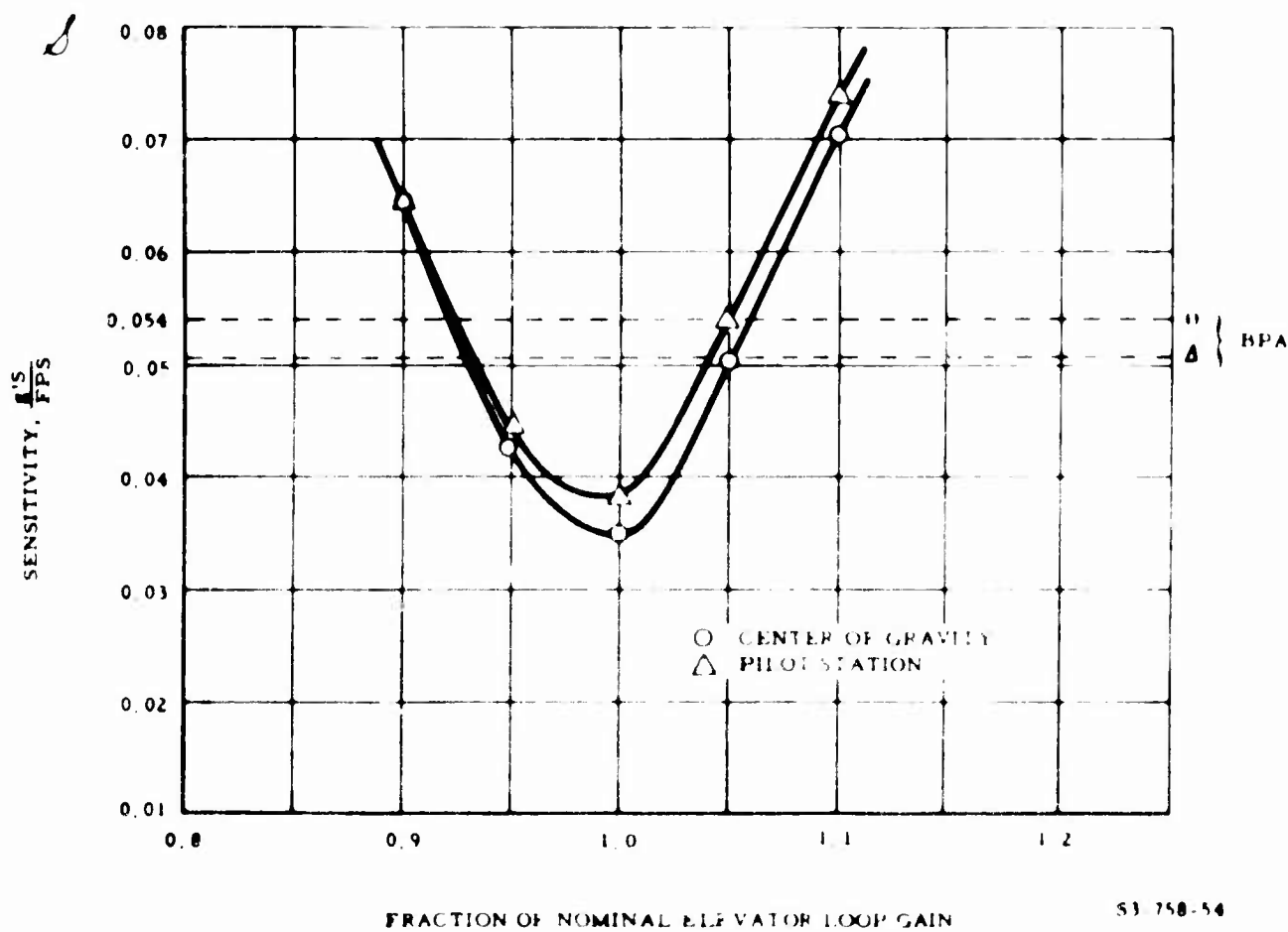
Figure 54. Measured Sensitivity With Simulated Gust System

160
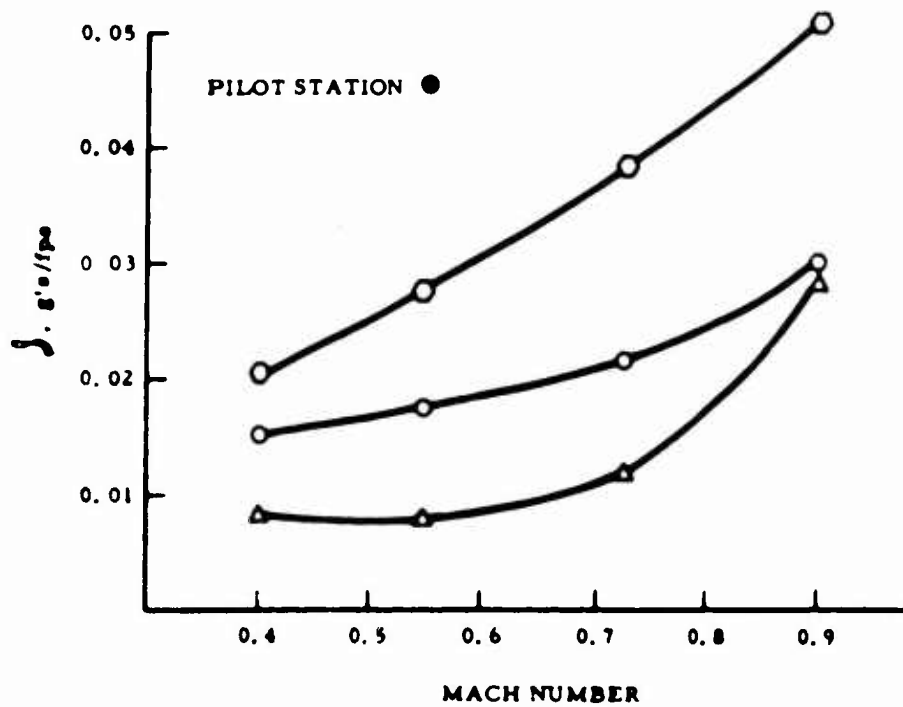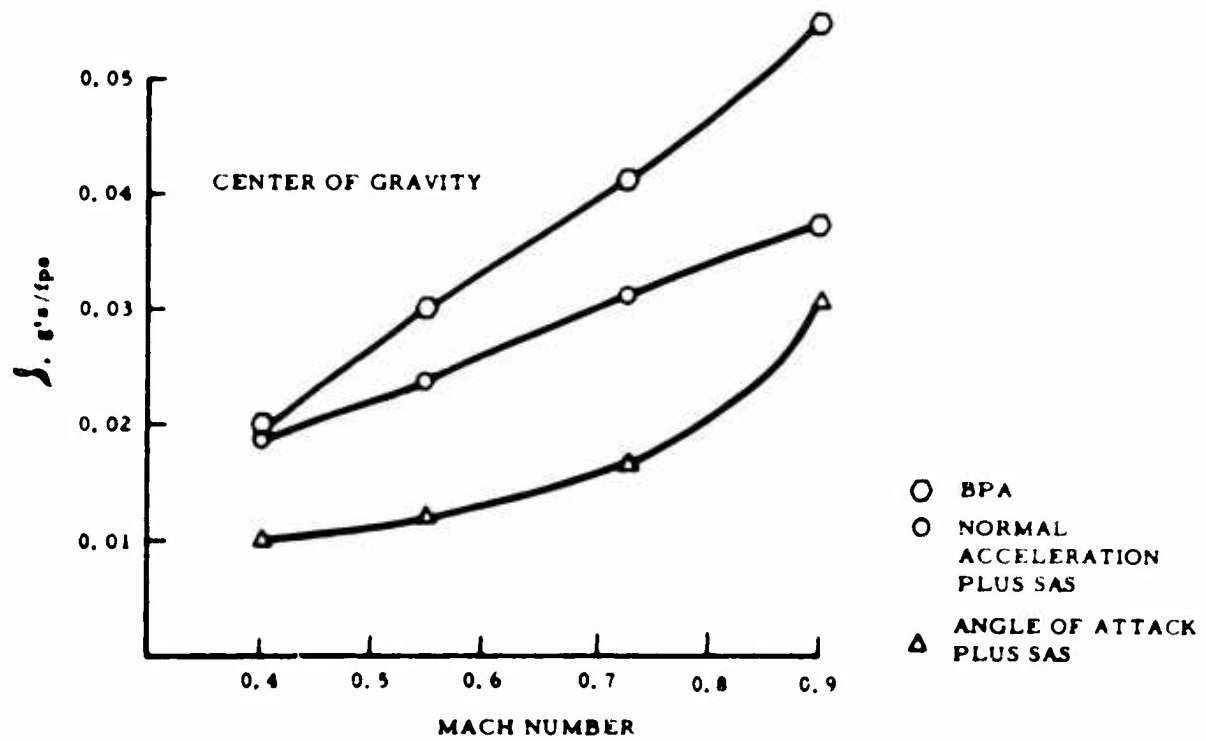
Figure 55. Gust Sensitivity With Active Systems

83-758-55

161
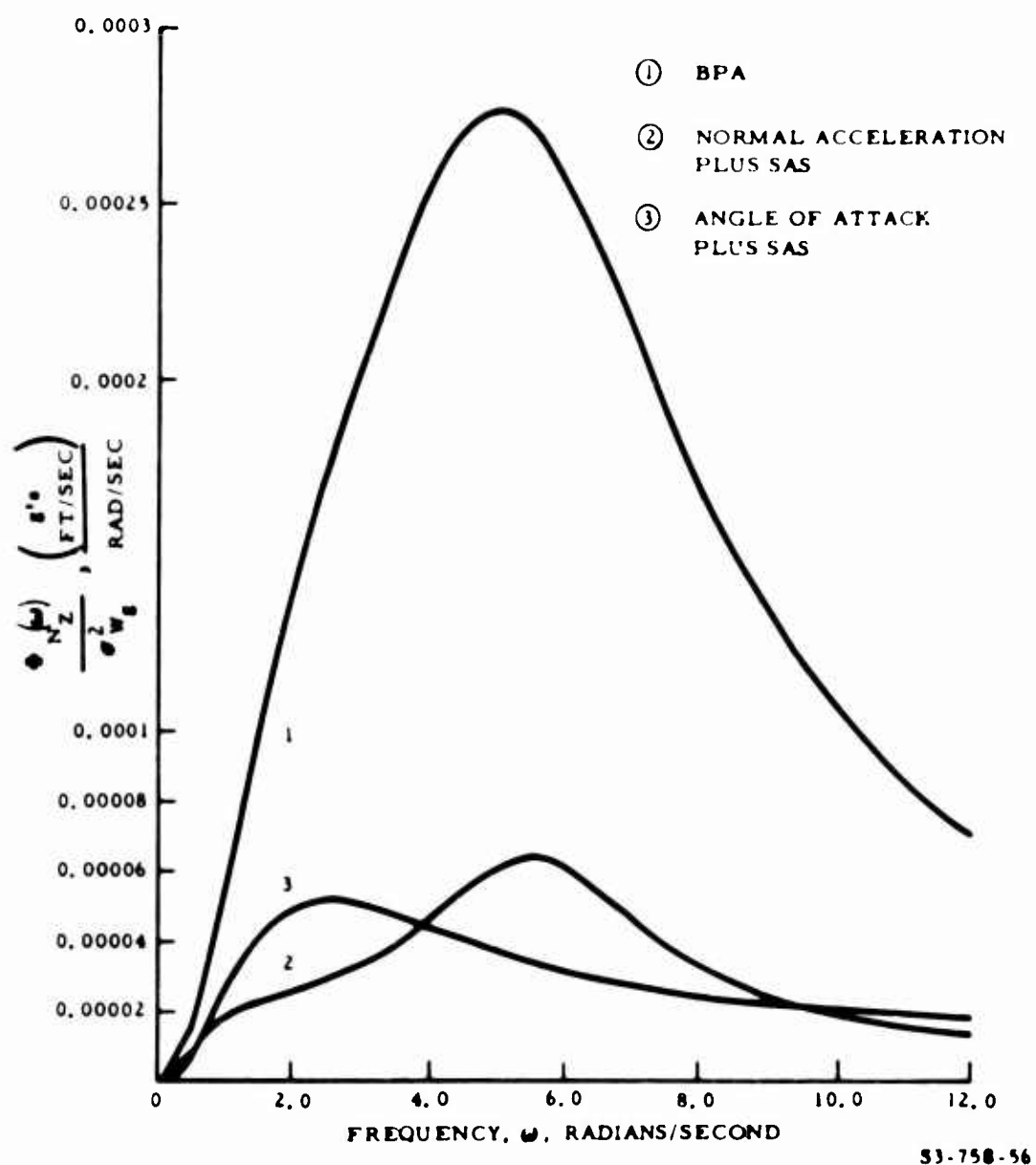
Figure 56. Acceleration Power Spectra With Active Systems
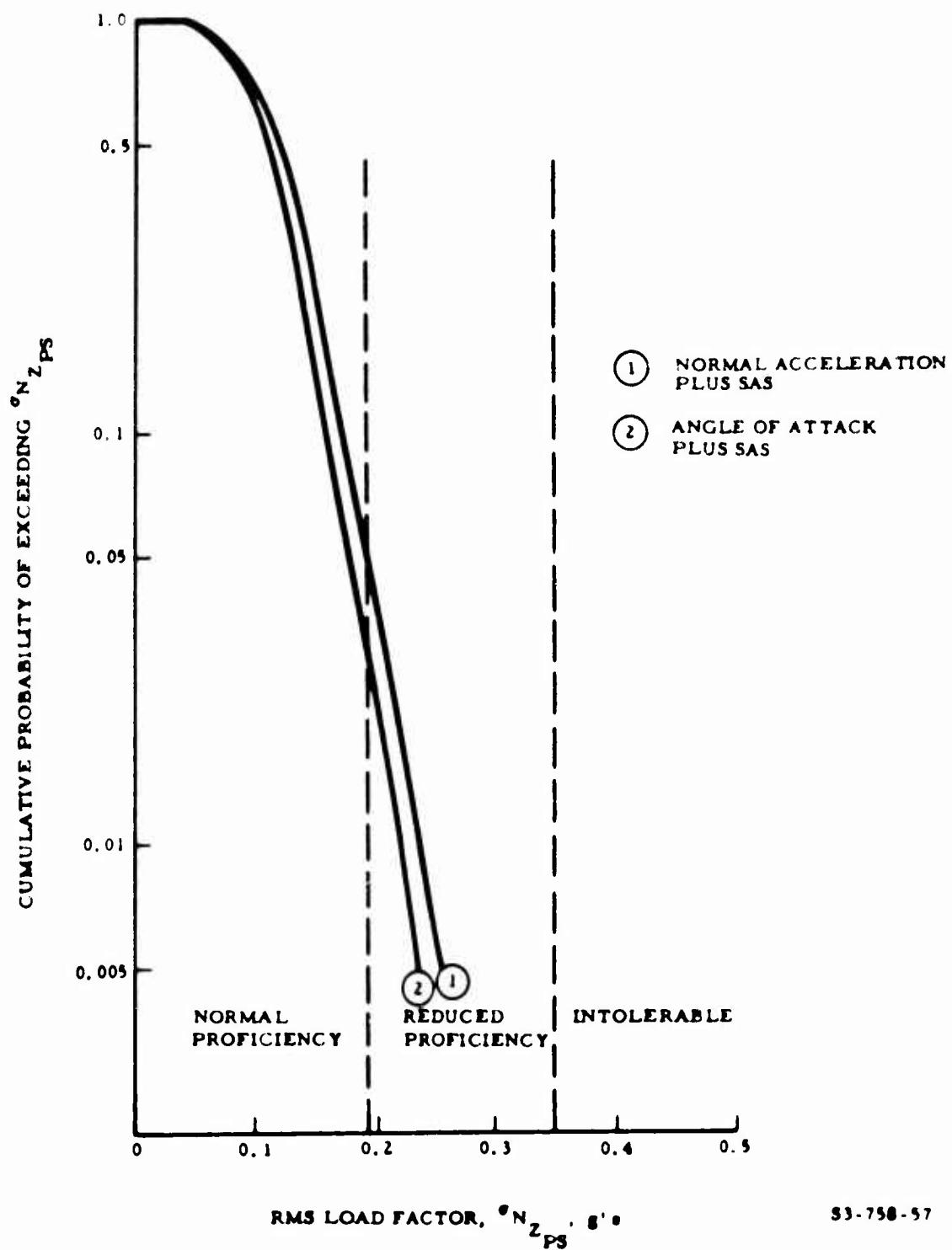
Figure 57.   Pilot Endurance Probability With Active Systems
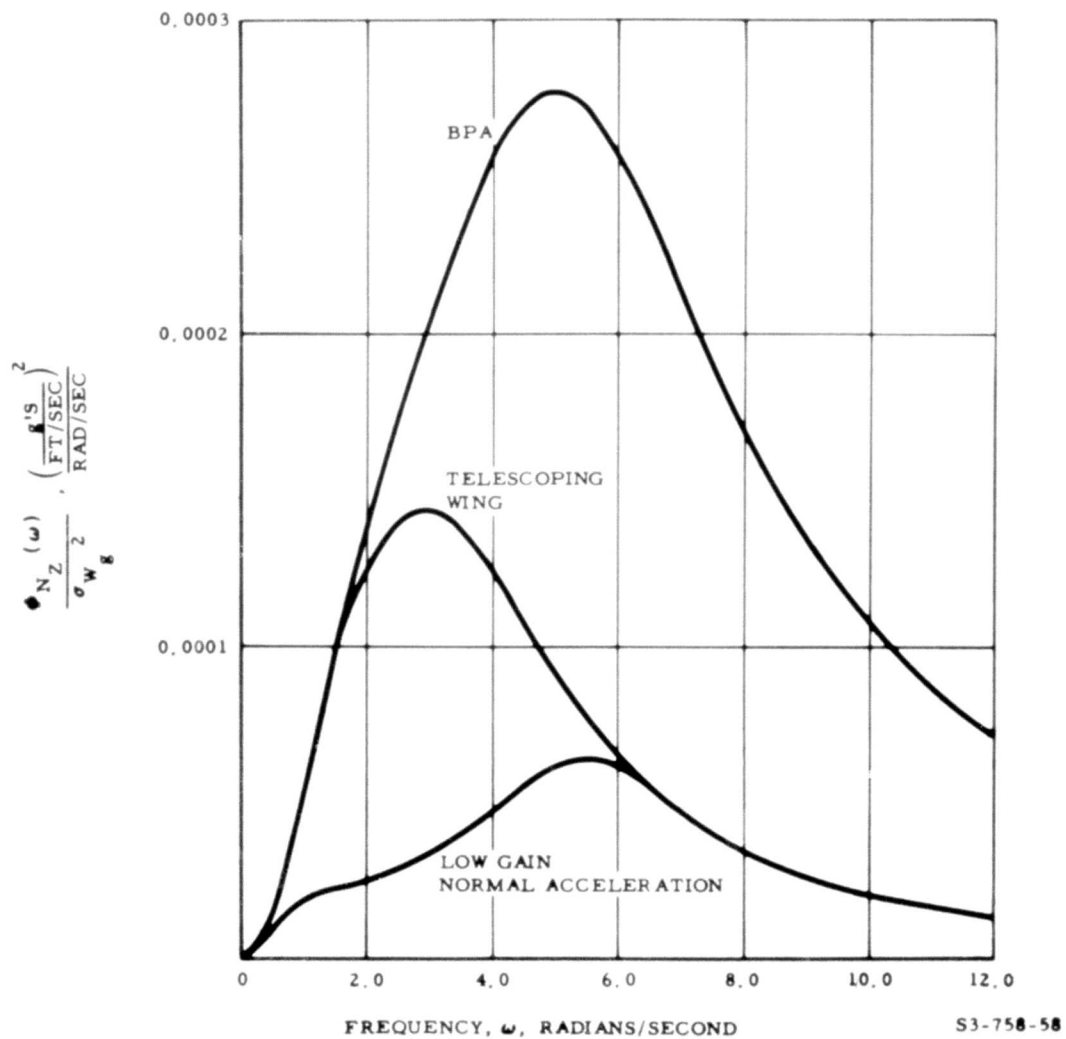
Figure 58. Comparison of Active and Passive Load
Spectra - Low Frequency
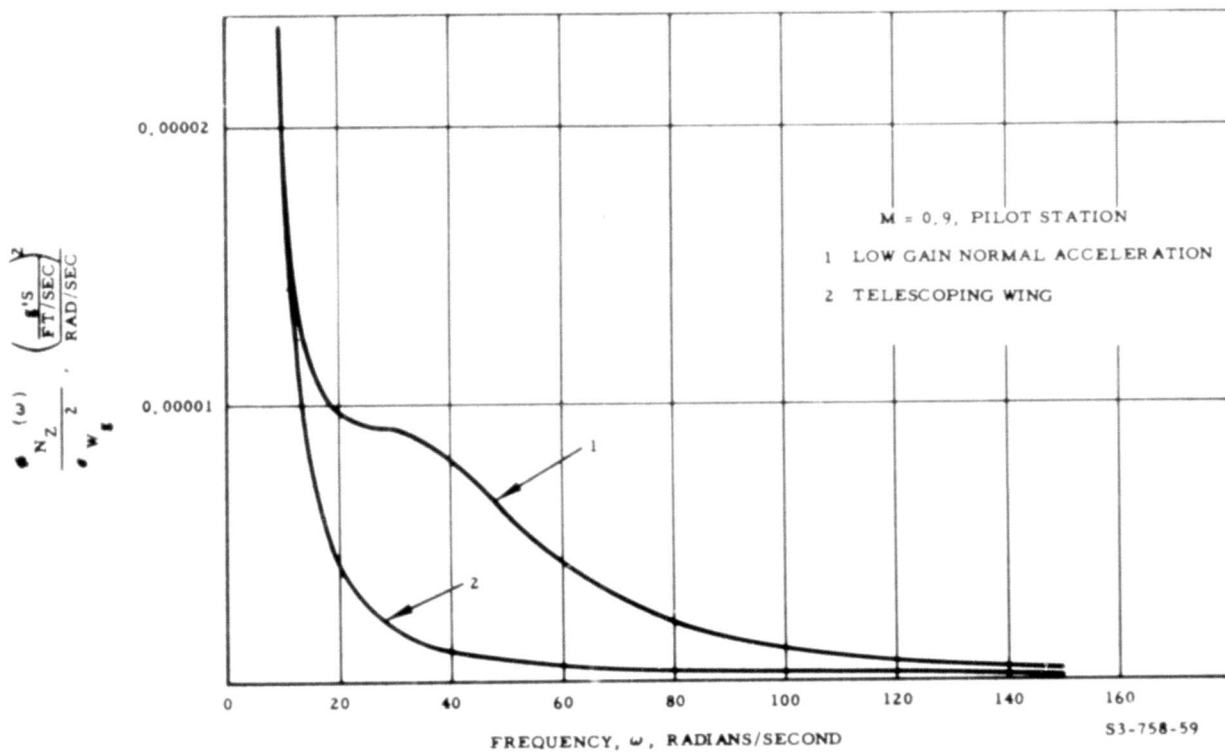
Figure 59. Comparison of Active and Passive Load
Spectra - High Frequency
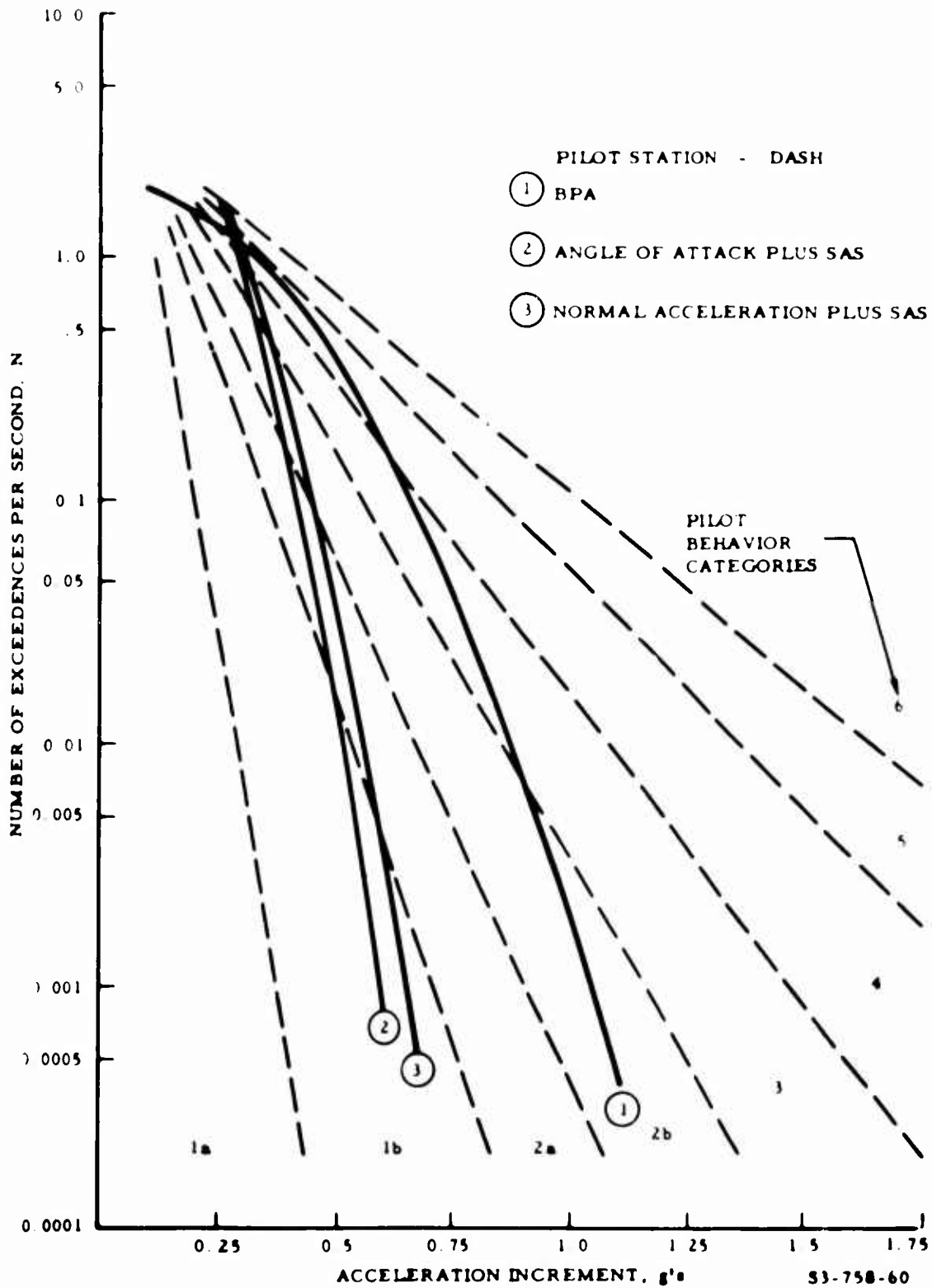
Figure 60.   Exceedances of Acceleration Levels
With Active Systems

166

BLANK PAGE

Figure 61. Active System Mechanization

S3-758-61

FOR USE WITH

$$C_{L_\alpha} = \frac{AR_e(.108)}{\dfrac{AR_e}{\cos\Lambda_{.5C}} + C}$$

WHERE: $C = 3.34 - .11\, AR_e$

FOR USE WITH

$$\frac{\partial C_{Di}}{\partial C_L^2} = \frac{1}{\pi\, AR_e}$$

CURVES BASED ON
TEST DATA IN REF. 38
(END PLATE ON EACH WING TIP)

EFFECTIVE AR/GEOMETRIC AR, AR_e/AR

END-PLATE HEIGHT/WING SPAN, h/b
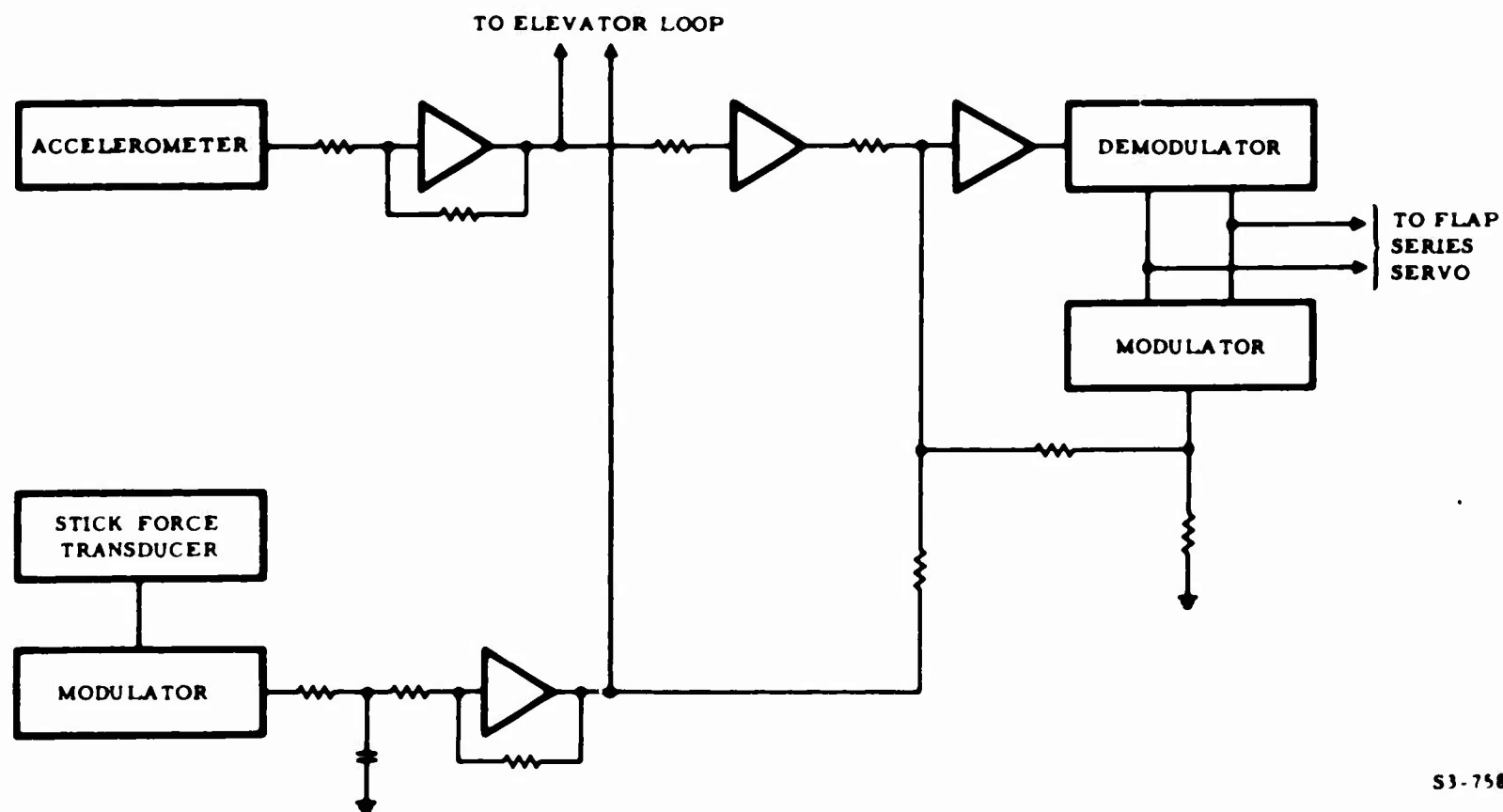
S3-758-62
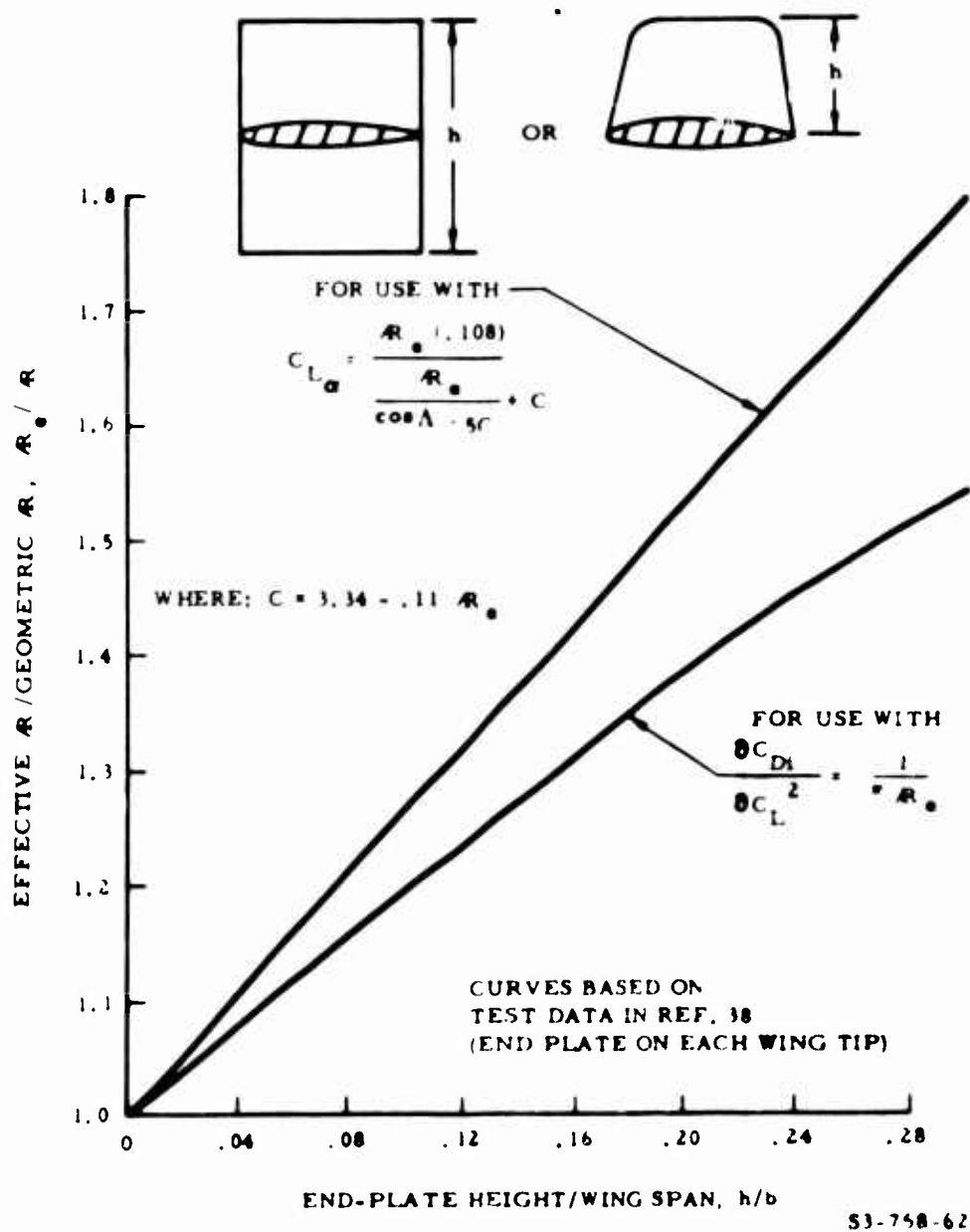
Figure 62. Effect of End Plates on Aerodynamic Characteristics
of Straight Wings
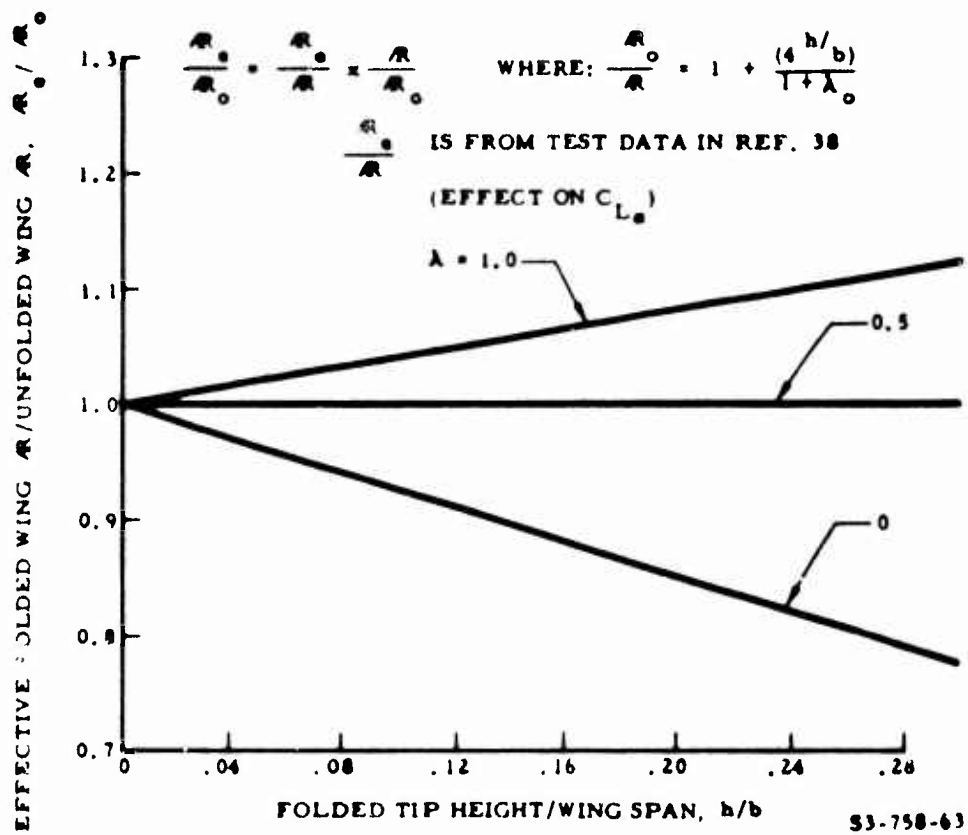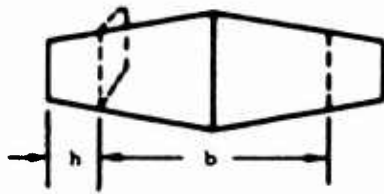
Figure 63. Effective Aspect Ratio of a Folded Wing
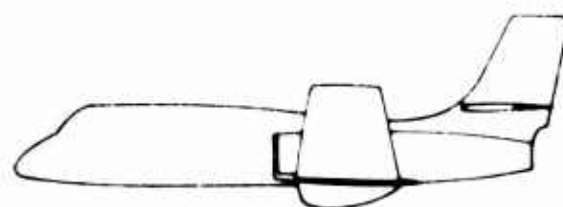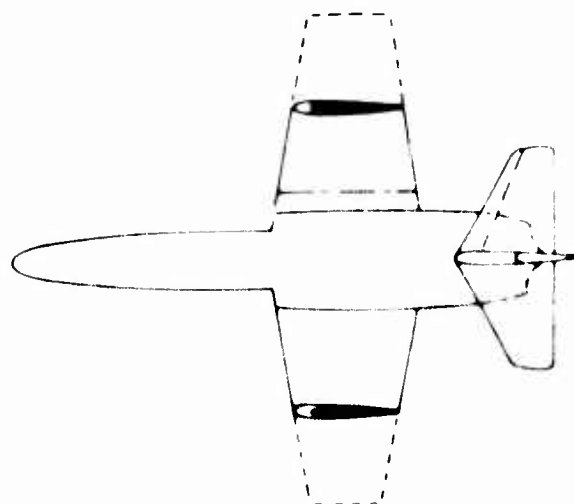
Figure 64.   Folding Wing Aircraft (FW)
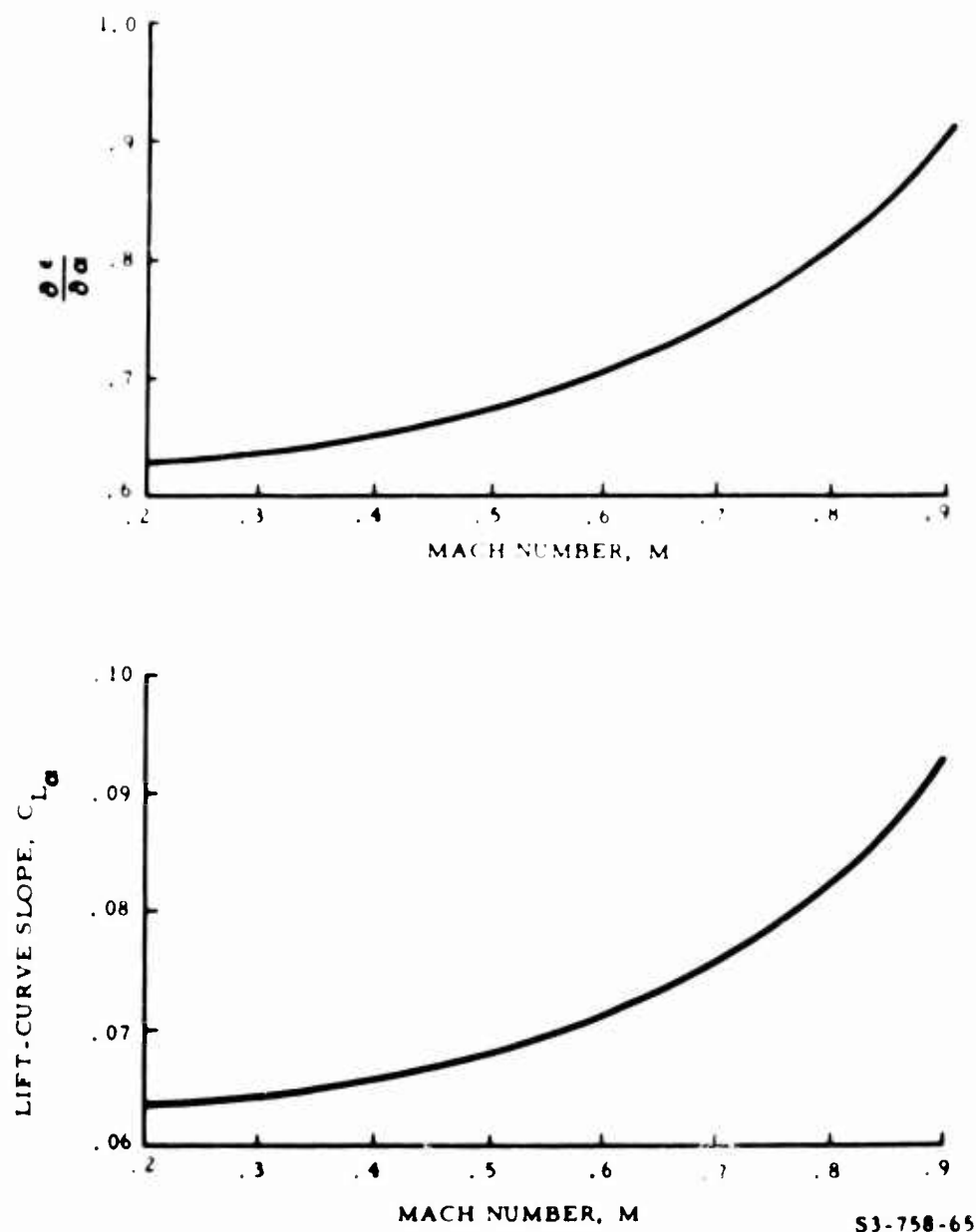
Figure 65. Effect of Mach Number on Lift-Curve Slope
And Downwash of FW
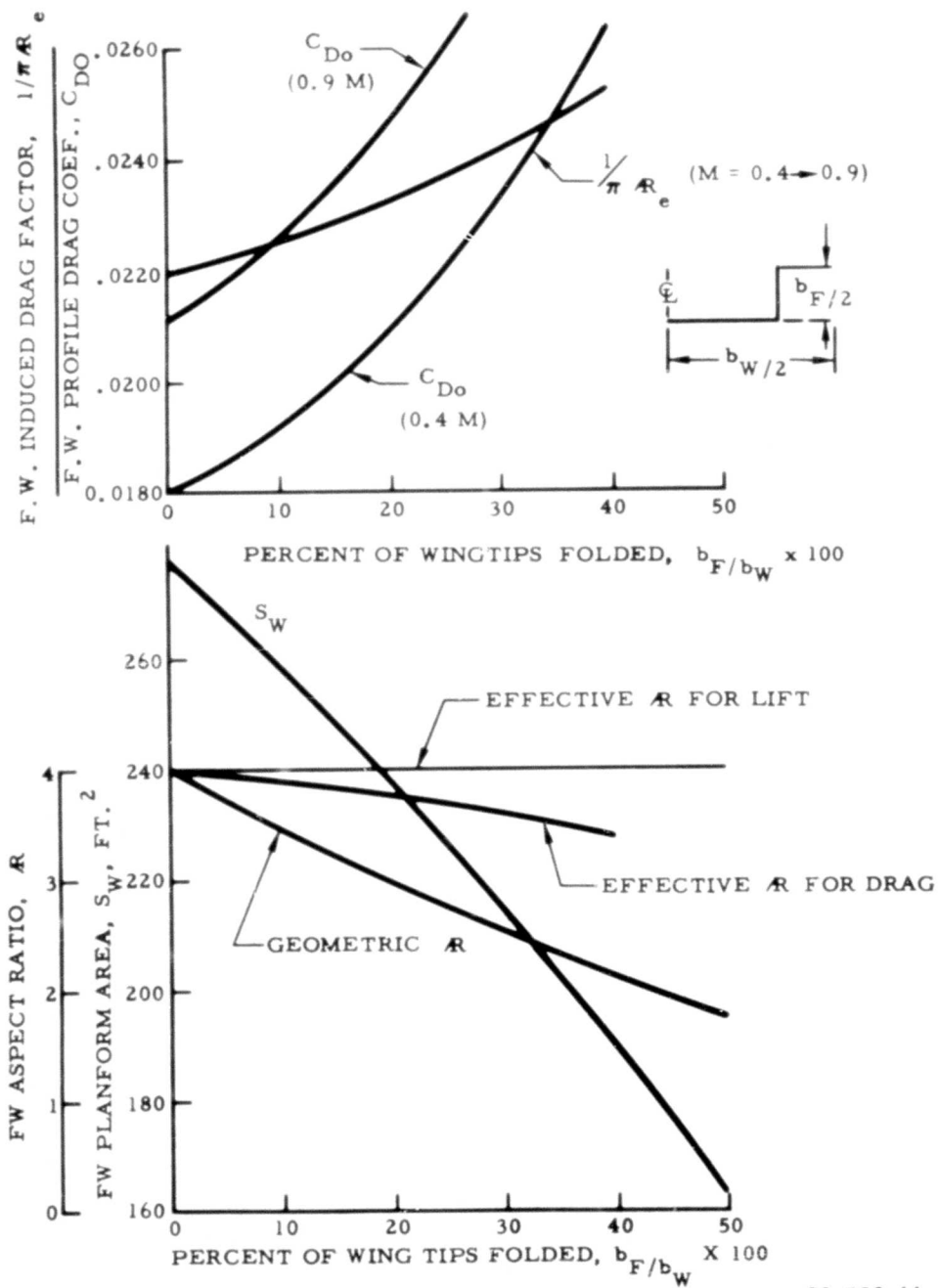
Figure 66.   Effect of Folded Wing Tips on Geometry and Drag

S3-758-66

172

FULL FOLDING

PARTIAL FOLDING

SK 758-67
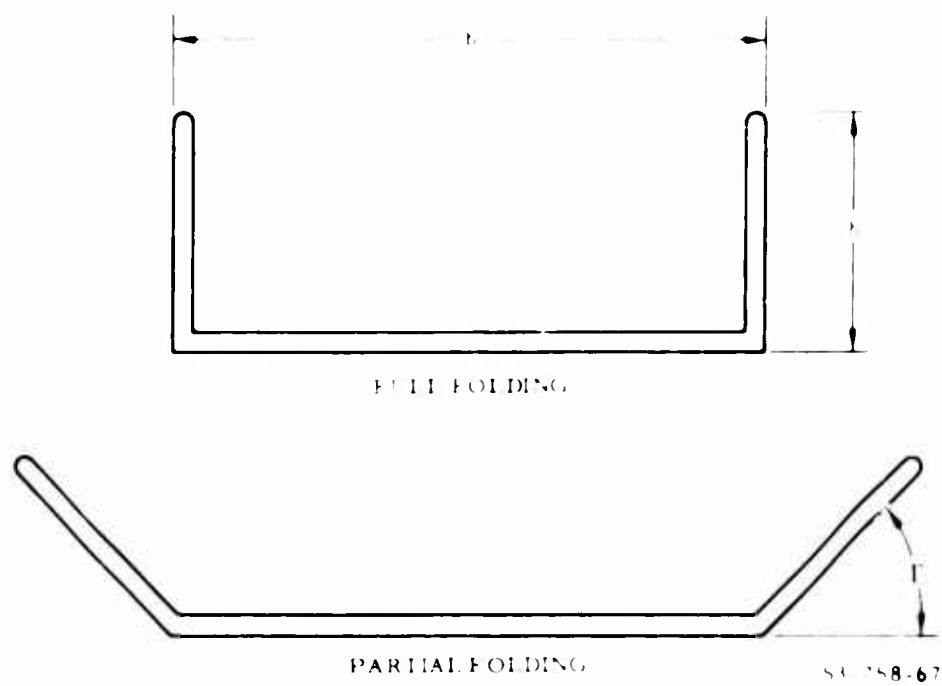
Figure 67. FW Wing Geometry
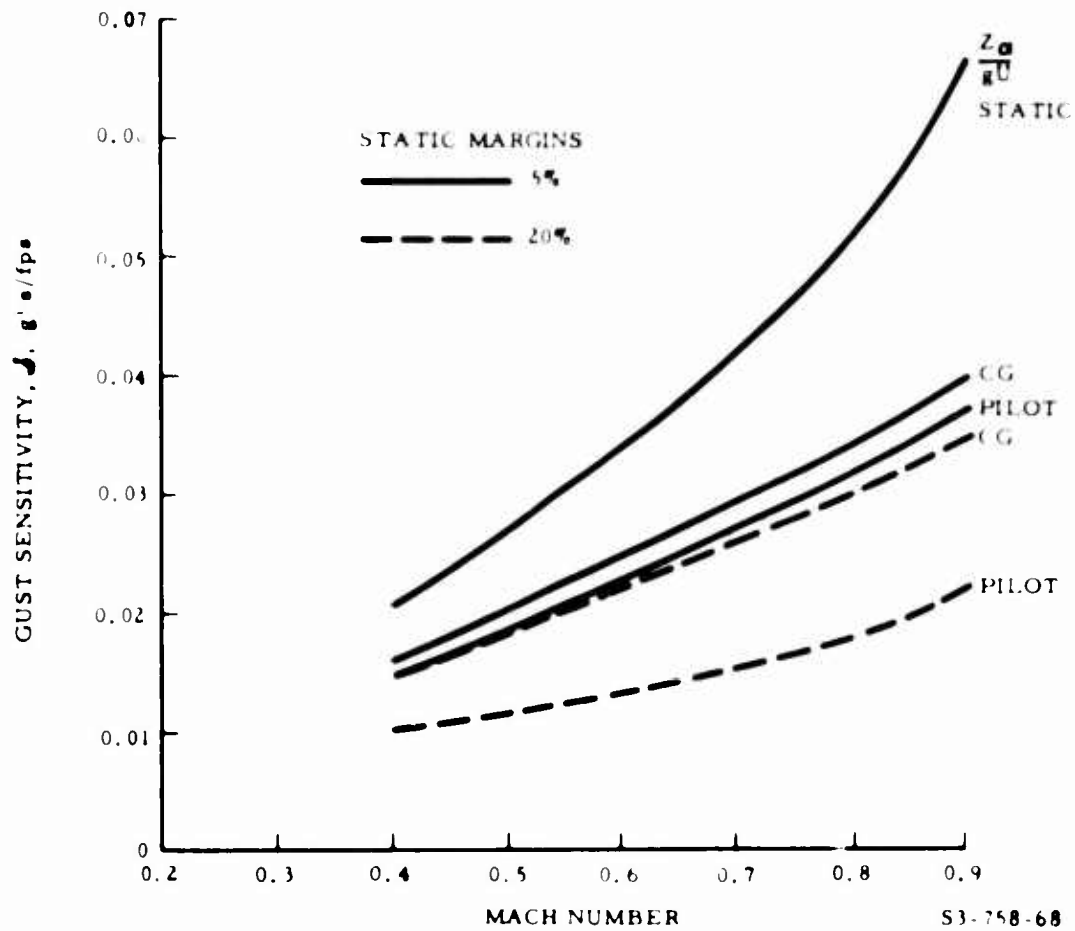
Figure 68. Gust Sensitivity of FW

174
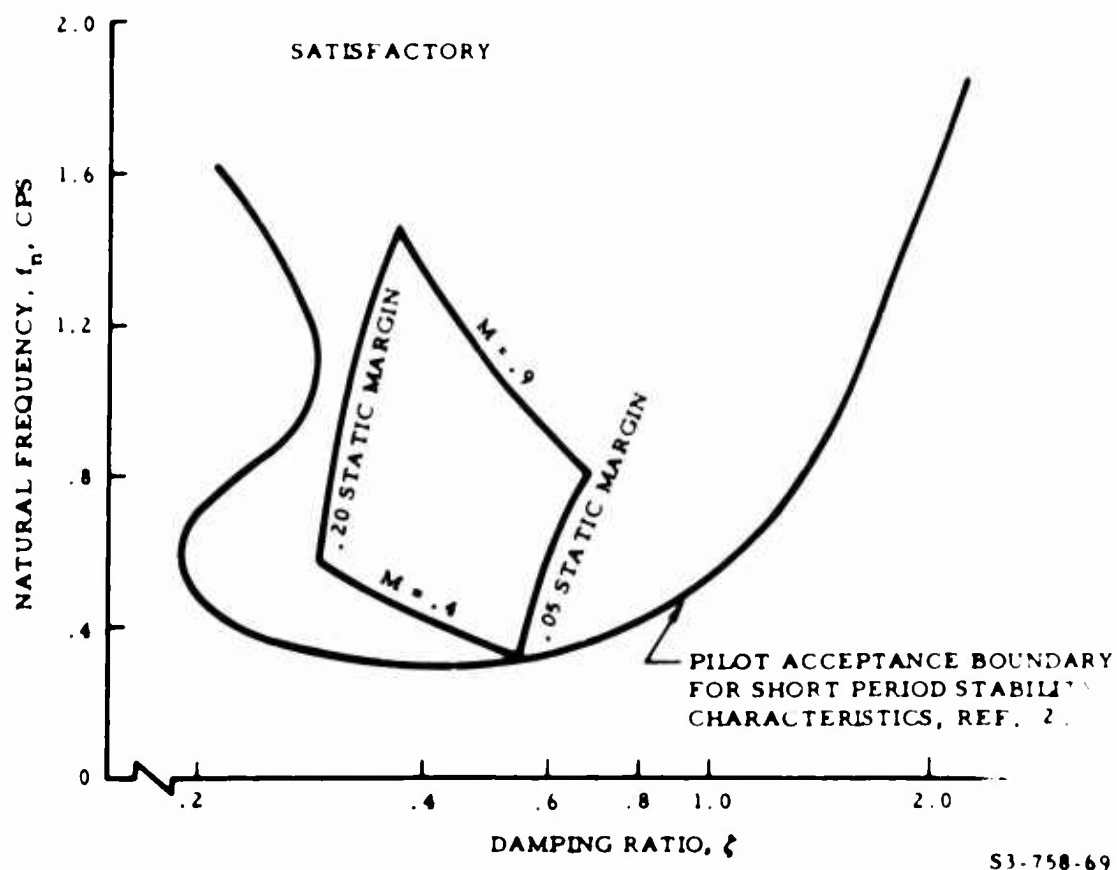
Figure 69.   Short Period Characteristics of FW
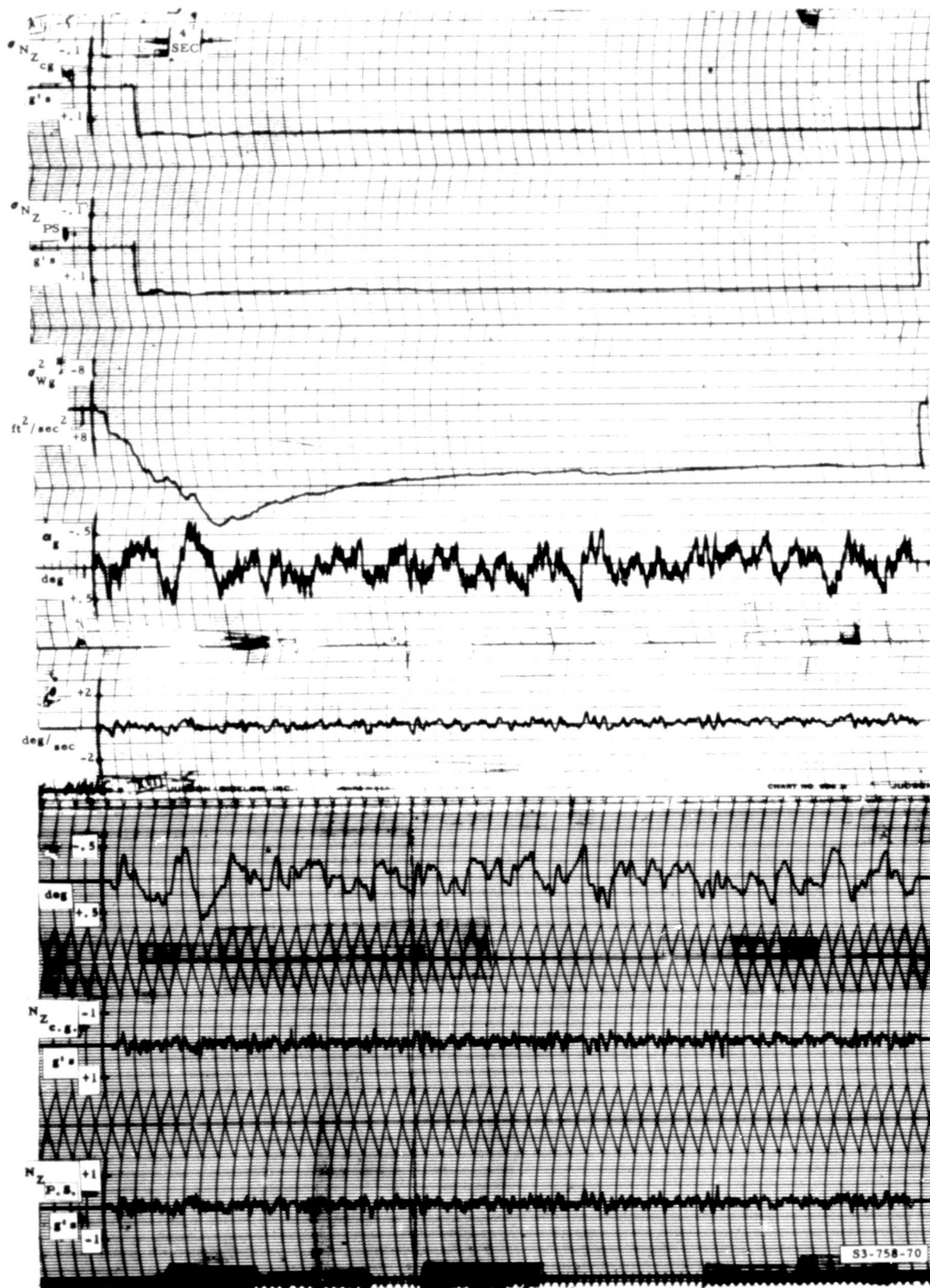
Figure 70.   Time History of FW Gust Response at 0.9 Mach

PERCENT OF WING TIPS FOLDED, b_F/b_W x 100

PERCENT CHANGE IN RANGE, $\left[\dfrac{R_A}{R_U} - 1\right]$ x 100

━━━ STRUCTURE AND FUEL WEIGHT ASSUMED
UNCHANGED FOR FW (W_F = 6300 LBS.)

O 20 MINUTE DASH AT 0.9M, WINGS FOLDED,
CRUISE AT 0.4 M, WINGS NOT FOLDED.
STRUCTURAL WEIGHT PENALTY DUE TO
WING FOLDING = +0.035 x (GROSS WEIGHT)
(W_F = 5670 LBS.)
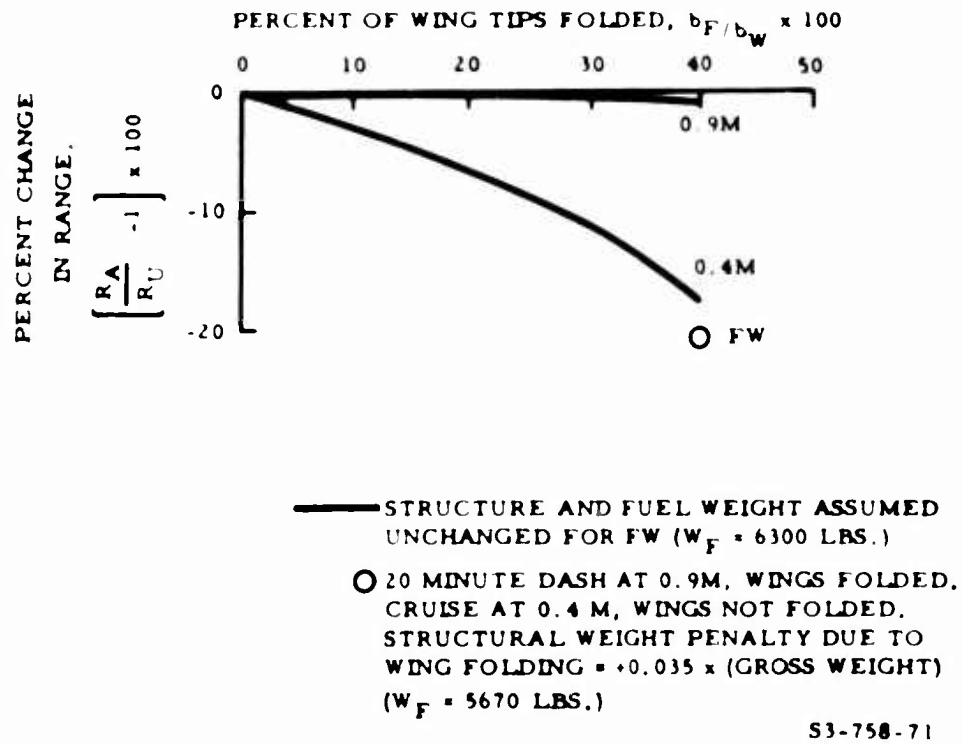
S3-758-71

Figure 71.   Effect of Wing Folding on Range
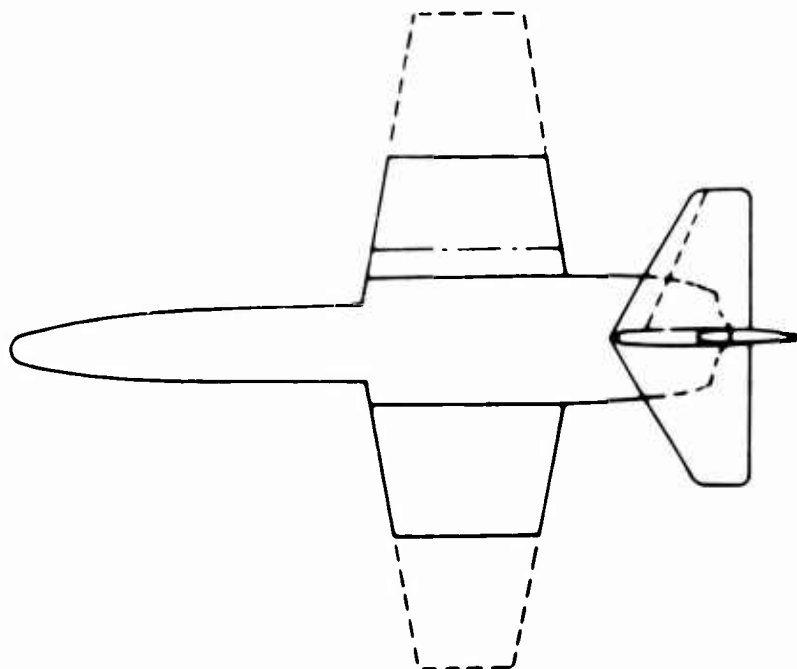
S3-758-72

Figure 72.   Telescoping Wing Aircraft (TW)
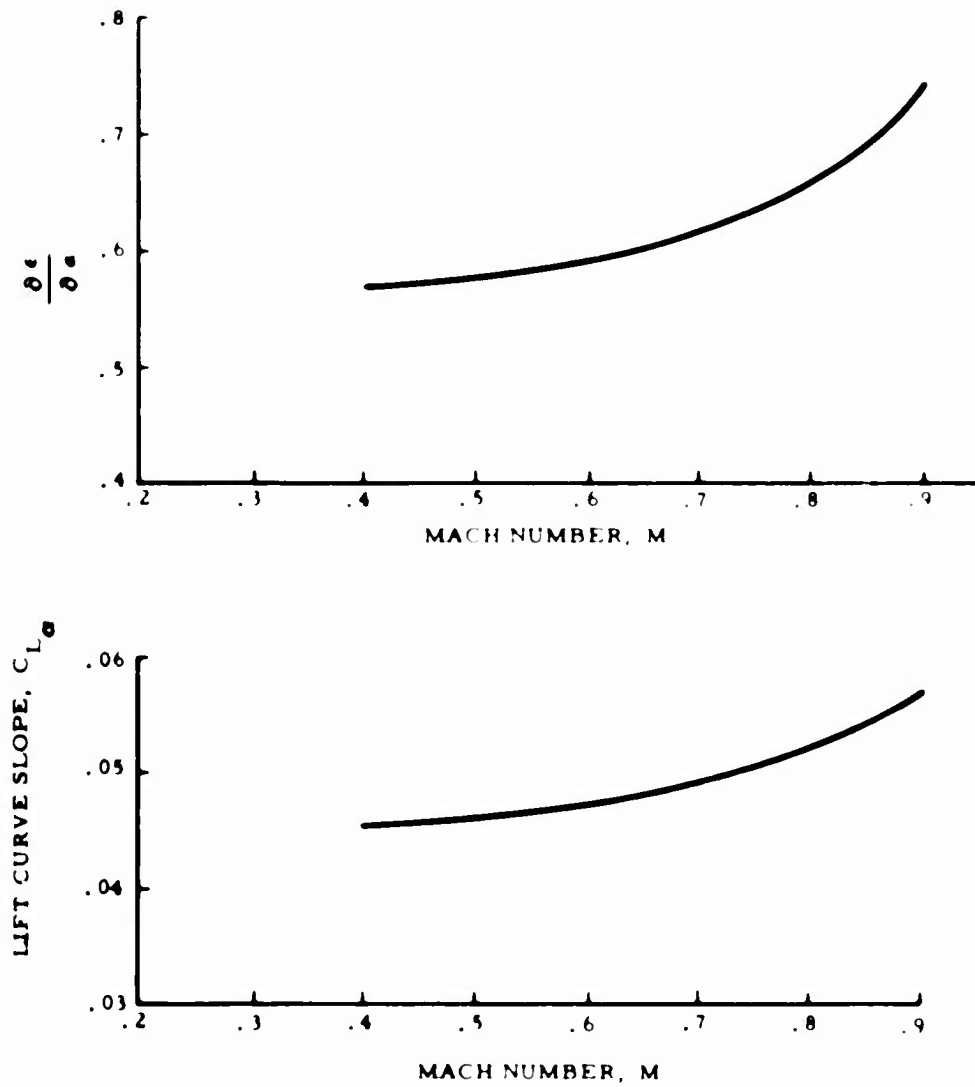
Figure 73. Effect of Mach Number on Lift-Curve Slope
and Downwash
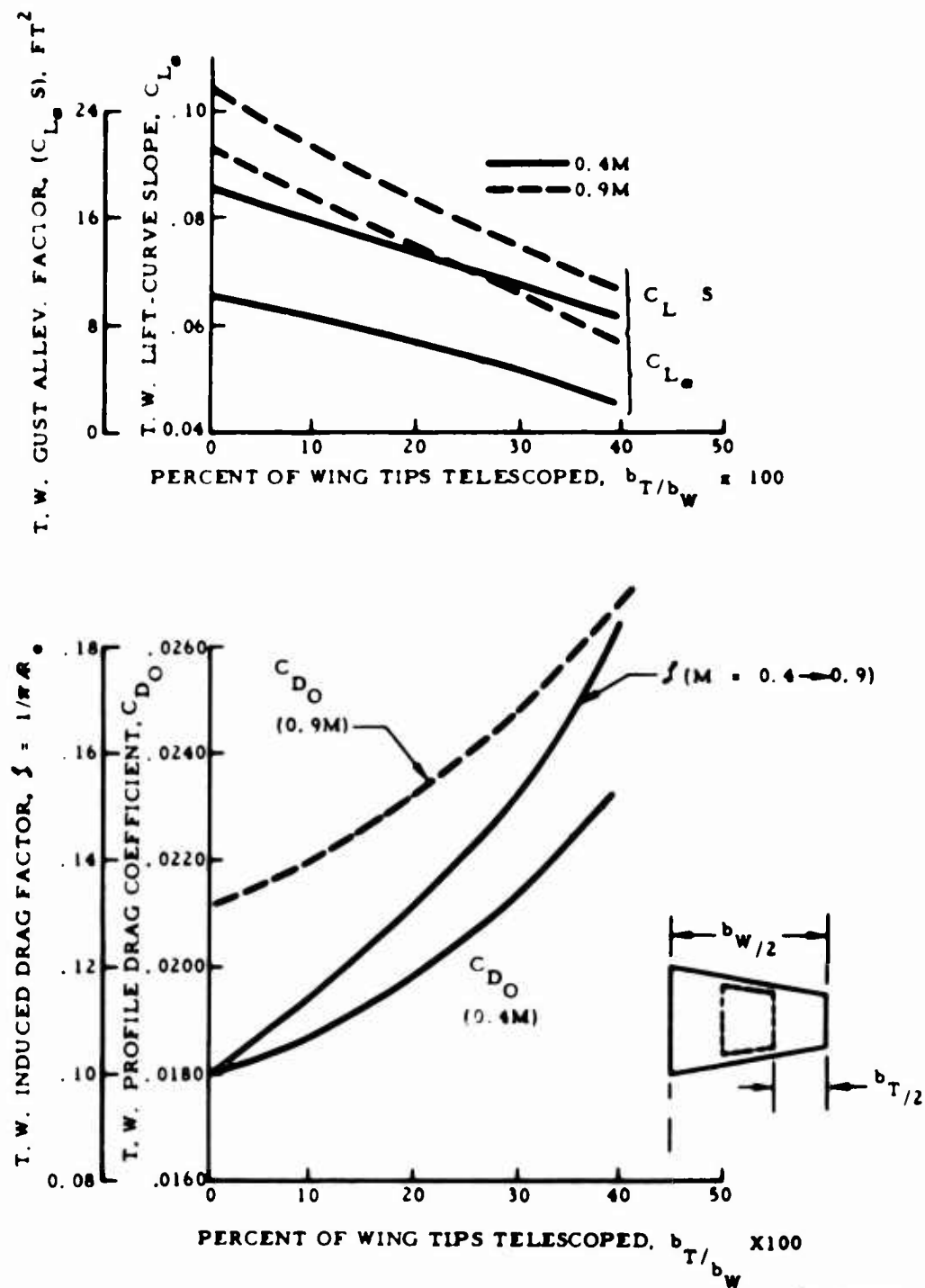
S3-758-73

Figure 74. Effect of Telescoping Wing Tips on Lift and Drag

S3-758-74

179
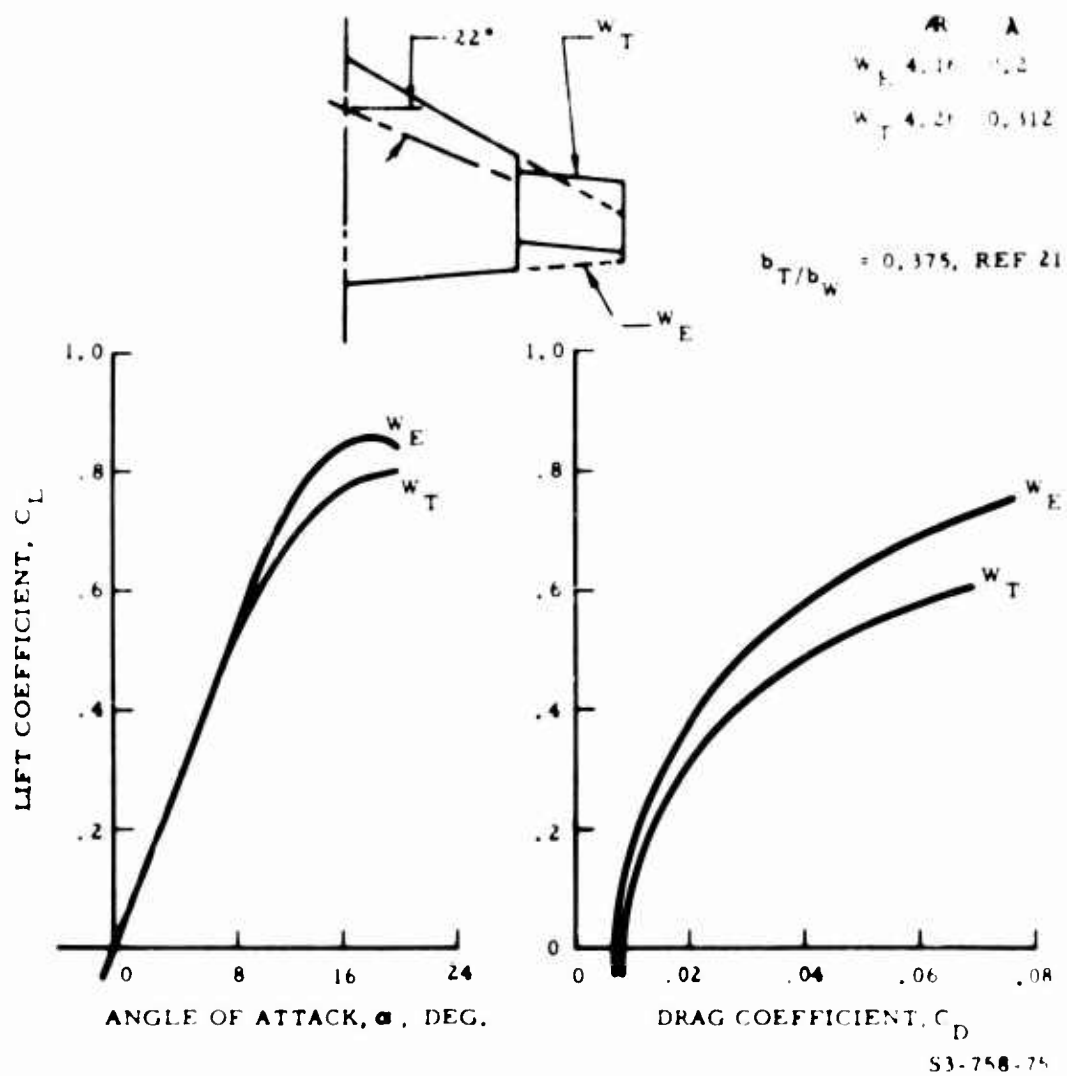
Figure 75. Effects of Wing Discontinuities Required to Accommodate a Telescoping Wing Tip

180

BLANK PAGE
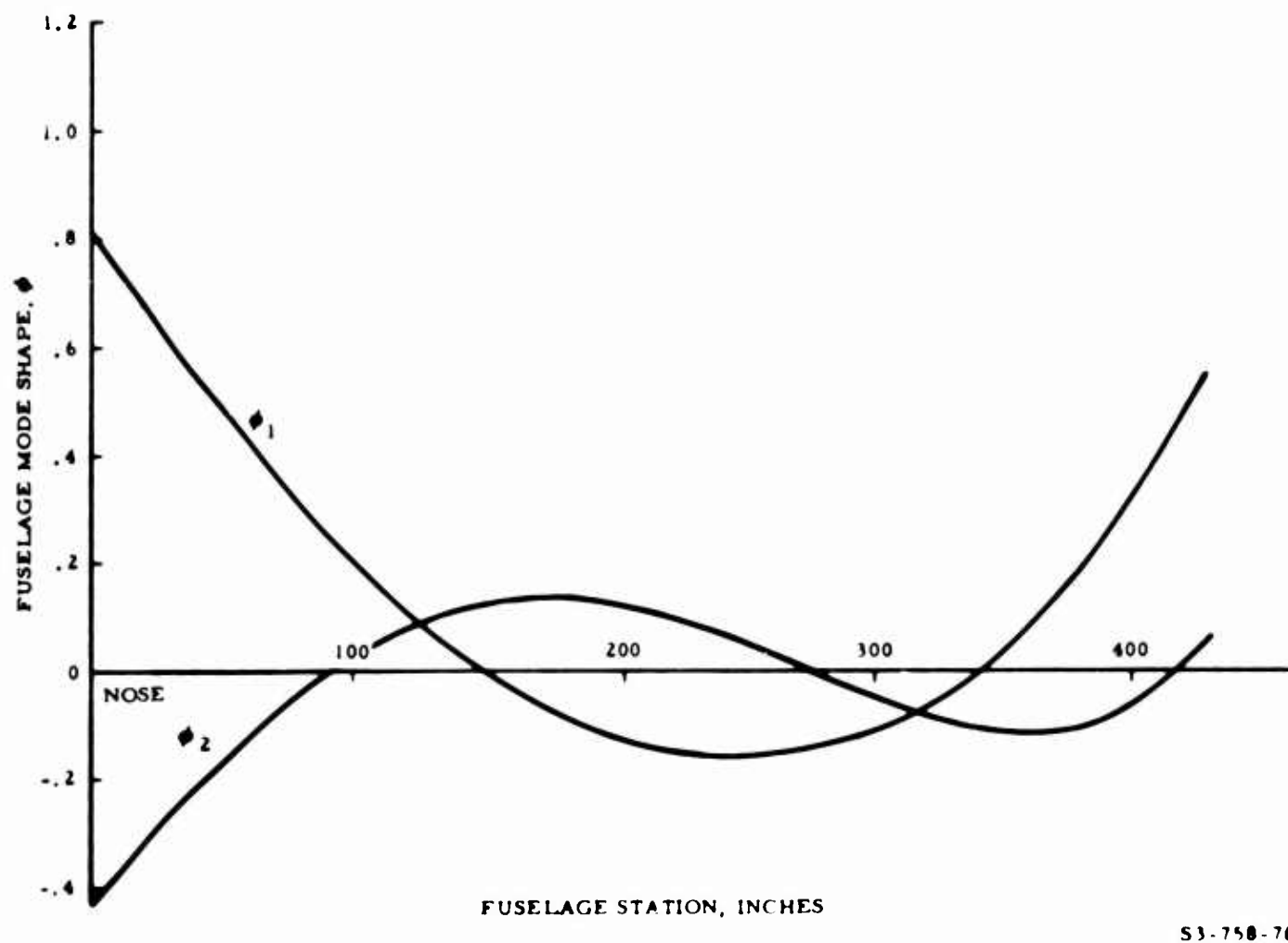
Figure 76.   Fuselage Mode Shapes in First Two Airplane Modes for TW

53-758-76
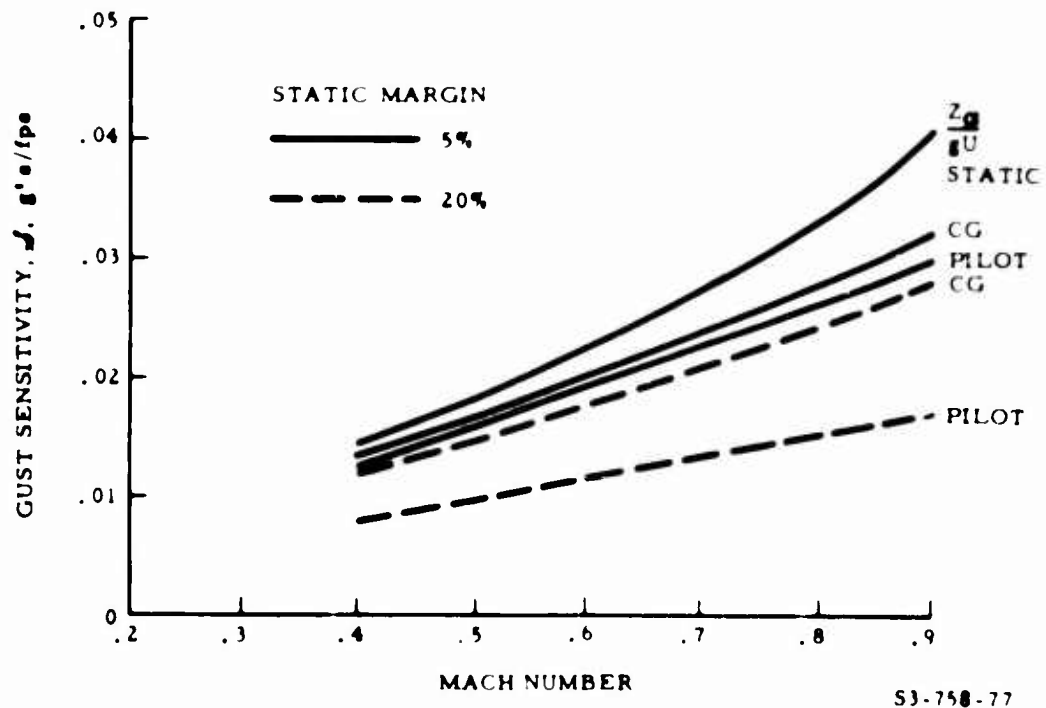
Figure 77.   Gust Sensitivity of TW
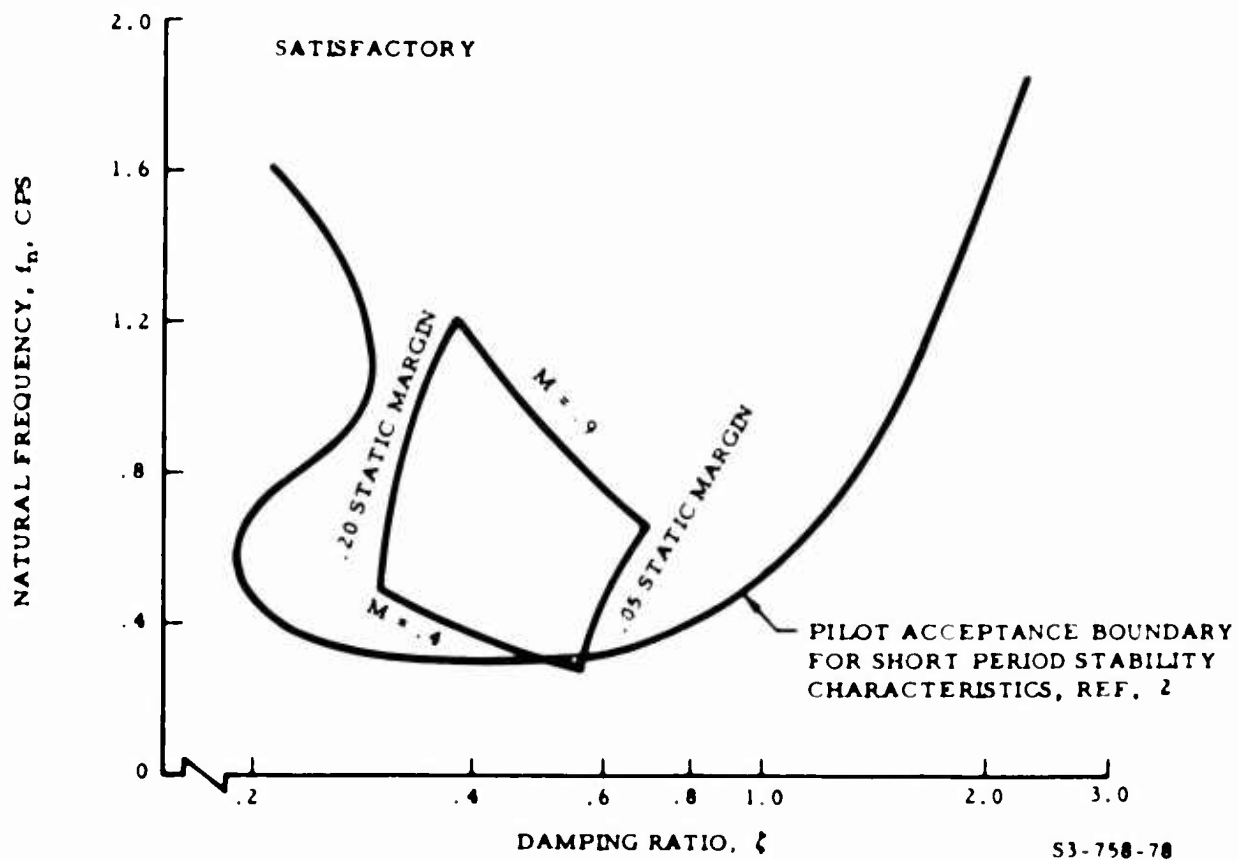
Figure 78.   Short Period Characteristics of TW

Figure 79. Time History of TW Gust Response at 0.9 Mach

183
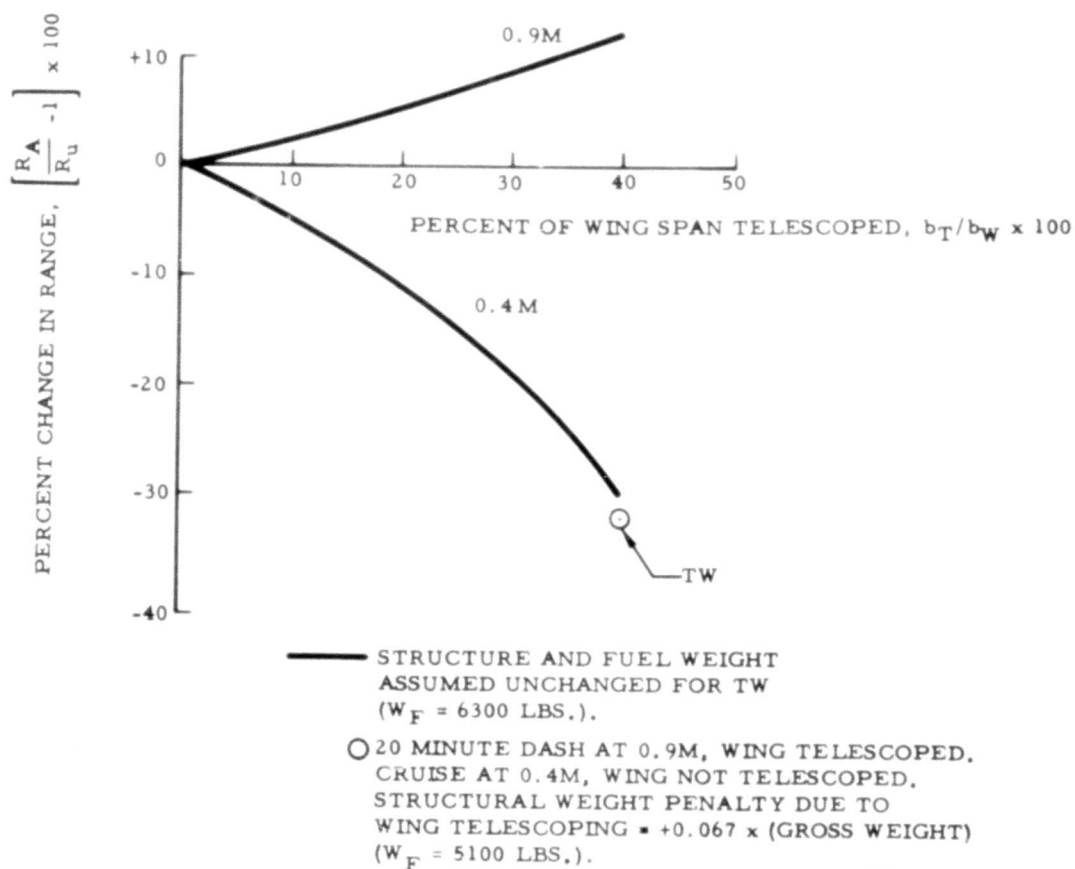
Figure 80. Effect of Wing Telescoping on Range
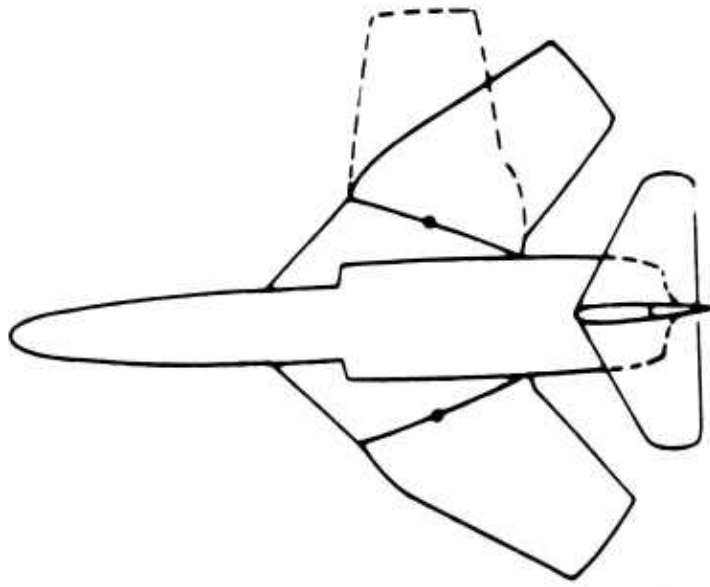
S3-758-81

Figure 81. Variable Sweep Aircraft (VS$_1$
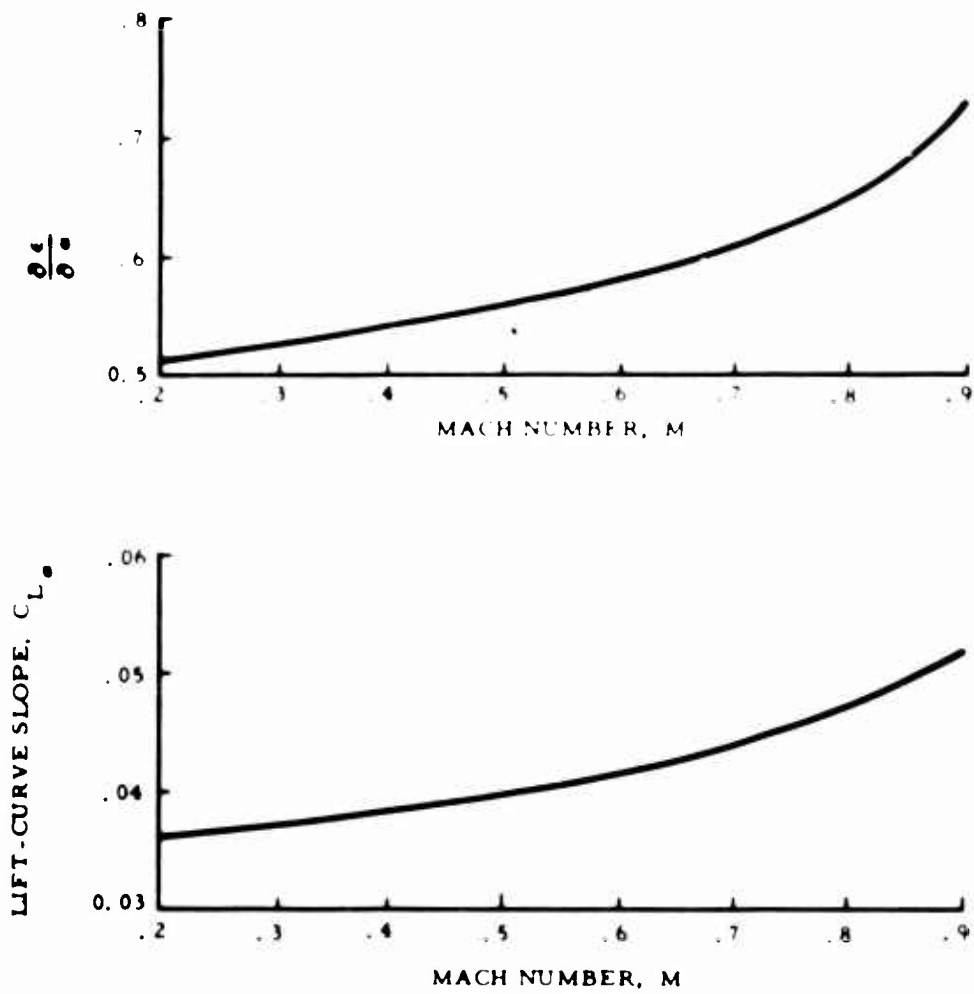
Figure 82. Effect of Mach Number on Lift-Curve Slope
and Downwash of VS₁
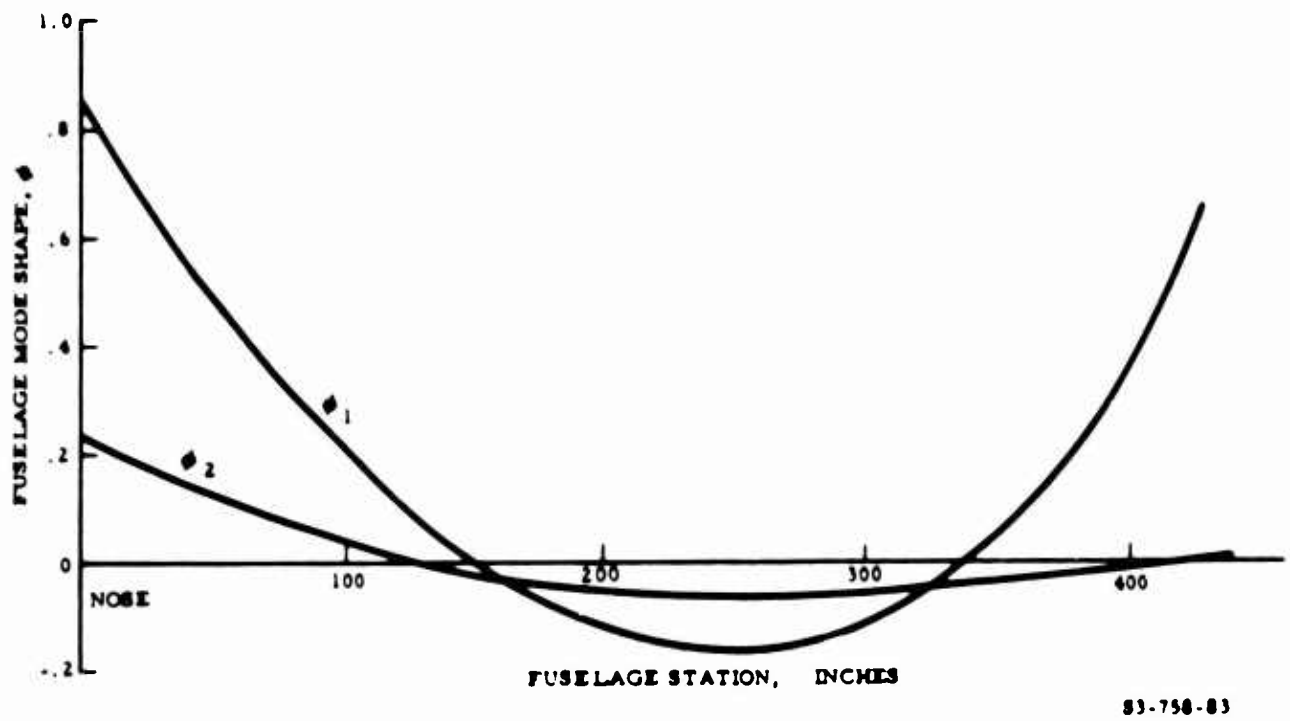
Figure 83.   Fuselage Mode Shapes in First Two Airplane
Modes for VS_1
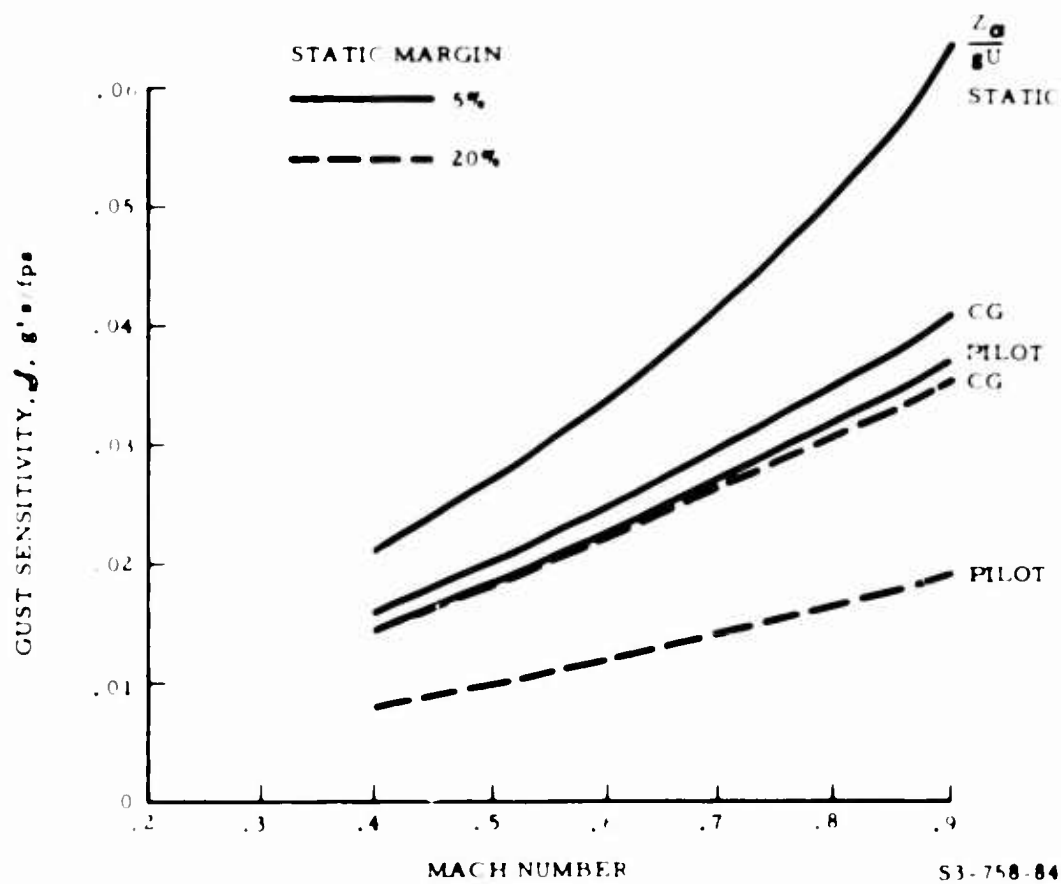
Figure 84. Gust Sensitivity of VS_1
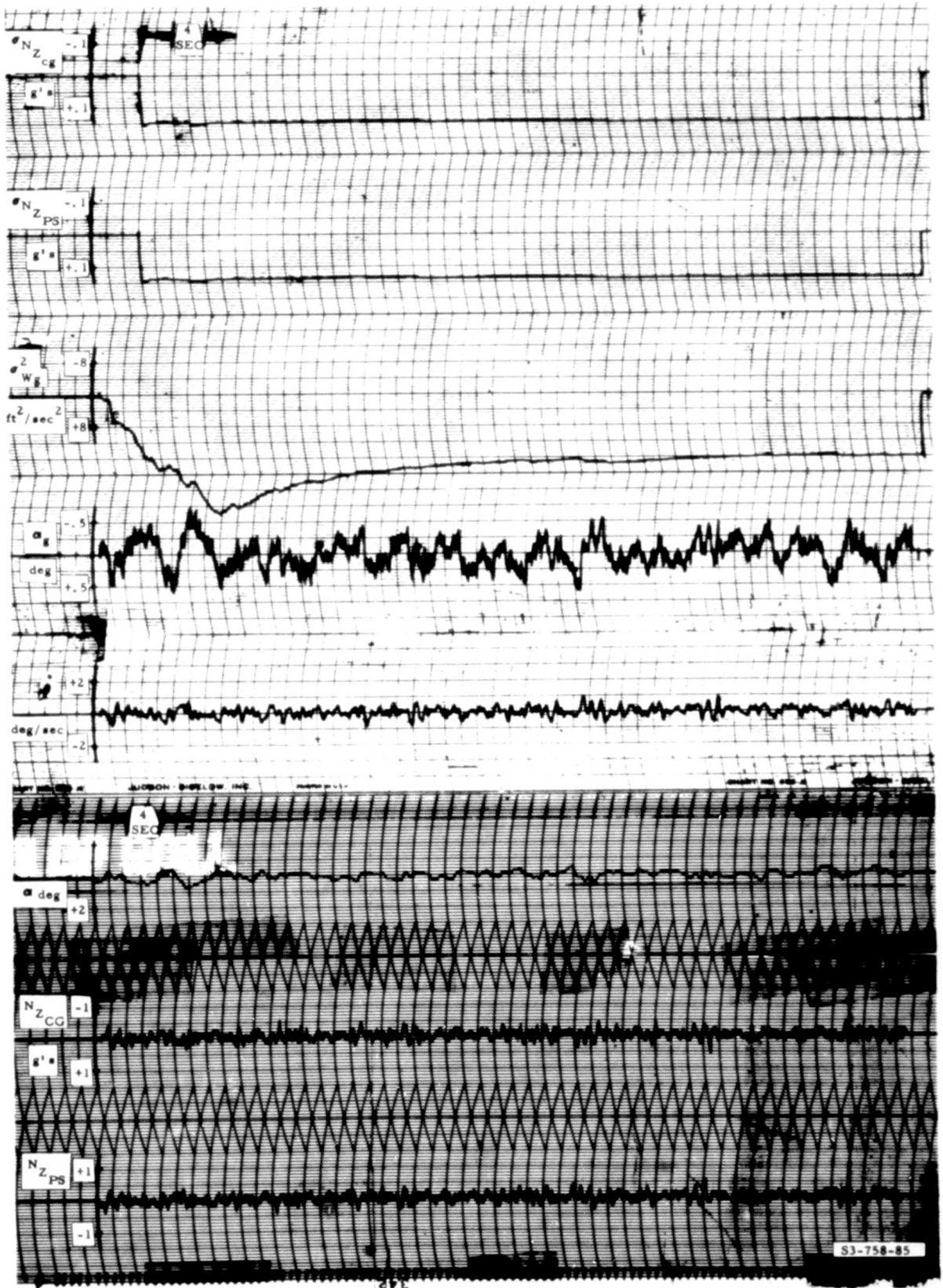
Figure 85.   Time History of VS_1 Gust Response at 0.9 Mach
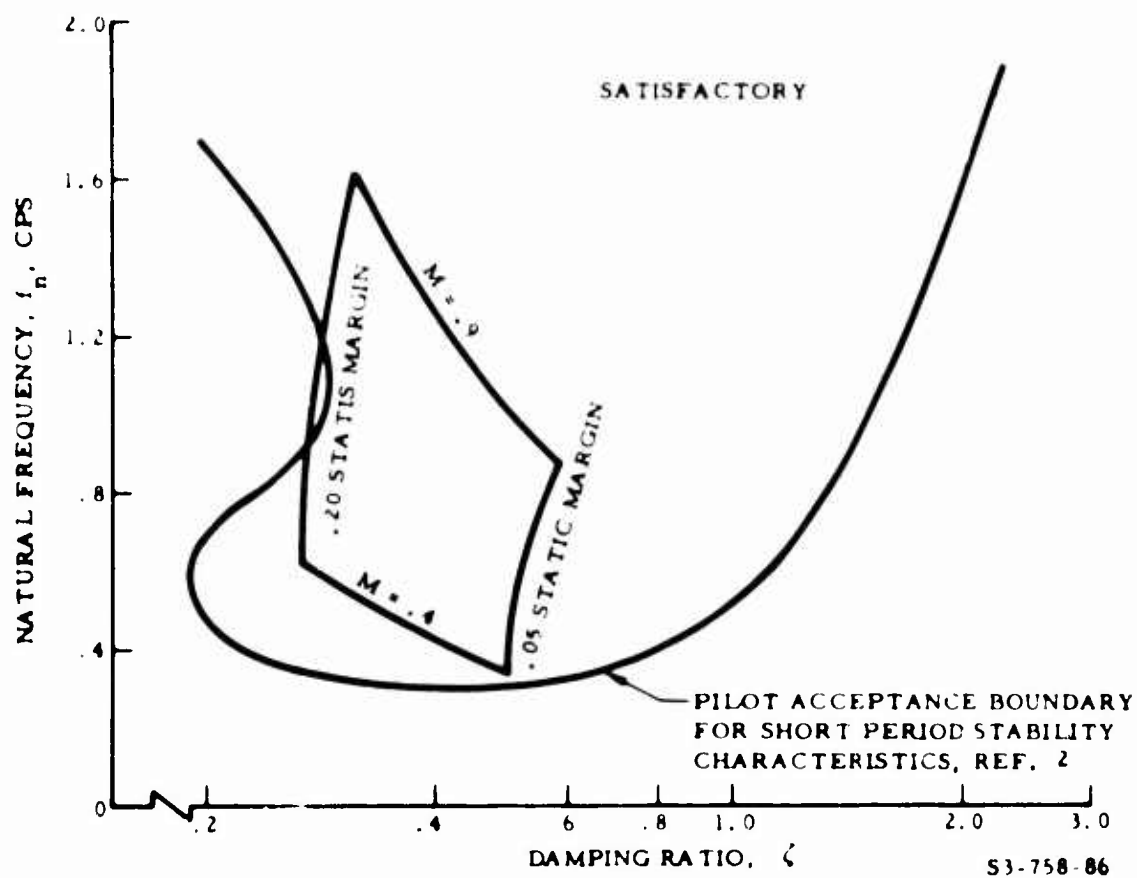
Figure 86. Short Period Characteristics of VS$_1$
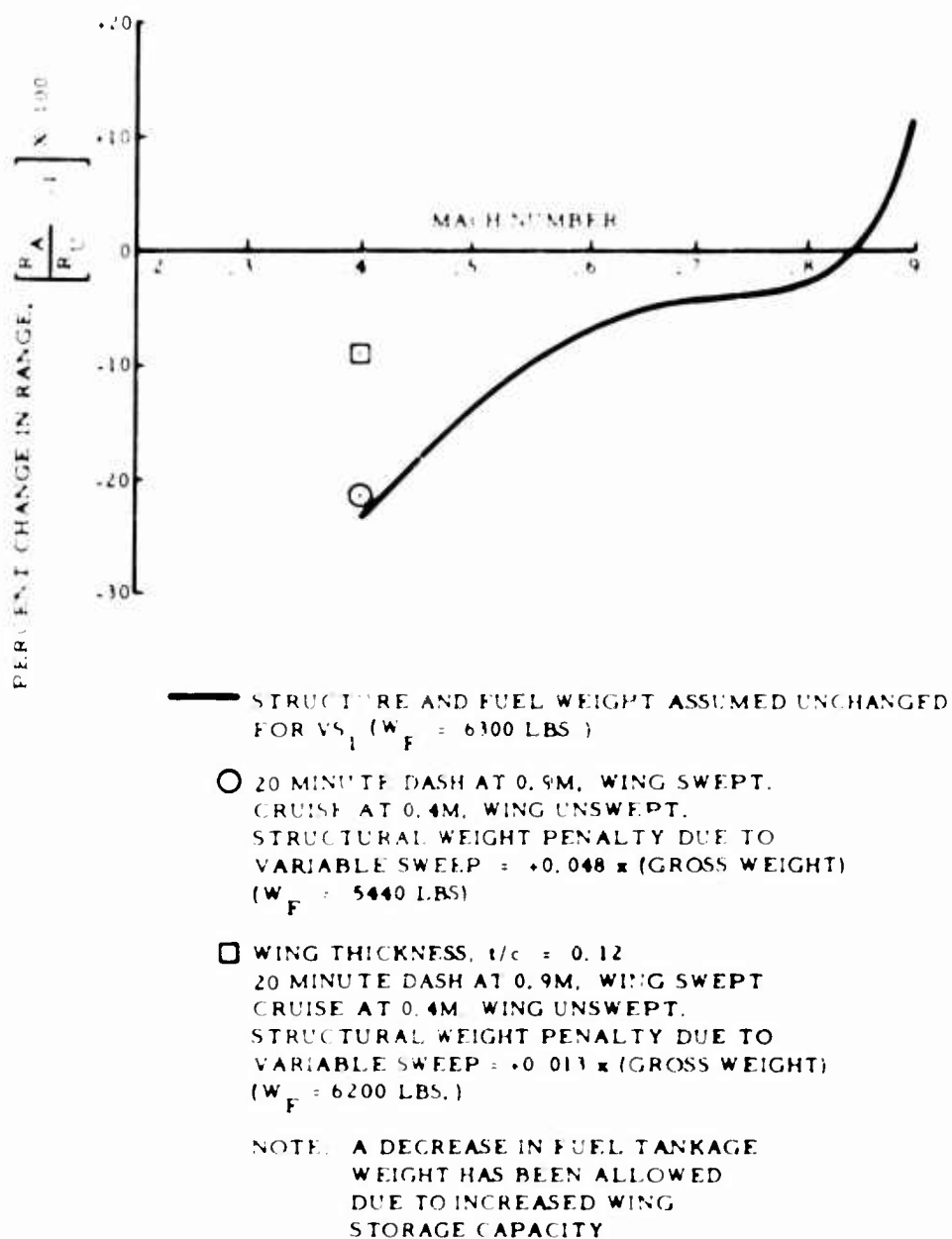
Figure 87. Effect of Variable Sweep VS₁ on Range
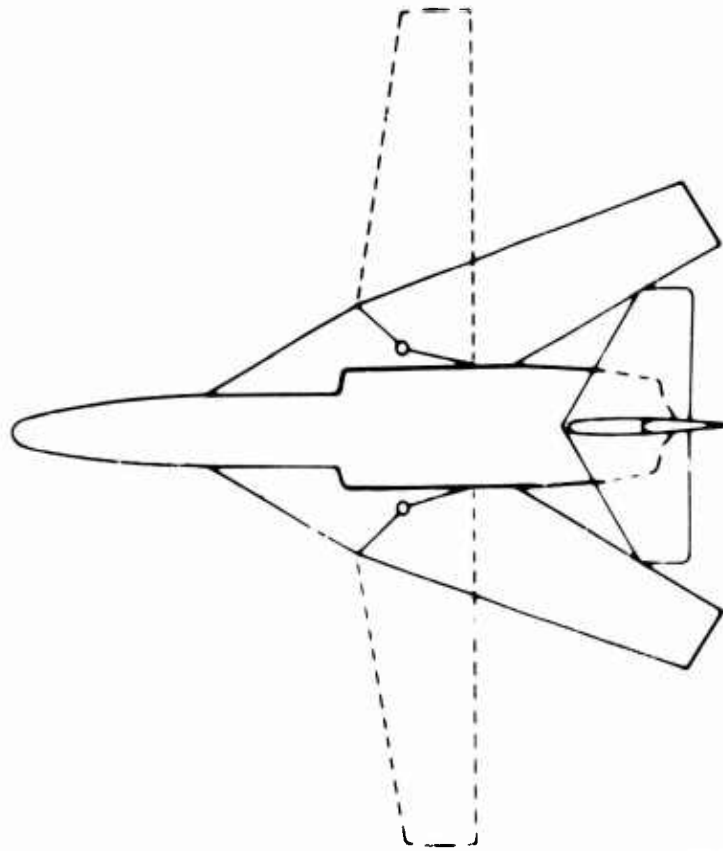
S1-758-88

Figure 88. Variable Sweep Aircraft (VS$_2$)
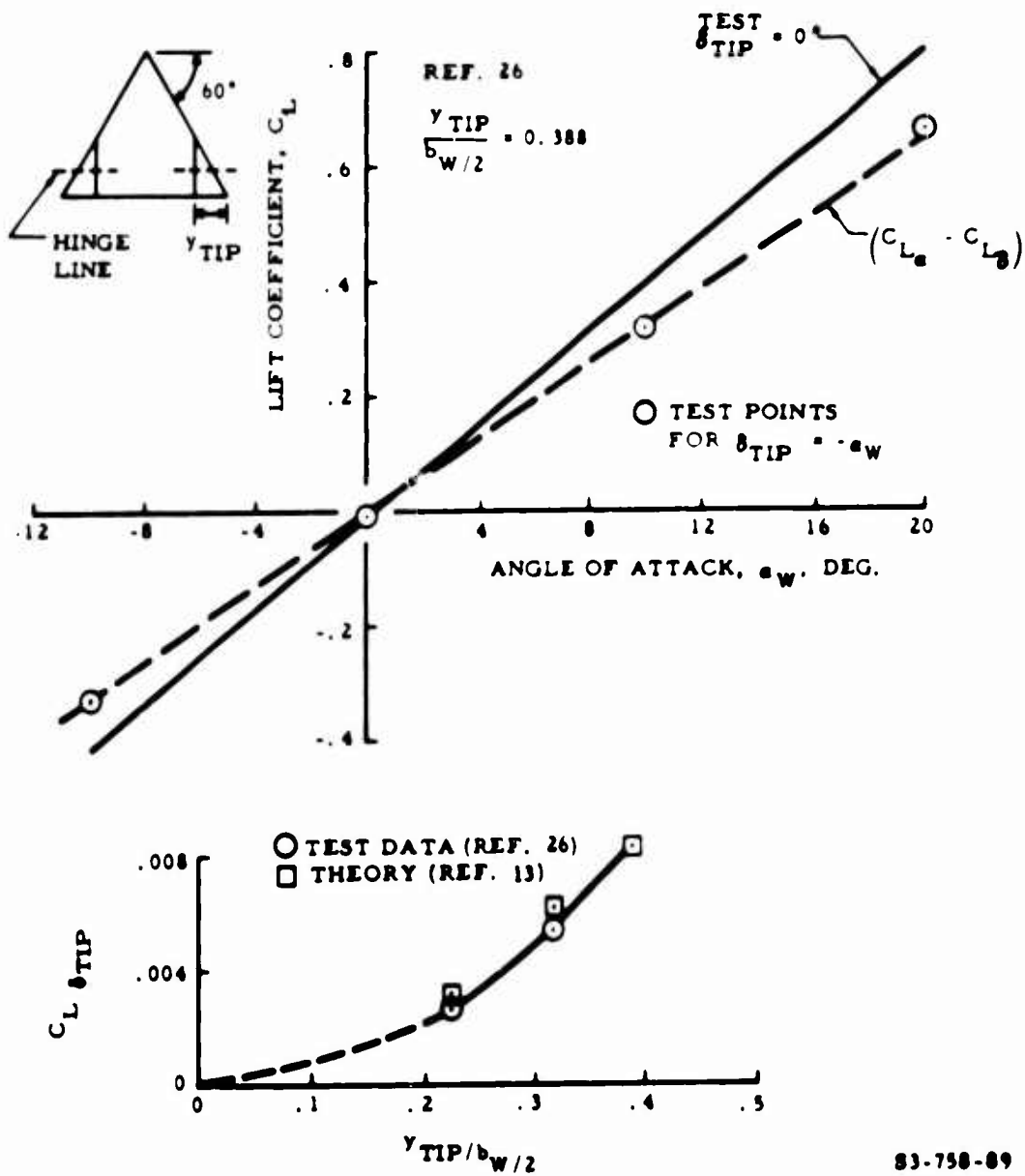
Figure 89. Comparison of Test Data and Theory for
Full-Chord Deflected Wing Tips
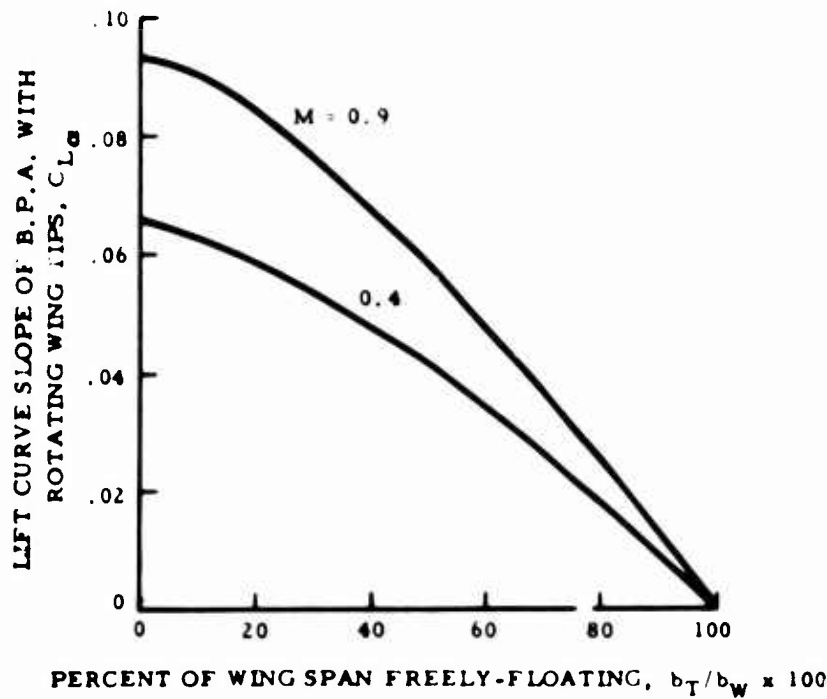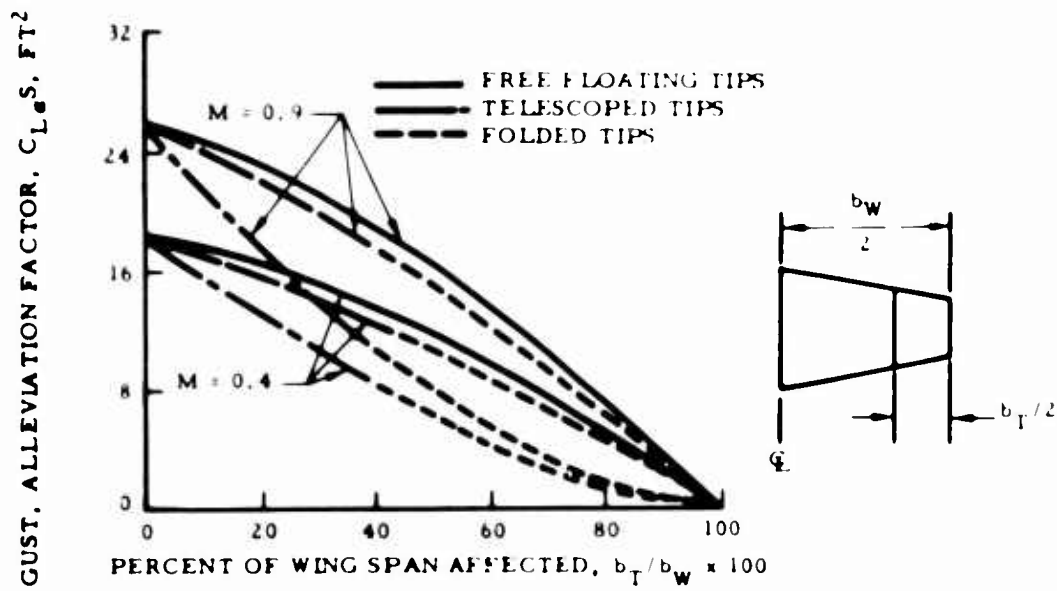
Figure 90. Effect of Free-Floating Wing Tips on Lift

194
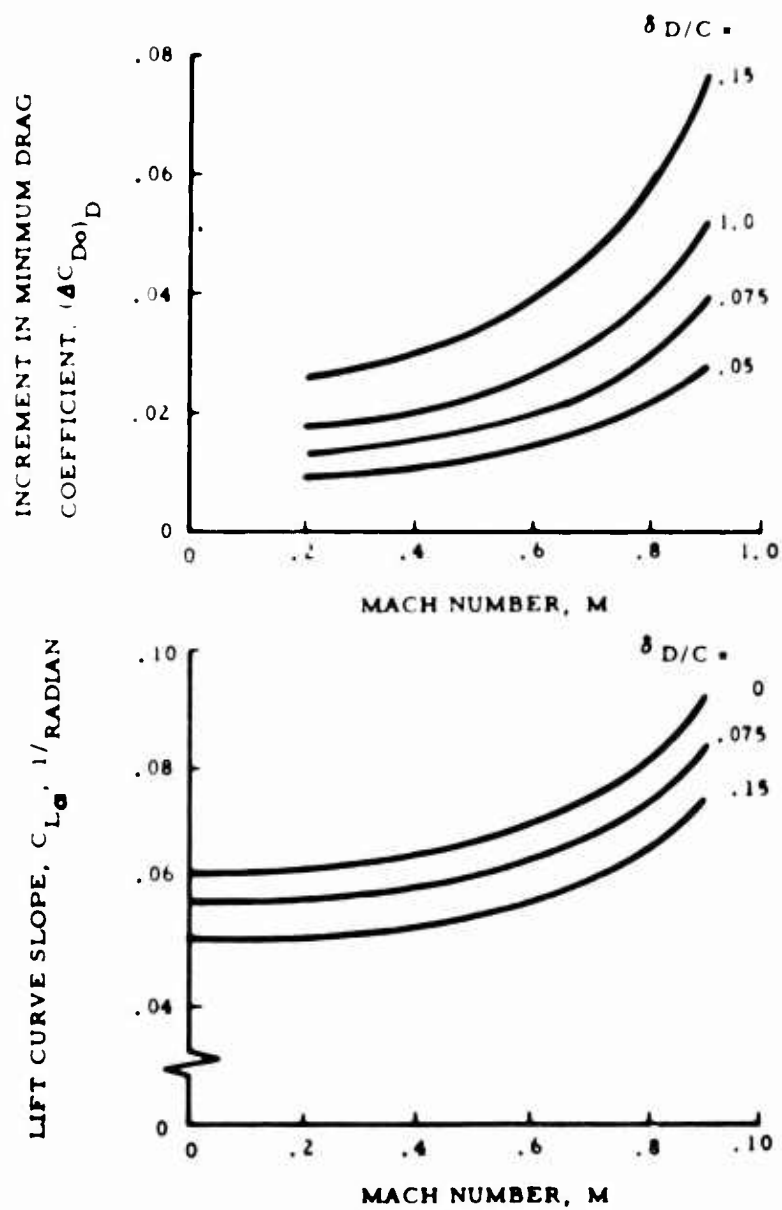
Figure 91. Effect of Deflectors on Lift and Drag of the BPA
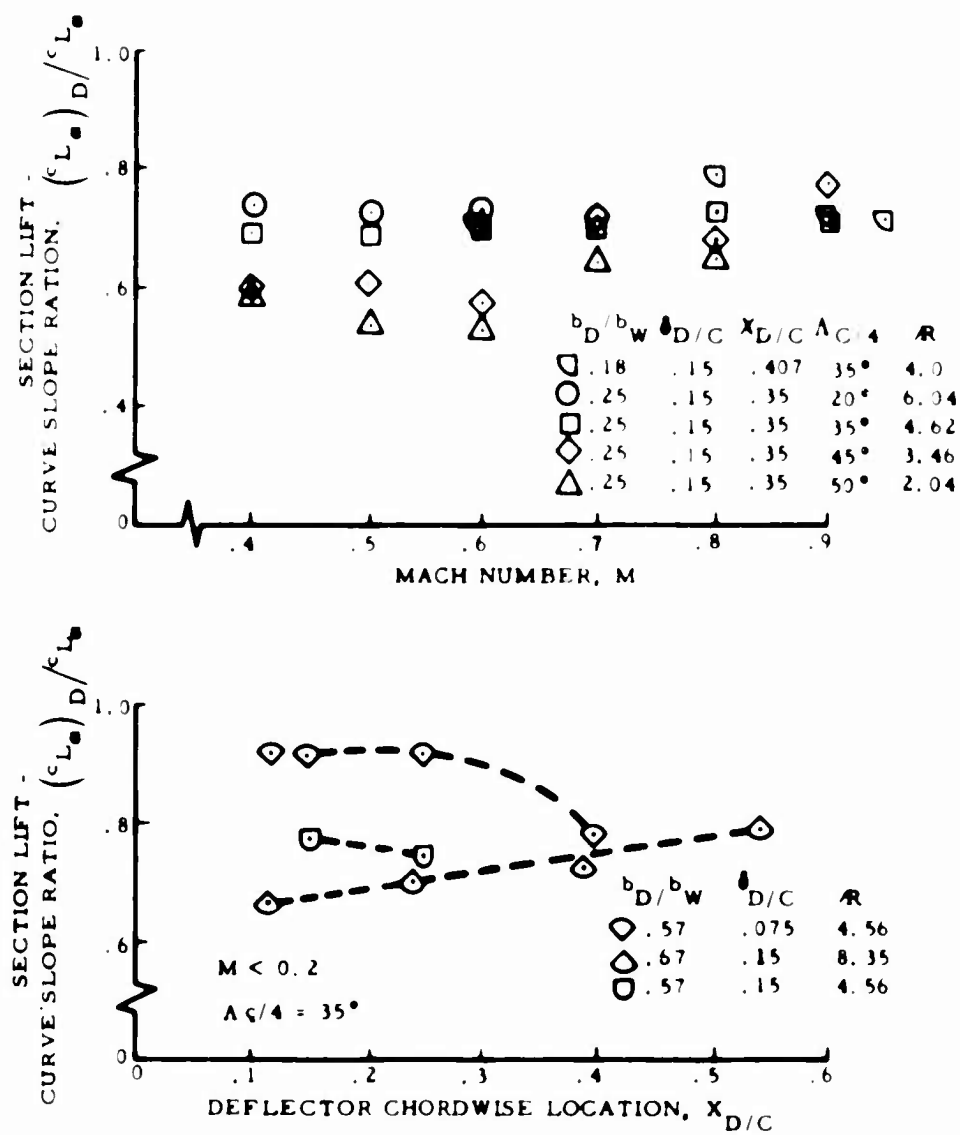
Figure 92. Effect of Deflectors and Location on
Section Lift-Curve Slope
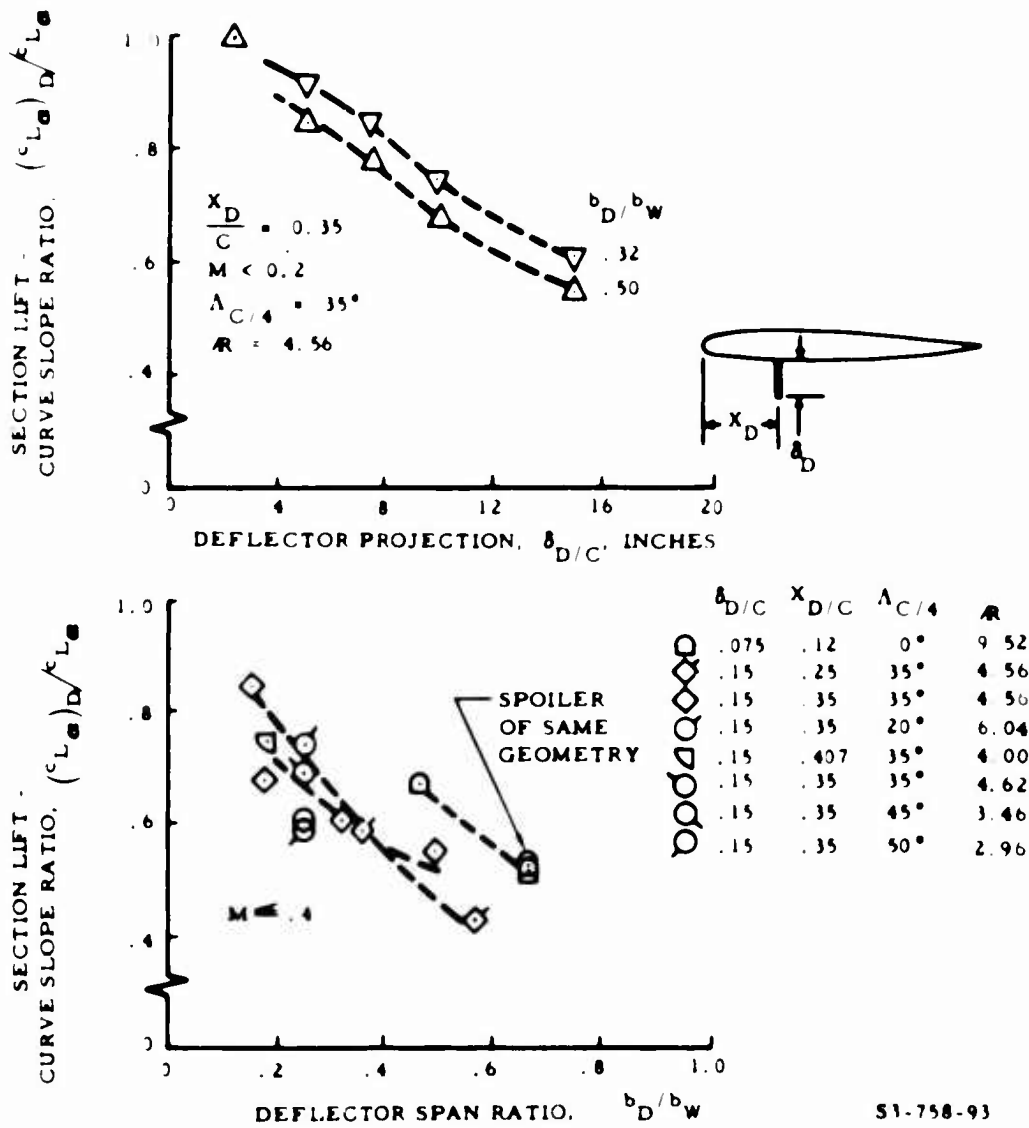
Figure 93. Effect of Span and Projection on Lift Curve Slope
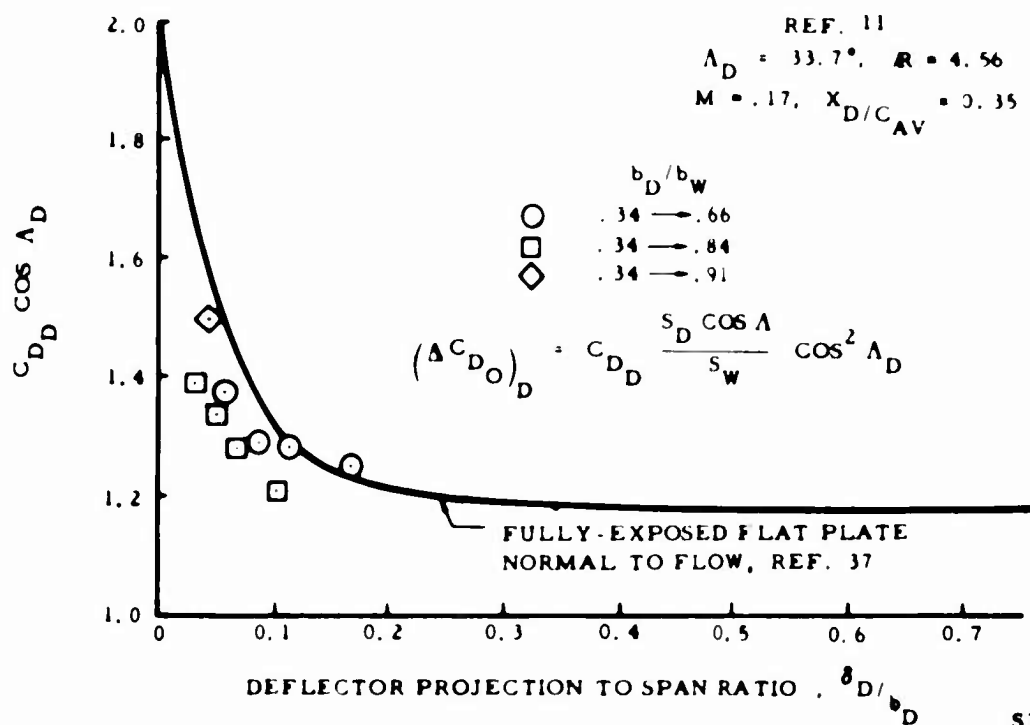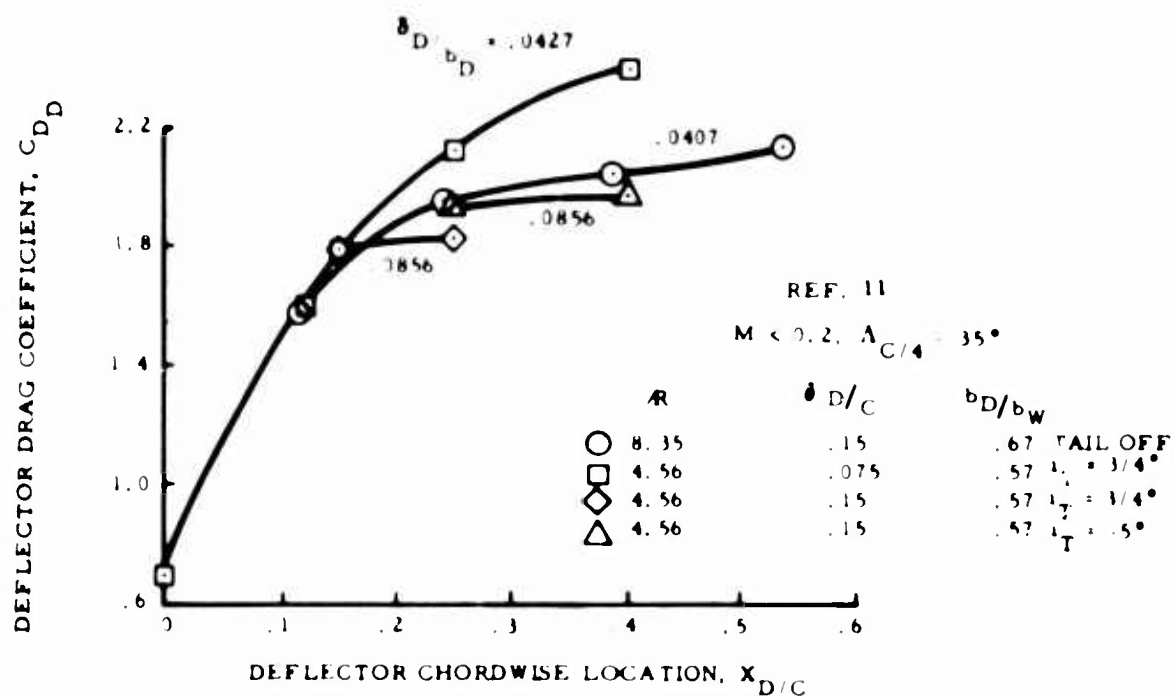
Figure 94. Drag Due to Deflectors
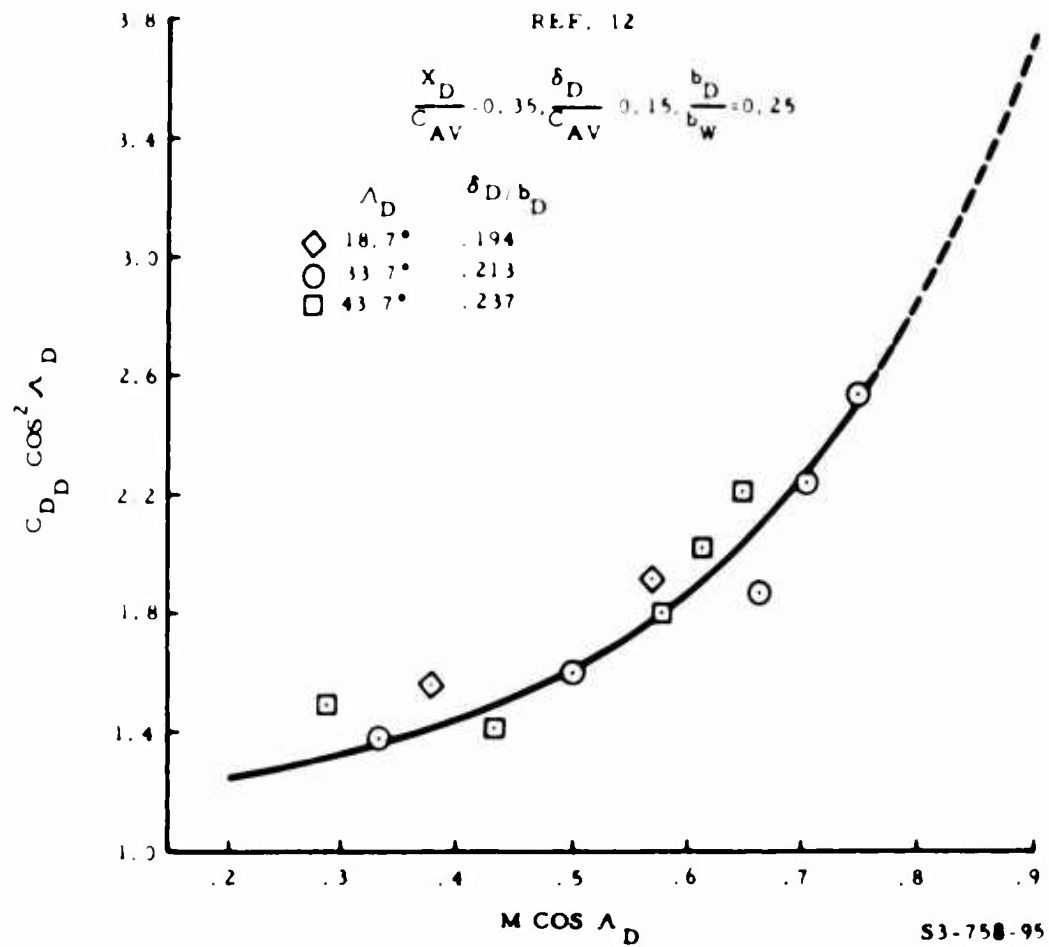
Figure 95. Deflector Drag Variation With Mach Number
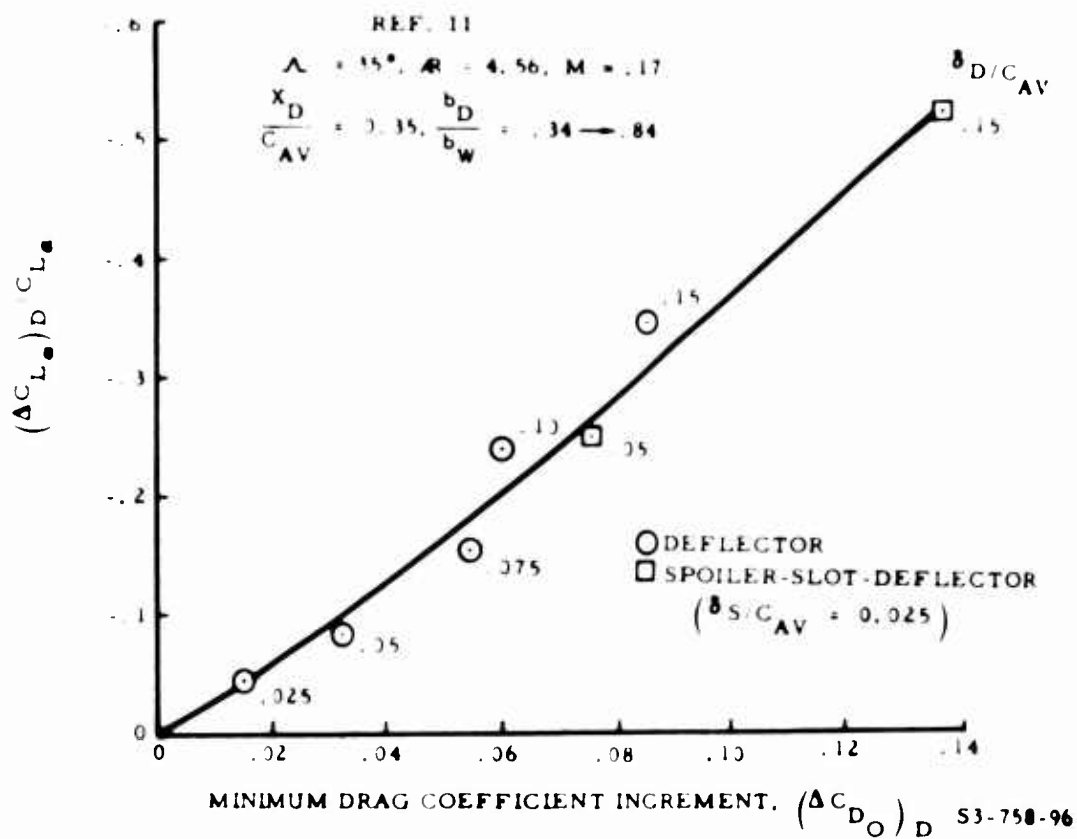
Figure 96. Effect on Lift and Drag of Spoilers and Deflectors in Combination
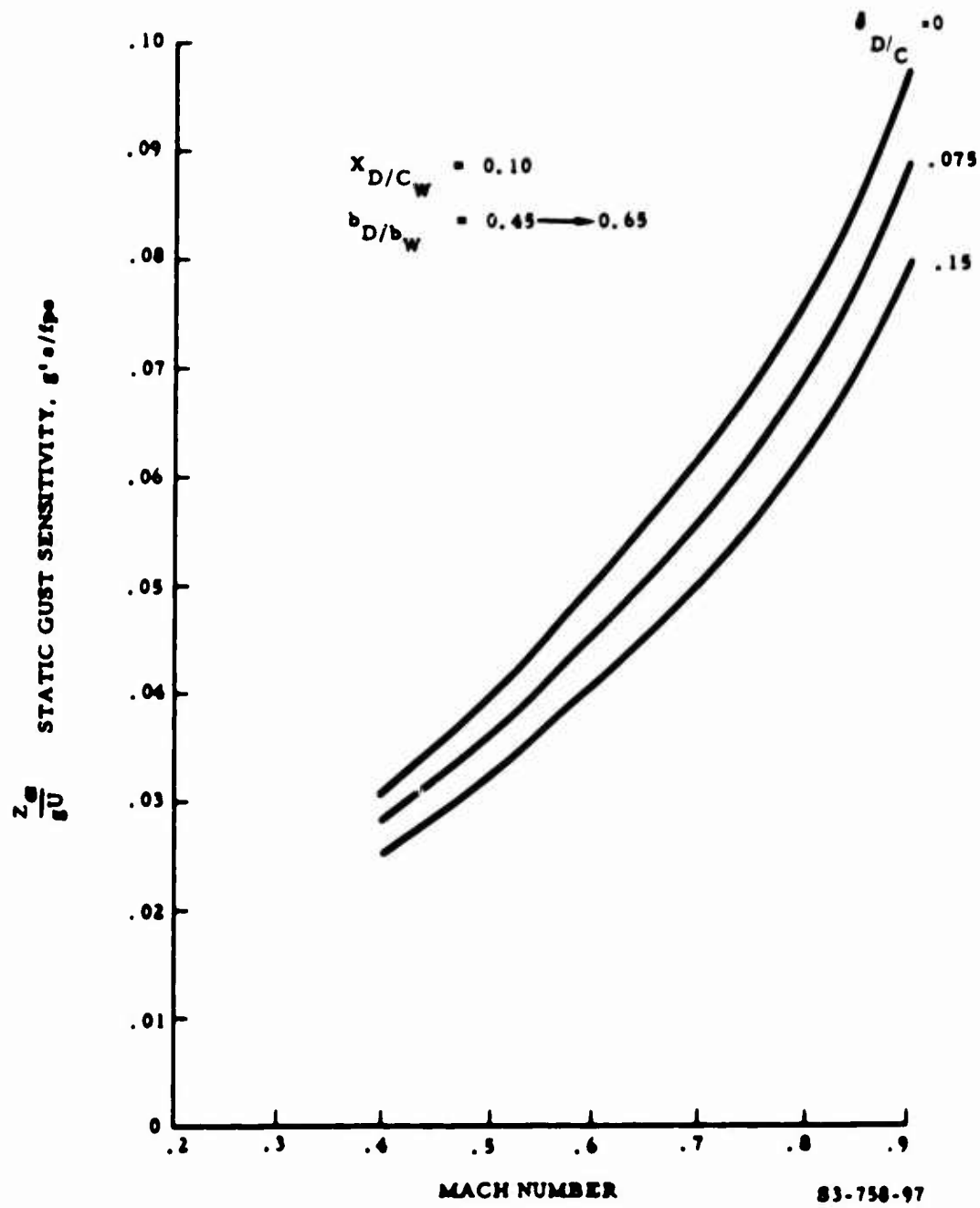
Figure 97. Effect of Deflectors on Gust Sensitivity
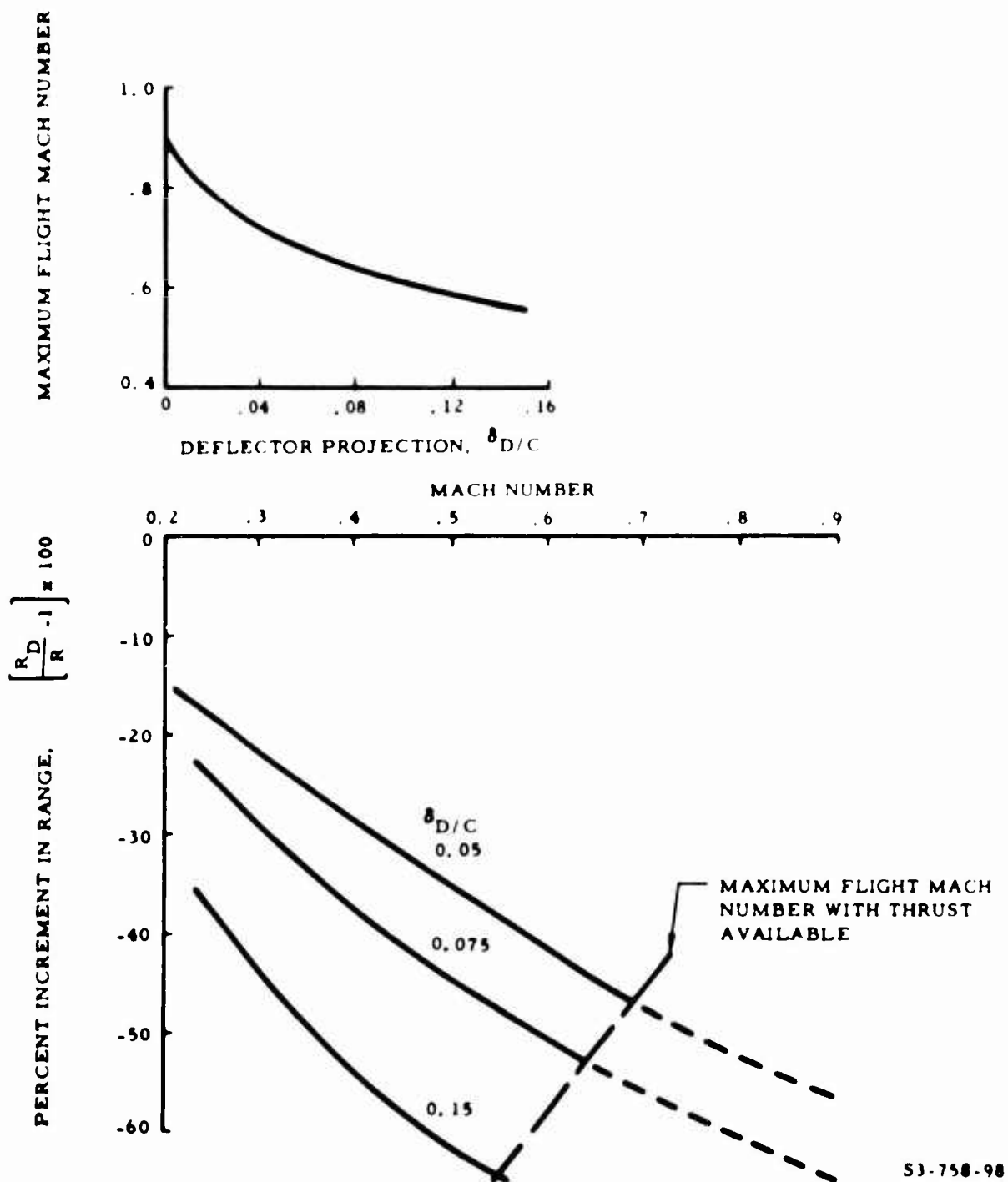
Figure 98. Effect of Deflectors on Maximum Speed and Range

202
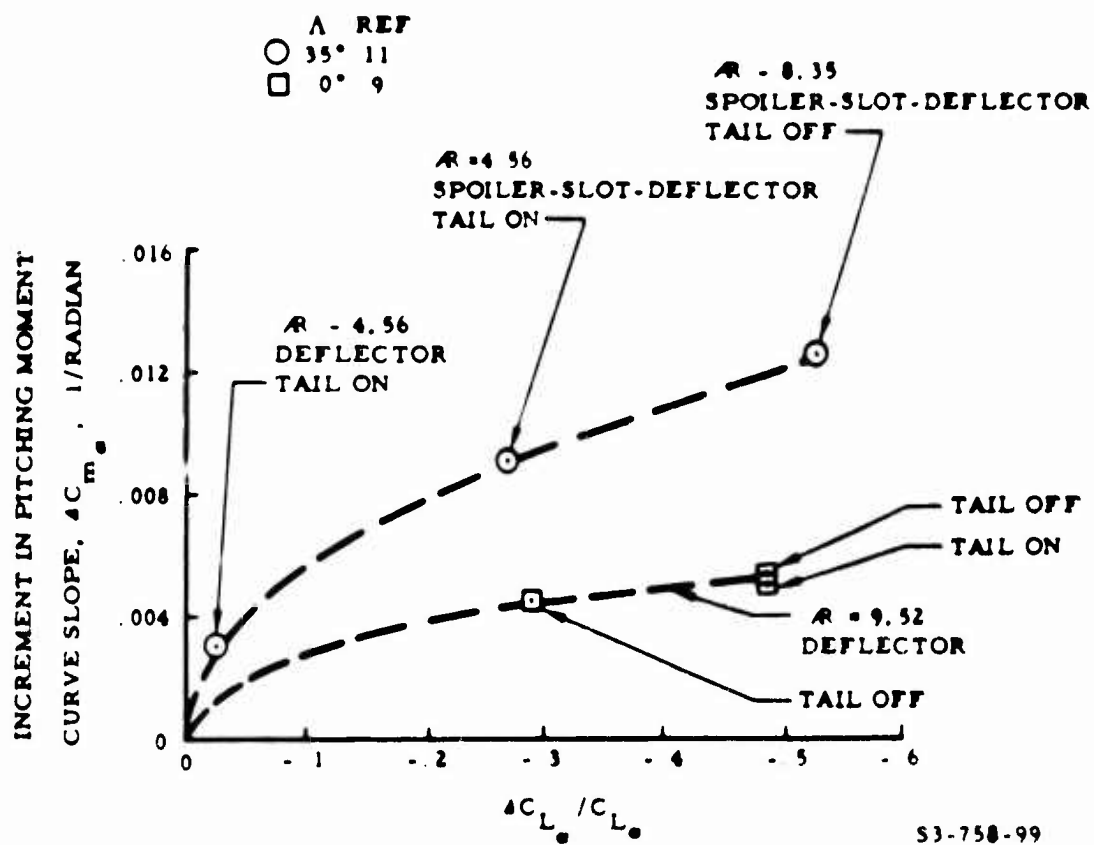
Figure 99. Effect of Spoilers and Deflectors on Static Stability
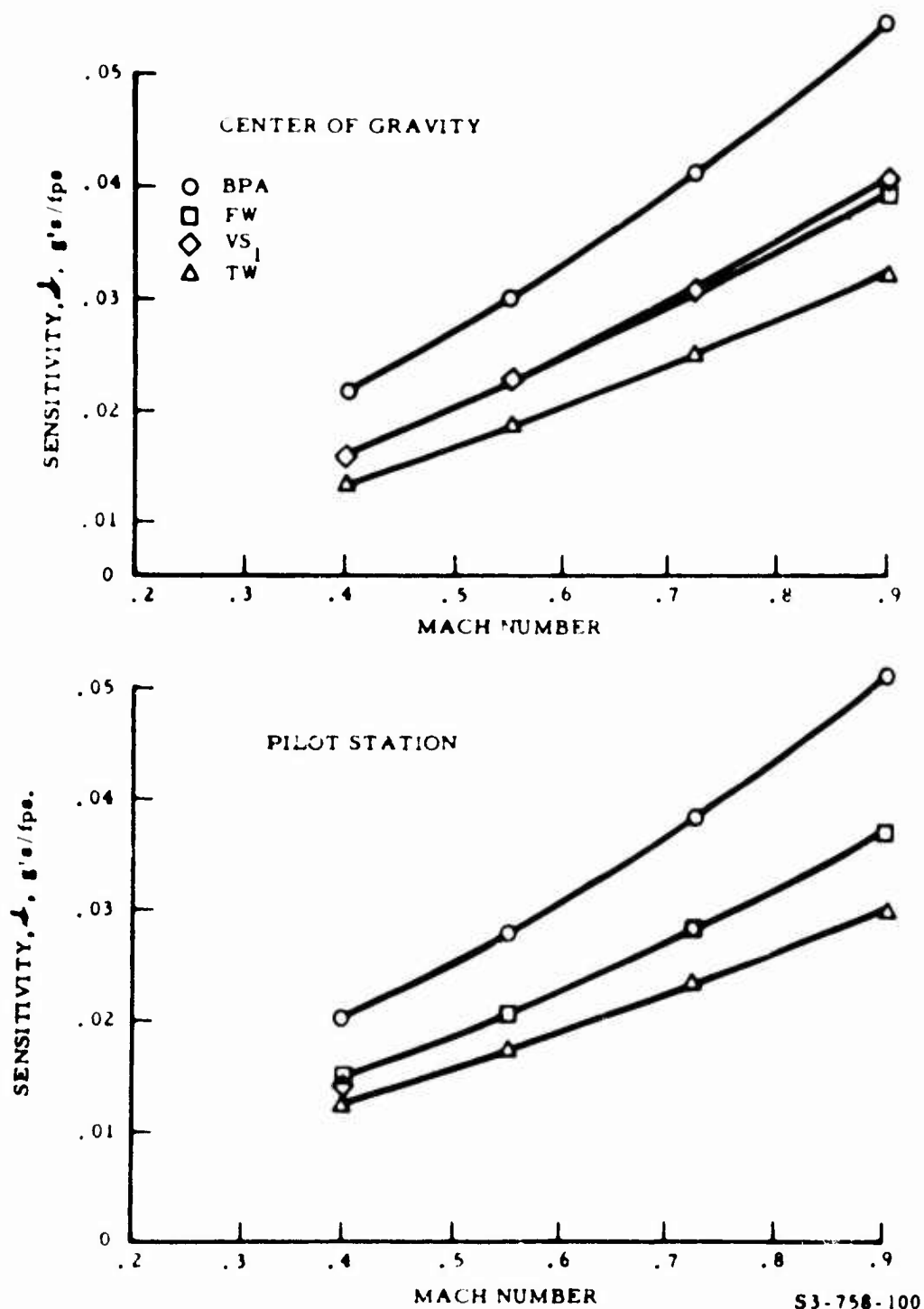
Figure 100. Gust Sensitivity With Passive Systems

S3-758-100
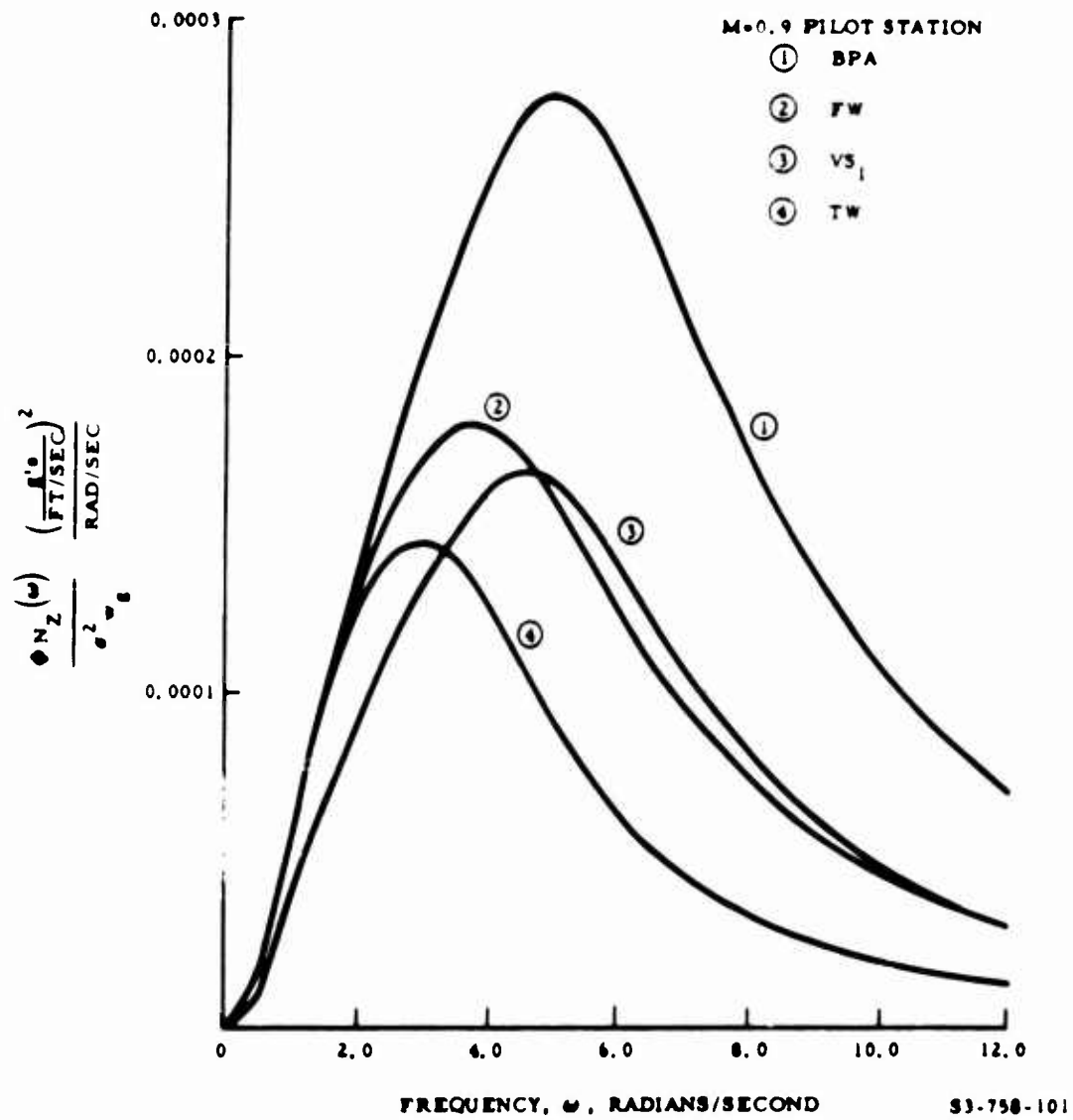
Figure 101. Acceleration Power Spectra With Passive Systems
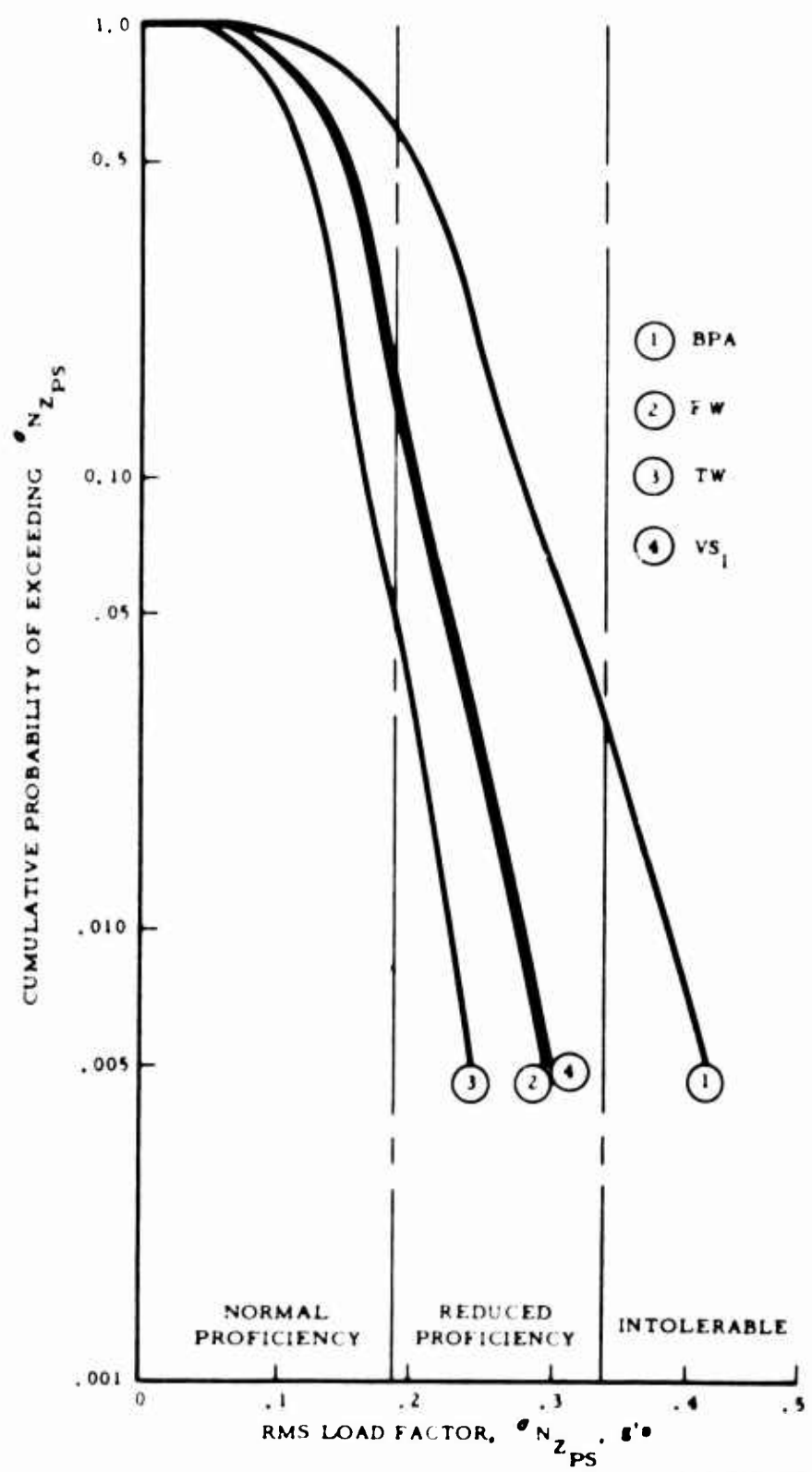
Figure 102. Pilot Endurance Probability With Passive Systems

206

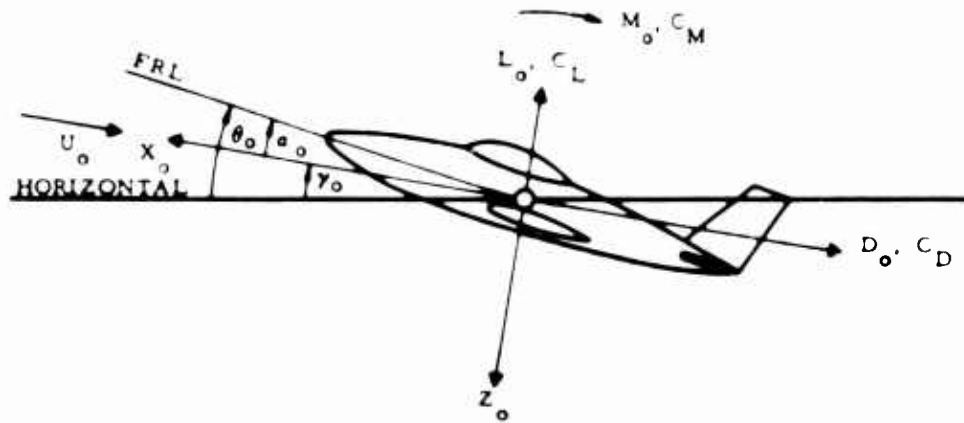Figure 103. Exceedances of Acceleration Levels
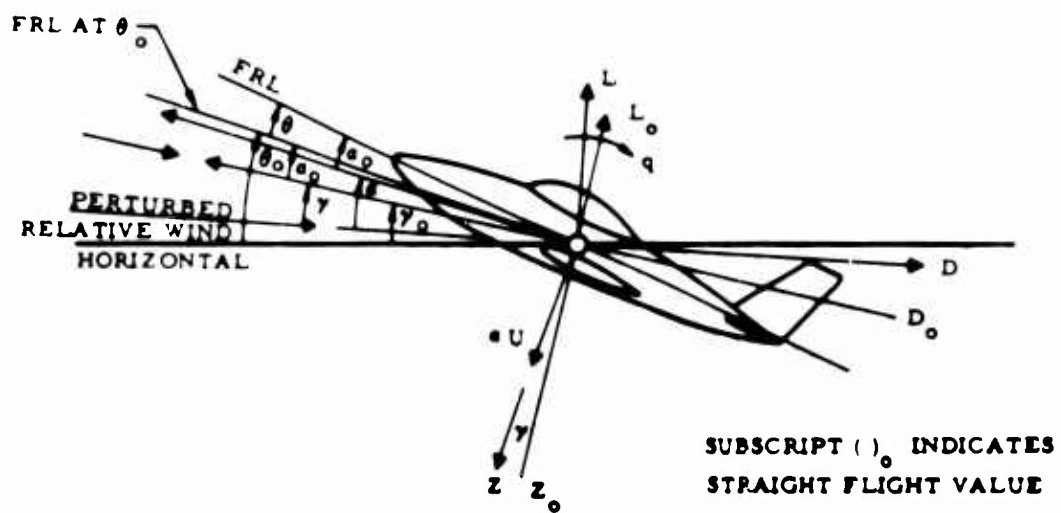With Passive Systems

207

Figure 103. Exceedances of Acceleration Levels
With Passive Systems

207
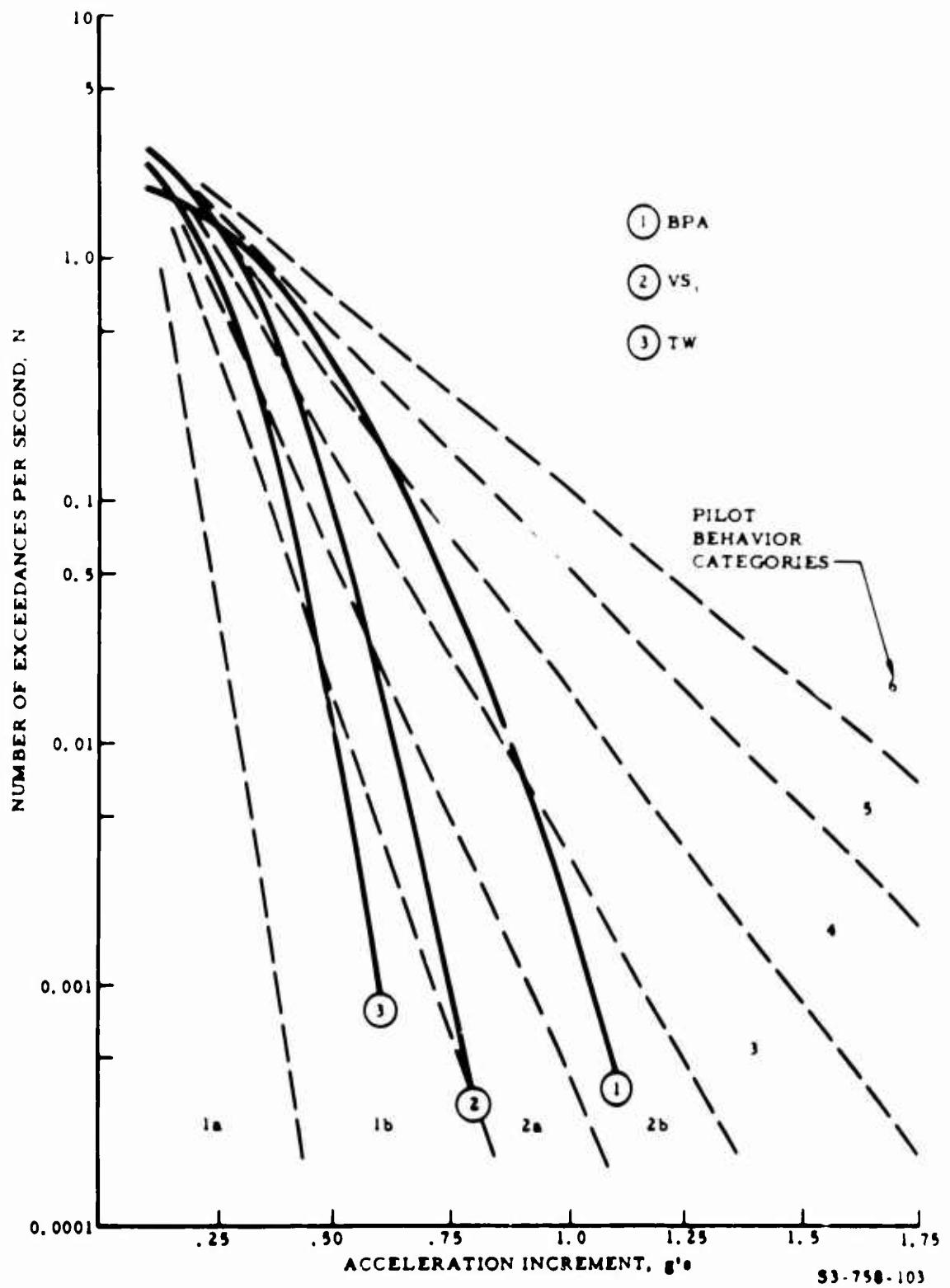
STRAIGHT FLIGHT

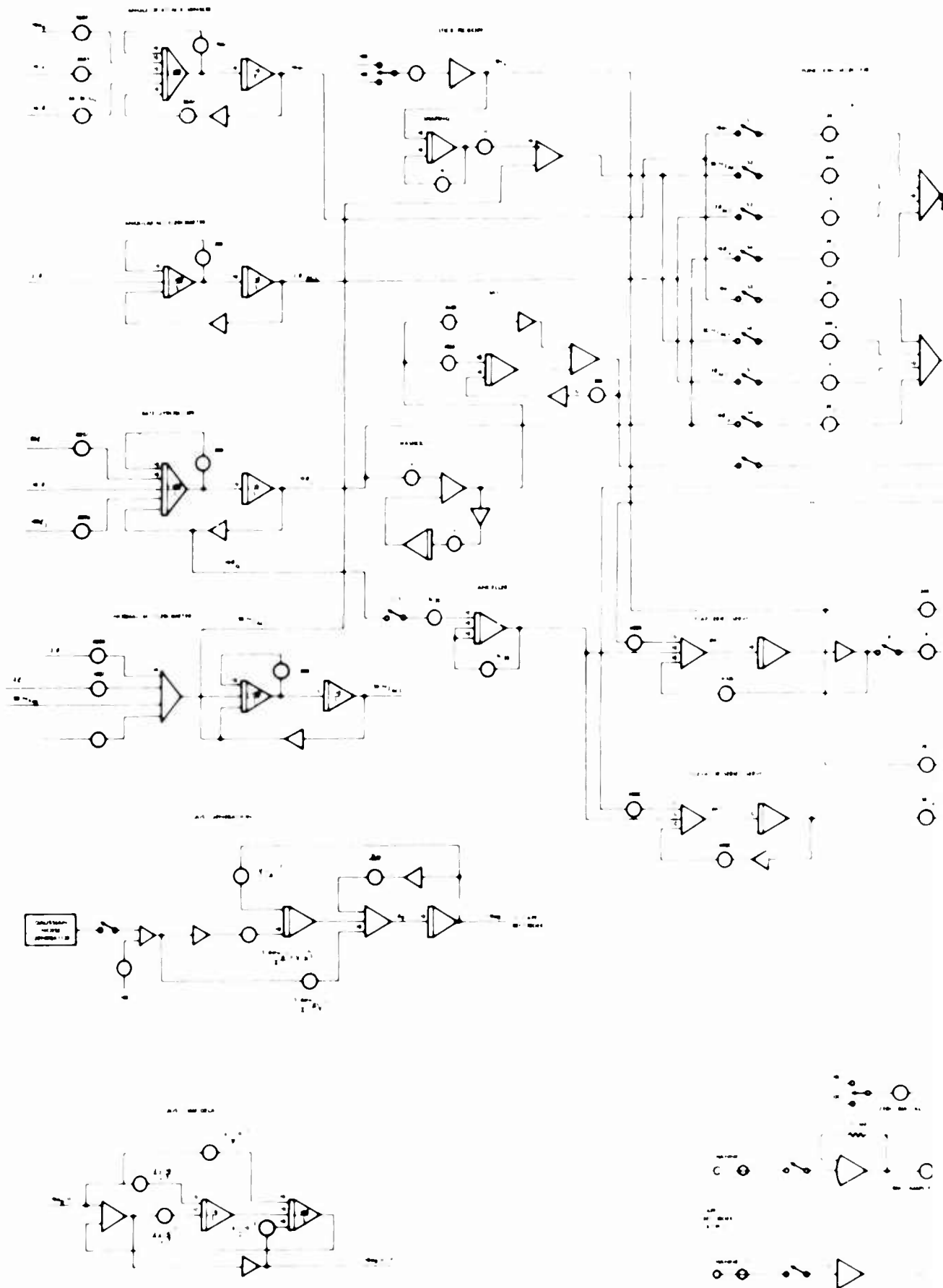NOTE: ALL ARROWS INDICATE POSITIVE DIRECTIONS

PERTURBED FLIGHT

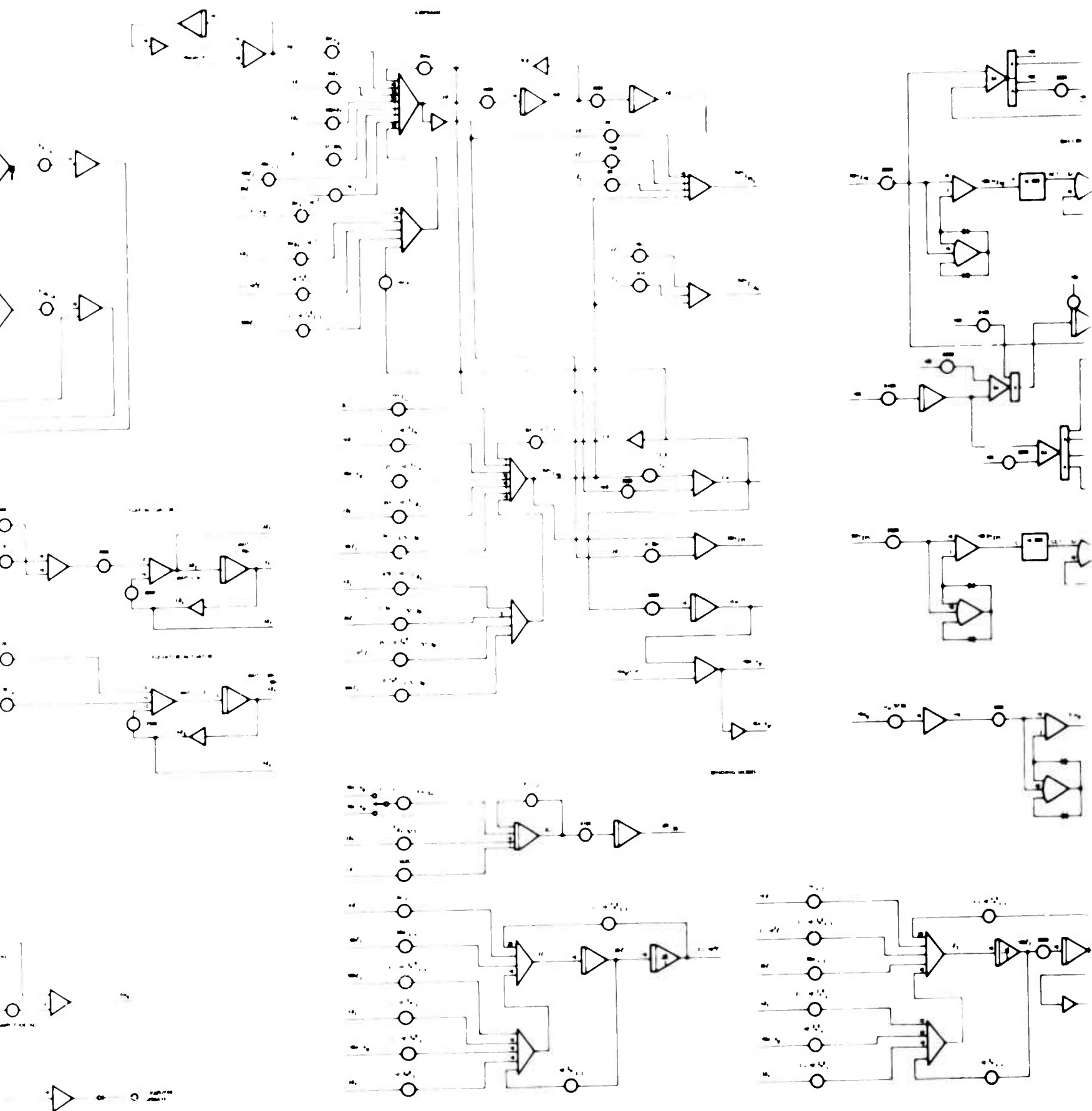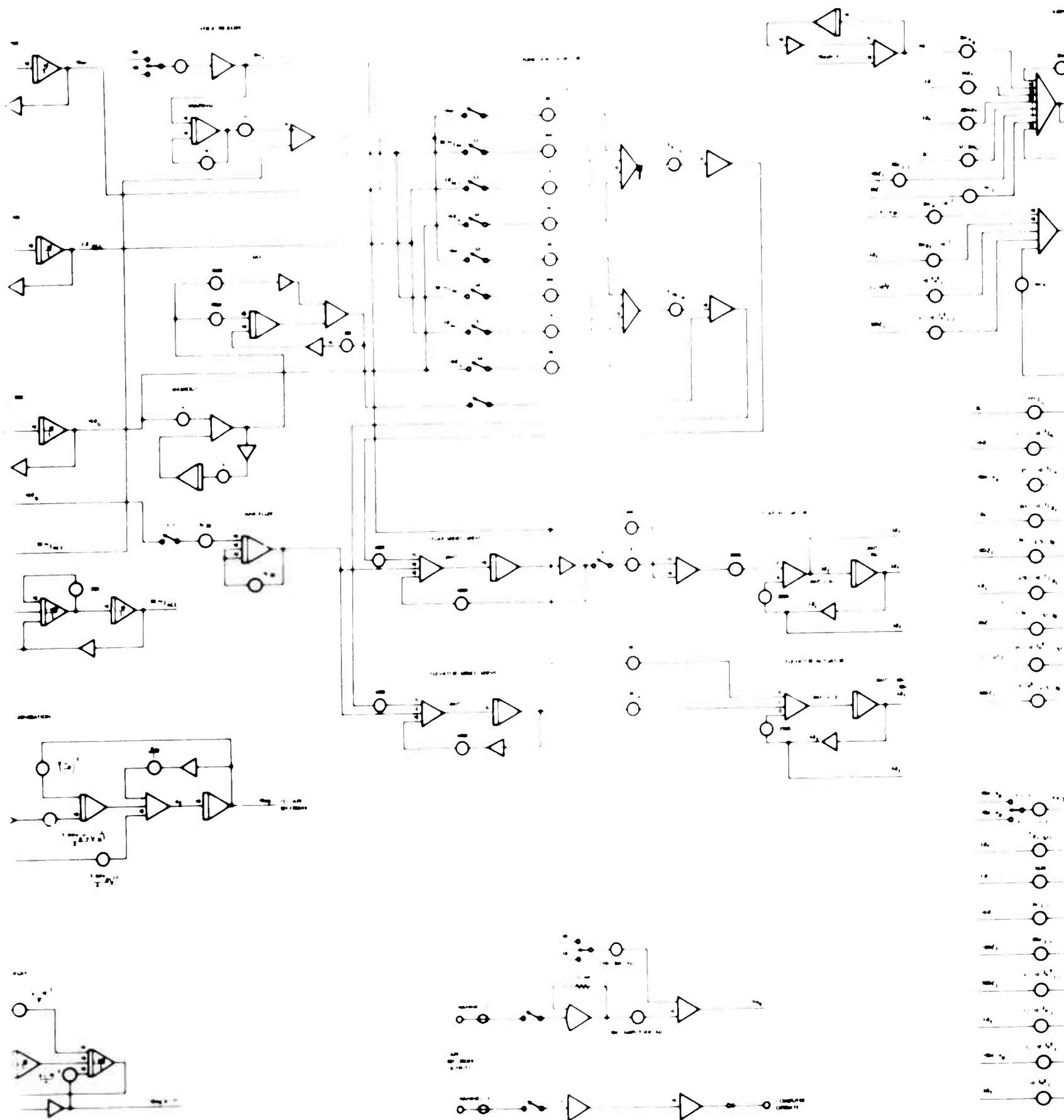Figure 105.   Axis System and Sign Conventions

Figure 106.   Analogue Computer C

211
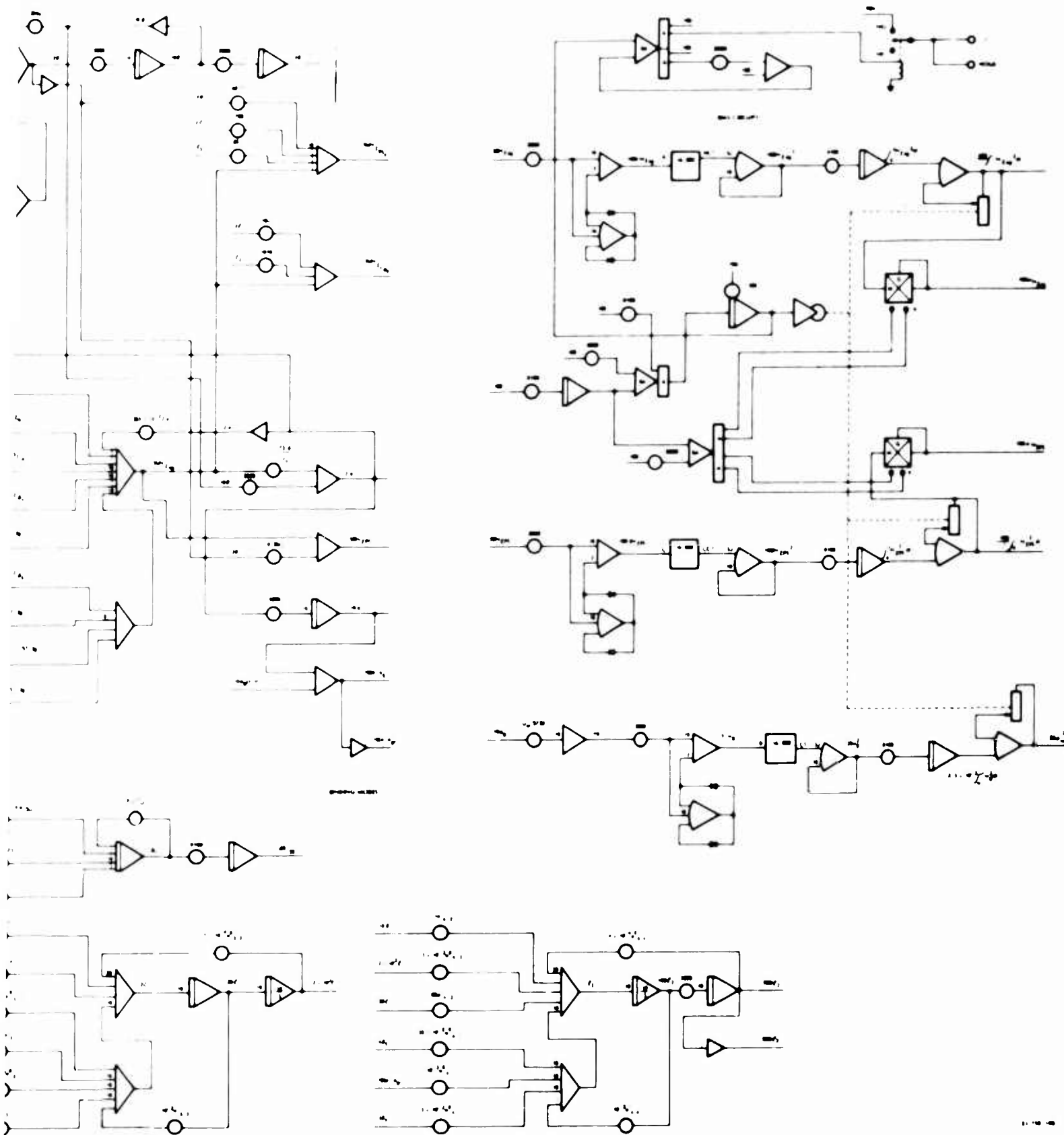
Figure 106. Analogue Computer Circuit Diagram

BLANK PAGE

DISTRIBUTION

U. S. Army Materiel Command	1
U. S. Army Mobility Command	2
First U. S. Army	1
Second U. S. Army	1
Third U. S. Army	1
Sixth U. S. Army	1
Eighth U. S. Army	1
U. S. Army, Pacific	1
U. S. Army Communications Zone, Europe	3
U. S. Army, Caribbean	1
U. S. Army, Hawaii	1
U. S. Army, Ryukyu Islands/IX Corps	1
U. S. Army Depot, Japan	1
Allied Land Forces Southeastern Europe	1
Office of Ordnance, D/A	1
Chief of R&D, D/A	1
U. S. Army Transportation Research Command	43
U. S. Army Research and Development Group (Europe)	1
U. S. Army Engineer Research and Development Laboratories	2
U. S. Army QM R&E Field Evaluation Agency	1
Army Research Office, Durham	1
U. S. Army Test and Evaluation Command	3
U. S. Army Engineer Waterways Experiment Station	1
U. S. Army Combat Developments Command	1
U. S. Army Combat Developments Command Aviation Agency	1
U. S. Army Combat Developments Command Transportation Agency	1
U. S. Army Combat Developments Command Quartermaster Agency	1
U. S. Army War College	1
U. S. Army Command and General Staff College	1
U. S. Army Transportation School	3
U. S. Army Aviation School	1
U. S. Army Quartermaster School	1
Deputy Chief of Staff for Logistics, D/A	2
U. S. Army Aviation Materiel Command	2
U. S. Army Transportation Center and Fort Eustis	4
U. S. Army Infantry Center	2
U. S. Army Aviation Maintenance Center	1
U. S. Army Armor Board	1
U. S. Army Aviation Test Board	1

U. S. Army Arctic Test Board	1
U. S. Army Transportation Board	1
U. S. Army Airborne, Electronics and Special Warfare Board	1
U. S. Army Terminal Command, Atlantic	1
U. S. Army Transportation Engineering Agency	1
Air Force Systems Command, Wright-Patterson AFB	5
Air Force Flight Test Center Edwards AFB	2
Air University Library	1
Bureau of Naval Weapons	4
Bureau of Supplies and Accounts	1
U. S. Naval Postgraduate School	1
Naval Air Test Center	2
David Taylor Model Basin	1
Hq, U. S. Marine Corps	1
Marine Corps Landing Force Development Center	1
Marine Corps Liaison Officer, U. S. Army Transportation School	1
Hq, U. S. Coast Guard	1
Ames Research Center, ·NASA	2
NASA-LRC, Langley Station	2
Lewis Research Center, NASA	1
Manned Spacecraft Center, NASA	1
NASA Representative, Scientific and Technical Information Facility	2
National Aviation Facilities Experimental Center	3
Human Resources Research Office	2
U. S. Army Standardization Group, Canada	1
Canadian Liaison Officer, U. S. Army Transportation School	3
British Army Staff, British Embassy	4
U. S. Army Standardization Group, U. K.	1
Defense Documentation Center	10

BLANK PAGE

Autonetics, a Division of North American Aviation, Inc., Anaheim, Calif., GUST ALLEVIATION FEASIBILITY STUDY - John D. Balducci, F. LeRoy Adams, and Milton A. Schwartzberg, November 1963, 214 pp. (Contract DA 44-177-AMC-858(T)) USATRECOM.   Unclassified Report

Analytical effort provides information for appraisal of capabilities and feasibility of known gust alleviation systems as applied to high subsonic operations. Gust alleviation systems are defined as methods which intentionally or incidentally reduce vertical

(Over)

1. Gust Alleviation

2. Contract DA 44-177-AMC-858 (T)

Autonetics, a Division of North American Aviation, Inc., Anaheim, Calif., GUST ALLEVIATION FEASIBILITY STUDY - John D. Balducci, F. LeRoy Adams, and Milton A. Schwartzberg, November 1963, 214 pp. (Contract DA 44-177-AMC-858(T)) USATRECOM   Unclassified Report

Analytical effort provides information for appraisal of capabilities and feasibility of known gust alleviation systems as applied to high subsonic operations. Gust alleviation systems are defined as methods which intentionally or incidentally reduce vertical

(Over)

1. Gust Alleviation

2. Contract DA 44-177-AMC-858 (T)

Autonetics, a Division of North American Aviation, Inc., Anaheim, Calif., GUST ALLEVIATION FEASIBILITY STUDY - John D. Balducci, F. LeRoy Adams, and Milton A. Schwartzberg, November 1963, 214 pp. (Contract DA 44-177-AMC-858(T)) USATRECOM.   Unclassified Report

Analytical effort provides information for appraisal of capabilities and feasibility of known gust alleviation systems as applied to high subsonic operations. Gust alleviation systems are defined as methods which intentionally or incidentally reduce vertical

(Over)

1. Gust Alleviation

2. Contract DA 44-177-AMC-858 (T)

Autonetics, a Division of North American Aviation, Inc., Anaheim, Calif., GUST ALLEVIATION FEASIBILITY STUDY - John D. Balducci, F. LeRoy Adams, and Milton A. Schwartzberg, November 1963, 214 pp. (Contract DA 44-177-AMC-858(T)) USATRECOM.   Unclassified Report

Analytical effort provides information for appraisal of capabilities and feasibility of known gust alleviation systems as applied to high subsonic operations. Gust alleviation systems are defined as methods which intentionally or incidentally reduce vertical

(Over)

1. Gust Alleviation

2. Contract DA 44-177-AMC-858 (T)

aircraft loading due to turbulence. Evaluation criteria include alleviation capability, pilot tolerance and endurance, stability, control, performance, structural effects, weight, cost, reliability, and fail-safety.